Neuronal dynamics of flexible motor control in the human subthalamic nucleus and cortex

Petra Fischer

Doctoral thesis

Nuffield Department of Clinical Neurosciences

MRC Brain Network Dynamics Unit

Oxford University & St John's College

August 2017

i) Declaration

I, Petra Fischer, confirm that the work presented in this thesis is my own. Where information has been derived from other sources, I confirm that this has been indicated in the thesis.

Signed:.....

Date:.....

ii) Abstract

Beta and gamma oscillations have long been associated with motor control, with beta generally assumed to be anti-kinetic and gamma pro-kinetic. This thesis aims to link these oscillations to several components of flexible motor control: inter-limb coordination, sensorimotor synchronization, abrupt stopping and regulation of the extent and speed of muscle contractions. The subthalamic nucleus (STN) plays an important role in controlling movements. In three separate experiments, I recorded local field potentials from the STN in Parkinson's disease patients on dopamine replacement therapy after they underwent deep brain stimulation surgery. In one task, EEG recordings were also obtained from healthy participants. In a stepping-in-place paradigm, STN beta oscillations were modulated relative to the contralateral step cycle, indicating segregated processing of the left and right limb in the contralateral STN at beta frequencies. Beta modulation was enhanced when auditory cues were provided and sensorimotor synchronization improved. During rhythmic finger tapping and sudden stopping, beta oscillations were again modulated. If post-movement beta was relatively high shortly before participants heard the stop signal, stopping was more successful. I hypothesize that post-movement beta reflects either evaluation of the motor plan according to sensory feedback from the last finger tap or processing related to timing adjustments in the next movement. In both cases, low post-movement beta suggests active neural processing and less reserve for stopping. The main correlate of successful stopping during the actual inhibition process directly following the stop signal, however, was a gamma power increase. Finally, both gamma and beta oscillations were modulated during motor imagery of three different force levels, indicating that their levels reflect motor vigour even in the absence of proprioceptive feedback and may be used as neurofeedback or BCI control signal. Altogether, these findings suggest that beta oscillations reflect wider motor control functions than just being anti-kinetic. Conversely, STN gamma oscillations do not only have a pro-kinetic role, as widely perceived, but are important for abrupt action stopping as well.

iii) Contents

iv) List of Figures

v) List of Supplementary Figures

vi) List of Tables

vii) Acknowledgements

I would like to thank Peter Brown and Huiling Tan for being incredibly supportive supervisors. I am particularly grateful for the instant feedback I have continuously received from the moment I started my studies – and was still gathering ideas – to the moment of finishing this thesis.

I couldn't have explored so many ideas without our safe and friendly lab environment, so I would also like to thank everyone who was and still is part of our lab, with special thanks to Alek without whom my first experiments would have never been set up so quickly. A big thank you also to Frauke and Juliana for many wide-reaching discussions.

Another heartfelt thank you also goes to my teachers, mentors and friends in Osnabrück: Peter König, Gordon Pipa, Kristoffer, Anna, Bene, Johannes, José and Christian – you taught me everything I needed to be accepted to the DPhil program and to enjoy even the challenges that come with research.

I would also like to thank the neurosurgical teams for enabling our research and all my study participants, especially all patients, who went through many repetitions of tapping or stepping without giving up.

My funding bodies, the Clarendon Fund and St. John's College have also played a crucial role in making this happen, not only financially but also by welcoming me into their friendly communities.

Finally, I would have never had the chance to pursue research within this fantastic environment if my family, especially my parents and Alasdair, would not have believed in me all along the way. It's been a great journey so far, and I am truly grateful for everyone who supported me.

viii) Abbreviations

ANOVA	Analysis of variance
BCI	Brain computer interface
CI	Confidence interval
CT	Computed tomography
CMC	Cortico-muscular coherence
DBS	Deep brain stimulation
ECoG	Electrocorticography
EEG	Electroencephalography
EMG	Electromyography
EOG	Electro-oculogram
FDI	First dorsal interosseous muscle
FDR	False discovery rate
fMRI	Functional magnetic resonance imaging
fNIRS	Functional near infrared spectroscopy
FOG	Freezing of gait
FOGQ	Freezing of gait questionnaire
GABA	Gamma amino-butyric acid

GPe	Globus pallidus externa
GPi	Globus pallidus interna
IFC	inferior frontal cortex
ISPC	Intersite phase clustering
L-DOPA	Levodopa
LFP	Local field potential
MEG	Magnetoencephalography
MSN	Medium spiny neuron
SD	Standard deviation
pre-SMA	Pre-supplementary motor area
SNc	Substantia nigra pars compacta
SNr	Substantia nigra pars reticulate
STN	Subthalamic nucleus
UPDRS	Unified Parkinson's Disease Rating Scale

ix) Publications incorporated into this thesis

1. Fischer, P., Tan, H., Pogosyan, A., Brown, P., 2016. *High post-movement parietal low-beta power during rhythmic tapping facilitates performance in a stop task.* Eur. J. Neurosci. 44, 2202–2213. doi:10.1111/ejn.13328

2. Fischer, P., Pogosyan, A., Herz, D.M., Cheeran, B., Green, A.L., Fitzgerald, J., Aziz, T.Z., Hyam, J., Little, S., Foltynie, T., Limousin, P., Zrinzo, L., Brown, P., Tan, H., 2017. *Subthalamic nucleus gamma activity increases not only during movement but also during movement inhibition.* Elife 6, 1–21. doi:10.7554/eLife.23947

3. Fischer, P., Pogosyan, A., Cheeran, B., Green, A.L., Aziz, T.Z., Hyam, J., Little, S., Foltynie, T., Limousin, P., Zrinzo, L., Hariz, M., Samuel, M., Ashkan, K., Brown, P., Tan, H., 2017. *Subthalamic nucleus beta and gamma activity is modulated depending on the level of imagined grip force.* Exp. Neurol. 293, 53–61. doi:10.1016/j.expneurol.2017.03.015

Other publications during the PhD:

1. Fischer, P., Ossandon, J.P., Keyser, J., Gulberti, A., Wilming, N., Hamel, W., Koppen, J., Buhmann, C., Westphal, M., Gerloff, C., Moll, C.K.E., Engel, A.K., Konig, P., 2016. *STN-DBS Reduces Saccadic Hypometria but Not Visuospatial Bias in Parkinson's Disease Patients.* Front. Behav. Neurosci. 10, 1–13. doi:10.3389/fnbeh.2016.00085

2. Herz, D.M., Tan, H., Brittain, J.S., Fischer, P., Cheeran, B., Green, A.L., Fitzgerald, J., Aziz, T.Z., Ashkan, K., Little, S., Foltynie, T., Limousin, P., Zrinzo, L., Bogacz, R., Brown, P., 2017. *Distinct mechanisms mediate speed-accuracy adjustments in cortico-subthalamic networks.* Elife 6, 1–25. doi:10.7554/eLife.21481

1 General Introduction

1.1 Impaired flexibility of motor control in Parkinson's disease

1.1.1 Parkinson's disease

Parkinson's disease is a movement disorder that starts unilaterally and is caused by progressive, but not exclusive, loss of dopaminergic neurons in the basal ganglia, a collection of nuclei at the base of the cerebrum. The disease is characterized by the cardinal symptoms tremor, rigidity, bradykinesia and postural instability (Jankovic, 2008). But patients also exhibit a more general wide-ranging impairment of flexible motor control. By flexible motor control I mean the dynamic competition between a motor strategy based on already accumulated information, i.e. determined by an internal forward model, and one determined by external cues driving adaption (Diedrichsen et al., 2010; Yeo et al., 2016). Patients struggle with rhythmic inter-limb coordination during bimanual or bipedal movements including gait (Almeida et al., 2002; Ponsen et al., 2006; Vercruysse et al., 2012), they find it more difficult to synchronize to external sensory cues (Bienkiewicz and Craig, 2015; Jones and Jahanshahi, 2014), and they also have deficits in action-switching (Byblow et al., 2002) or inhibition (Gauggel et al., 2004; Obeso et al., 2011). All these motor control functions depend on processing of proprioceptive or external sensory information to adjust or terminate the current movement strategy.

Gait, an automated movement that frequently needs to be flexibly adjusted, can be heavily affected in Parkinson's disease. Underlying causes may be abnormal gait pattern generation or posture, perceptual malfunction, problems with movement automaticity or frontal executive dysfunction (Heremans et al., 2013a). Most likely a combination of all these factors results in impairments such as freezing of gait, which can be caused by a wide variety of triggers.

Rhythmic sensory cues can improve gait rhythmicity and freezing substantially (Arias and Cudeiro, 2010, 2008; Hausdorff et al., 2007; Mazilu et al., 2015). This suggests an important role of sensory information for rhythmic motor control.

Interval timing in sensorimotor synchronization tasks can be strongly impaired in some patients while others perform similarly well as healthy participants (Merchant et al., 2008). This heterogeneity improved after dopamine replacement therapy. Dopaminergic signalling seems to be important for interval timing also as it can be affected in schizophrenia, Huntington's disease, attention deficit hyperactivity disorder and multiple system atrophy (Allman and Meck, 2012; Beste et al., 2007; Högl et al., 2014) – all involving dysregulated dopamine.

In contrast to the timing deficit, patients needed more time for inhibiting a movement irrespective of medication intake (Obeso et al., 2011). Motor inhibition deficits thus were hypothesized to depend not primarily on the action of dopamine but rather on diffusely dysfunctional fronto-striatal coordination that affect both response initiation and inhibition (Sinha et al., 2013).

1.1.2 The basal ganglia

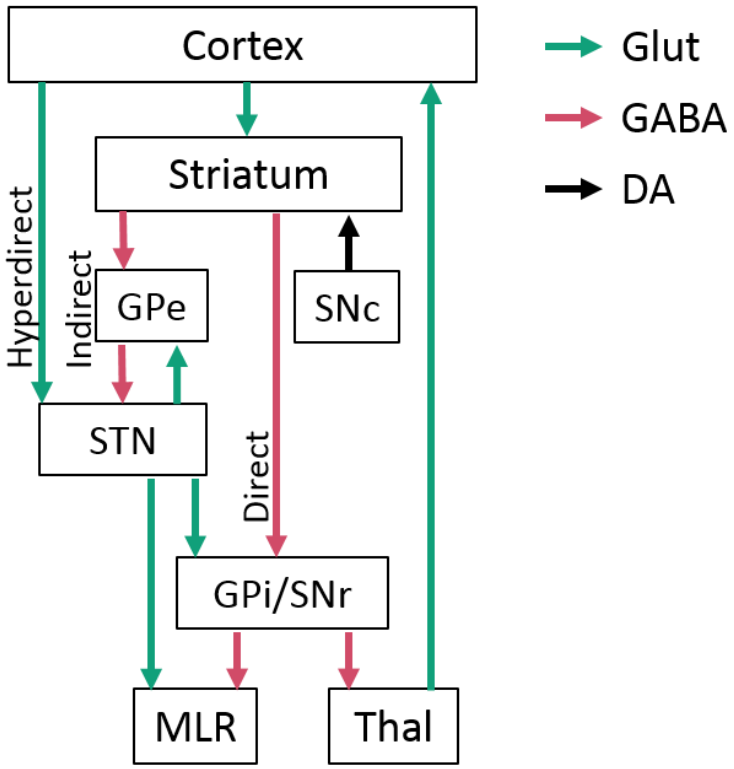

Figure 1.1 Diagram of the basal ganglia showing the hyperdirect, indirect and direct pathway.

The basal ganglia are a complex subcortical structure that have been put forward to act as an action selection mechanism (Mink, 1996; Redgrave et al., 1999), as estimator for time (Gouvêa et al., 2015; Jones and Jahanshahi, 2014) as regulator for movement kinematics (Desmurget and Turner, 2010; Dudman and Krakauer, 2016; Redgrave et al., 1999; Rueda-Orozco and Robbe, 2015) and as tutor for motor learning (Turner and Desmurget, 2010).

Anatomical and electrophysiological studies of the basal ganglia have led to the distinction between three main processing pathways (Figure 1.1): The direct, the indirect and the hyperdirect pathway (Nambu et al., 2002).

Both, the direct and indirect pathways are modulated by dopaminergic input from the Substantia Nigra pars compacta (SNc). When dopamine binds to D1-receptor medium

spiny neurons (MSNs) projecting to the direct pathway, their firing rates increase, whereas indirect pathway D2 MSN activity decreases (Surmeier et al., 2007). The gradual loss of dopaminergic neurons in the SNc in Parkinson's disease thus appears to bias the balance between the two pathways towards the indirect pathway.

The direct and indirect pathways receive inputs from cortex and the thalamus via the striatum (Smith et al., 1998). Cortical input to the hyperdirect pathway travels directly to the subthalamic nucleus (STN) and thus bypasses the striatum. The two main output structures are the internal segment of the globus pallidus (GPi) and the substantia nigra pars reticulata (SNr) projecting to the thalamus (Rinvik, 1975), which in turn again innervates motor cortex and the superior colliculus (Chevalier et al., 1984). The superior colliculus also receives direct projections from the GPi/SNr and projects back to the striatum and the STN via a tecto-thalamic route (Redgrave et al., 2010). The thalamus also receives direct projections from the STN (Lanciego et al., 2012). The STN furthermore also di-synaptically projects to the cerebellum, presumably via the pontine nuclei (Bostan et al., 2010). Additionally, most nuclei of the basal ganglia have reciprocal connections to the mesencephalic locomotor region (MLR) of the brainstem (Martinez-Gonzalez et al., 2011; Mena-Segovia et al., 2004). Importantly, direct and indirect pathway projection neurons were shown to regulate MLR glutamatergic cells in an opposing manner, which directly seem to control gait (Roseberry et al., 2016).

As the GPi/SNr tonically inhibit the thalamus, inhibition of the GPi/SNr via direct pathway-MSN projections results in disinhibition and thus net excitation of the thalamus and cortex (see Figure 1.1). Indirect pathway MSNs, instead, first inhibit the globus pallidus externus (GPe) and thus reduce inhibition of the STN, which in turn has a net excitatory effect on the GPi/SNr. Complexity is added by numerous recurrent connections, among them glutamatergic projections from the STN to the GPe and striatum (Alkemade et al., 2015), as well as GABAergic projections from the GPe to the striatum (Abdi et al., 2015).

Albin et al. (1989) put the net excitatory and inhibitory effects of the direct and indirect pathway, respectively, in the context of basal ganglia disorders. Indirect pathway lesions result in hyperkinesia (Carpenter et al., 1950; Hamada and DeLong, 1992) and the same pathway also is pathologically overactive in hypokinetic disorders such as Parkinson's disease (Remple et al., 2011). An early idea was that direct pathway activity is important for movement initiation while indirect pathway activity mediates inhibition. But the relatively simplistic view of two parallel pathways, one being strictly pro- and the other anti-kinetic, has recently been critically reviewed (Calabresi et al., 2014).

First, rodent tracing studies showed that almost 60% of direct pathway MSNs also send collaterals to the indirect pathway's GPe (Fujiyama et al., 2011; Kawaguchi et al., 1990; Wu et al., 2000). Second, both pathways were found to be active during movement (Cui et al., 2013; O'Hare et al., 2016) and stimulation of the indirect pathway did not only result in a downregulation of cortical neurons but also in an upregulation of a subset of cells (Oldenburg and Sabatini, 2015). Additionally, optogenetic inhibition of not only the direct but also of indirect pathway MSNs resulted in delayed movement initiation (Tecuapetla et al., 2016). This suggests that not only well-timed direct but also indirect pathway activity is required for action initiation. Surprisingly, optogenetic activation of either population also resulted in delayed movement initiation and even already ongoing actions were disrupted by inhibition of either pathway. Notably, only during indirect pathway MSN stimulation the animal left the vicinity of the lever, i.e. pursued an alternative action (Tecuapetla et al., 2016). These results suggest that activity patterns need to be well-balanced between the two pathways for fully functioning action control.

It is assumed that the basal ganglia are structured in channels (Hoover and Strick, 1993; Romanelli et al., 2005) that receive segregated inputs from small patches of M1 motor territories (Donoghue et al., 1992). A recent computational modelling study suggests that alternative actions are suppressed by cross-channel inhibition within the GPe and activation of a very small number of STN cells that encode the executed

action and project diffusely to the pallidum, which inhibits the competing actions (Blenkinsop et al., 2017). The authors linked this to the experimentally observed triphasic response of GPi cells during movements, consisting of early excitation, subsequent inhibition and late delay excitation (Nambu et al., 2002). Only those indirect pathway cells that code for the executed action are thought to exhibit a biphasic response, without the late excitation but a longer period of GPi inhibition instead (Blenkinsop et al., 2017). The GPi inhibition then can result in cortical disinhibition. Each pathway seems to have an important role in generating this response: The early excitation is thought to arrive via the fast hyperdirect pathway, the inhibition via direct pathway MSNs, whereas the late excitation (or inhibition in case of a biphasic response) would be mediated by the indirect pathway (Nambu et al., 2002).

This raises three questions: How can this fine balance and segregation be reliably achieved? Information must be extensively reorganized within the basal ganglia as output neurons are considerably fewer in number than afferents to the striatum (Oorschot, 1996; Zheng and Wilson, 2002). How can information routing be performed selectively and adaptively? This fascinating aspect of neural processing still seems to be poorly understood. And how does outgoing basal ganglia activity shape downstream firing rates (Bosch-Bouju et al., 2013; Goldberg et al., 2013)?

The STN certainly is a key hub for motor control with all its in- and outgoing connections and thus understanding its role in flexible behaviour may bring us closer to answers.

1.1.3 Deep brain stimulation

Deep brain stimulation (DBS) of the STN is a surgical procedure that was first performed 30 years ago and has been celebrated as the most important discovery for treating the symptoms of Parkinson's disease since levodopa (Hariz, 2017). The electrode is typically positioned within the STN or the GPi and contains either four or

eight contacts. After successful implantation, one of the contacts, or a combination, is activated to stimulate with a default pulse width of 60 µs and frequency of 130 Hz, which can be modified but works well in most cases (Moro et al., 2002). The voltage or current is individually adjusted and determines the spread of the stimulation field depending on the surrounding tissue (Yousif and Liu, 2008).

Despite the widespread popularity of this procedure, the precise mechanisms of action on the surrounding nerve cells and fibres are still not well understood (Chiken and Nambu, 2016). STN DBS has been shown to result in both excitatory and inhibitory postsynaptic potentials through activation of glutamatergic and GABAergic afferents. Overall it seems to reduce firing rates of neighbouring cells but increase firing of GPi/SNr neurons while activating afferent axons antidromically. One leading hypothesis is that DBS disrupts abnormal information flow (Chiken and Nambu, 2016).

Naturally, stimulating a large set of cell bodies and axons can also cause unwanted side effects. Depending on the electrode placement, stimulation can cause dysarthria, i.e. speech impairments (Skodda, 2012), dystonia or psychiatric side effects, such as disinhibition, depression or hypomania (Cyron, 2016; Michael Schüpbach, 2012).

The contacts surrounding the stimulating contact can also be used to record local field potentials (LFP) that reflect local STN population activity (also see Chapter 2.2.1.). In an attempt to reduce side effects and prolong battery life, several studies have shown that using the LFP and stimulating only when pathological activity exceed a certain threshold resulted in equivalent or even superior motor improvement (Little et al., 2016a, 2013) while dyskinesia or speech side effects were reduced (Little et al., 2016b; Rosa et al., 2017). This adaptive deep brain stimulation algorithm works by stimulating only during periods of excessively elevated beta oscillations – oscillations in the range of 12-35 Hz.

1.1.4 Pathological oscillations in Parkinson's disease

Numerous studies have shown a pathological increase in beta oscillations in the STN in unmedicated patients (Brown, 2003; Levy et al., 2002; Moshel et al., 2013). As Parkinson's disease progresses and dopamine levels become more and more depleted, neurons in the basal ganglia seem to lose the ability to function individually and instead become synchronized with each other. The strength of beta synchrony correlates with rigidity and bradykinesia and is reduced by dopamine replacement therapy and DBS (reviewed in Little and Brown, 2014; Neumann and Kuehn, 2017). Attenuation of beta oscillations has also been shown to correlate with motor improvement and even seems to outlast brief withdrawal of DBS after being active for 6-12 months, indicating long-term plastic changes (Trager et al., 2016). DBS also seems to selectively improve hypersynchrony in the STN and between the STN and mesial premotor regions (Oswal et al., 2016).

Where or how beta band oscillations originate in Parkinson's disease is still an open question: Beta hypersynchrony may be driven by cortex (Kato et al., 2014; Litvak et al., 2011), may depend on recurrent loops between the striatum and GPe (Blenkinsop et al., 2017; Corbit et al., 2016) or the STN and GPe (Cagnan et al., 2015; Mallet et al., 2008; Nevado-Holgado et al., 2014; Pavlides et al., 2015; Tachibana et al., 2011) or may even be locally generated (Kondabolu et al., 2016; Lienard et al., 2017; McCarthy et al., 2011).

In progressively dopamine-depleted monkeys, first symptoms appeared before a distinct increase in firing synchrony could be observed (Leblois et al., 2007). Slowing of movements was one of the earliest symptoms, which was accompanied by a shift in the ratio of cells that decreased/increased during movement execution towards a much larger percentage of cells that increased their firing rates. Although pairs of spike trains likely are less sensitive in detecting neural synchrony than LFP recordings, these findings suggest that synchronous activity does not contribute much to bradykinesia. Instead of causing early slowing of movements, the authors speculated that pathological

synchrony may play a role in the emergence of later motor symptoms, such as rigidity or freezing (Leblois et al., 2007).

Recent studies have furthermore shown that the amplitude of high-frequency oscillations (HFO) was coupled to the phase of beta oscillations in motor cortex (for HFO between 50-200 Hz, de Hemptinne et al., 2013) and in the STN (for HFO between 200-400 Hz (van Wijk et al., 2016)), which was most pronounced in the more severely affected hemisphere (Shreve et al., 2017). This phase-amplitude coupling was reduced by DBS (de Hemptinne et al., 2015) and during movement (Kato et al., 2016; Kondylis et al., 2016) and was interpreted to reflect hyper-synchronized spiking in cortex that prevents information processing (de Hemptinne et al., 2015; Voytek and Knight, 2015).

Pathological hypersynchrony may not only arise from the decline of dopaminergic cells but also from long-term potentiation of synapses between the GPe and the STN (Chu et al., 2015; Mastro and Gittis, 2015). Circuit dysfunction may thus persist even when dopamine levels are restored.

It is important to note that markers of beta hypersynchrony or phase-amplitude coupling have also been shown in patients with dystonia (Wang et al., 2016; Whitmer et al., 2013) although this may be related to medication therapy resulting in dopamine depletion (Kühn et al., 2008). Finally, it is still a matter of debate how well hypersynchronized beta episodes correlate with Parkinsonian motor symptoms on a moment-to-moment basis (Pan et al., 2016).

Involuntary motor blocks, such as freezing of gait or of upper limb movements, have also been linked to excessive synchrony (Scholten *et al.*, 2016; Shine *et al.*, 2014; Singh *et al.*, 2013). Gait freezing seems to be a prime example of how sensory input, such as narrow doors or cognitive load, can result in a dysfunctional network state that completely blocks motor output. It suggests that network dynamics for motor control are tightly interwoven with those for sensory processing.

1.2 Oscillations in the STN and motor cortex during motor control

1.2.1 Oscillations and motor control

Flexible motor control requires a fine-tuned machinery that regulates multiple components. Imagine a dancer that copies a choreography. How can muscle groups of multiple body parts be activated to different degrees (or relaxed) in a temporally complex coordinated manner? And when the music suddenly stops, how does the dancer switch from moving to postural standstill right in the middle of the dance?

For the brain to communicate separate movement intentions to different muscles, it needs to be able to 1) *simultaneously* target muscle-groups *selectively*, 2) have a fine-tuned *scaling mechanism* to control movement vigour, 3) have a fine-tuned *timing-mechanism*, and 4) if need be, quickly *cancel motor commands,* again *selectively.*

Oscillations are thought to be an important information filter and carrier mechanism in the brain (Cannon et al., 2014; Fries, 2015) and may provide a framework for addressing all these problems. The frequency composition of oscillatory inputs to motor neurons strongly affects their firing pattern (Parkis et al., 2003). Importantly, spike synchronization can occur in the absence of firing rate modulation, as for example during stimulus expectation, indicating a role for top-down cognitive function (Riehle et al., 1997). Synchronization also seems to be important for binding cells into functionally coherent ensembles: Cells with similar muscle fields that were either more activated at the onset or during the holding period of the same movement, were synchronized whereas cells with opposing effects in the same muscle were less likely to fire when the other was active (Jackson et al., 2003).

1.2.2 Movement-related changes in oscillatory power and coherence

To stay within the scope of this thesis, I will focus on movement-related modulation of oscillations in the beta (12-30 Hz) and gamma band (35-100 Hz) as both are robustly observed in the motor cortex and the STN.

Cortico-muscular coherence (CMC) is a means to quantify phase-locking between oscillations recorded from the brain and from muscles. In M1 electrocorticography (ECoG) recordings it was shown that both frequency bands can be coherent with muscle activity during both phasic and tonic contractions (Marsden et al., 2000). The speed, i.e. frequency, of oscillations also seems to correlate well with motor unit and pyramidal neuron firing during movements; they fire rapidly at movement onset and maintain slower discharge rates at beta frequencies during sustained contractions (Hagbarth et al., 1983; Jackson et al., 2003). Gamma CMC seems to be particularly high during phasic movements (Marsden et al., 2000; Muthukumaraswamy, 2011), during very strong isometric contractions (Brown et al., 1998; Mima et al., 1999) and even at low force levels when the contraction had to be dynamically adjusted in a visuomotor matching task (Andrykiewicz et al., 2007; Omlor et al., 2007). Gamma CMC also rose in expectation of rapid force adjustments prompted by a visual cue (Schoffelen et al., 2005), while beta power decreased.

Cortico-subcortical gamma synchrony has also been found between M1, the STN and the GPi (Cassidy et al., 2002; Litvak et al., 2012). Subcortical gamma seems to lead cortical activity, and thus has been suggested to drive cortical gamma. A recently published computational model suggested that gamma oscillations in the basal ganglia originate within the GPe-STN feedback loop (Blenkinsop et al., 2017). Gamma oscillations can also be observed in the striatum during movement initiation in rats (Masimore et al., 2005).

Cortical gamma power (60-90 Hz) increases focally in the contralateral M1 and post-central gyrus only during movement (Cheyne et al., 2008; Pfurtscheller et al., 2003) but not when an effector is passively moved (Muthukumaraswamy, 2010). Importantly,

finely-tuned gamma in this range was found to begin at movement onset and was highly transient, whereas 35-50 Hz low-gamma started slightly later but remained high during sustained contractions (Crone, 1998). Power in both bands furthermore increased not only during movement initiation but also during movement completion when the muscles relaxed (Ball et al., 2008; Szurhaj et al., 2005).

Beta CMC is high during low to medium isometric muscle contractions (Chakarov et al., 2009; Spinks et al., 2008; Witte et al., 2007) but reduced during pinching of unstable objects in comparison to stable ones (Reyes et al., 2017) and reduced in the above-mentioned low-force visuomotor matching task that resulted in high gamma CMC (Andrykiewicz et al., 2007; Omlor et al., 2007). When the same task was performed by a deafferented patient, who performed considerably worse, only beta coherence but no gamma coherence was observed (Patino et al., 2008), indicating a functional role of gamma CMC. Beta CMC also was shown to be higher after visuo-motor learning (Perez et al., 2006) and lower when attention had to be divided (Kristeva-Feige et al., 2002).

Although beta CMC can persist or even increase during phasic movements (Marsden et al., 2000), average sensorimotor beta power, reflecting summed population activity, is clearly reduced (van Wijk et al., 2012). It is also relatively suppressed during muscle relaxation (Toma et al., 2000), passive movement (Cassim et al., 2001), somatosensory stimulation (Cheyne et al., 2003; Gaetz and Cheyne, 2006; van Ede et al., 2011) and motor imagery (Kühn et al., 2006; Pfurtscheller et al., 2005; Schnitzler et al., 1997). Any change in the current sensorimotor state thus seems to perturb beta synchrony. Movement-related modulation of beta oscillations has not only been observed in primary and pre-motor areas (Lee, 2003; Sanes and Donoghue, 1993) and in several nuclei of the basal ganglia (Courtemanche et al., 2003) but also in parietal areas (Brovelli et al., 2004; Murthy and Fetz, 1992), the cerebellum, (Courtemanche, 2004; Soteropoulos, 2005) and the thalamus (Paradiso et al., 2004). All these areas were found to be coupled with sensorimotor cortex at beta frequencies, which hints at a role

of beta oscillations in linking spatially segregated areas and supporting information integration.

After movement completion, beta power in M1 and the STN rebounds to levels exceeding the resting baseline (Toma et al., 2000). During these periods, beta CMC was also increased (Feige et al., 2000). The rebound is sharp after muscle relaxation but returns only gradually when sustained contractions are maintained (Toma et al., 2000). The post-movement rebound is also more pronounced when more muscle mass was activated in the preceding movement (Pfurtscheller et al., 1998) and when the movement was normally terminated and not suddenly interrupted (Alegre et al., 2008). It is lateralized, i.e. highest in the contralateral sensorimotor cortex (Jurkiewicz et al., 2006; Parkes et al., 2006; Ritter et al., 2009; Salmelin et al., 1995), STN (Androulidakis et al., 2007b) and thalamus (Brücke et al., 2013) although it can be observed also in other areas. It has been registered in bilateral sensorimotor, premotor, medial frontal (Ohara et al., 2000; Szurhaj et al., 2003), inferior parietal and temporal regions (Sochůrková et al., 2006) although the precise frequency and time of onset may differ (Pfurtscheller et al., 2003). It is important to note that when individual trials are examined, episodes of beta de- and re-synchronization are not strictly locked to movement onset or offset, and that the beta rebound seems to lack clear somatotopic organization (Crone et al., 1998; Feingold et al., 2015).

Intriguingly, the amplitude of the beta rebound is relatively suppressed when sensory feedback signalizes that a just completed movement did not result in the expected outcome (Tan et al., 2014a, 2014b). This feedback-dependent modulation was interpreted to reflect updating of a forward model (Cao and Hu, 2016) and may thus pose an important mechanism to interact flexibly with the world.

1.2.3 Deterioration of movement-related changes in oscillations in Parkinson's disease

In Parkinson's disease, the movement-related beta decrease is delayed and reduced compared with healthy controls (Devos et al., 2003a, 2003b; Magnani et al., 2002). The movement-related gamma increase is also reduced and seems to be relatively restored by dopamine replacement therapy (Androulidakis et al., 2007b), which partially normalizes also the concurrent beta decrease (Devos et al., 2003a, 2003b). When patients were withdrawn from dopaminergic medication and performed tonic contractions, both beta and 35-60 Hz gamma CMC were reduced (Salenius et al., 2002). The post-movement beta rebound is also diminished in patients compared with healthy controls (Pfurtscheller, 1998) but seems to be unaffected by administration of dopamine (Androulidakis et al., 2007b; Doyle et al., 2005).

1.2.4 Oscillations during rhythmic movements including gait

Treadmill walking has been associated with increased 24-40 Hz cortico-muscular coupling in EEG recordings from healthy participants (Petersen et al., 2012). In another study, sensorimotor 24-40 Hz beta and 70-90 Hz gamma was modulated in an opposite way with respect to the gait cycle (Seeber et al., 2015). Two additional studies have furthermore found modulation of motor cortical beta oscillations relative to the contralateral heel strike (Bradford et al., 2015; Cheron et al., 2012).

In hemiparkinsonian walking rats, STN and SNr beta activity was similarly modulated by paw movements around 30 Hz (Brazhnik et al., 2014; Delaville et al., 2015). Another study in rodents showed cortico-striatal theta-gamma phase amplitude coupling during running (von Nicolai et al., 2014). These studies all suggest involvement of cortical and subcortical beta and gamma oscillations in gait control. However, to date no study has yet investigated how oscillations in the human STN evolve with the gait cycle.

More generally, between consecutive repeated movements, beta increases more strongly if the inter-movement-interval is longer, for example 2s instead of 0.5s in a tapping task (Joundi et al., 2013). When movements were performed in immediate succession, beta did not increase (Manuel Alegre et al., 2004). Recent studies furthermore provided evidence for a role of beta oscillations in the initiation of movement sequences (Bartolo and Merchant, 2015), interval timing (Kononowicz and van Rijn, 2015), beat perception (Fujioka et al., 2015) and for learning rhythmic sequences (Edagawa and Kawasaki, 2017). Interestingly, in patients with Parkinson's disease, entrainment of beta oscillations to rhythmic auditory cues seems to be preserved in sensory but impaired in motor areas (te Woerd et al., 2017).

Recordings from monkeys performing a sensorimotor synchronization task have led Merchant and Bartolo (2017) to speculate that gamma rather than beta oscillations mediate sensory processing within the motor cortico-basal ganglia-thalamo-cortical loop. When the metronome stopped but the rhythmic movement had to be continued, beta oscillations were more pronounced, thus taking over control of timing and acting as "bonding signal" across the circuit (Merchant and Bartolo, 2017). Notably, one major challenge for studying repetitive movements is the difficulty of distinguishing between post-cue/-movement evaluative and pre-cue predictive processing and their neural correlates (Meijer et al., 2016).

1.2.5 Neural correlates of motor inhibition

So far, this introduction has focused on oscillatory dynamics during movement execution. The following section will move on to describe first the network and then the neuronal dynamics associated with movement cancelation.

Imaging, lesion and stimulation studies point towards an important role of the right inferior frontal cortex (rIFC), pre-supplementary motor area (pre-SMA) and the STN in motor inhibition (reviewed in Aron et al., 2014; Bari and Robbins, 2013; Jahanshahi et al., 2015a). Lesions of the STN seem to impair stopping accuracy even when the stop

signal was presented early in a trial (Eagle et al., 2008) while rIFC lesions seem to prolong stop signal reaction times, meaning that the stop signal had to be presented earlier to allow successful stopping (Aron et al., 2003; Chambers et al., 2006).

The pre-SMA and IFC project directly to the STN (Aron et al., 2007; Inase et al., 1999) and seem to work together to generate a stopping command to interrupt an action via the basal ganglia (Aron, 2011; Rae et al., 2015). Pre-SMA activity was found to precede rIFC activity during stopping and when preparing to stop. The pre-SMA may thus have a role in registering the salient stop cue to subsequently alert other areas, such as the rIFC that may then perform action control (Swann et al., 2012). A paired-pulse TMS study also seemed to confirm that inhibitory control of the rIFC over M1 depends on the pre-SMA (Neubert et al., 2010). Other work furthermore suggests that the dorsal rIFC, i.e. the right inferior junction, implements attentional detection while only the ventral part implements braking or actual inhibitory control (Aron, 2011; Aron et al., 2015; Chikazoe et al., 2009; Levy and Wagner, 2011; Verbruggen et al., 2010). According to an fMRI study, the rIFC modulates the excitatory drive from the pre-SMA to the STN (Rae et al., 2015), which seemed to determine inter-individual stopping performances. Yet, a recent ECoG study challenged the notion that rIFC implements actual motor inhibition (Fonken et al., 2016).

Some studies have also suggested a role of the striatum in stopping, although the striatum seems to be more specifically involved in proactive and selective control (Aron, 2011). The next paragraphs will outline what we know about the dynamics of oscillations during motor inhibition so far.

Human electrophysiological studies reported an increase in beta activity over rIFC (Huster et al., 2017; Swann et al., 2009) and over pre-SMA, which seemed to be higher and more coherent for successful compared to failed stop trials (Swann et al., 2012). A MEG study also reported higher beta power over pre-SMA and IFC after successful vs. unsuccessful stopping but it seemed to be too late to implement stopping (Jha et al., 2015). Recently it has been proposed that this beta increase may be more related to

task complexity rather than motor inhibition per se as bilateral ECoG recordings in a simple stop task failed to detect differences between successful and unsuccessful stops (Fonken et al., 2016). Additionally, when a complex movement (writing a signature) had to be terminated midway, frontal beta did not increase but rather failed to show the post-movement increase that was observed during normal movement termination (Alegre et al., 2008).

Some studies also have argued that beta oscillations mediate motor inhibition at least in the STN. For example, high STN beta activity was related to stronger suppression of cortico-spinal excitability during speech inhibition (Wessel et al., 2016a). Two studies also reported that a movement-related STN beta decrease was interrupted earlier and reversed to an increase during successful stopping (Alegre et al., 2013; Benis et al., 2014). Yet in two other stop signal experiments, STN beta power did not significantly differ between successful and failed stops although it still increased relative to go-trials (Bastin et al., 2014; Ray et al., 2012). In the basal ganglia of rats, beta power did not only increase after stop- but also after go-cues and the beta difference between successful and unsuccessful stopping was too late to influence the stopping process (Leventhal et al., 2012). Instead, the firing rate of a specific GPe subpopulation was closely linked to stopping (Mallet et al., 2016).

Response inhibition can be subdivided into action cancellation (i.e. stopping an already ongoing movement) and action withholding (i.e. withholding the execution of a planned movement that has not yet been initiated). Ample evidence has associated beta oscillations with the latter. STN beta increased during action withholding in a Go/NoGo (Kühn et al., 2004) and a Stroop task (Brittain et al., 2012). Lateralized inhibition of the non-selected hand in an action selection task also coincided with up-regulated corticospinal beta coherence (van Wijk et al., 2009). In EEG/MEG studies, beta furthermore increased frontally in NoGo trials, when performing anti-saccades (Alegre et al., 2004; Hwang et al., 2014) and when holding a posture stable against external perturbations (Androulidakis et al., 2007a). Moreover, when finger abduction movements were prompted during periods of elevated beta microtremor as surrogate for

cortical beta, the movement was significantly slower (Gilbertson et al., 2005). Additionally, in high-conflict trials of an Eriksen flanker task, STN single-cell activity was significantly more strongly locked to the phase of STN beta oscillations than in low-conflict trials, where reaction times were shorter, although beta power was similar in both trial types (Zavala et al., 2015). Finally, beta oscillations in Parkinson's disease seem to impair normal motor control as discussed in section 1.1.4, although it needs to be emphasized that beta oscillations in these patients differ from physiologically healthy beta activity.

It is important to note that in some reports the label "inhibitory" may not even have been clearly defined (Bari and Robbins, 2013). One may refer to inhibition when "a definite response [...] mediated by a given process in the nervous system is decreased or abolished by another central process [...] (Konorski, 1967)". However, inhibition once also was defined as "some sort of interference exerted by one mental process upon another (Skaggs, 1929)". Many studies appear to mix up the actual inhibitory process, which abolishes movement-related activity, with other neural events, such as processing of the salient stop cue or retrieval of the correct cue-action association according to the task instruction. Electrophysiological changes that have been described as neural correlates of inhibition may thus in some cases fall under the latter definition, which should be carefully considered when interpreting results.

As outlined in section 1.2.2., gamma activity increases at movement onset and thus has repeatedly been labelled pro-kinetic (Cassidy et al., 2002; Fogelson et al., 2005; Litvak et al., 2012). But curiously, a gamma increase was also observed during outright stopping in electrocorticography (ECoG) recordings from the pre-supplementary motor area and right inferior frontal gyrus (Swann et al., 2012). The increase was interpreted as attentional monitoring while a concurrent increase in beta coherence was associated with inhibitory control. Another ECoG study similarly linked pre-frontal gamma to attentional monitoring, as it increased bilaterally after a stop signal but did not differ between successful and unsuccessful stop trials (Fonken et al., 2016). An alternative interpretation would be that the gamma increase nevertheless triggers an inhibitory

process that may result in successful or unsuccessful stopping elsewhere – in the basal ganglia, for example. But then in line with the view that STN gamma activity is pro-kinetic, it was found to be lower during successful stopping (Alegre et al., 2013).

Finally, a fronto-central slow-wave response has been put forward as key marker for motor inhibition as it correlated well with stopping speed and success (Wessel and Aron, 2016). Such a slow-wave response was also associated with response slowing during high-conflict decisions (Cavanagh et al., 2011). Interestingly, disrupting the STN with DBS speeded up suboptimal decisions during high-conflict trials and resulted in a reversal of the relationship between the slow-wave increase and response time. Thus, the relationship between this electrophysiological response and response inhibition does not seem to be fixed. Furthermore, very similar responses can also be elicited by violations of sensory expectations that do not even involve intentional motor inhibition (Huster et al., 2013; Wessel et al., 2016b).

Taken together, motor inhibition is a topic that has attracted much interest in recent years. Yet many questions are still unresolved, and it is debatable whether the power increases that were reported in various frequency bands are merely epiphenomenal or may have a functional role.

1.3 Thesis objectives

Much research has already been done on oscillations and motor control but a clear consensus about the functional role of oscillations has not yet emerged. Some evidence suggests that beta oscillations carry information through sensorimotor networks about the outcome of a movement. Would we find the same for rhythmic movements that are performed in direct succession? And how does post-movement beta activity relate to the execution of the next movement?

Focussing on the possible roles of oscillations in flexible motor control in this thesis, I set out to answer the following questions:

- How can two or more limbs be flexibly coordinated and this coordination be adjusted to external events in the environment? Will we find a special role of post-movement beta oscillations?
- Are beta oscillations indeed related to stopping? How else may fast stopping be mediated?
- What mechanisms could contribute to regulating the extent and speed of transient muscle contractions separately for multiple effectors? Are basal ganglia gamma oscillations only present during movement or can they be generated by the intention to move?

As the STN seems to have an important role in motor control, we recorded local field potentials from Parkinson's disease patients, who underwent implantation of deep brain stimulation electrodes, to investigate its activity correlates in three different motor tasks. Patients took their medication as usual to limit pathological synchronization and to record basal ganglia activity that is closer to normal than in the dopamine-depleted state.

2 General Methods

2.1 Ethics

All participants gave their informed written consent in accordance with the Helsinki Declaration guidelines. The experimental protocols were approved by the local ethics committees: the National Research Ethics Committee A, Oxford, the Medical Sciences Interdivisional Research Ethics Committee, Oxford, and the National Hospital for Neurology & Neurosurgery and Institute of Neurology Joint Research Ethics Committee, London, UK.

2.2 Electrophysiological recordings

2.2.1 Local field potential recordings

Bilateral STN local field potentials (LFP) were recorded from patients with Parkinson's disease who had undergone DBS surgery. Patients were selected for the surgical procedure if motor symptoms were inadequately controlled by medication and after ensuring that no significant psychiatric conditions were present (Foltynie and Hariz, 2010). Electrode implantation and targeting was performed based on pre-operative MR or combined CT/MR imaging. Electrode extension cables were externalized through the scalp to enable post-operative recordings by connecting the cables to an amplifier (TMSi Porti amplifier, TMS International, Netherlands). In a second surgical procedure, up to 7 days later, the cables were connected to a subcutaneously implanted pacemaker that provides chronic high-frequency deep brain stimulation. The electrode models implanted contained either four (Medtronic 3389) or eight (Boston Scientific, Vercise, DB-2201 and Vercise directional, DB-2202) platinum-iridium contacts. After optimal electrode placement, the lower most contact (contact 0) should be below or in the lower border of the STN while the upper most contact should be above or at the upper most border of the STN.

The ground electrode was placed on the inside of the wrist. The LFPs were recorded with a common average reference and were re-referenced offline to bipolar montages resulting in spatially focal voltage deflections. LFP bipolars were computed by subtracting neighbouring channels of the same recording electrode. If single channels were saturated or inactive, the remaining surrounding contacts were subtracted instead.

Synaptic currents are relatively slow and thus more likely to overlap and sum up in the population average (Buzsáki et al., 2012). The LFP is therefore thought to predominantly capture postsynaptic membrane potential fluctuations resulting from firing of presynaptic excitatory and inhibitory populations (Haider et al., 2016). It reflects the spatially averaged activity of many cells that are concurrently active, as random activity would cancel itself out. It is important to note that LFP oscillations capture a multitude of extracellular processes in the vicinity of the recording electrode. These processes include any type of transmembrane currents that may also result from synchronous local spiking activity, from afterhyperpolarizations and from hyperpolarization-induced opening of ion channels. Voltage-dependent membrane responses can result in intrinsic resonance properties in response to inputs at preferred frequencies that can give way to self-sustained oscillations (Buzsáki et al., 2012). Importantly, the LFP tracks integrative synaptic processes that could not be inferred from firing activity alone. Although subcortical nuclei lack the structure of cortical columns, LFP recordings from the STN also seem to capture synchronous sub- and suprathreshold population activity (Magill et al., 2004).

2.3 EEG recordings

In the studies presented in Chapter 4 and 5 we also obtained electroencephalography (EEG) recordings. The EEG was recorded from actively shielded Ag/ACl electrodes placed on the scalp with a conductive gel. They were connected to the same TMSi amplifier that also recorded the LFP and movement parameters, such as

electromyographic (EMG) activity, grip force or finger flexion during tapping. LFP and EEG data were recorded at a sampling rate of 2048 Hz using in-house software. The amplifier had an in-built first order low-pass filter before the analog-to-digital converter at 4,8kHz and a digital sinc3 filter with a cutoff frequency at 553 Hz to avoid aliasing.

The EEG is thought to capture large-scale synchronous postsynaptic potentials of thousands to millions of geometrically aligned pyramidal cells (Cohen, 2017). Often, high amplitudes in the LFP would simultaneously be expressed in high amplitudes in the EEG, but these signals can also be dissociated. Sodium channel blockage by administration of lidocaine for example decreased LFP power but increased EEG power as a result of stronger synchronization between distributed electrode sites, where oscillations of the same frequency had lower amplitudes (Musall et al., 2014). It is even harder to draw inferences about microscopic events from EEG phenomena in comparison to the LFP because of larger recording distances from the electrophysiological source and volume conduction through the skull. Thus, I would like to acknowledge the considerable explanatory gap between EEG and LFP recordings and investigations of single-cell or multi-unit discharge rates (Cohen, 2017). Yet broadband spatially-resolved LFP recordings, which were obtained for three of my chapters, have still been put forward as "most useful signal for understanding neuronal computations" as they can capture both inputs and outputs, although high-frequency oscillations reflect the output only indirectly, of a large number of cells (Buzsáki et al., 2012).

2.4 Data pre-processing

Events for stimulus or movement onsets were created in Spike 2 (Cambridge Electronic Design). After removal of the DC component (2 sec time constant), data were further processed with custom routines in MATLAB (v. 2014b, The MathWorks Inc., Natick, Massachusetts).

Off-line filtering was performed using the fieldtrip functions *ft_preproc_lowpassfilter* and *ft_preproc_highpassfilter* (Oostenveld et al., 2011). Data were subsequently down-sampled to 1000 Hz and EEG channels were re-referenced to the average of all EEG channels or to linked earlobes, if recorded. Eye movement artefacts were removed from the EEG signals by subtracting the filtered EOG (40Hz low-pass Butterworth filter with a filter order of 6, passed forwards and backwards) after amplitude matching via least-squares optimization (MATLAB function *fminocn*). Trials contaminated by movement artefacts were discarded following visual inspection.

2.5 Time-frequency decomposition

In this thesis, two different time-frequency decomposition methods were used: The wavelet-transform and the filter-Hilbert method. It has been shown that these methods are formally equivalent (Bruns, 2004) although results depend on the precise parameters chosen to resolve the time-frequency trade-off.

For the wavelet-transform, the signal is convolved with complex Morlet wavelets, which are sinusoidal waveforms of any frequency of interest that is multiplied, i.e. tapered, by a Gaussian kernel. Free parameters are the frequencies of interest and kernel width, i.e. number of cycles. The squared amplitude of the convolution result constitutes the power of the signal.

For the filter-Hilbert method, the signal y(t) was band-pass filtered for a range of frequencies of interest and then Hilbert-transformed to derive the complex (analytic) signal Y(t):

$$Y(t) = y(t) + i*H(t)$$

The complex signal has a real part, y(t), which is the original data, and an imaginary part, i*H(t) that contains the Hilbert transform H(t), which is a version of the original data phase-shifted by 90° in the frequency-domain (sines are

transformed to cosines and conversely). H(t) can be obtained by performing the following convolution in the time-domain:

$$H(t) = \frac{1}{\pi * t} * y(t)$$

The free parameters of the filter-Hilbert method are the filter bandwidth and filter order. The Hilbert-transform can provide high temporal resolution as it returns instantaneous estimates of the power and phase. If any frequency from within the filter-range increases strongly in amplitude, this would also be strongly reflected in the power of the filtered signal, which can be beneficial if peak frequencies differ slightly across subjects. But particularly for high frequencies, subsequent smoothing of the continuous power time course was necessary in this analysis pipeline as cluster-based permutation tests (see section 2.5.2) rely on continuous segments that consistently differ in one direction across all participants. If the data were not smoothed, minor temporal between-subjects variability of strong effects that peak only briefly would have resulted in a failure to detect significant clusters.

Both time-frequency decomposition methods were performed on the continuous signal, which was subsequently cut into epochs, baseline-normalized, averaged across trials and subjected to statistical tests.

2.6 Intersite phase clustering

For Chapter 6, phase-based connectivity between the contralateral STN and the five EEG channels of interest (Fz, C3, C4, Cz, Pz) was computed based on the phase information of the Hilbert-transformed filtered signal (band-width and frequency shifts as described in Data pre-processing). Intersite phase clustering (ISPC) can be defined over trials or over time. As we did not expect high-frequency oscillations to be phase-locked across trials, we calculated ISPC for each trial over multiple fixed-width moving windows to get an estimate of changes in ISPC over time. The fixed width was 200 ms for 50-120 Hz and 250 ms for 6-40 Hz. The frequency cut-off was

6 Hz as 250 ms would have included only one and a quarter cycle of a 5 Hz oscillation or even less for lower frequencies.

The window width was chosen to be longer for lower frequencies such that more cycles contributed to the estimate. 250 ms would for example encompass 4 cycles of a 16 Hz oscillation. ISPC was computed within each of these windows, which were shifted by 10ms such that the overlapping bins resulted in a smooth image. ISPC was obtained by calculating the length of the average vector of phase (φ) differences represented as vectors with length one on a unit circle (Lachaux et al., 2000) based on the following equation (n=number of samples, MATLAB code provided):

$$\left| \frac{\sum_{t=1}^{n} e^{i*(STN\varphi_t - EEG\varphi_t)}}{n} \right|$$

The amplitude of the signal thus did not contribute to the ISPC estimate. To assess whether ISPC changed in response to the stop signal, we compared whether it differed significantly from zero after normalizing it by the pre-stop signal period ranging from -350 to 0ms before the stop cue.

2.7 Statistical analysis

2.7.1 Parametric and non-parametric statistics

Differences were considered statistically significant if $p < 0.05$. Pairwise comparisons were performed with t-tests or Wilcoxon signed-rank tests if the normality assumption was violated, which was assessed with a Lilliefors test. To analyse multi-factorial designs in Chapter 5 and 7, repeated-measures ANOVAs were computed in SPSS (v. 22, IBM SPSS Statistics for Windows, Armonk, NY: IBM Corp.). Greenhouse-Geisser correction was applied and the correction factor ε reported if the sphericity assumption was violated.

Correlations between power changes and behaviour were computed as Spearman's rank correlation coefficients with 95% bootstrapped confidence intervals using the *Spearman* function from the Robust correlation toolbox (Pernet et al., 2013).

2.7.2 Permutation testing

Multiple-comparison correction in time-frequency or time windows of interest was performed by using a *cluster-based permutation procedure* (Maris and Oostenveld, 2007, MATLAB code provided): The original paired samples were randomly permuted 2000 times such that each pair was maintained but its order of subtraction may have changed to create a null-hypothesis distribution. If relative power was tested for significant differences from zero, then the sign changed from *"+power"* to *"-power"* if a data point was permuted. For each permutation, the sum of the z-scores within suprathreshold-clusters (pre-cluster threshold: $p < 0.05$) was computed relative to the permutation distribution to obtain a distribution of the 2000 largest suprathreshold-cluster values. If the sum of the z-scores within a suprathreshold-cluster of the original difference exceeded the 95th percentile of the largest sums of z-scores from the permutation distribution, it was considered statistically significant.

3 Bipedal coordination during stepping in place

3.1 Introduction

Gait disturbances are an early sign and prominent feature of Parkinson's disease. In advanced stages many patients suffer from motor blocks (so-called freezing), festination or balance problems (Ebersbach et al., 2013), which suggests that the basal ganglia contribute to the control of human gait. Sensory cues can trigger freezing, which thus seems to reflect a failure to adjust interlimb coordination to the environment or to maintain control despite environmental changes.

Gait disturbances are a major clinical challenge as they may be refractory to medication or deep brain stimulation (DBS) of targets within the basal ganglia, and drastically reduce patients' quality of life (Fasano et al., 2015; Heremans et al., 2013b). Continuous DBS at a fixed high frequency, the current standard, may at some point be replaced by temporally flexible stimulation strategies (Arlotti et al., 2016; Beudel and Brown, 2015), which increases the importance of understanding the neuronal population dynamics associated with gait control. Past studies recording EEG or subthalamic nucleus (STN) local field potentials (LFPs) have shown abnormally exaggerated neuronal synchronization when gait deteriorates (Shine et al., 2014; Singh et al., 2013), but they have not disclosed how basal ganglia activity is modulated during gait. To demonstrate modulation within the gait cycle, neural activity must be recorded with sufficiently high temporal and spatial precision. LFP recordings from the STN in patients who have undergone deep brain stimulation surgery to alleviate motor symptoms provide the necessary resolution, and have helped to establish features of STN activity that correlate with upper limb movements in the past (Anzak et al., 2012; Tan et al., 2016a). In particular, beta oscillations (over about 15-30 Hz) have been shown to be modulated during rhythmic movements of the contralateral upper limb with a beta trough during movement followed by a rebound between two consecutive movements (Androulidakis et al., 2008; Joundi et al., 2013).

Here I test the primary hypothesis that beta activity in the STN is also rhythmically modulated during gait. I sought to find out if beta modulation is time-locked to the movement of the contralateral leg or synchronous in both STN. Since gait involves coordinated and rhythmic movements of both lower limbs, I would expect beta modulation (relative power attenuation followed by a rebound) to alternate in an opposite manner between the two STN if it is locked to the contralateral step. EEG recordings during gait in healthy subjects also support this idea as beta oscillations in motor cortex seem to be modulated relative to the contralateral leg (Bradford et al., 2015; Cheron et al., 2012).

To assure patients' safety and to reduce movement artefacts, we recorded STN LFPs during visually-guided stepping in place while sitting. Auditory cues should improve stepping performance, such as stepping accuracy, considering that auditory cues improve gait impairments in patients with Parkinson's disease (Arias and Cudeiro, 2010, 2008; Hausdorff et al., 2007; Mazilu et al., 2015). Additionally, auditory cues alone already modulate sensorimotor beta oscillations even in the absence of movement (Fujioka et al., 2015, 2012; Iversen et al., 2009; Saleh et al., 2010). My second hypothesis was therefore that auditory cues would not only be associated with behavioural benefits in our paradigm, but also with enhanced beta modulation, considering that beta oscillations provide information about sensorimotor consequences (Tan et al., 2014b; Torrecillos et al., 2015).

*Table 3.1 Clinical details. Age and disease duration are given in years. Dom. Hand = Dominant hand: Right (R) or left (L), UPDRS-III: Unified Parkinson's disease rating scale part III OFF/ON levodopa. * = recorded in both the soundOff and soundOn condition. Levodopa equivalent dose (mg/day) was calculated according to Tomlinson et al. (2010).*

ID	Age/Sex /Dom. hand	UPDRS-III OFF/ON levodopa	Disease duration (years)	Main symptom	Levodopa equivalent dose (mg / day)	DBS lead
1	62/m/r	27/4	12	Freezing of gait	955 mg	Medtronic 3389™
2	60/m/r	52/30	8	Freezing of gaits	1282 mg	Medtronic 3389™
3*	59/m/r	53/18	7	Tremor, bradykinesia, dyskinesia	1195 mg	Boston Scientific DB-2202™
4*	64/f/r	66/36	16	Rigidity, tremor	1628 mg	Boston Scientific DB-2202™
5*	59/m/r	36/8	14	Fluctuations, tremor	1062 mg	Medtronic 3389™
6*	56/m/l	42/26	7	Fluctuations, dyskinesia	1365 mg	Medtronic 3389™
7*	62/m/r	59/15	12	Tremor, rigidity, dyskinesia	1000 mg	Medtronic 3389™
8*	71/m/r	36/18	15	Gait, tremor	785 mg	Boston Scientific DB-2201™
9*	61/m/r	33/11	9	Rigidity	1293 mg	Medtronic 3389™
10*	57m/r	49/18	12	Tremor	1881 mg	Boston Scientific DB-2201™
11*	59/m/r	28/8	10	Tremor	1010 mg	Boston Scientific DB-2201™
12	59/m/r	23/6	22	Fluctuations	1658 mg	Medtronic 3389™
13	65/m/r	16/8	8	Tremor	1434 mg	Medtronic 3389™

3.2 Methods

3.2.1 Participants

We recorded 16 Parkinson's disease patients who had undergone bilateral implantation of DBS electrodes in the STN. Three full data sets and one electrode that was located on the right had to be excluded because of severe movement artefacts (see exclusion

criteria below). Clinical details of the patients included (mean age 61 ± (SD) 4 years, mean disease duration 12 ±4 years, 1 left-handed, 1 female) are listed in Table 3.1. Patients took their prescribed dopaminergic medication as usual and recordings were performed 3-7 days after the surgery at one of the following three surgical sites: King's College hospital in London, University College hospital in London, or the John Radcliffe hospital in Oxford, UK. For each patient, one of the following three macroelectrode models was used: Medtronic 3389 (quadripolar, n=8), Boston Scientific DB-2201 Vercise (octopolar, n=3) and Boston Scientific DB-2202 Vercise directional (octopolar, directional, n=2).

3.2.2 Task

Patients sat in a chair in front of a laptop and a plate mounted by foot pedals placed on the floor such that their feet could comfortably reach the pedals (Scythe, USB 3FS-2). The laptop displayed a video of a walking cartoon man (see *Figure 3.1*), which was looped after one walk cycle (i.e. one right and left step, separated by 1 second) such that the man was walking in place. Patients were instructed to step onto the left- and rightmost pedal with their left and right foot, respectively, in synchrony with the footsteps of the man in the video, while resting their arms on their lap. In a first condition (soundOff), patients were stepping while sitting and had to rely on the video only. In a second condition (soundOn), a metronome sound was provided at the time of each heel strike displayed in the video and thus provided additional information about the timing of heel strikes via the auditory system. For a control condition, patients were instructed to think of anything unrelated to walking, such as upcoming or past holiday plans, and to watch the video without moving. The duration of the video shown in each run was 42 seconds and thus contained 21 left and 21 right heel strikes.

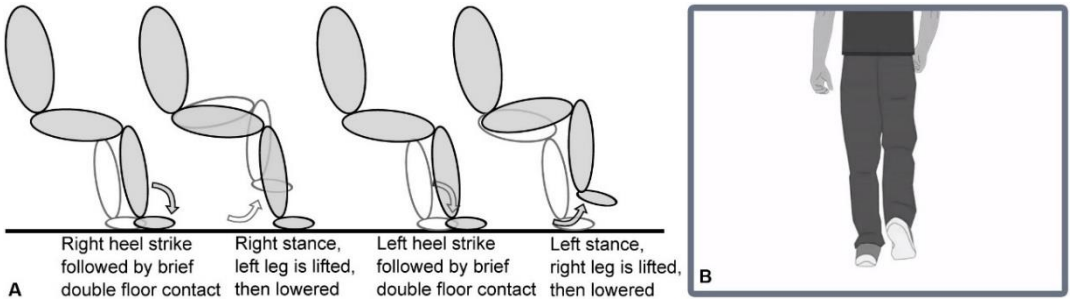

Figure 3.1 Schematic of stepping in place and snapshot of the visual stimulus. (A) After each heel strike, the contralateral leg was lifted. (B) One example picture from the video that dictated the stepping rhythm.

After a short practise run, we recorded the four conditions (N = NoSound + movement, S = SoundOn + movement, C = Control condition (watching only)) in the following order:

2x N, 2x S, 3x C, 2x S, 2x N

This order was chosen such that one stepping in place condition without sound (N) preceded the condition with sound (S) to make sure patients performed one stepping in place condition without prior exposure to the sound. For the first two patients, the soundOn condition was not recorded and thus was present only in seven of nine patients.

After each of the "watching only" (C) runs, subjects rated their performance with a questionnaire asking "How well were you able to think of something else rather than walking?" for the control condition (C). Patients indicated their rating on a visual analogue scale ranging from 0 to 10 with 10 corresponding to "Very well" and 0 to "Not at all".

After the recording was completed, patients filled out the *gait and falls questionnaire* to assess the presence of pre-operative gait problems (Giladi et al., 2000).

3.2.3 Recordings

Monopolar LFPs, foot pedal activation, and triggers for the heel strikes displayed in the video were recorded with the TMSi Porti amplifier. The triggers were registered with a light-sensitive sensor attached to the top left corner of the presentation laptop. In the video underneath the light-sensitive sensor, a black square turned white for one frame (= 41.7ms at a frame rate of 24 frames/second) with each right heel strike, and grey (RGB = [179, 179, 179]) with each left heel strike.

3.2.4 Data processing

The triggers of the first two heel strikes and of the last one were deleted to exclude start and stop-related activity. To exclude channels that were strongly contaminated by movement artefacts, we included only bipolar combinations, where the standard deviation of the 1 Hz high- and 40 Hz low-pass filtered event-related potential did not exceed 1.5 µV (6the average SD of the included channels was 0.40 ± 0.31 µV). The event-related potential was computed as the average across all right steps in a 2s-wide window around the right heel strike ranging from -0.5:1.5s, which thus also included left steps. Activity for each STN was computed by averaging across all bipolar channels of the electrode to avoid any channel selection bias. The downside of the latter is that by averaging all channels we increased the likelihood of a negative result, as not all contact pairs are likely to have been in the STN.

The two main behavioural variables of interest were *step-to-cue offsets* and *step interval durations*. *Step-to-cue offsets* denotes the difference between each real step and the closest corresponding heel strike displayed in the video. *Step interval duration* denotes the length of the interval between the current and the consecutive (contralateral) step registered by the foot pedal. *Step-to-cue offsets* longer than 1s and *step interval durations* longer than 2s were discarded as outliers (mean number of outliers = 10 ± (SD) 9.9). This resulted in an average number of 51 ± 30 left and 49 ± 30 right steps in the soundOff condition and 44 ± 20 left and 43 ± 17 right steps in the soundOn condition.

Then the median of the remaining *step-to-cue offsets* and *step interval durations* was computed. One patient started with the wrong foot and was stepping with the opposite foot to the one shown in the video in some runs. Those steps were excluded for the correlation analyses as these *step-to-cue offsets* could arbitrarily be interpreted as close to -1 or 1.

If patients found it hard to step on time with the cue, it resulted in a larger spread of *step-to-cue offsets,* which could be negative or positive and averaging may thus result in a number close to zero irrespective of variability. To quantify *step timing variability,* we thus computed the median absolute deviation of all *step-to-cue offsets,* which is a robust measure of variability (Williams, 2011) . We also computed the median absolute deviation of all *step interval durations*, which we will call *step interval variability.*

As we specifically explored lateralized stepping control and this would necessarily be out of phase between the two sides, we did not average across the right and left STN for each patient but treated them separately for the soundOn and soundOff comparison, which increased the number of samples from seven patients to 14 STN.

3.2.5 Time-frequency decomposition

The data were down-sampled to 1000 Hz and high-pass filtered (1 Hz cut-off, Butterworth filter, filter order = 6, passed forwards and backwards) before applying continuous Morlet-wavelet transforms using the *fieldtrip*-function *ft_freqanalysis* (Oostenveld et al., 2011). The wavelets were set to span 6 cycles for frequencies between 5-45 Hz and to span 12 cycles for frequencies between 50-80 Hz. The resulting time-frequency decomposition was down-sampled to 200 Hz and smoothed by averaging within a 0.3s sliding window to reduce noise in the data, which aids in performing cluster-based permutation statistics. Relative power was obtained for each subject and frequency by normalizing the absolute power by its average across a 2s time window around the heel strike encompassing one full gait cycle: *(power – average power) / average power * 100.*

3.2.6 Statistical analysis

Behavioural variables or relative power changes are reported as mean ± standard deviation (SD). For the soundOn vs. soundOff comparison, the data from both STN aligned to the contralateral heel strike were averaged. This resulted in a sample size of 10 subjects for these comparisons.

Multiple-comparison correction for power across multiple time and frequency bins was performed by using a cluster-based permutation correction approach as outlines in section 3.1.1. To control for multiple comparisons of burst properties in several time windows, the false discovery rate (FDR) correction procedure was performed (Benjamini and Hochberg, 1995).

Effect sizes are reported as *Hedges g* and its 95% bootstrapped CIs, which were estimated with the *MATLAB Measures of Effect Size toolbox* (Hentschke and Stüttgen, 2011). Spearman's correlation coefficients that were computed across trials within each subject were Fisher's z-transformed and then also subjected to the cluster-based permutation correction procedure to test if the direction of these correlations was consistent across patients.

3.2.7 Beta burst properties

We also examined if increased beta power, appearing in the trial-average, resulted either from a consistent amplitude increase of beta oscillations across trials or instead from an increased likelihood of much bigger oscillations or beta bursts in some trials. In the trial-average, these two possibilities cannot be distinguished. Beta bursts were classified as periods where the amplitude exceeded a threshold defined as the 75% percentile of the amplitude concatenated across conditions (Tinkhauser *et al*, 2017). The beta amplitude was filtered between 28-30 Hz according to the power difference in the soundOn-Off comparison (Butterworth filter, filter order = 6, passed forwards and backwards, and smoothed by a 0.3s moving average to avoid misclassification of noise as bursts). The median amplitude and median duration of these bursts, were computed

within a 0:1s window after the contralateral heel strike, averaged for each patient in the soundOn and soundOff condition and then compared.

3.3 Results

3.3.1 Behavioural results

The average *step-to-cue offset* (n=13, averaged across soundOff and soundOn if present) was -0.09 ± (SD) 0.1s, which shows that the real step was on average 100ms earlier than the heel strike displayed in the video. This so-called *negative mean asynchrony* shows that patients were able to anticipate the next step correctly, a common phenomenon in sensorimotor synchronization tasks (Repp and Su, 2013). The average *step interval duration* was 0.99 ± 0.03s confirming that patients successfully matched their step intervals to the 1s interval in the video.

When the sound was provided, a significant reduction in *step timing variability* relative to the soundOff condition was observed (soundOff = 0.13 ± 0.11s, soundOn = 0.06 ± 0.02s, Wilcoxon signed-rank test (n=9): $P = .020$, Hedges g = 0.85 [0.54, 1.85]). We found no significant difference in *step-to-cue offsets* (soundOff = -0.10 ± 0.09s, soundOn = -0.13 ± 0.09s, $t_8 = 1.0$, $P = .331$, Hedges g = 0.29 [-0.27, 0.91]), *step interval durations* (soundOff = 0.97 ± 0.08s, soundOn = 1.0 ± 0.01s, Wilcoxon signed-rank test (n=9): $P = .125$, Hedges g = 0.57 [0.23, 1.26]) or *step interval variability* (soundOff = 0.09 ± 0.05s, soundOn = 0.07 ± 0.04s, $t_8 = 1.5$, $P = .171$, Hedges g = 0.50 [-0.07, 1.47]). Note though, that the 95% CI of the effect size for the difference in step interval duration comparison did not include zero, which indicates that step intervals were slightly longer in the soundOn condition.

To synchronize with the heel strikes in the video separated by 1s intervals, the timing of the next step had to be delayed if the current step was very early and it had to be advanced if the current step was late. Hence, *step interval duration* should be negatively correlated with the preceding *step-to-cue offset*. T-tests on the Fisher's z-transformed correlations of each subject showed that this was the case for both

conditions (soundOff: rho = -0.35 ± 0.23, t_8 = -4.9, P =.001; soundOn: rho = -0.55 ± 0.19, t_9= -7.51, $P < .001$). Remarkably, the correlations were significantly stronger for the soundOn condition ($rho_{soundOn - soundOff}$ = -0.22, t_6= -2.79, P = .032, Hedges' g = 1.21 [0.63, 2.41]) even though the spread of both variables was higher when no sound was provided (see SDs above). This indicates that auditory feedback facilitated step interval adjustments as evidenced by a stronger relationship between *step-to-cue offsets* and the duration of the subsequent step interval.

Patients' self-reports suggested that they were successful in thinking of something unrelated to walking in the control condition, as the question "How well were you able to think of something else rather than walking?" resulted in 7.7 ±1.8 points out of 10 (= Very well).

3.3.2 Correlation between task performance and gait questionnaire

We also examined if step timing variability, the only performance measure that improved with the sound, was worse in patients with more severe pre-operative gait problems. Severity of gait problems was assessed with the freezing of gait questionnaire (FOG-Q, Giladi *et al.*, 2000). The FOG-Q scores correlated with step timing variability in the soundOn condition (

Figure 3.2, Spearman's rho = 0.73, [0.16, 1.00], P = .026), although the small sample size (n=9) should be noted.

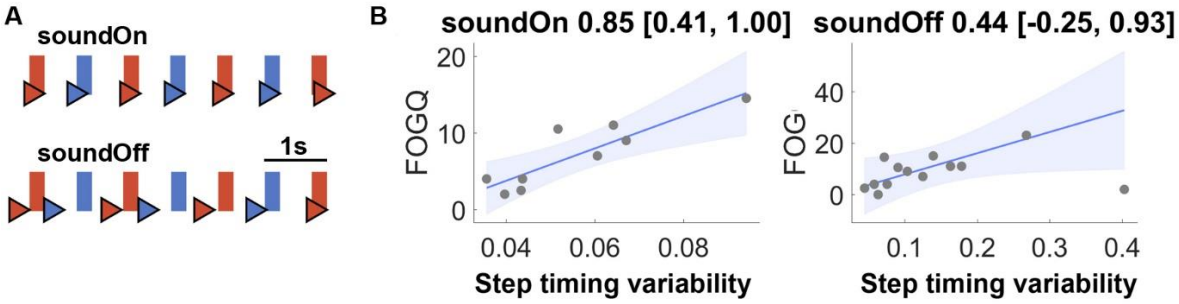

Figure 3.2 Example of step timing variability and correlation with gait impairment. (A) Example of the timings of heel strikes (triangles) and cues presented in the video (rectangles) in the soundOff (top row) and soundOn (bottom row) condition of one subject (subject 5, red = right heel strike, blue = left heel strike). The difference between a cue and the corresponding heel strike is the step-to-cue offset and the STD of these differences is the step timing variability. When the sound was off, heel strikes were less rhythmic than when it was on. (B) Correlation between step timing variability and freezing-of-gait questionnaire (FOG-Q) scores in the soundOn (left) and soundOff condition (right). The title shows the Spearman correlation coefficient. The line denotes the linear regression fit with 95% CIs.

These clinical correlates of step timing variability support the use of the latter measure as a surrogate index relevant to gait performance in our paradigm. We would have expected to find an even stronger relationship in the soundOff condition but only a weak trend was seen in the same direction in the soundOff condition (*Figure 3.2* right, rho = 0.21 [-0.47, 0.84], P = .485). One patient reported only minor gait problems but exhibited very high step timing variability without the sound, such that the correlation would have only been significant after excluding this patient. However, it is well-established that gait impairments in everyday life are reflected by increased step time variability and impaired gait rhythmicity in experimental settings (Gilat et al., 2013; Plotnik and Hausdorff, 2008).

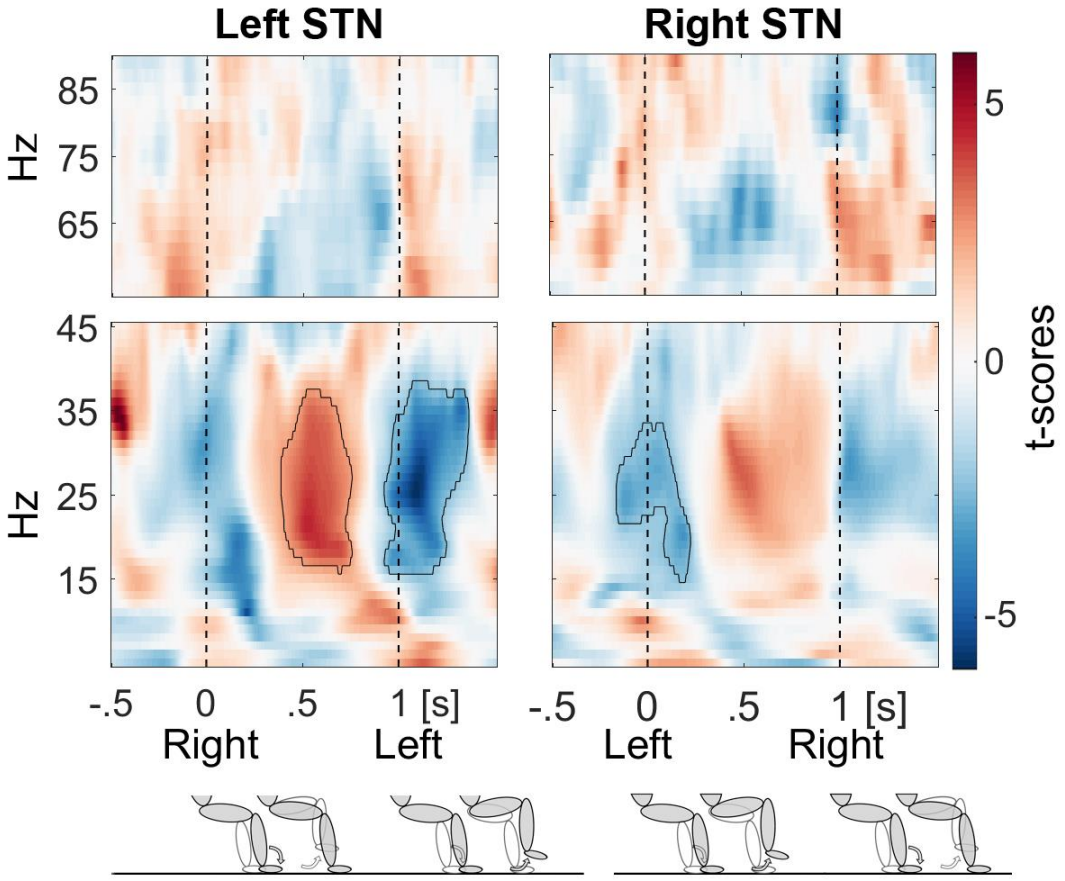

Figure 3.3 Beta and gamma step-related power modulation. Beta power was modulated in an opposite manner in the left and right STN during active stepping (data aligned to the contralateral heel strike and pooled across the sound ON and OFF condition). The bottom row shows the concurrent leg movements. Encircled clusters denote significant power increases in red and decreases in blue relative to the average within the gait cycle.

3.3.3 Power modulation

Beta power was significantly modulated during stepping in place in both STN (*Figure 3.3*, data averaged across the soundOn and soundOff condition) with the strongest decrease after the ipsilateral heel strike when the contralateral foot was lifted. Lifting the leg is more effortful than lowering it; thus, this is consistent with the notion that beta oscillations correlate inversely with effort (Tan et al., 2015). Beta oscillations were most likely to occur or to be largest after the contralateral heel strike when the contralateral foot rested on the pedal as shown by the red power increase in *Figure 3.3*. Beta power in the two STN was thus modulated in an opposite manner.

Figure 3.3 also suggests that gamma activity was modulated opposite to beta activity within each STN. However, cluster analysis failed to identify significant clusters in the gamma band and so changes in this frequency band were not considered further.

The step-specific modulation was particularly pronounced in the high-beta band (20-30 Hz) and less so in the low-beta band (12-20 Hz). The degree of left/right-alternating modulation was quantified as median squared power difference between the right and left STN: $median\ (power_{riSTN} - power_{leSTN})^2$

Figure 3.4 shows that this measure was significantly higher in the high-beta band compared to the low-beta band during stepping in place (Wilcoxon signed-rank test, n=13, $P = .021$, Hedges' g = 0.60 [0.28, 1.07]), but not during video watching without movement (Wilcoxon signed-rank test, n=13, $P = .733$, Hedges' g = -0.35 [-0.87, 0.26]).

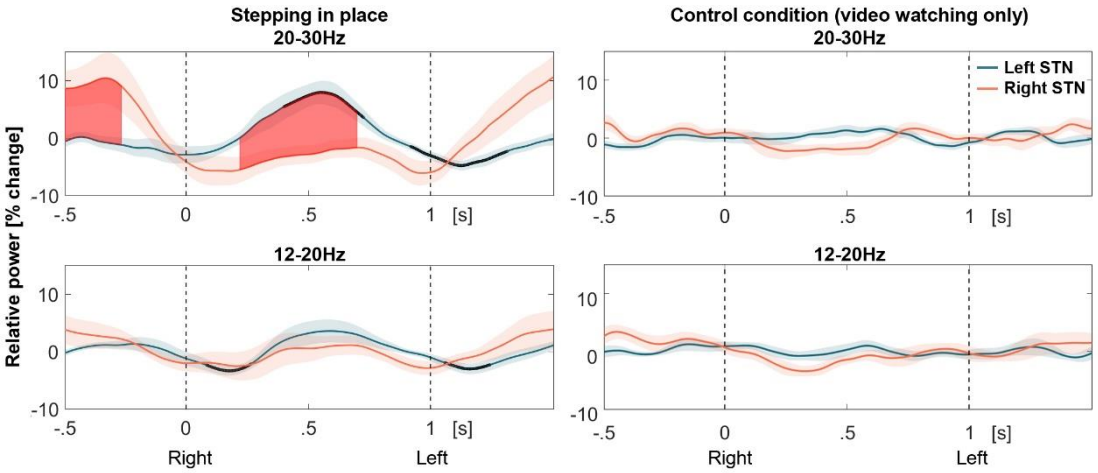

Figure 3.4 High- and low-beta power modulation. Black bold lines denote significant differences to 0 and the red filled area shows significant differences between 20-30 Hz beta power in the left and right STN after cluster-based multiple comparison correction (top row). Shaded areas denote standard errors of the mean. No significant modulation was present when patients were not moving but were only watching the video (right column).

3.3.4 Modulation increased with the sound

Next, we tested if beta modulation was stronger when the metronome was provided during stepping in place. Power modulation was computed for each condition as the difference between the maximum and minimum within 0:1s and -0.5:0.5s, respectively, so as to extract the peak and trough relative to the contralateral heel strike (see *Figure 3.3* and *Figure 3.4*). Beta modulation was significantly higher in the soundOn condition between 28-30 Hz. This modulation difference was driven by increased 28-30 Hz beta synchronisation when the contralateral foot was resting on the pedal (*Figure 3.5A*, diff = 2.5%, t_8 = 3. 05, P = .016, Hedges g=0.30 [0.13, 0.68]) while the difference at the time of the trough at the contralateral heel strike was not significant (diff = -0.7%, t_8 = -0.64, P = .542, Hedges g=-0.12 [-0.83, 0.20]).

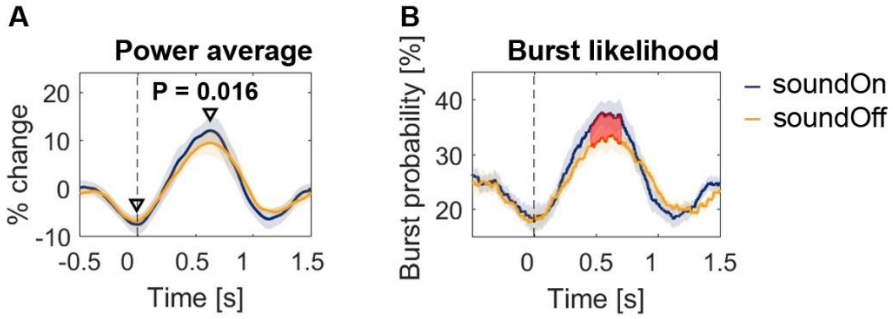

Figure 3.5 Beta bursts after contralateral heel strikes were more likely when auditory cues were provided.(A) Power modulation [max-min(power)] was significantly higher between 28 and 30 Hz during stepping with the metronome in comparison to stepping without the sound (n=9, cluster-based multiple comparison corrected). Shaded error bars denote standard errors of the mean. This difference was mainly driven by an increased 28-30 Hz beta power peak after the contralateral step (dashed vertical line at 0s). (B) 28-30 Hz beta bursts (defined as exceeding the 75th percentile of the amplitude) were more likely to occur when the sound was on. This probability mirrors the power average to the left.

3.3.5 Sound-related differences in beta burst properties

The observed increased power peak in the soundOn condition may be due to consistently increased amplitude of beta oscillations or alternatively due to an increased occurrence rate of enhanced beta periods or bursts in some trials (which would also be expressed as higher amplitude in the average). If we would find that the amplitude was different, then this may indicate that a larger number of cells were more synchronized. If we find an increase only in the number of bursts, it would show that similar events of beta synchronization occurred more frequently. Indeed, the probability of 28-30 Hz burst events irrespective of their amplitude was significantly higher in the soundOn condition (*Figure 3.5B*). The median burst amplitude and burst duration did not differ significantly, indicating that the shape of the beta oscillation profile was not consistently different in the two conditions (burst amplitude: soundOn =0.35, soundOff =0.35, Wilcoxon signed-rank test (n=9): $P = 0.570$, burst duration: soundOn = 265 soundOff=255, $t_8 = 0.5$, $P = 0.169$).

3.3.6 Within-subject correlations between power and behaviour

To test if beta modulation relates to the interval between two consecutive steps, we computed within-subjects correlations between trial-wise (i.e. for each step) beta power and the *step interval duration*. We tested if the Fisher's z-transformed correlations were significantly different from zero at the group level, separately in the soundOff and soundOn condition (*Figure 3.6*, left and right column). If the timing of the beta rebound is locked to the timing of the contralateral heel strike, then this should be visible when the power is shown for the 1s window preceding the ipsilateral heel strike. The variability of the timing of the contralateral heel strike relative to time=0s should affect the timing of the post-movement rebound, which is captured in this window when the contralateral foot was on the ground. The co-variation of the beta rebound and the relative timing of the contralateral heel strike should thus be best reflected with this alignment. Indeed, if the contralateral heel strike preceded the current one by more than 1s, then the beta rebound also occurred earlier (*Figure 3.6*, the green x denotes the average time of the 50% of all contralateral heel strikes that were earliest). This was the case in both conditions. The positive correlations (encircled green blobs) show that 20-30 Hz beta power was higher when the interval between the two steps was longer (see also the line plots below that depict the power average of the 50% longest and shortest interval durations in green and grey respectively). Interestingly, the beta decrease at the current step (time = 0s) appeared to differ only in the soundOn condition.

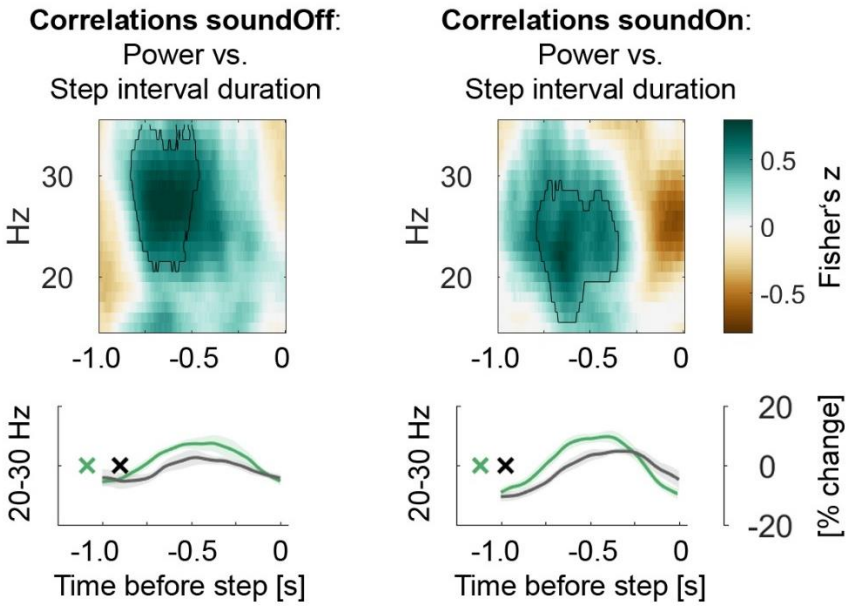

Figure 3.6 Correlations between STN power and step interval duration. Fisher's Z-transformed Spearman correlations were computed between power and the behavioural variables step interval duration between the ipsilateral step at 0 and the preceding step. Encircled green clusters show that when the interval between the two steps was longer, beta power was higher. The same relationship is shown in the power average below (median split data, green = longest intervals, black = shortest intervals).

3.4 Discussion

We found that, during stepping in place, beta oscillations are modulated relative to the contralateral foot step-cycle in the left and right STN. Rhythmic auditory cues, which can alleviate gait disturbances (Arias and Cudeiro, 2010, 2008; Hausdorff et al., 2007; Mazilu et al., 2015), assisted patients in synchronizing their steps to those shown in the video and promoted power modulation in the beta band selectively. More precisely, when auditory cues were provided, the likelihood of beta bursts was increased after the contralateral heel strike.

Our results are in line with reports that STN beta power is modulated during repetitive tapping (Androulidakis *et al.*, 2008; R. A. Joundi *et al.*, 2013) and single limb movements (reviewed in Brown, 2007). During contralateral movement, beta decreases and then rebounds. Often these studies report homogenous power changes over a broad

beta band covering 12-35 Hz whereas we found step-specific modulation to be most pronounced between 20-35 Hz.

Is step-cycle-locked modulation of high-beta oscillations primarily physiological?

We recorded from patients with Parkinson's disease, and as such the modulation of high-beta frequencies might be pathological rather than primarily physiological. However, there are reasons for thinking that the modulation patterns disclosed here may reflect broadly similar modulation patterns in healthy subjects. First, patients performed the task on dopaminergic medication to minimize pathological activity linked to low levels of dopamine (Weinberger *et al.*, 2006). Second, modulation patterns resembled those recorded from cerebral cortex in healthy subjects (Cheron *et al.*, 2012; Storzer *et al.*, 2016), with which STN beta activity is coherent, especially in the higher beta range (Hirschmann et al., 2011; Litvak et al., 2011). Finally, similar modulation patterns are seen in the STN and its output target, the substantia pars reticulata, in hemi-parkinsonian walking rats (Brazhnik *et al.*, 2014; Delaville *et al.*, 2015).

Does the degree of step-cycle-locked modulation of high-beta oscillations relate to performance?

Within-subject correlations showed that the timing of the beta rebound was locked to the contralateral heel strike in both conditions. Interestingly, in the soundOn condition the beta rebound was not only higher when an interval was longer but it also decreased faster before the ipsilateral heel strike. Immediately after each ipsilateral heel strike the contralateral foot is lifted. This faster beta decrease may thus support faster lifting of the contralateral foot, which may help to shorten the next interval to stick with the rhythm. The increased modulation of beta power during long intervals may thus be an important contributor to the improved synchronization performance when auditory cues were provided. This resembles the increase in movement-related modulation of beta activity that can be observed after intake of antiparkinsonian medication, which generally enables patients to move faster (Doyle *et al.,* 2005; Androulidakis *et al.,* 2007). The possible significance of step-cycle-locked modulation of high-beta oscillations

is heightened by the fact that those patients, who found it harder to synchronize their steps to the rhythm given by the video even when auditory cues were provided, tended to have more severe clinical gait impairments, in line with past findings (Gilat *et al.*, 2013; Plotnik and Hausdorff, 2008). Moreover, just as auditory cues can improve gait (Arias and Cudeiro, 2010, 2008; Hausdorff et al., 2007; Mazilu et al., 2015), we found that they improved patients' ability to match their steps to the heel strikes in the video, which was associated with increased contralateral post-movement synchronization in the upper beta frequency band. This increase in average synchronization predominantly originated from an increased likelihood of individual bursts rather than a consistent increase in the degree of synchronization (i.e. amplitude) in all trials. Stronger modulation of activity across the whole beta band has also been associated with improved Parkinsonian motor symptoms before (Doyle et al., 2005).

What is the nature of the relationship between step-cycle-locked modulation of high-beta oscillations and performance?

Although stronger modulation of high-beta activity in the STN was associated with improved synchronisation of stepping to the rhythm given by the video, we cannot distinguish whether this was due to the fact that less affected patients had more physiological patterns of beta reactivity or if stronger beta modulation emerged as a more successful compensatory strategy. In patients suffering from freezing of gait, enhanced synchronization of >20 Hz oscillations was reported as prominent feature both at rest (Toledo *et al.*, 2014), and before and during freezing episodes (Scholten *et al.*, 2016; Shine *et al.*, 2014; Singh *et al.*, 2013, note that hypersynchronization was also observed in lower frequencies). This might be reconciled with our observation that stronger modulation of high-beta activity in the STN is associated with improved stepping performance, if as proposed for upper limb movements, exaggerated beta activity and lack of dynamic modulation of beta are correlates of motor impairment in Parkinson's disease (Androulidakis et al., 2007b). In short, strong synchronization in the beta band and limited task-related modulation of this have been proposed to

restrict local processing through rate coding and the dynamic configuration of neural assemblies on a finer spatio-temporal scale (Brittain and Brown, 2014). The inference from the present results is that this compromises local basal ganglia processing related to gait control.

We would like to acknowledge, though, that in this purely correlative study we cannot distinguish whether beta modulation is involved in the feed-forward control of gait, or more indirectly involved, as a response to gait-related sensory afference or feedback-related error processing. The latter may have contributed to the observed association between poor performance and low modulation as previous studies have shown that post-movement beta oscillations are less likely after erroneous movements (Tan *et al.*, 2014; Tan, Wade, *et al.*, 2016). Another possibility is that post-movement beta oscillations are less likely due to increased cognitive load (Fischer *et al.*, 2016) when patients with poor performance struggled to step on time with cues. Maximally occupied cognitive resources, irrespective of whether auditory cues were present, may also explain why in some patients, performance improved while beta modulation remained similar. The within-subjects correlation between increased beta and longer step interval durations similarly may merely reflect delayed movement onset (Kühn et al., 2004) or an active role in interval timing as reported before (Kononowicz and van Rijn, 2015).

Study limitations

One limitation of this study is that we investigated stepping in place during sitting and not upright walking, which may include arm swing. However, freezing episodes can also be observed during stepping in place (Nantel et al., 2011), which suggests overlap between neuronal control of stepping in place and gait, although no distinct freezing episodes were observed in our study. Stepping on a foot pedal has also been used as a task for fMRI studies to investigate gait-related network dysfunctions in Parkinson's disease (Gilat et al., 2017; Shine et al., 2013a, 2013b). Ultimately, it remains to be tested if STN power during real walking is modulated as it was during stepping in

place. Yet, the positive effect of auditory cueing on both gait and stepping in place in the current paradigm supports the validity of the latter as a safe surrogate for gait while ensuring that activity changes reflect leg movements and not arm swing.

Implications for DBS

The present results suggest a link between rhythmic stepping performance and modulation of high-beta oscillations. The clear step-locked modulation pattern and its amplification with auditory cues raise the possibility that patients with gait problems may benefit from temporally patterned left-right alternating DBS more than from continuous, uniform stimulation that would attenuate beta activity throughout the whole gait cycle. Instead, beta oscillations could be permitted at those points in the cycle at which they would naturally occur by briefly deactivating DBS to assist beta modulation, similar to the way in which auditory cues seemed to redistribute beta bursts during stepping. Entrainment of motor cortical beta to auditory cues has only recently been shown to be impaired in Parkinson's disease (te Woerd et al., 2017) and thus the benefit from auditory cueing alone will be limited. The hope is that alternating DBS patterns may provide a means to alleviate gait disturbances in those patients with impairments that are refractory to conventional DBS.

3.5 Summarized findings

The main findings of this chapter are:

- 20-30 Hz STN beta activity decreases and increases relative to the contralateral step cycle
- The beta increase after the heel strike is enhanced when auditory cues are provided and when steps are better synchronized to the cues
- Stimulating with an alternating DBS pattern, which provides a rhythmic structure and allows beta to increase briefly, may be beneficial for gait control

4 Sensorimotor synchronization and stopping in healthy participants

4.1 Introduction

Growing evidence associates elevated beta power in motor regions of the cerebral cortex and the basal ganglia with reinforcement of the current motor state (Engel and Fries, 2010). Relatively high post-movement beta activity has been linked to increased confidence in the internal model underlying an action (Tan et al., 2014a, 2014b, Tan et al. 2016). It was also suggested that when beta power was relatively reduced after performance errors, this may reflect subsequent behavioural adaptation as it was followed by increased reaction times on the next trial (Jha et al., 2015).

If repetitive actions need to be timed to external events, they need to be constantly evaluated. Tapping to a metronome involves repetitive actions that require the subject to generate an action plan, monitor its timing based on incoming sensory information and adapt it to what the task requires. Again, this presents a trade-off between maintaining the current motor program and adjusting to the environment. We hypothesized that when the action plan does not need to be adjusted, i.e. when confidence in performing an action timely and appropriately is high, beta power between two consecutive movements increases more strongly than when the motor plan needs to be adapted. This would also be in line with the beta modulation increase during auditory cueing reported in the previous chapter.

Elevated post-movement beta oscillations now may either reflect action reinforcement, which should thus make it harder to adjust the upcoming action to unpredictable events, or sparing of cognitive resources, which should result in faster reaction times.

To test this, we selected auditory-paced rhythmic finger tapping as primary motor task, and determined how motor performance was affected in anticipation of, and in response to, a second instruction, which was to abruptly stop tapping. We hypothesized

that movement-related beta modulation would grow with the first few taps in each trial as an internal model of the task develops. Conversely, if this modulation indeed reflects the degree of confidence in repeating the same movement, it should be reduced when subjects are preparing themselves to stop the movement abruptly.

We deliberately selected the timing of the stop signal such that abrupt stopping would be challenging. As the timing of auditory-paced finger tapping crucially seems to depend on posterior parietal cortex activity (Krause et al., 2014, 2012), beta modulation within this region was of particular interest. Finally, in Go/NoGo tasks and stopping paradigms, elevated beta in the STN, inferior frontal cortex and pre-SMA has been linked to successful suppression of upcoming movements. (Jha et al., 2015; Kühn et al., 2004; Swann et al., 2009, 2012) If beta oscillations are indeed relevant for motor inhibition, we would expect to find increased beta power during successful stopping in the tapping task.

4.2 Materials and methods

4.2.1 Participants

We recorded 21 healthy right-handed participants after obtaining informed written consent. Right-handedness was evaluated with the Edinburgh handedness inventory (Oldfield, 1971). Three subjects were excluded because of low tap-to-sound synchronization accuracy, defined as more than 20% of their taps being not within 200ms of the corresponding sound. One subject had to be excluded because of technical problems with the stop signal delivery time resulting in n=17. The participants analysed were aged between 18-38 years (median 26 ± IQR 13 years). Nine participants were female, eight were male.

4.2.2 Task

We investigated EEG oscillations during regular rhythmic tapping and abrupt stopping with the right index finger, which was guided by an isochronous metronome (700ms inter-sound interval, 700 Hz pitch, 40ms duration).

Participants were instructed to tap synchronously to a metronome sound and to start tapping immediately after hearing the first sound. They were asked to make only brief contact with the pressure pad serving as tapping surface and otherwise keep the finger lifted. Additionally, they were encouraged to settle on a movement pattern that was comfortable and to keep the movement amplitude and force the same throughout the whole duration of the experiment. The tapping hand was hidden under an opaque cardboard box to avoid visual processing of the movement. Each participant performed the task in two conditions: 1) the STOP-condition and 2) the CONTINUE-condition (*Figure 4.1*). In the STOP-condition, subjects had to resist making one last tap as soon as they heard the stop signal.

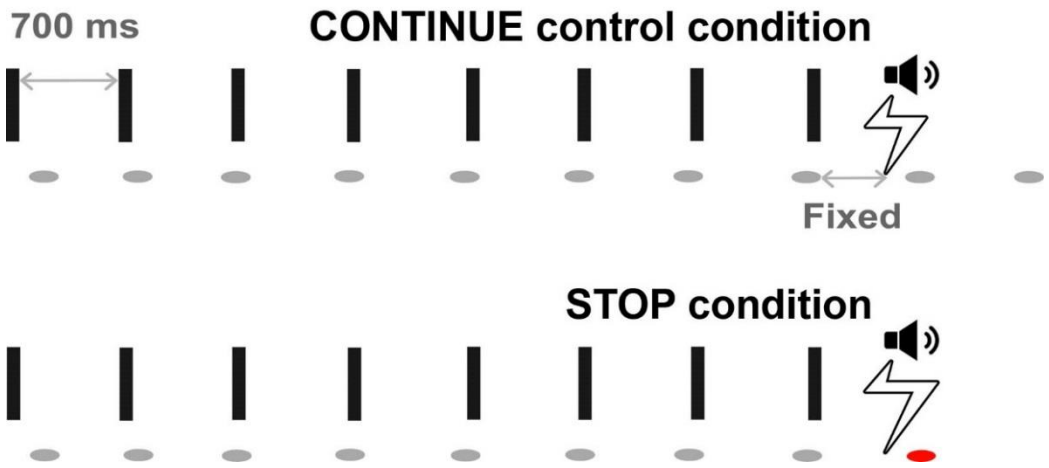

Figure 4.1 Schematic of the CONTINUE and STOP condition in the upper and lower row respectively. Black rectangles depict metronome sound cues, grey ellipses represent taps. The bolt indicates the stop signal, a sound higher in pitch than the regular tones that was delivered at an individually fixed delay relative to the previous last regular tap. The red rightmost ellipse in the lower panel would represent an unsuccessfully inhibited tap.

In the CONTINUE-condition, participants were asked to continue with two more taps after an auditory cue that was identical to the stop signal. The CONTINUE-condition was designed to examine the response to the stop signal without sudden movement inhibition, and therefore did not demand the same level of cognitive control, i.e. alertness or enhanced readiness to stop, as in the STOP-condition. The stop signal was a higher pitched tone (2000 Hz pitch, 40ms duration) delivered after a random number of 6-10 metronome cues. Thus, subjects had to stop after 6-10 taps. The minimum number of 6 sounds was chosen to establish regular cyclic tapping before stopping. Stopping was classified online as successful when the pressure sensor positioned below the finger was not touched.

The subject-specific stop signal delay time was determined in an initial training period (20-50 trials) for each participant so that successful interruption of the planned tap would occur in 50-60% of all trials. A success rate that was slightly higher than 50% was favoured to allow for more observations of halfway interrupted taps providing a graded response for subsequent correlative analyses (see *Figure* 4.2). For some participants, performance was more variable, while the time on the task was restricted to about an hour. The actual mean success rate was 58 ± 9% (range=35-69%). The selected subject-specific stop signal delay time was kept constant throughout the subsequent experimental session of at least 100 trials and ranged between 500-565ms for different participants (544 ± 19ms). Importantly, in each trial the stop signal was triggered relative to the tap registered by the pressure sensor upon contact (i.e. surpassing a threshold low enough to register each tap), and not to the sound. This was to prevent participants from delaying their taps to achieve a better performance. After each block of 10 trials, participants received feedback about the number of successful stops.

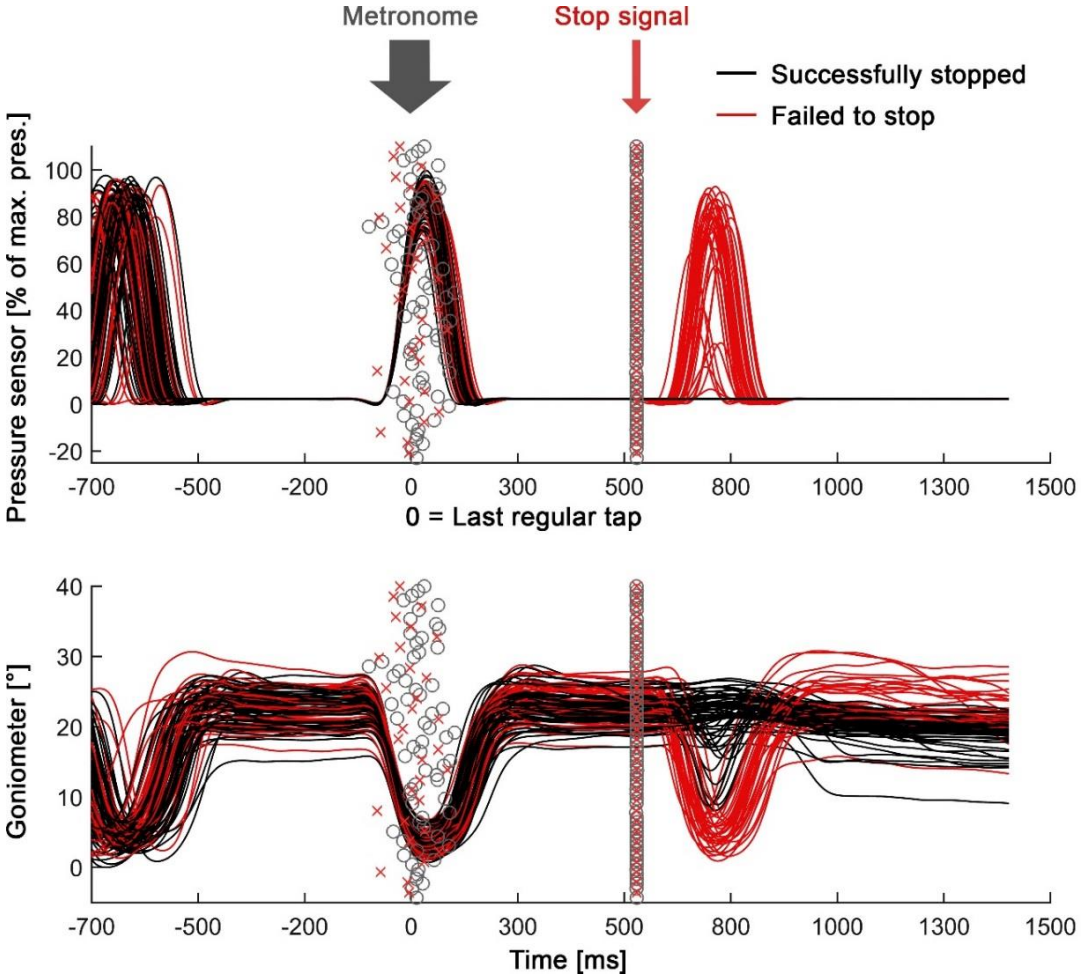

Figure 4.2 Behavioural data from the first subject. The upper panel shows pressure sensor data. The stop signal was delivered relative to the time of the finger touching the sensor when the pressure signal passed a threshold (time=0ms). For this subject, the stop signal delay time was 550ms relative to 0ms, marking the last regular tap. Black lines are trials where the tapping movement after the stop signal was successfully interrupted, red lines are trials where the tap was not inhibited before touching the sensor. The markers around 0ms represent the temporal offset between the sound and the tap (o = stopped, x = failed to stop). The markers o and x are overlapping rather than separated showing that random fluctuations of the tap-to-sound offset were not crucial in determining stopping performance. The lower panel displays the extent of finger flexion as recorded by the goniometer. Note that successfully stopped trials frequently contained downward movement of the finger, which was interrupted timely enough to stop touching of the sensor stopping.

Both tasks were practised for at least 10 trials prior to the recording. To help control for slow drifts in performance and EEG measures over time, we recorded the conditions in blocks of 10 trials in the following order:

2 blocks (=20 trials) CONTINUE – 10 blocks (=100 trials) STOP – 3 blocks (=30 trials) CONTINUE

The very first CONTINUE block after the STOP blocks was discarded to avoid inclusion of data confounded by conflict, which some subjects might have experienced for a few trials after being trained to stop. Participants were allowed to take breaks in between blocks of 10 consecutive trials whenever they required one. We recorded substantially more trials in the STOP condition to make sure we had enough trials with both successful and unsuccessful stops after discarding irregularly timed taps. Additionally, if time allowed, a few more trials were recorded to make up for trials containing artefacts or tapping irregularities. The experiment was programmed in Spike 2 (Cambridge Electronic Design) and the auditory cues were delivered via speakers (Creative Inspire T10) at a volume such that the sounds were clearly audible but not perceived as uncomfortable.

4.2.3 Data acquisition

23 EEG channels positioned according to the 10-20 system with additional linked earlobes were recorded and referenced to a common average. *Electro-oculogram* (EOG), and three more channels at fronto-central locations (FCz, FC3, FC4) were additionally recorded. Behavioural data were collected with a goniometer (TMSi Goniometer F35, 1D) attached to the index finger over the metacarpophalangeal joint to measure the degree of finger flexion, and a force sensitive resistor to register the timing upon finger contact with the tapping surface.

4.2.4 Behavioural data pre-processing

Tap-to-sound offset was calculated for each individual tap as the difference between the timing of the metronome sound and the timing of tap pressure onset. Taps with an absolute tap-to-sound offset larger than 150ms were excluded to discard taps that were not performed accurately on time with the metronome considering that an offset of 150ms would exceed three times the average expected negative mean asynchrony in non-musicians (Krause et al., 2010). Furthermore, offsets smaller than 150ms are shorter than usual reaction times and thus may still be considered anticipatory (Mates et al., 1992). Any further behavioural outliers (such as spurious goniometer deflexion) prior to the stop signal were removed following visual inspection. On average 12 ± 10% of all attempted stops and 26 ± 3% of all regular taps were excluded. The goniometer traces and tap-to-sound offset distributions were similar and strongly overlapping in successfully stopped vs. unsuccessfully inhibited taps (Figure 4.2).

Note that successfully stopped trials frequently contained downward movement of the finger, which was interrupted in time before touching the pressure sensor. This graded performance was captured by a measure we call *movement extent*. The measure was computed by normalizing the extent of the downward movement by the amplitude of the upward movement done before. Thus, it does not reflect the absolute amount of downward movement but constitutes the relative amount as fraction of the height of the preceding finger lift. 0% movement extent would be a full stop, whereas 50% refers to a movement that was interrupted halfway on the way down. Failure to stop would be captured by a *movement extent* of 100%.

4.2.5 EEG pre-processing

Time-frequency spectrograms were computed on the continuous data by filtering the data into 3 Hz-wide frequency bands around centre frequencies shifted by 1 Hz ranging from 3 to 30 Hz (Butterworth, filter order=6, two-pass, using the Fieldtrip toolbox (Oostenveld et al., 2011) functions *ft_preproc_lowpassfilter* and *ft_preproc_highpassfilter)* and calculating the power of the Hilbert transform.

4.2.6 EEG processing

4.2.6.1 Evolving reactivity

In each trial, participants performed 6-10 continuous taps. To investigate how power modulation changed over time within a trial, we subdivided taps into early (tap number 2-3), middle (3-4) and late (>5, excluding taps directly followed by a stop signal) taps within each trial. Behavioural analyses suggested that tapping became more anticipative as the series of taps evolved and that this was more marked in the CONTINUE condition than the STOP condition. Accordingly, we sought progressive changes in the EEG during the tapping series, and differences between these in the two conditions, which might shed light on the neural processes underpinning the behavioural observations.

To assess how modulation evolved in the low-beta (12-20 Hz) and high-beta (20-30 Hz) bands, we computed three-way (2x3x2) repeated measures ANOVAs on the power modulations. The three factors were task (STOP, CONTINUE), time (early, middle and late taps) and electrode location (C3, Pz). From the STOP condition, 201 early, 204 middle and 201 late taps were included on average per subject given that two taps were collated per trial for the early and middle taps whereas a variable number (depending on trial length) were collated for late taps. From the CONTINUE condition 84 early, 87 middle and 77 late taps were included.

Modulation of the respective band was quantified by computing first the overall power average in the individual channel (averaged first over all taps for each subject and then over subjects and the two conditions) to determine the time of the maximum and minimum overall power average (including all taps and subjects, averaged across both conditions). These were selected from within a 700ms time window that started -100ms relative to the tap onset to capture both the minimum around the tap onset as well as the peak of the subsequent increase.

Thus, time points denoting maxima and minima (indicated as arrows in *Figure 4.4*) were the same for all time windows in both conditions. In a second step, the difference between the means of activity over 100ms wide windows centered around these points was computed to obtain the modulation while accounting for small variabilities in peak timings across subjects. The difference was then normalized by the average power within this window.

4.2.6.2 EEG features preceding the stop signal and correlating with performance

To test for correlations in a time window preceding the stop signal, we aligned the EEG data to the onset of the last regular tap registered by the pressure sensor and examined a time window ranging from 150ms after the tap (disregarding most of the upward movement) to 500ms. The earliest stop signal delay time within our group was 500ms, hence the window was restricted to 500ms to avoid including reactive responses.

4.2.7 Statistical testing

To control for multiple comparisons of several behavioural variables we performed the false discovery rate (FDR) correction procedure, which controls the expected proportion of falsely rejected hypotheses (Benjamini and Hochberg, 1995).

To test in whether behavioural correlations were significantly different from zero on a group-level, correlation coefficients were Fisher's z transformed and underwent a one-sample t-test (n=17). Partial correlations were computed to control for movement properties when examining the relationship between EEG power and the movement extent. We controlled for each movement variable individually, as well as for two components obtained via principal component analysis (PCA) that explained most of the variance (see Results).

Before testing for differences in power, each time-frequency matrix was normalized for each subject by the average across all regular taps (excluding tap 1 and those followed

by a stop signal) to obtain a relative power change in percent. Effect sizes reported are calculated based on Cohen's d.

To evaluate statistical significance of mean power differences in time-frequency spectrograms, we used the same cluster-based permutation procedure as in the previous chapter.

We concentrated our analyses on electrodes overlying the contra- and ipsilateral motor cortices (C3, C4), pre-supplementary motor area (FCz) and right pre-frontal cortex (F8) because of the role of these regions in motor inhibition (Rae et al., 2015) and overlying the parietal cortex (Pz) due to its role in anticipatory motor control (Krause et al., 2014). Because we selected these regions according to prior knowledge, no additional multiple-comparison correction was performed beyond the cluster-based permutation procedure for each electrode.

4.3 Results

4.3.1 Behavioural results

We hypothesised that tapping would become more regular and anticipative as each short series of taps evolved and more so in the CONTINUE condition than the STOP condition, where sudden stopping was required and participants may have been more hesitant. First, we determined how tapping characteristics evolved over time on each trial, and whether these characteristics and their temporal evolution differed between the STOP and the CONTINUE condition (*Table 4.1*). Taps were split into early (tap number 2-3), middle (3-4) and late taps (>5, excluding taps directly followed by a stop signal). In both conditions, inter-tap intervals became more regular over time in each trial as indicated by a reduced disparity between two consecutive intertap intervals (ITI_diff).

Table 4.1 Differences in the temporal development from the early (2-3) to the late (>5) taps in the STOP and CONTINUE condition (mean±STD). Values in bold are significantly different between the STOP and CONTINUE condition after FDR correction. P-values are in brackets below the significant contrasts and were marked with an asterisk if Wilcoxon signed-rank tests were used. ITI_diff=difference between the post-tap and pre-tap inter-tap intervals (ms, positive values denoting longer post-tap inter-tap intervals), maxPrs=peak pressure during the tap, downTime=duration of finger contact with the pressure sensor, soundOffset=offset between sound and tap (negative values represent taps that occurred before the sound), peakVelDown=peak velocity of the downward movement of the previous tap, upMvmt=amount of up-movement, peakVelUp=peak velocity of the upward movement.

Variable	Tap Nr: 2-3	4-5	>5
STOP soundOffset	6.0 ±26.6	-46.2 ±31.0	**-45.9 ±32.3**
CONT soundOffset	3.6 ±32.2	-52.3 ±25.9	**-60.8 ±28.3**
P-value soundOffset			**(*P* = .008*)**
STOP downTime	**123.8 ±42.7**	**121.4 ±42.8**	**116.6 ±40.9**
CONT downTime	**141.1 ±57.0**	**140.8 ±57.8**	**137.7 ±54.7**
P-value downTime	**(*P* = .002)**	**(*P* = .002)**	**(*P* = .001*)**
STOP ITI_diff	83.9±14.3	9.9±6.5	0.7±4.3
CONT ITI_diff	73.2±21.7	10.3±9.8	-1.5±4.7
STOP maxPrs	59.9 ±14.7	57.4 ±15.0	58.2 ±14.4
CONT maxPrs	61.3 ±14.7	59.0 ±15.3	58.7 ±14.7
STOP peakVelDown	159.4 ±64.6	158.0 ±63.6	154.8 ±61.5
CONT peakVelDown	166.4 ±65.3	163.0 ±63.8	167.3 ±65.2
STOP upMvmt	15.0 ±6.7	14.4 ±6.5	14.4 ±6.4
CONT upMvmt	15.7 ±6.2	15.2 ±6.1	15.6 ±5.9
STOP peakVelUp	116.6 ±65.3	113.2 ±65.6	114.5 ±63.6
CONT peakVelUp	114.6 ±69.3	108.3 ±66.9	112.5 ±70.7

After the third tap, participants showed a tendency to tap slightly ahead of the sound (tap-to-sound offset), which is known as negative mean asynchrony and can be observed during stable sensorimotor synchronization (Repp and Su, 2013). Although tap-to-sound offsets were similar in the beginning of each trial in both conditions, the development of the negative mean asynchrony seemed to be more limited when participants anticipated to stop abruptly. This was particularly evident for late taps in the STOP condition when compared to the CONTINUE condition. A 3x2 repeated-measures ANOVA resulted in a significant main effect of time (Greenhouse-Geisser corrected $F_{2,\,32} = 81.0$, $\varepsilon = .56$, $P < .001$) and interaction between condition and time (Greenhouse-Geisser corrected $F_{2,\,32} = 5.2$, $\varepsilon = .64$, $P = .026$) but no significant main effect for condition ($F_{1,\,16} = 3.8$, $\varepsilon = 1.0$, $P = .070$).

These findings suggest that the development of anticipatory tapping was relatively compromised when participants expected stopping and particularly when expectancy of the stop signal was highest after the 5^{th} tap. In addition to this, the duration the pressure sensor was pressed was shorter (downTime) in the STOP condition than in the CONTINUE condition straight from the start of each trial. The significant interaction (Greenhouse-Geisser corrected $F_{2,\ 32} = 4.8$, $\varepsilon = .95$, $P = .017$) in a 3x2 ANOVA indicates that in addition to the main effect of condition ($F_{1,\ 16} = 15.0$, $\varepsilon = 1.0$, $P = .001$) and time (Greenhouse-Geisser corrected $F_{2,\ 32} = 5.0$, $\varepsilon = .80$, $P = .020$), the contact duration with the pressure sensor was shortened even more in the STOP condition.

Second, within the STOP condition, we sought evidence to support the hypothesis that stopping success would be partly dependent on the confidence in the internal model of the synchronization task.

We thus examined the relationship between the movement parameters of the preceding tap and stopping success, and quantifyied this via rank correlation coefficients (*Table 4.2*). If the last regular tap was performed relatively early with respect to the metronome sound instead of lagging behind, stopping was more successful (soundOffset, $P < .001$, 12 of 17 subjects significant). This relationship is visible in the scatter plot showing all participants indivdiaully in *Figure 4.3*. If the last tap was relatively vigorous (maxPres, $P < .001$), and the duration of contact with the pressure sensor was relatively long (downTime, $P = .001$), then stopping was also more successful. Note though, that a significant relationship with maxPres or downTime was only present in 5 of the 17 subjects in total. In most participants, the sign of the correlation was negative, hence the significant group level results. But compared to the 12 of 17 significant correlations with the soundOffset, the relationship between tapping vigour and movement extent was clearly weaker.

Table 4.2 Correlations between movement parameters of the last regular tap and the movement extent after the stop signal (mean±SD). Values in bold are FDR-corrected significant based on one-sample t-tests of the Fisher's z-transformed intra-individual correlation coefficients of the 17 subjects. tapNr=number of taps preceding delivery of the stop signal. The remaining variable names are the same as in Table 4.1.

Variable	Rho ±SD	p-value	Nr. of sub <.05
soundOffset	**0.29 ±0.13**	**<0.001**	12
downTime	**-0.10 ±0.11**	**0.001**	4
maxPres	**-0.10 ±0.09**	**<0.001**	1
tapNr	**-0.11 ±0.16**	**0.012**	5
peakVelDown	0.04 ±0.12	0.238	3
upMvmt	**0.08 ±0.11**	**0.013**	3
peakVelUp	**0.07 ±0.11**	**0.020**	2

The more taps participants performed prior to presentation of the stop signal, i.e. the later it was delivered in a series, the easier it was for subjects to stop (tapNr, $P = .012$, 5 of 17 subjects individually significant) consistent with growing expectancy of the stop signal. Prior to successful stopping, the movement also seemed to be smaller (upMvmt, $P = .013$, 3 of 17 subjects individually significant), which translated to slower speed (peakVelUp, $P = .020$, 2 of 17 subjects individually significant). In summary, the strongest predictor of successful stopping was an increased tap-to-sound offset, i.e. relatively early timing, of the last regular tap.

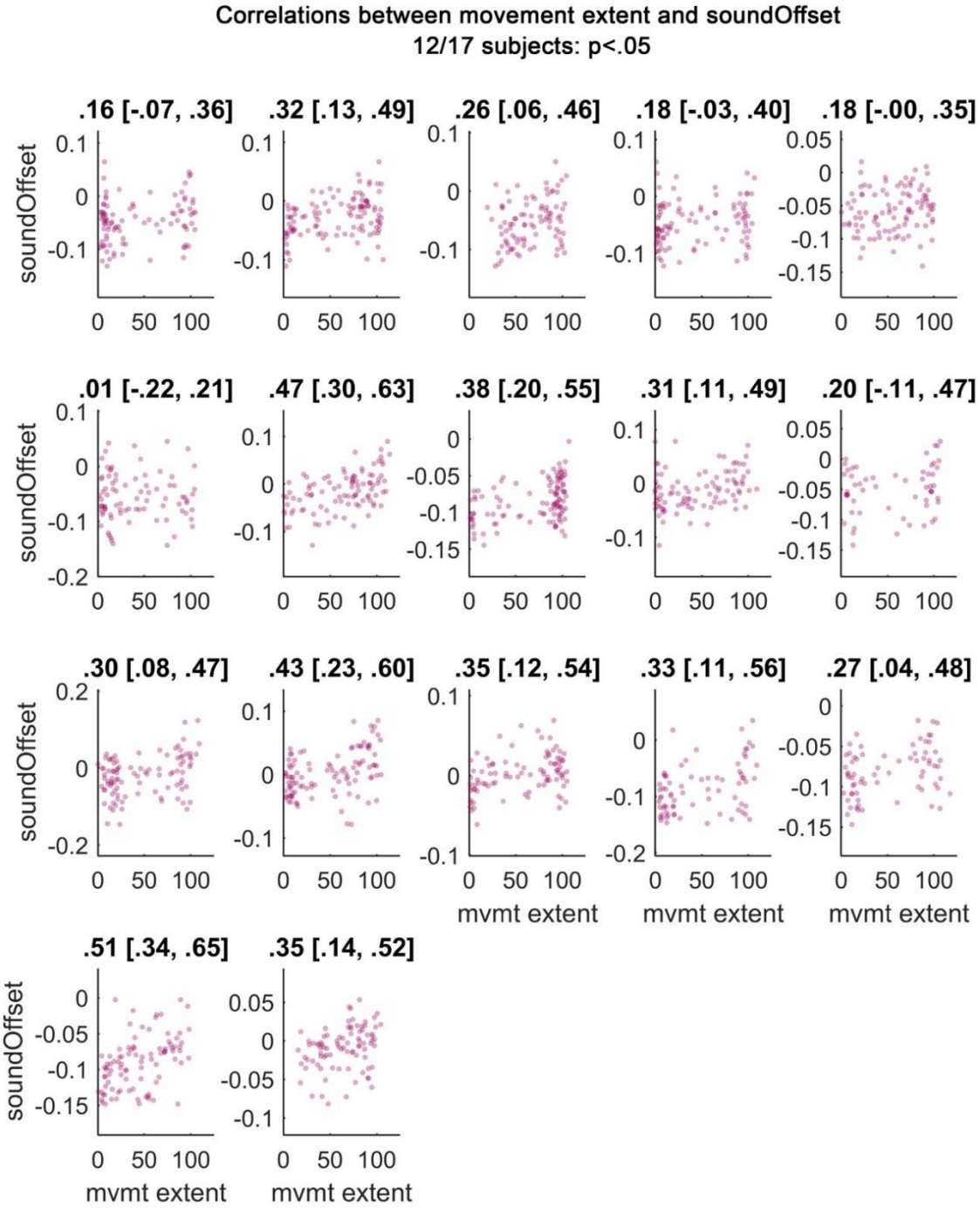

Figure 4.3 Scatter plot of correlations between movement extent (x-axis) and tap-to-sound offset (y-axis).Subplots show individual participants. Plot titles denote Spearman's rho followed by its 95% bootstrapped confidence interval. Participants were less likely to stop when the last regular tap was relatively late with respect to the metronome sound. 12 of 17 subjects had significant correlations.

4.3.2 EEG

Power modulation within a tap-cycle occurred predominantly in theta and high-beta frequencies (

Figure 4.5A). After the tap (at 0ms), power increased first in the theta band. 20-30 Hz beta activity decreased after the tap onset and then peaked right in the middle between two consecutive taps and was most strongly modulated in electrodes overlying the contralateral motor cortex (C3) and preSMA (FCz). High-beta modulation was less pronounced over parietal cortex (Pz). For subsequent quantitative analyses of spectral changes we therefore selected C3 and Pz as representatives of these two patterns of EEG response.

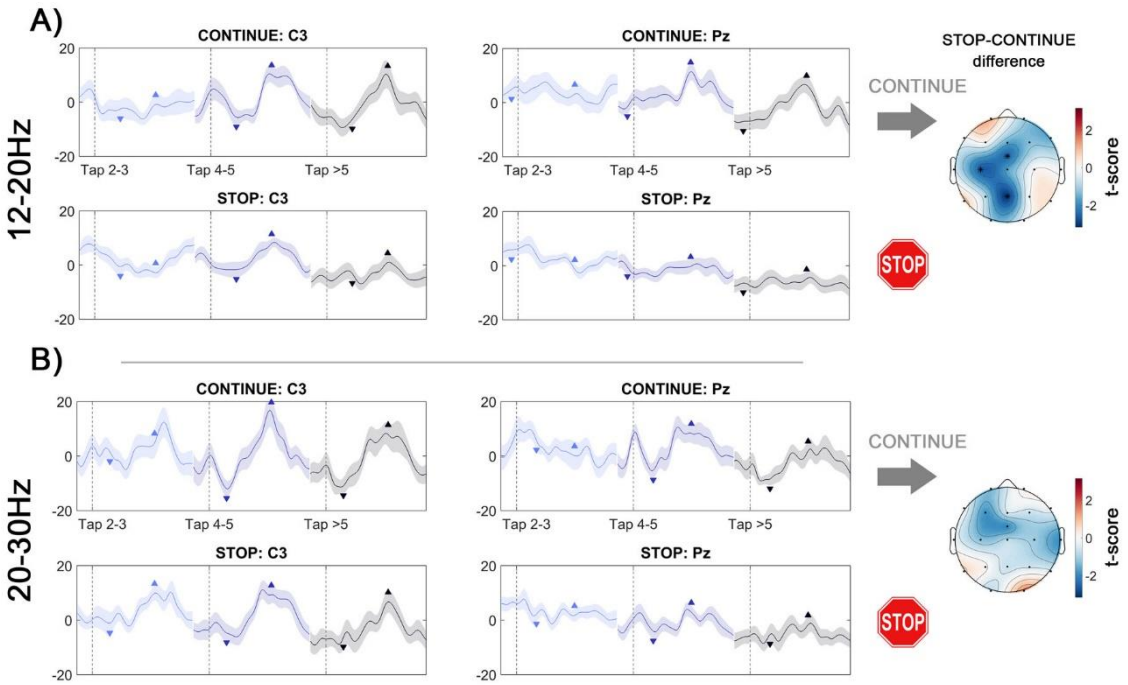

Figure 4.4 Temporal development of the % change in A) 12-20Hz and B) 20-30Hz power. The left and right column depict modulation in the electrodes C3 and Pz, respectively. Data are aligned to taps as denoted in the legend showing one tap-cycle within a -100:600ms window. The left, middle and right traces depict early (2-3), middle (3-4) and late (>5) taps, respectively. Downward arrows denote the location of the average power trough, and upward arrows denote the location of the average power peak, which was used to compute the modulation. In A) the 12-20 Hz modulation developed in the CONTINUE condition (upper row) after the third tap both in C3 and Pz. In the STOP condition, modulation was strongly attenuated, particularly in Pz. In B) the average 20-30Hz modulation was again stronger in C3 than in Pz, and modulation increased after the third tap. Topoplots to the right show the

distribution of negative t-scores of the condition differences in modulation, which were significant in Pz, C3 and FCz for the low-beta band.

4.3.3 EEG results: Evolving reactivity

4.3.3.1 Low-beta power

The ANOVA with low-beta power as dependent variable (*Figure 4.4*) resulted in two significant main effects of time ($F_{2, 32} = 14.2$, $\varepsilon = .95$, $P < .001$) and condition ($F_{1, 16} = 10.7$, $\varepsilon = 1.0$, $P = .005$, mean $_{\text{CONTINUE}}$ =7.8, mean $_{\text{STOP}}$ =1.2): the average modulation increased steeply from early taps to taps 4-5 (mean $_{\text{early}}$ = -2.5, mean $_{\text{middle}}$ = 8.0, mean $_{\text{late}}$ = 8.0; $P_{\text{early vs. middle}} < .001$, $P_{\text{early vs. late}} = .001$, $P_{\text{middle vs. late}} = .993$). *Figure 4.4A* shows how the 12-20 Hz modulation developed in the CONTINUE condition after the third tap both in C3 and Pz. In the STOP condition, however, modulation seemed to be attenuated in C3 and even more so in Pz, although it should be noted that we did not find a significant main effect of electrode location ($F_{1, 16} = 2.0$, $\varepsilon = 1.0$, $P = .173$) nor significant interactions ($P_{\text{loc*cond}} = .349$, $P_{\text{loc*time}} = .432$, $P_{\text{cond*time}} = .507$, $P_{\text{loc*cond*time}} = .954$).

To explore the validity of the comparison between the STOP and CONTINUE condition, we performed two additional control analyses. First, we verified that neither tap-to-sound offsets nor low-beta modulation differed between the first and second block of the CONTINUE condition. We performed three separate 3x2 ANOVAs with tap-to-sound offsets, downTime and low-beta modulation as dependent variables and the two factors time (early, middle and late taps) and recording block (block 1 vs. 2). The ANOVA with soundOffset as dependent variable resulted only in a significant main effect of time (Greenhouse-Geisser corrected $F_{2, 32} = 66.0$, $\varepsilon = .55$, $P < .001$) but no significant main effect of block ($F_{1, 16} = 0.3$, $\varepsilon = 1.0$, $P = .614$) or interaction (Greenhouse-Geisser corrected $F_{2, 32} = 2.7$, $\varepsilon = 0.67$, $P = .107$). The ANOVA with downTime as dependent variable showed no significant effects (time: Greenhouse-Geisser corrected $F_{2, 32} = 0.6$, $\varepsilon = .61$, $P = .491$; block: $F_{1, 16} = 0.2$, $\varepsilon = 1.0$, $P = .698$; time*block: Greenhouse-Geisser corrected $F_{2, 32} = 0.1$, $\varepsilon = .68$, $P = .800$). Hence blocks in the CONTINUE condition did not differ.

The ANOVA with low-beta modulation as dependent variable resulted again only in a significant main effect of time ($F_{2, 32} = 7.7$, $\varepsilon = .91$, $P = .002$, mean $_{early}$ = -0.9, mean $_{middle}$ = 11.2, mean $_{late}$ = 13.4) but not block number ($F_{1, 16} = 0.4$, $\varepsilon = 1.0$, $P = .560$, mean $_{BLOCK1}$ =7.1, mean $_{BLOCK2}$ =8.8). Hence neither tap-to-sound offsets nor low-beta modulation differed between the first and second block of the CONTINUE condition.

Second, we made sure that the condition difference did not result from a different number of trials. To this end, trials from the two conditions were matched in number by selecting a reduced subset of trials from the middle of the STOP condition, discarding the same amount of data at the beginning and end of each participant's recording block. The two main effects found in the original ANOVA containing all trials were again significant (condition: $F_{1, 16} = 7.0$, $\varepsilon = 1.0$, $P = .017$, mean $_{CONTINUE}$ =7.6, mean $_{STOP}$ = 0.4; time: $F_{2, 32} = 7.7$, $\varepsilon = .86$, $P = .003$, mean $_{early}$ = -2.6, mean $_{middle}$ = 7.3, mean $_{late}$ = 7.2).

4.3.3.2 High-beta power

The ANOVA with 20-30 Hz power as dependent variable (*Figure 4.4B*) resulted in two significant main effects of electrode location ($F_{1, 16} = 8.7$, $\varepsilon = 1.0$, $P = .009$) and time ($F_{2, 32} = 17.5$, $\varepsilon = .98$, $P < .001$). Power over C3 was more strongly modulated than over Pz (mean $_{C3}$ = 13.1, mean $_{Pz}$ = 4.0), and modulation was again established more strongly after the third tap (mean $_{early}$ = 1.8, mean $_{middle}$ = 13.1, mean $_{late}$ = 10.7; $P_{early\ vs.\ middle} < .001$, $P_{early\ vs.\ late} < .001$, $P_{middle\ vs.\ late} = .286$).

To evaluate whether the condition difference is specific to the low-beta band, we performed the same ANOVA for 8-12 Hz alpha modulation, and found no significant main effects ($P_{channel} = .173$, $P_{condition} = .219$, $P_{time} = .719$) or interactions ($P_{chan*condition} = .337$, $P_{channel*time} = .538$, $P_{condition*time} = .521$, $P_{channel*condition*time} = .450$).

In summary, movement-related modulation in both low-beta and high-beta frequency ranges increased in C3 and Pz with the number of taps. We only observed condition differences in the low-beta band, showing that modulation of low-beta power was reduced in the STOP condition, where participants had to be prepared to interrupt their movement quickly and the tap-to-sound offset was smaller.

4.3.4 EEG results: Features preceding the stop signal and correlating with performance

Our behavioural results raised the possibility that stopping success was partly dependent on the timing of the last regular tap relative to the metronome and in some also on tapping vigour. Our EEG findings suggest that the gradual increase in low-beta modulation might be a candidate marker for the neural processes underpinning the development of stable sensorimotor synchronization. Importantly, low-beta modulation was reduced in the STOP condition when participants could not be confident that they would hold on to the current motor plan for the next tap. If low-beta modulation indeed reflects confidence in the current action plan, we would expect it to be higher after taps that were more similar to the CONTINUE condition, i.e. with a relatively high tap-to-sound offset and downTime, and thus also higher before successful stopping.

First, we computed power differences and tested for significance via cluster-based permutation testing (

Figure 4.5B). The data were subdivided into successful and unsuccessful stops. To select a principled cut-off for this division, we iteratively varied the threshold of movement extent for definition of trial outcome following the stop signal. Splitting the data with a range of movement extent thresholds from 36-48% consistently yielded significant clusters in both Pz and C3. Accordingly, we selected a movement threshold of 40% to discriminate successful and unsuccessful stops for further analysis, in the knowledge that the results would be similar had we chosen a threshold from 36-48% of movement extent. The mean difference was strongest in Pz (

Figure 4.5B+C, t_{16}=3.3, $diff_{avgPeak}$ = 23.1% at 330ms, 15Hz, effect size = 1.1, P = .004), whereas the highest t-score was found in C3 (t_{16}=4.1, $diff_{avgPeak}$ = 21.2% at 375ms,

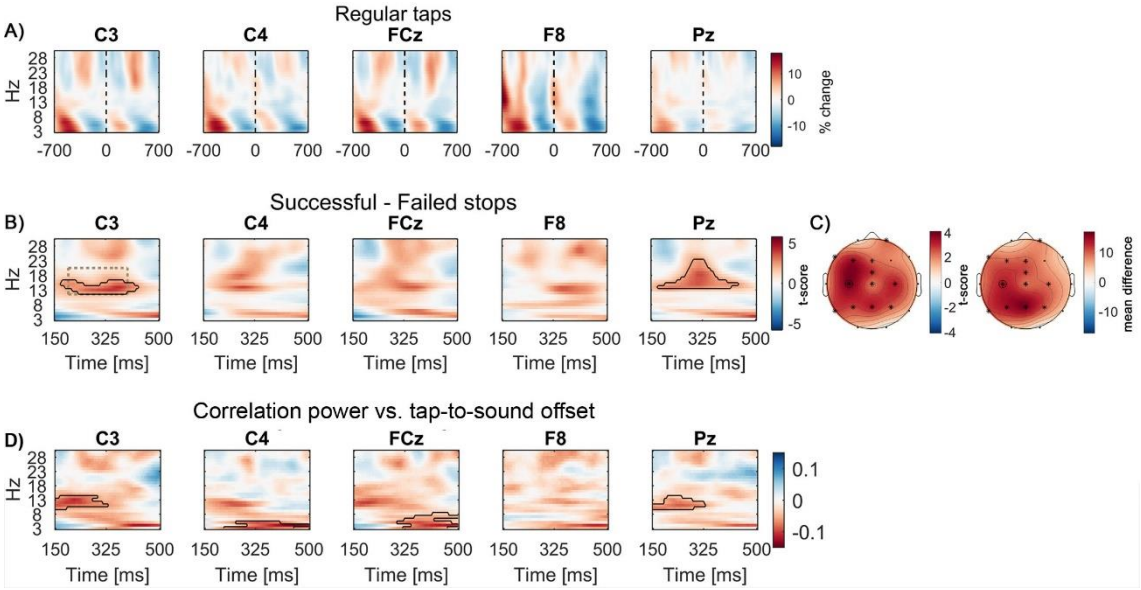

Figure 4.5 EEG preceding the stop signal. A) Power aligned to regular taps (time=0) in the STOP condition. The black dashed line denotes the finger contact with the pressure sensor. Power was z-transformed for each frequency within the time window displayed before being averaged across subjects for better visual display. B) T-scores of power differences between successful and failed stops prior to the stop signal. Clusters surrounded by black outlines denote that power was significantly higher when participants interrupted their movement more successfully (movement extent threshold<40%). C) Topoplots show the distribution of t-scores and mean differences. In locations marked with a star, 12-20Hz beta was significantly higher prior to successful stops averaged within the window outlined by the dashed rectangle in B) in C3. The channel location of C3 in the topoplots is highlighted with a black circle surrounding the star. D) Correlation between power and the tap-to-sound offset. 10-15 Hz power was higher in C3 and Pz when tap-to-sound offsets were more negative (i.e. earlier).

14Hz, effect size = 1.3, P = .001), which was due to a larger between-subjects variability in Pz (*Figure 4.6B*).

Importantly, this power difference preceded the stop signal. Aligning the low-beta band power average to the stop signal showed that the significant difference in C3 and Pz had in fact already ended about 100ms before the stop signal (*Figure 4.6A*). To see if a similar difference is present when the split threshold was not fixed to 40% movement extent, we also split the data into two clusters (one close to 0 and one close to 100% movement extent) detected by a k-means clustering algorithm. *Supplementary*

Figure A.1 shows that the difference in C3 is still significant but that the difference in

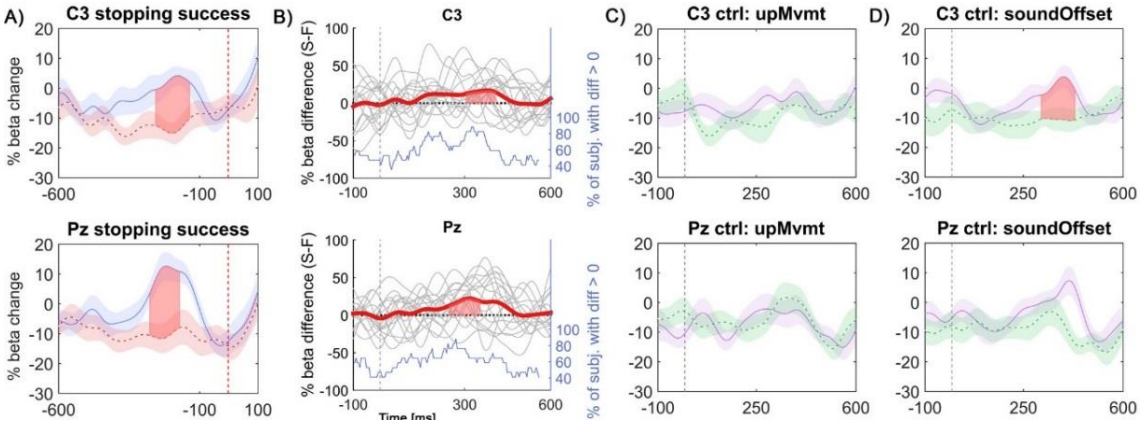

Figure 4.6 A): 12-20 Hz beta power time course preceding the stop signal (vertical dashed line). Data were subdivided according to stopping performance (movement extent <40%: solid curve; >40%: dashed curve). B) Time courses of individual differences between the power of successful and unsuccessful stops subdivided as in A). Data are aligned to the last regular tap (vertical dashed line) preceding the stop signal. The bold line denotes the mean difference. The bottom stepped line shows for each point in time the fraction of participants who had higher beta power prior to successful stops. C) Data are aligned to the last regular tap and median split according to the amount of upward movement upMvmt (smaller upMvmt = solid curve; bigger upMvmt = dashed curve). D) Data are aligned to the last regular tap and median split according to soundOffset (more anticipatory soundOffset = solid curve; delayed soundOffset = dashed curve). Filled areas between lines indicate significant differences, which were cluster-based multiple comparison corrected. Shaded error bars around curves denote standard errors. Note that successful stopping was associated with a pattern of beta power modulation that was more similar to the regular tapping beta profile in the CONTINUE condition (compare with the right-hand upper panel for Taps > 5 in Figure 4.4A).

Pz does not survive the multiple comparison correction procedure. Furthermore, although differences in power occurred around the time when the finger was held still between taps, power differences in Pz and C3 disappeared when trials were subdivided according to the median extent of finger upward movement (*Figure 4.6C*).

Subdividing the data according to the median tap-to-sound offset resulted in a significant difference that survived multiple-comparison correction in C3 but not Pz and resembled the power difference related to stopping performance (*Figure 4.6D*).

In a next step, we investigated how many of the recorded subjects presented a significant correlation between stopping performance and power at any frequency in the beta band (12-30 Hz) in a 200-500ms time window after the last regular tap. 16 of 17

participants showed a significant correlation between activity in the beta band in C3 and movement extent (*Figure 4.7*). This was reduced to 10 of 17 participants after controlling for tapping parameters by performing partial correlations. Partial correlations were performed because several movement parameters also correlated with stopping performance *Table 4.2*). To reduce the seven potentially related movement variables to two components accounting for most of the variance, we conducted a principal component analysis. The first two components accounted for on average 40 and 22% of the variance, respectively. Scatter plots for Pz were similar to those from C3, with 14 significant correlations (9 when computing partial correlations).

Although we controlled for the variability in tap-to-sound offset with the partial correlation, we were additionally interested if the tap-to-sound offset of the last regular tap also affected subsequent beta power. This should be the case if beta oscillations reflect processing of the tap timing.

Figure 4.5D shows the correlation between power and the tap-to-sound offset and suggests that this was the case. 10-15 Hz power was higher in C3 and Pz when tap-to-sound offsets were more negative (i.e. earlier). A similar relationship was also seen for lower frequencies over C4 and FCz.

Taken together, when post-movement beta power was relatively high, stopping was more successful. Beta power also seemed to be modulated by the previous tap-to-sound offset, which correlated with stopping as well.

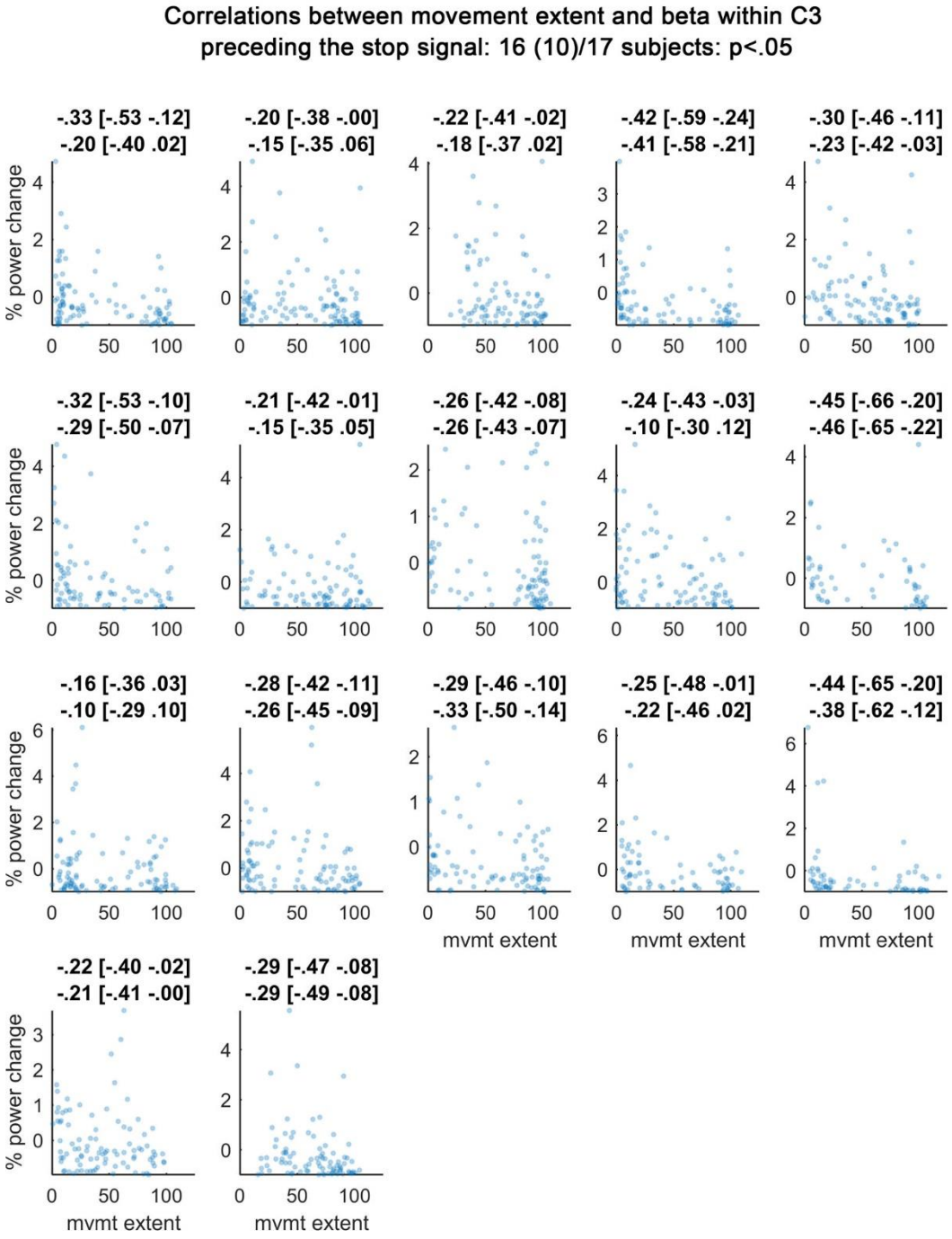

Figure 4.7 Scatter plot of correlations between movement extent (x-axis) and beta relative to baseline (y-axis). Subplots show individual participants. For each participant, beta power yielding the maximum correlation (detected anywhere between 12-30 Hz and 200-500ms after the last regular tap considering that optimal frequencies and time points may differ across subjects) is shown. Plot titles denote Spearman's rho followed by its 95% bootstrapped confidence interval. The second line denotes the correlation coefficient resulting from the partial correlation controlling for the first two components obtained by principal component analysis of the behavioural variables. 16 of 17 subjects (10 if partial correlations were considered) had significant correlations.

4.3.5 EEG features that follow the stop signal and are linked to stopping performance

Finally, we asked if beta also was higher after the stop signal when the movement was inhibited. Immediately after the stop signal, power increased significantly in low frequencies (*Figure 4.8A*) as observed in classical stop signal reaction time tasks (Huster et al., 2013). In the STOP condition, the largest increase was observed in FCz (t_{16} = 8.3, $diff_{avgPeak}$ = 428.3% at 240ms, 3Hz, effect size = 2.7, $P < .001$). All but one subject displayed a significant power increase, thus this increase was highly consistent (*Figure 4.8D*). Around 350ms after the stop signal, parietal beta was lower than in the aftermath of the tap before (t_{16} = -3.7, $diff_{avgPeak}$ = -19.9% at 365ms, 19Hz, effect size = -1.1, $P = .002$).

Both effects were also present in the first block of the CONTINUE condition (*Figure 4.8B*) even though no immediate movement interruption was required or had been performed before. This power increase thus seemed to be linked to the processing of the salient stop signal rather than to actual motor inhibition. The reduced colour intensity in *Figure 4.8B* compared to *A* suggests that the low-frequency increase was smaller when tapping was continued than when it had to be stopped.

In a next step, we compared whether power differed between successful and unsuccessful stops (*Figure 4.8C*). When stopping was more successful, the low-frequency power increase after the stop signal was significantly stronger than when it failed. The peak increase was strongest in FCz (t_{16} = -4.9, $diff_{avgPeak}$ = 166.5% at 225ms, 3Hz, effect size = 0.7, $P < .001$), yet when the average within 0-200ms and 3-8 Hz was computed, the topoplot showed clear lateralization with a stronger power increase over contralateral motor cortex (*Figure 4.8C*). Correlations between movement extent and power within a 3-8Hz and 0-200ms time window after the stop signal were significant in 14 of 17 subjects (12 of 17 when computing partial correlations).

Taken together, following the stop signal only low-frequency, and not beta power, was associated with improved stopping ability. As it was higher in the STOP condition and during successful stops, this increase may have been modulated by the degree of

attention to the signal, although we cannot directly test this hypothesis with the present data.

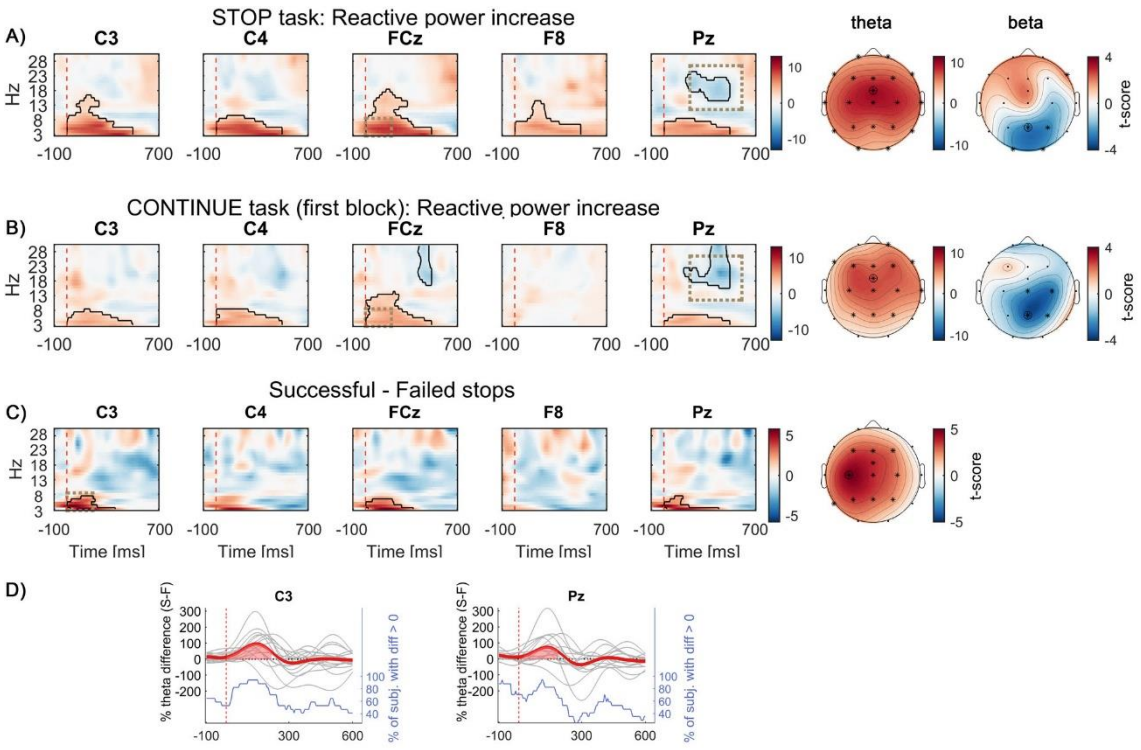

Figure 4.8 A) T-scores of the contrast between power aligned to the stop signal (vertical dashed line) averaged across all STOP trials irrespective of stopping performance and the regular tap done before. B) as A) but computed on all CONTINUE trials of the first block instead. In clusters surrounded by black outlines, power differed significantly from power observed during the regular tap done before. Cluster-based statistics were computed within 0:500ms after the stop signal. Straight after the stop signal, power increased in low frequencies in all channels in both tasks. The cluster in the beta range denotes that beta power was lower relative to regular tapping. Topoplots show t-scores from the average within the dashed rectangular windows: The low-frequency power increase peaked fronto-centrally, whereas the difference in beta was most pronounced over parietal and ipsilateral sites. C) T-scores of power differences between more successful and less successful stops (movement extent threshold=40%). Clusters denote that low-frequency power was significantly higher when participants interrupted their tap before touching the pressure sensor. The corresponding topoplot shows that the t-score was highest over contralateral M1. D) Time courses of individual theta (3-8 Hz) power differences following the stop signal (vertical dashed line) corresponding to the difference depicted in C). The bold line denotes the mean difference. The bottom stepped line shows for each point in time the fraction of participants who had higher theta power during successful stops.

4.4 Discussion

We found that movement-related modulation of power at beta frequencies increased with time in each tapping sequence. This modulation was task-dependent and less pronounced in the STOP condition when the tapping movement had to be abruptly interrupted. In this condition, tapping also seemed to be more cautious as captured by reduced negative mean asynchrony and shorter contact time with the pressure pad. Modulation over the contralateral motor cortex was visible after the first three taps in both tasks, but similar modulation over parietal cortex appeared to develop only in the CONTINUE condition.

Given that successful stopping was preceded by stronger beta power modulation, we hypothesise that participants may have reacted faster to the stop signal when confidence in the current motor plan was high, i.e. when cognitive resources were relatively free and not occupied with adjusting the current motor plan. Alternatively, the observed difference in beta may reflect an intention to perform the next tap later, which would also facilitate stopping. The correlation between low-beta power and the previous tap-to-sound offset points towards a role of beta in timing evaluation although correlations between beta and stopping success were still successful after controlling for the tap-to-sound offset. This may be the case when beta oscillations would reflect timing intentions that may be partially driven by but do not need to perfectly correspond with the preceding tap-to-sound offset.

The detection of power differences over parietal cortex is well in line with the idea that parietal cortex plays a crucial role in maintaining an internal model during tapping to a metronome (Pollok et al., 2008, 2006). Interestingly, negative mean asynchrony can be reduced by reducing excitability of the posterior parietal cortex via cathodal tDCS or rTMS (Krause et al., 2014, 2012).

High post-movement beta power has been linked to greater confidence in the internal model of a task (Tan et al., 2014a). We thus propose that within the STOP condition, confidence in the internal model of the rhythm fluctuated, and when it was higher,

post-movement beta power was increased. A recent study has also reported increased beta power after successful stopping and a relative decrease following failed stops (Jha et al., 2015). The relative beta decrease was interpreted as error detection mechanism that would result in reorganizational processes drawing cognitive resources, as it was followed by increased reaction times.

The relative decrease of parietal beta activity following the stop signal would be consistent with this. Attenuation of the post-movement beta rebound seemed to occur irrespective of whether the tapping movement was continued or not, presumably because the stop signal interfered with the internal representation of the sensorimotor synchronization model needed for accurate tapping in both tasks.

How can our findings and interpretation be reconciled with the prevailing view that elevated beta power reinforces the current motor state, which in our paradigm was continued tapping (Engel and Fries, 2010)? It could be reconciled if increased beta activity reinforced postural holding of the lifted finger between taps to delay the reaction time of the next tap. This would be in line with previous findings of prolonged reaction times when beta was high due to conflict, accuracy demands or uncertainty (Berchtold et al., 2012; Pastötter et al., 2013; Tzagarakis et al., 2010). However, if elevated beta activity promoted stopping by keeping the finger still, we would expect the power difference to be sustained rather than vanishing 100ms prior to the stop signal. Moreover, this would not explain why the average modulation was reduced in the STOP condition. Rather we posit that increased beta modulation may imply more flexible motor control, possibly through facilitating intra- or inter-cortical communication (Rubino et al., 2006). Note that enhanced pre-stimulus parietal beta oscillations have previously also been linked to improved sensory detection and faster reaction times (Kamiński et al., 2012; Linkenkaer-Hansen et al., 2004). In this context it has been proposed that increased beta may reflect a state of enhanced arousal rather than the status quo (Kamiński et al., 2012). However, against this interpretation speaks that we observed higher beta modulation in the undemanding CONTINUE condition, which was unlikely to induce greater arousal. Our results instead point towards a more

complex involvement of beta oscillations in flexible motor control depending both on task demands and instantaneous performance evaluation.

I would like to note that the difference in beta power over parietal cortex was weaker when the data was not split at a fixed threshold of 40% movement extent but divided into two clusters for each individual. Splitting the data according to whether the pressure sensor registered a tap would have also resulted in a reduced effect size. In some participants, the movement extent was bimodally distributed with distinct clusters around 0 and 100% while in others it was more uniformly distributed. Correlations, which are particularly well-suited for the latter case and do not depend on arbitrary thresholds, were also significant. Thus 40% as threshold appears to be an acceptable choice to illustrate the nature of the difference between successful and failed movement inhibition.

The present study might be considered preliminary in that EEG sampling and hence spatial resolution was relatively limited. This, together with the relatively inferior signal-to-noise ratio of EEG, might explain why we could not confirm that successful stopping may be dependent on a beta increase in right inferior frontal cortex as reported in electrocorticography studies (Swann et al., 2009, 2012). In addition, it should be stressed that the correlations identified between beta power preceding the stop signal and stopping performance were relatively small, which might result from the noisy nature of EEG signals or genuinely weak relations. Another limitation of the current study is the fact that the STOP and CONTINUE conditions were not counter-balanced and did not include matched numbers of trials. Contrasts between these conditions should therefore be treated with caution, although relevant control analyses suggested that these confounds had relatively little effect.

Yet our findings begin to link modulation of low-beta oscillations to the evaluation of an internally generated model of repetitive actions, which is continuously updated based on information from the environment. In particular, oscillations in this frequency band may not only promote the current motor state or plan, as previously suggested

(Engel and Fries, 2010; Gilbertson et al., 2005) but may have a wider role in adjusting movements flexibly to external events.

Given that successful stopping was preceded by stronger beta power modulation, we hypothesise that participants may have reacted faster to the stop signal when confidence in the current motor plan was high, i.e. when cognitive resources were relatively free and not occupied with adjusting the current motor plan. Alternatively, the observed difference in beta may reflect an intention to perform the next tap later, which would also facilitate stopping. The correlation between low-beta power and the previous tap-to-sound offset points towards a role of beta in timing evaluation although correlations between beta and stopping success were still successful after controlling for the tap-to-sound offset.

4.5 Summarized findings

- Beta modulation with beta peaking between two taps developed during rhythmically paced finger tapping over parietal and contralateral motor cortex
- If sudden movement inhibition was required and anticipated, this modulation was reduced
- When stopping was required, the negative mean asynchrony was also reduced
- Tapping was more likely to be successfully interrupted if the previous post-movement beta increase was relatively high
- The beta difference preceded the stop signal, and might reflect delayed movement intentions or increased confidence in the current motor plan and thus less cognitive load

5 Sudden stopping of rhythmic movements in patients with Parkinson's disease

The previous chapter examined the neuronal dynamics during sensorimotor synchronization and stopping of rhythmic tapping but was limited to cortical EEG recordings. As outlined in the General Introduction, the basal ganglia are important for action timing and stopping. Thus we recorded the same task that was used in the previous chapter in patients with Parkinson's disease from which we could also record STN LFPs.

5.1 Introduction

Previous studies have described a neuronal stopping network involving prefrontal and supplementary motor cortical regions, as well as the subthalamic nucleus (STN) (Aron et al., 2014; Jahanshahi et al., 2015; Rae et al., 2015). The STN is well-positioned to cancel actions as it receives cortical input via the hyperdirect pathway and can inhibit the thalamus and brainstem via the basal ganglia output nuclei as well as the striatum via the globus pallidus externus (GPe) (Mink, 1996; Wei and Wang, 2016). In spite of recent advances in understanding functional and effective connectivity within the stopping network using fMRI (Rae et al., 2016, 2015; Xu et al., 2016), the fast temporal dynamics of population activity accompanying the stopping process are not entirely clear.

When rats attempted to cancel an action, increased STN firing activity was found irrespective of whether cancellation was successful or not (Schmidt et al., 2013), but more recently, micro-electrode recordings in the human STN revealed two distinct subpopulations that selectively increased firing rate either during successful response inhibition or during motor execution (Bastin et al., 2014; Benis et al., 2016). Also in

the GPe a subpopulation termed arkypallidal cells, which seem to receive input not only from the striatum but also from the STN (Nevado-Holgado et al., 2014), has specifically been linked to action cancellation (Mallet et al., 2016). It is unclear, though, how different populations within the basal ganglia are activated in a selective and flexible way. Oscillations, particularly in the gamma band (> 30 Hz), have been proposed to be a key mechanism for coordinating spatially separate but functionally related assemblies (Bosman et al., 2012; Fries, 2015; Nikolic et al., 2013; Schoffelen et al., 2005). We hypothesized that gamma activity may thus also facilitate coordinated activation of task-relevant subpopulations for efficient movement cancelation. A local field potential study in Parkinson's disease patients, however, has shown increased 55-75 Hz gamma activity when patients failed to stop (Alegre et al., 2013), which is in line with the prevailing view that gamma activity is pro-kinetic (Cassidy et al., 2002; Fogelson et al., 2005; Litvak et al., 2012) or related to response vigour (Jenkinson et al., 2013). Beta activity, instead, is widely viewed as a marker of broad motor suppression within the STN (Wessel et al., 2016a) as well as cortex (Swann et al., 2012). High STN beta activity for example was linked to elongated response times during incongruent trials in a Stroop task (Brittain et al., 2012) and to stronger suppression of cortico-spinal excitability during speech inhibition (Wessel et al., 2016a). However, as movements are known to coincide with decreasing beta and increasing gamma activity (Joundi et al., 2012; Lalo et al., 2008), comparisons between executed and withheld movements might reflect the lack of movement rather than the stopping process per se.

Ideally, stopping would be recorded as a continuous variable that captures how fast an ongoing movement is terminated by measuring how much movement distance was covered from the time of the stop signal until it was stopped. A continuous measurement of the inhibition process would be useful for computing correlations between the speed of the stopping process and electrophysiological changes.. Motor inhibition has traditionally been investigated with stop signal or Go/NoGo tasks, in which movements are triggered by cues (Huster et al., 2013; Swick et al., 2011). In the

stop signal paradigm, subjects press a button in response to a go cue and in some trials a stop signal instructs them to withhold the movement. Based on reaction times in go-trials and the stop signal delay time, a stop signal reaction time can be calculated for each subject. But as each trial only captures whether the button was pressed or not, it is impossible to infer the speed of the stopping process in individual trials. Go/NoGo tasks instead rely on a large fraction of go trials to catch participants out on rare trials, in which a NoGo cue signals them to withhold the pre-potent motor response. Both tasks require participants to decide whether to stay or move but not to interrupt an ongoing action. Successful stopping is achieved in these tasks by successfully delaying or canceling action initiation rather than terminating an action that is already ongoing. Our aim was to extend existing studies by investigating rhythmic movements that can be interrupted halfway and are not directly preceded by go-cues but are self-initiated. Patients were asked to tap rhythmically to a metronome. Under these circumstances, subjects anticipate the metronome instead of reacting only after each sound, and so movements can be considered self-initiated. They were instructed to stop upon hearing a different cue that was timed such that they were able to stop only in approximately half of their attempts (*Figure 5.1*). The neural response to the stop signal was not intermixed with a foregoing response to a go cue as the last metronome sound was delivered about 700 ms prior to the stop signal.

The delay of the stop signal was set by the experimenter after a training period at the start and then kept constant for the rest of the experiment. It was delivered relative to the tap instead of the metronome sound to keep movement variability to a minimum and to prevent the strategy of delaying the tap relative to the metronome sound. This, in combination with the instruction to synchronize accurately to the metronome, provided trains of self-initiated actions that were well-matched across trials. The task was also well-suited to investigate endogenous fluctuations in readiness to stop. We analyzed STN local field potentials (LFP) and scalp electroencephalography (EEG) activity recorded in this task from nine Parkinson's disease patients, who underwent deep brain stimulation surgery. To differentiate volitional motor inhibition from

salience detection, six of them were recorded in an additional control condition with identical auditory cues but different instructions. Their task in this condition was to finish the tapping sequence with two more taps upon hearing the stop signal instead of attempting to stop (*Figure 5.1*).

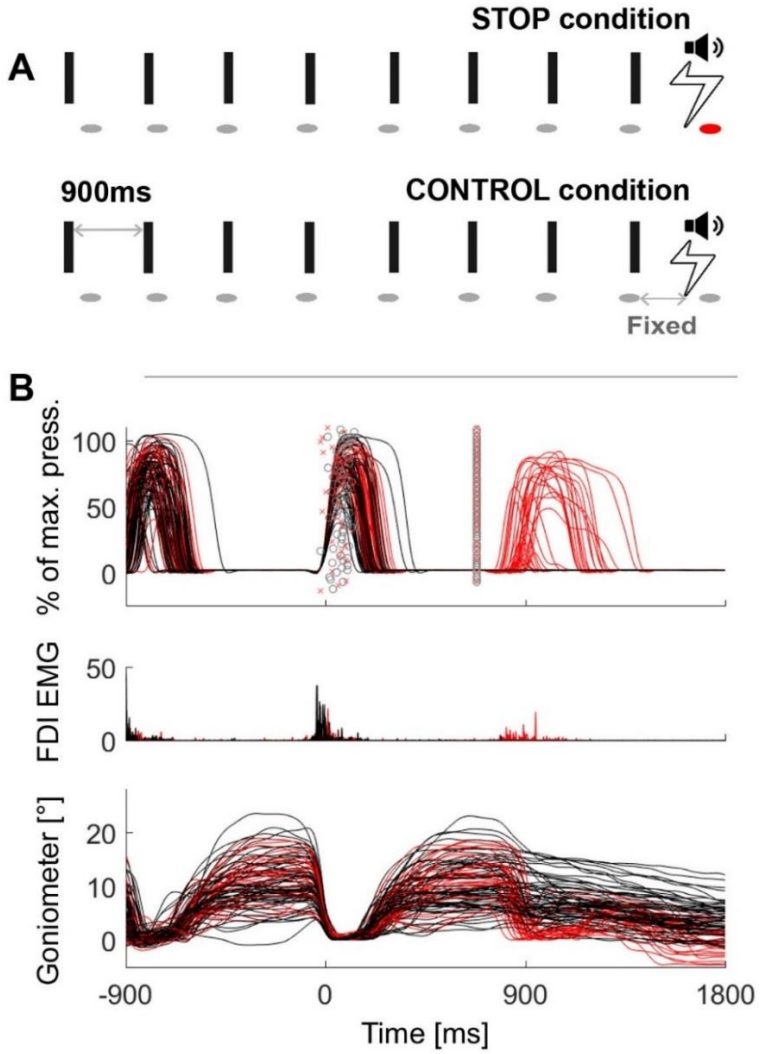

Figure 5.1 Behavioural task and representative data. (A) Schematic of the task in the STOP condition (top row) and in the control condition (2nd row). In the STOP condition participants had to tap (=ellipses) to a metronome (=rectangles) and stop after 5-9 taps. The red ellipse denotes a tap that was unsuccessfully stopped. (B) Pressure sensor, FDI muscle activity and goniometer data from one representative patient. Black lines are trials where the tapping movement after the stop signal was successfully stopped, red lines are trials where stopping failed. The markers around 0ms represent the temporal offset between the last regular sound and the tap (o = successful stop trials, x = failed stop trials). The markers at 680ms show the time of the stop signal, which was always triggered relative to the last regular tap that was registered by the pressure sensor at 0ms. Note that the black and red trajectories overlap, which shows that stopping performance did not depend on the preceding movement trajectory.

5.2 Materials and Methods

5.2.1 Participants

Ten Parkinson's disease patients (mean disease duration = 8 ±4 years, mean age = 59 ±8 years; one left-handed/ambidextrous; two female) were recorded after obtaining informed written consent to take part in this study. One patient had to be excluded from the analysis as they intermittently fell asleep during the testing. All patients underwent bilateral implantation of deep brain stimulation electrodes into the STN two to six days before the recording with the aim to alleviate symptoms through chronic high-frequency deep brain stimulation. Surgeries and recordings were performed either at the University College hospital in London or the John Radcliffe hospital in Oxford, UK. For each patient one of the following three macroelectrode models were used: Medtronic 3389 (quadripolar, for P1-4 and 8), Boston Scientific, Vercise, DB-2201 (octopolar, for P6) and Boston Scientific, Vercise directional, DB-2202 (octopolar, directional, for P5, 7 and 9).

Table 5.1 Clinical details. Age and disease duration are given in years. UPDRS-III: Unified Parkinson's disease rating scale part III ON/OFF levodopa. Levodopa equivalent dose (mg / day) was calculated according to Tomlinson et al. (2010).

ID	Age/Sex/dom. Hand	UPDRS-III	Disease durat.	Main symptom	Levodopa equivalent dose	DBS lead	Surgical Centre
1	65/f/r	33/11	5	Tremor/Dyskinesia	807 mg	Medtronic 3389™	Oxford
2	55/m/r	49/25	10	Leg dragging + tremor (left side)	2022 mg	Medtronic 3389™	Oxford
3	66/f/r	25/14	17	Freezing of gait, balance	1089 mg	Medtronic 3389™	London
4	50/m/r	37/17	5	Tremor, Dyskinesia, esp. in right foot	958 mg	Medtronic 3389™	London
5	48/m/ambi	46/18	6	Frequent OFFs	800 mg	Boston Scientific DB-2202™	Oxford
6	54/m/r	61/32	8	Motor fluctuations	455 mg	Boston Scientific DB-2201™	Oxford
7	60/m/r	37/6	6	Rigidity left side, bradykinesia, dyskinesia	2084 mg	Boston Scientific DB-2202™	Oxford
8	67/m/r	31/13	3.5	Bradykinesia, Rigidity	2173 mg	Medtronic 3389™	London
9	68/m/r	33/15	10	Motor fluctuations	1765 mg	Boston Scientific DB-2202™	Oxford

Clinical details of the patients are given in *Table 5.1*. Patients were tested on medication to ensure task performance and motor function were as normal as possible, although acknowledging that functional impairments, albeit lessened, still persist in this state.

5.2.2 Task

Similar as in Chapter 5, participants were asked to tap to an isochronous metronome (900 ms inter-trial interval, ITI, 700 Hz pitch, 40 ms duration) and to interrupt tapping in response to a high-pitched auditory stop cue (2000 Hz pitch, 40 ms duration) after a random number of 5-9 taps. The taps had to be initiated already before the metronome sounds instead of in reaction to them to achieve synchronization. If the movement would be reactive, the tap would always lag behind the sound, which was not the case as evidenced by a negative tap-to-sound offset. Thus, this task is special as the metronome cues are not equivalent to go cues.

The timing of the stop signal was again adjusted in a training period at the beginning such that patients would be able to stop only in 50-60% of all trials. The stop signal was again triggered relative to the tap registered by the pressure sensor and not to the sound to prevent patients from delaying their taps relative to the metronome, which would improve stopping performance if the latter were the case. A ~50% success rate was desirable to capture fluctuations in alertness or stopping readiness and to distinguish related brain processes. The actual average stopping probability was 55% ± (SD) 10%. Six patients were additionally recorded in the CONTINUE control condition, where patients were asked to end the tapping sequence with two more taps after hearing the high-pitched sound instead of stopping immediately. This was to assess if stopping-related activity was linked to active motor inhibition or whether it merely reflected registration of the more salient stop tone. The CONTINUE condition thus posed much less of a challenge than the main stopping task. We did not evaluate if beta modulation during regular tapping differed between the STOP and the

CONTINUE condition as in Chapter 5 because of the small number of patients and an increased tap timing variability across patients and between tasks.

The task recorded in Chapter 5 differed from the present patient study only in the metronome interval duration, which was shorter (700 ms instead of 900 ms in the patients) and the number of taps (6-10 taps until the stop signal may appear instead of 5-9 taps in the patients). Intervals were chosen to be longer because stopping proved to be more feasible for patients with longer intervals, and the number of taps was reduced to increase the number of trials obtained in the time-limited recording sessions. We planned to record 100 trials in the stopping condition and 20 trials before and after the main block in the CONTINUE condition. Due to fatigue and time constraints in some cases less trials were recorded. As three patients (P4, P7, P9) had severe motor symptoms on the right side, they performed the task with their left index finger. The remaining six patients used the right index finger. As we would expect the contralateral hemisphere to be more involved in the tapping, we analysed the data not separated between left and right motor cortex and STN, but between contra- and ipsilateral C3/C4 and STN.

5.2.3 Behavioural analysis

Behavioural outliers (such as spurious goniometer deflexions) prior to the stop signal were removed following visual inspection. After further exclusion of arrhythmic taps as defined by taps that deviated more than 300 ms from the metronome sound, an average number of 65 ± (SD) 24 trials remained for further analyses. Goniometer traces and the distribution of tap onsets were strongly overlapping prior to successfully vs. unsuccessfully stopped taps (*Figure 5.1*). To get a graded measure of stopping performance for correlations, the amount of downward movement measured by the goniometer was again quantified as *movement extent*. It was defined as the extent of the downward movement normalized by the amplitude of the upward movement done

before. The time between the stop signal and subsequently failed stops was quantified as median across trials for each patient and then averaged over subjects.

5.2.4 Electrophysiological recordings

Bilateral STN local field potentials and EEG was recorded at a sampling frequency of 2048 Hz. EEG electrodes were placed over (or close to if sutures had to be avoided) Fz, Cz, Pz, Oz, C3 and C4 according to the international 10-20 system. Electrooculogram was recorded to remove eye blink artefacts in a subsequent procedure. For one patient, EEG channels could not be recorded because of large DC drifts causing amplifier saturation. Tap onsets were registered by a force-sensitive resistor measuring the pressure of the finger on its surface. Finger flexion, i.e. the tapping trajectory, was recorded with a goniometer (TMSi Goniometer F35) attached to the index finger over the metacarpophalangeal joint. To capture muscle activity, electromyogram (EMG) was recorded from the first dorsal interosseous muscle (FDI).

5.2.5 Data pre-processing

EEG channels were re-referenced to linked earlobes if the latter were recorded (n=5) or to the average of all EEG channels if not (n=3). Power between 3-40Hz was obtained by filtering the data into 3 Hz wide frequency bands shifted by 1 Hz (Butterworth, filter order=6, two-pass, using fieldtrip functions *ft_preproc_lowpassfilter* and *ft_preproc_highpassfilter* (Oostenveld et al., 2011)) and calculating the power of the Hilbert transform. Power between 50 and 120 Hz was calculated within 10 Hz wide frequency bands in 2 Hz steps. To reduce noise, power subsequently was temporally smoothed with a 100ms sliding window.

5.2.6 LFP bipolar selection

As we recorded from three different electrode models, with multiple contacts of which some may not have been located in the STN, we decided to pre-select the bipolar configuration that recorded the strongest gamma reactivity during regular tapping. We chose to select the contacts based on gamma activity because gamma has been found to be highly focal to the STN (Trottenberg et al., 2006). For the quadripolar (Medtronic 3389) and the unsegmented octopolar model (Boston Scientific DB-2201), bipolars were computed between neighbouring contacts or if channels saturated and thus could not be recorded, the surrounding contacts were instead used for the bipolar subtraction. For the directional contacts (Boston Scientific DB-2202), bipolar combinations were computed between the small segmented ones (C2-C7), plus C1 and C8 if more than two of these channels were saturated to increase the likelihood of including activity from the presumably focal gamma source. As power was converted into relative power changes with respect to a baseline, normalized power estimates were relatively comparable despite differently sized contact surfaces or distances between contacts, as was the case for the directional electrode model.

For the selection process, we first computed the 60-90 Hz median power over all taps for each of the multiple bipolar pairs on each electrode in a time window spanning twice the tapping interval around each tap. Then the range between the maximum and minimum of the resulting power time course was divided by the average power within this window, providing the amount of movement-related gamma modulation captured by each bipolar configuration. For each recording electrode only the bipolar configuration with the highest modulation was analysed further. Note that these contacts also recorded significant movement-related beta modulation as shown in *Figure 5.2*.

5.2.7 Statistical testing

It should be noted that we analysed LFPs from electrode contact pairs of different surface areas (according to electrode type) and EEGs that had different references between subjects. Accordingly, we only considered normalised changes in power to mitigate this variability. Correlations between stopping performance (quantified as movement extent after the stop signal) and movement parameters or features in the EEG/LFP were calculated as Spearman's rank correlation coefficients with bootstrapped confidence intervals (using the *Spearman* function from the Robust correlation toolbox (Pernet et al., 2013)). To test if correlations with movement parameters differed significantly from zero on a group-level, correlation coefficients were Fisher's z transformed for each patient and then subjected to a one-sample t-test (n=9). The maximum correlation with EEG/LFP gamma power (*Supplementary Figure A.4*) was determined for each patient by finding the maximum correlation within 60-90 Hz and 0:156 ms after the stop signal.

Each time-frequency matrix was normalized for each subject and frequency by the average power across all regular taps (excluding tap 1 and those directly followed by a stop signal) to obtain a relative power percentage change before testing for differences.

Multiple-comparison correction for power or ISPC comparisons in time-frequency or time windows of interest was performed by using a cluster-based permutation procedure as described in 3.1.1.

5.3 Results

5.3.1 Behavioural results

The mean stop signal delay time with a 55% ± (SD) 10% successful stopping rate was 707±49 ms (range = 620-760 ms). The mean interval between the preceding tap and the unsuccessfully inhibited tap in trials where stopping failed was 864±36 ms, and was significantly shorter than the 900 ms interval dictated by the metronome (Wilcoxon

signed-rank test, $P = .004$). In these trials, patients would have still had on average 156 ms to stop.

Movement trajectories preceding successfully or unsuccessfully inhibited stops were overlapping (*Figure 5.1*, trajectories measured by a pressure sensor and goniometer). Thus any electrophysiological differences in this window are unlikely related to movement differences per se.

Stopping performance was quantified as *movement extent*, which was the extent of downward movement after the stop signal relative to the amplitude of the preceding upward movement. 0% movement extent thus refers to a full stop. 50% describes a movement that was interrupted halfway and 100% would correspond to a full tap, i.e. failed stopping. Correlations between *movement extent* and various properties of the last regular tap were computed for each patient and then subjected to t-tests to assess if the Fisher's z-transformed correlation coefficients significantly differed from 0 on the group-level. In 7 of 9 subjects, movement extent correlated with the tap-to-sound offset, which indicates that stopping performance was worse when the foregoing tap was relatively late in a trial corresponding to previous results (Fischer et al., 2016). However, none of the tested variables were associated with successful stopping after FDR-correction of the resulting p-values (see *Table 5.2*).

Previous research suggests that a surprising sound alone already elicits motor slowing of verbal reports (Wessel and Aron, 2013). We thus checked if the tap performed after the salient "stop signal" (which served as "continue signal" in the control condition) was delayed or slowed down in the CONTINUE condition when stopping was not even required. The median intertap interval directly preceding the stop signal (median ITI=893 ms) did not differ significantly from the one directly after the stop signal (median ITI =889 ms, Wilcoxon signed-rank test $P = 1.0$).

Table 5.2 Correlations between movement parameters of the last regular tap and the movement extent after the stop signal (mean±SD).In 7 of 9 subjects, movement extent correlated with the soundOffset (=tap-to-sound offset; negative values represent taps that occurred before the sound). But none of the p-values resulting from one-sample t-tests of the Fisher's z-transformed intra-individual correlation coefficients of the 9 subjects survived FDR-correction. downTime=duration of finger contact with the pressure sensor, maxPrs=peak pressure during the tap, tapNr=number of taps preceding delivery of the stop signal, peakVelDown=peak velocity of the downward movement of the previous tap, upMvmt=amount of up-movement, peakVelUp=peak velocity of the upward movement.

Variable	Rho±SD	p-value	FDR-corrected p-value
soundOffset	0.29 ±0.18	0.020	0.137
downTime	-0.10 ±0.19	0.174	0.407
maxPres	-0.04 ±0.23	0.460	0.644
tapNr	-0.13 ±0.20	0.061	0.215
peakVelDown	-0.05 ±0.23	0.377	0.644
upMvmt	0.00 ±0.23	0.952	0.952
peakVelUp	0.04 ±0.29	0.810	0.945

5.3.2 LFP and EEG power differences following the stop signal

We tested for rapid LFP and EEG power changes between the stop cue and the average timing of the tap when inhibition failed, which was on average 156 ms after the cue and puts a limit on the window within which successful movement inhibition had to occur.

The STN contralateral to the tapping hand responded to the stop signal with a 60-90 Hz gamma power increase when compared to activity from the tap before (*Figure 5.3A*) shows the reference data from the tap before aligned to where the stop signal would have occurred if it would have been presented one tap earlier; *Figure 5.3B* shows the response to the stop signal; *Figure 5.4A* shows the contrast between the two). Importantly, this gamma increase was significantly and consistently higher during successful movement inhibition (*Figure 5.3C* + *Figure 5.3D*, and *Figure 5.4B*). The effect size of this difference was very large (60-90 Hz power difference between

successful-failed stops: Cohen's d $\text{mean}_{\text{winOfInt}} = 1.2$, $\text{max}_{\text{winOfInt}} = 2.6$). Note that during regular tapping we observed the typical pattern of movement-related gamma power increase and beta power decrease (*Figure 5.3A* and *Figure 5.5*). Gamma power thus increased during both movement execution and movement inhibition. The movement-related peak was broader and weaker than the stop-related increase that peaked around 70 Hz (*Supplementary Figure A.2*).

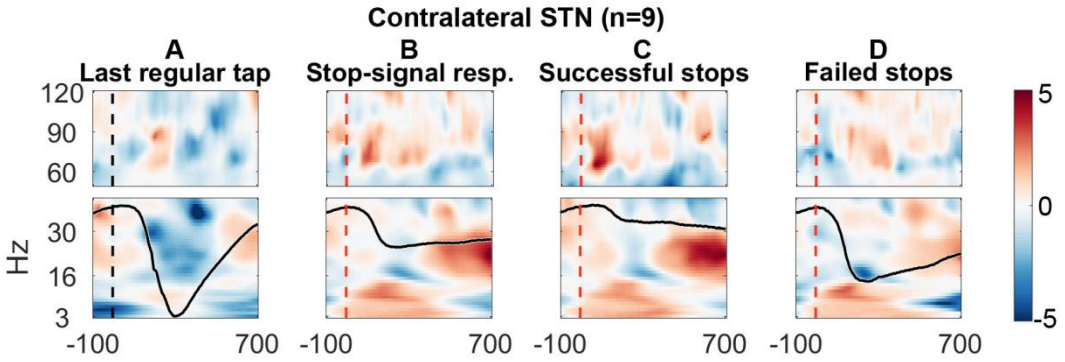

Figure 5.3 Contralateral STN power changes around the stop signal. T-scores calculated over all patients (n=9, normalized by the average power during regular tapping) for (A) the last regular tap aligned to the timepoint when the stop signal would have occurred if it would have been delivered one tap earlier (vertical dashed line). The black line shows the tapping movement measured by the goniometer. The downward movement was accompanied by a beta decrease and gamma increase as expected. The following three columns show changes in response to the stop signal (vertical dashed line) (B) irrespective of whether stopping was successful or not, (C) during successful stops only, and (D) during failed stops only. Note that when a stop signal was present and especially when stopping was successful (column 3), gamma increased strongly. Differences between 2-1 and 3-4 are contrasted in Figure 5.4. The tapping trajectory of failed stops does not reach the bottom line even though the finger touched the table because trajectories were normalized to the minimum of all four trajectories, which occured with the last regular tap, where the spring was extended more vigorously than during attempted inhibition.

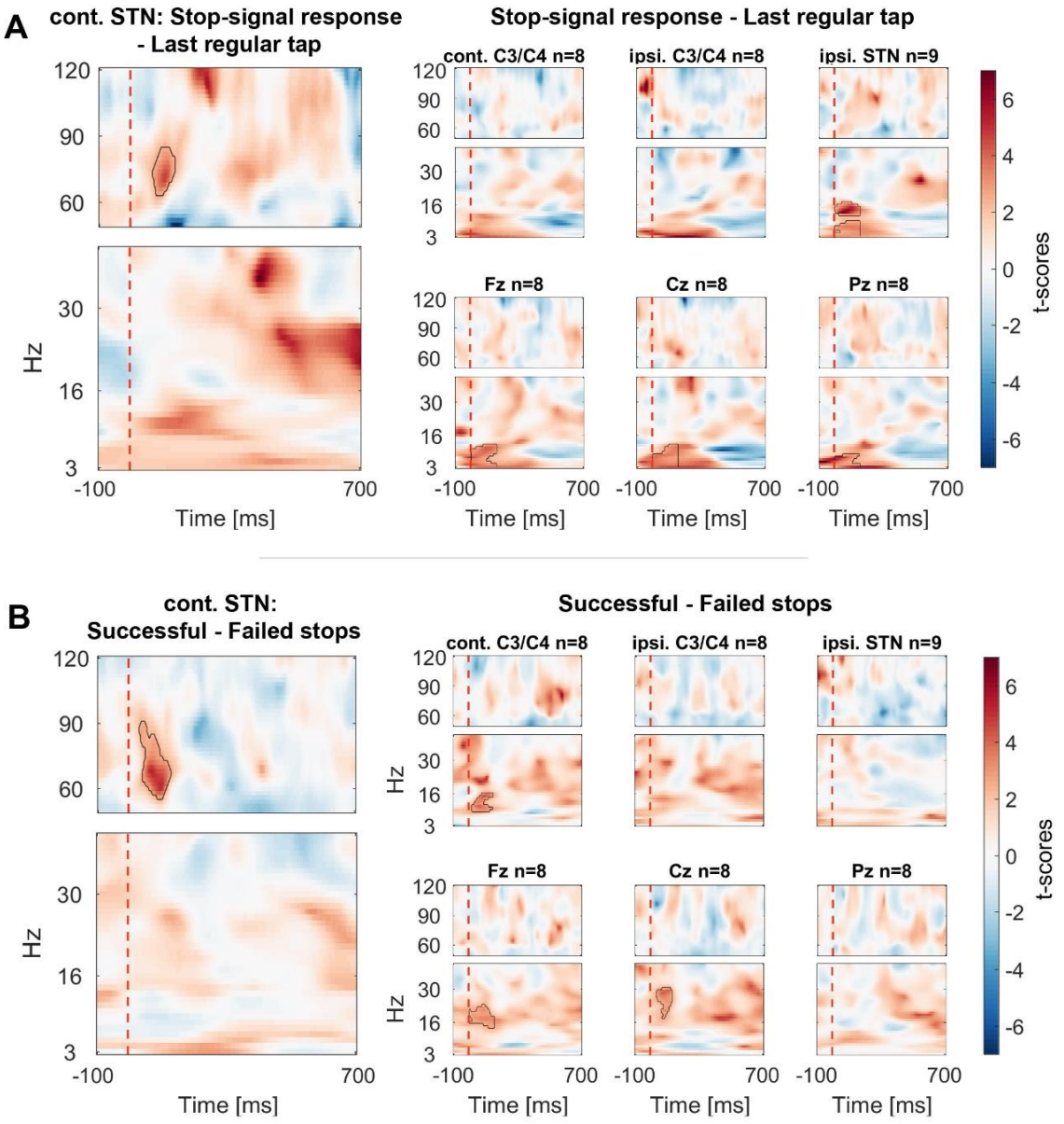

Figure 5.4 Contrasts between power changes following the stop signal. (A) T-scores calculated over all patients of the contrast between power aligned to the stop signal (vertical dashed line) averaged across all trials irrespective of stopping performance (Figure 5.2B) and the regular tap made before (Figure 5.2A, aligned to where the stop signal would have occurred if it would have been presented one tap earlier). Red clusters denote that power significantly increased in response to the stop signal. (B) T-scores of power differences between successful and failed stops. Red clusters denote that power was significantly higher if participants successfully inhibited the upcoming tap (Figure 5.2C-D).

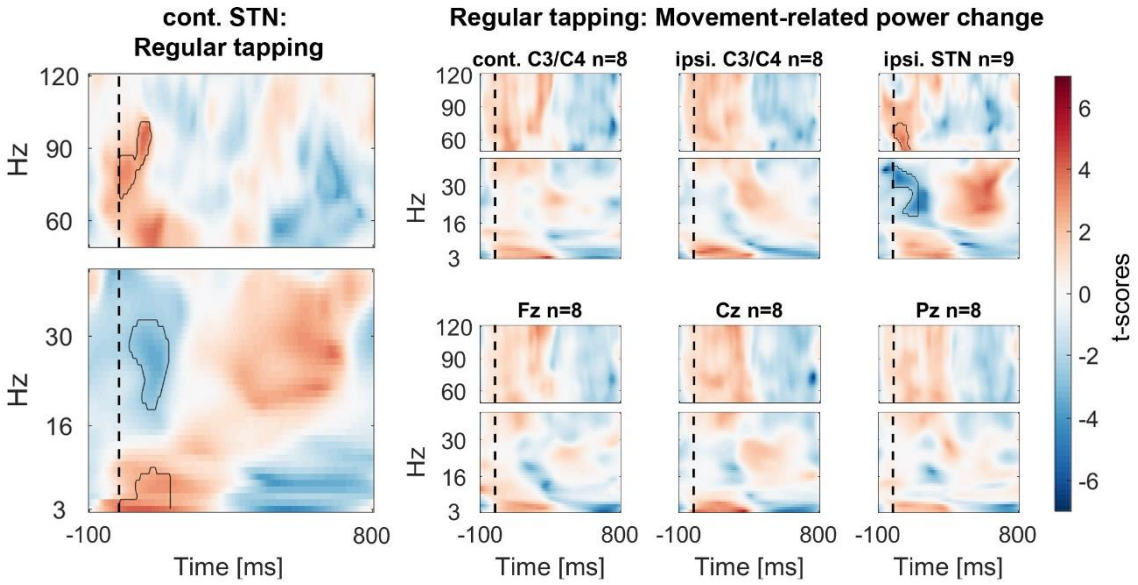

Figure 5.5 Power time-course during regular tapping averaged across all patients. Spectra were tested for significant power modulation locked to the tap in a 0:156ms window (matched in size to the test-window for the main Figure 5.3) after tap onset (= dashed line). As power was normalized by the average power of one full tap cycle including movement, the effects were relatively small and would not survive multiple-comparison correction over the full time-window. However, movement-related beta decrease and gamma increase relative to a pre-movement baseline has been repeatedly reported before (Androulidakis et al., 2007b; Tan et al., 2013).

Cortical EEGs recorded a low-frequency increase in response to the stop signal in all channels (*Figure 5.3A*), which was – in contrast to STN gamma activity – not significantly higher during successful stopping (*Figure 5.3B*). Only 8-30 Hz power over contralateral C3/C4, Cz and Fz was significantly higher when stopping was successful. However, there was no overall power increase following the stop signal in the 8-30 Hz band in these channels when compared to the tap before (*Figure 5.3A*), not even when only successful stop trials were considered (*Supplementary Figure A.3*). In previous studies, such increase was observed when an action had to be withheld before being initiated (Kühn et al., 2004; Swann et al., 2009).

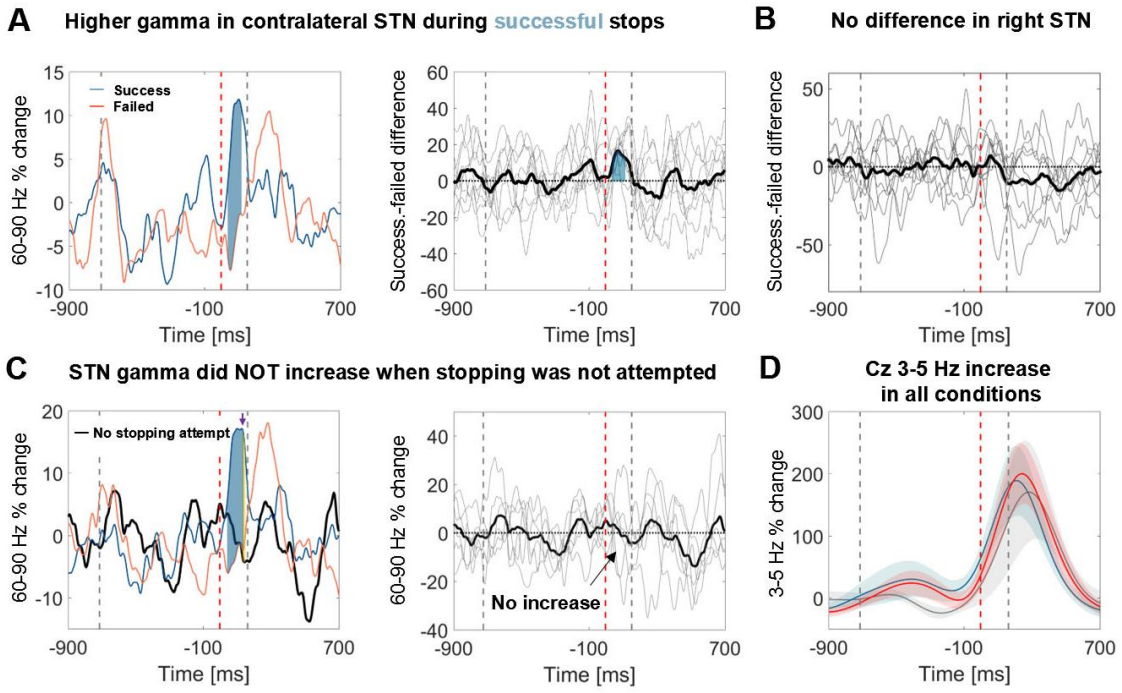

Figure 5.6 Power time course in the STN averaged across patients relative to the stop signal.(A) 60-90 Hz gamma power was significantly higher when stopping was successful (left, blue line). The first grey dashed line denotes the average time of the last regular tap. The grey dashed line after the stop signal (red dashed line) denotes the average time of all failed taps. This difference was consistent across patients (middle panel; bold black line denotes the average difference between successful and failed trials with the individual differencess in grey; n=9). Filled blue areas show cluster-based corrected significant differences. (B) This difference was not present in the right STN (n=9; ipsilateral in 6). (C) Gamma in contralateral STN did not increase when stopping was not attempted (black line = control condition, the plot in the middle column shows individual power time courses in the control condition; n=6). Filled blue areas show cluster-based corrected significant differences between successful and unsuccessful stopping. The yellow filled area indicated by the purple arrow in the leftmost plot shows where power from successful stopping significantly differed from the control condition if uncorrected for multiple comparisons. (D) The 3-5 Hz increase in Cz (n=6) was similar irrespective of whether stopping was successful (blue), unsuccessful (red) or whether it was not even attempted (grey). Shaded areas denote standard errors of the mean.

To exclude that the STN gamma increase merely reflects processing of the salient stop cue, six patients additionally performed a control condition before and after the main stopping task. The stimulus sequence of the control condition was identical to the main condition and the instruction differed only in that patients had to finish the tapping sequence with two more taps upon hearing the stop signal instead of inhibiting the tap immediately. Importantly, no gamma increase was observed in this control condition,

even though the difference between successful and unsuccessful stops was still significant despite the reduced sample size of 6 patients (*Figure 5.6C*).

It has been suggested that specifically the right STN may mediate stopping (Aron and Poldrack, 2006). To evaluate the role of the right STN alone, individual gamma differences between successful and unsuccessful stops of all right STNs are displayed in *Figure 5.6B*, showing no significant increase. Three right-handed patients performed the task with the left hand and thus in those the right STN was the contralateral one. However, in the remaining six, the right STN was the ipsilateral STN, and thus the lack of significant right STN gamma increase indicates that the gamma increase was specific to the contralateral STN.

To further corroborate the functional significance of our finding we also tested whether the average gamma increase peaked earlier during successful stops than during failed stops. Indeed, the average gamma peak of successful stops at 106 ± (SD) 59 ms occurred earlier than the average unsuccessful tap (at 156 ±50 ms), whereas the average gamma peak of failed stops occurred later (at 179 ±84 ms). These gamma peak timings significantly differed from each other (t_8 = -2.9, P = .019, CI_{diff} = [-131, -16ms], Cohen's d = 1.0).

We also examined within-subject correlations between movement extent (i.e. inhibition failure) and gamma within the stopping window (0-156ms) after the stop signal (see *Supplementary Figure A.4*). This was significant in 8 of 9 patients (uncorrected tests; P3's confidence intervals were borderline significant, Spearman's rho P = .049) when gamma was taken from the contralateral STN, meaning that in all but one patient we found that when gamma was higher, movement extent was less and stopping was more successful. In contralateral C3/C4 and in ipsilateral STN such a relationship was present only in three patients, and in ipsilateral motor cortex only in one patient, further indicating specificity to the correlation with contralateral STN activity. Note though that correlations might be harder to detect with EEG data due to the reduced signal-to-noise ratio in comparison with LFPs.

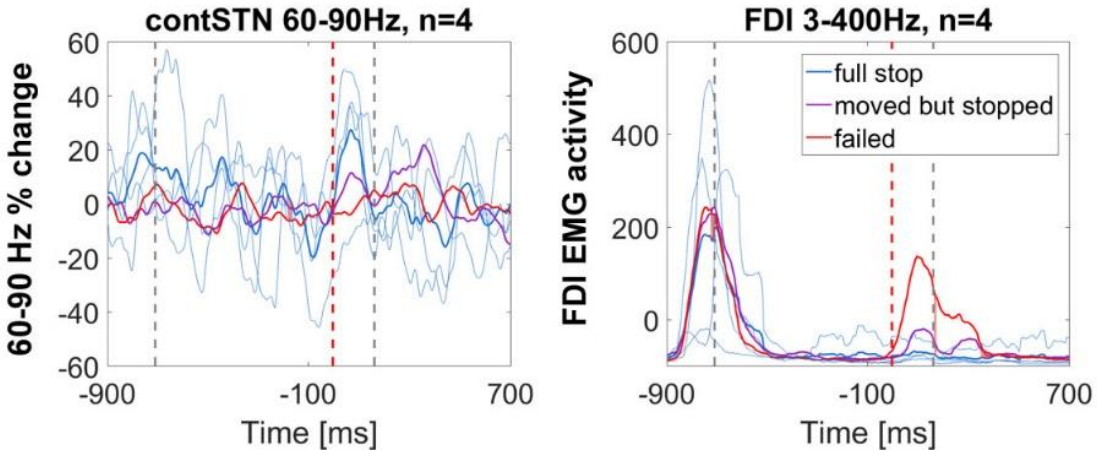

Figure 5.7 Power time course relative to the stop signal in patients who stopped fully in at least 5 trials. 60-90 Hz gamma power was highest during full stops (defined as <10% movement extent), it increased halfway when the tap was interrupted halfway and it did not increase when stopping failed. Thin blue lines denote the time course of full stops from the four individual subject. The FDI EMG activity to the left shows that the muscle activity pattern was reversed, i.e. EMG activity was absent when gamma increased quickly, which demonstrates that gamma did not only increase when the tap was interrupted halfway.

To see if the gamma increase was highest specifically during full stops, we classified the movement after the stop signal into full stops (<10% downward movement), intermediate stops (>10% but pressure sensor was not touched) and failed stops (all trials where the pressure sensor was touched). Only four patients made five or more full stops (mean number of full stops = 9.5), so formal statistics were not applied. Still, in full stop trials, gamma increased most strongly. It increased moderately for intermediate stops and remained flat for failed stops (

Figure 5.7). As expected, activity recorded from the first dorsal interosseous muscle of the tapping hand (presented to the right in

Figure 5.7) suggests an inverse relationship to the gamma increase.

Finally, we examined if the cortical 3-5 Hz power increase, which was clearly present in the stop condition (*Figure 5.3A*), was also present in the CONTINUE control condition when movement inhibition was not even attempted. The grey power trajectory representing the control condition shows a very similar peak in Cz (*Figure 5.6D*, n=6). Significance testing within the crucial reaction time window (ranging from the stop signal to the average time of the failed tap, 156 ms later) resulted in no significant differences between the control condition and either the power increase during failed or successful stopping. The direct comparison between failed or successful stops was not significant either. Also, a peak-extraction analysis failed to detect a difference between low-frequency peaks (Cz successful stops vs. continue: $t_5 = 0.2$, $P = .848$, $CI_{diff} = [-205.1, 240.2\%]$; failed stops vs. continue: $t_5 = 0.5$, $P = .641$, $CI_{diff} = [-149.4, 220.8\%]$). The 3-5 Hz increase only seemed to be reduced in the control condition in Fz and both M1 (*Supplementary Figure A.5*), however this was also not significant.

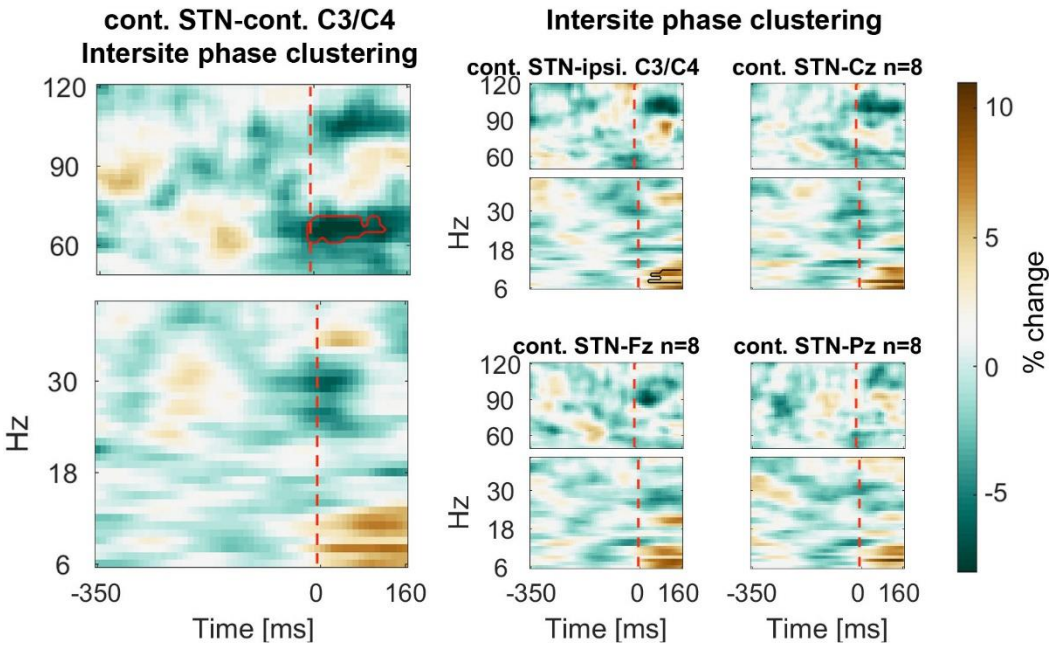

Figure 5.8 Connectivity changes following the stop signal. Intersite phase clustering (ISPC) values are normalized by a -350:0ms baseline preceding the stop signal. The dashed line denotes the time of the stop signal. Gamma ISPC between contralateral STN and contralateral C3/C4 decreased significantly between 60-80 Hz (encircled in red), whereas ISPC in low frequencies between STN and cortical electrodes increased.

5.3.3 Changes in cortex-STN connectivity following the stop signal

In a next step, we computed intersite phase clustering (ISPC) values between filtered oscillations in the EEG recordings and the LFP signal from the STN contralateral to the tapping hand. To get an estimate of the temporal development, we subdivided a -350:160 ms time window around the stop signal into equal bins in which ISPC was computed for each trial and then averaged over trials (see *Materials and Methods*). ISPC describes whether phase differences between two sites are randomly distributed (small ISPC → low connectivity) or clustered (high ISPC → high connectivity) and was obtained by taking the length of the mean vector of all phase differences from all time points within one bin.

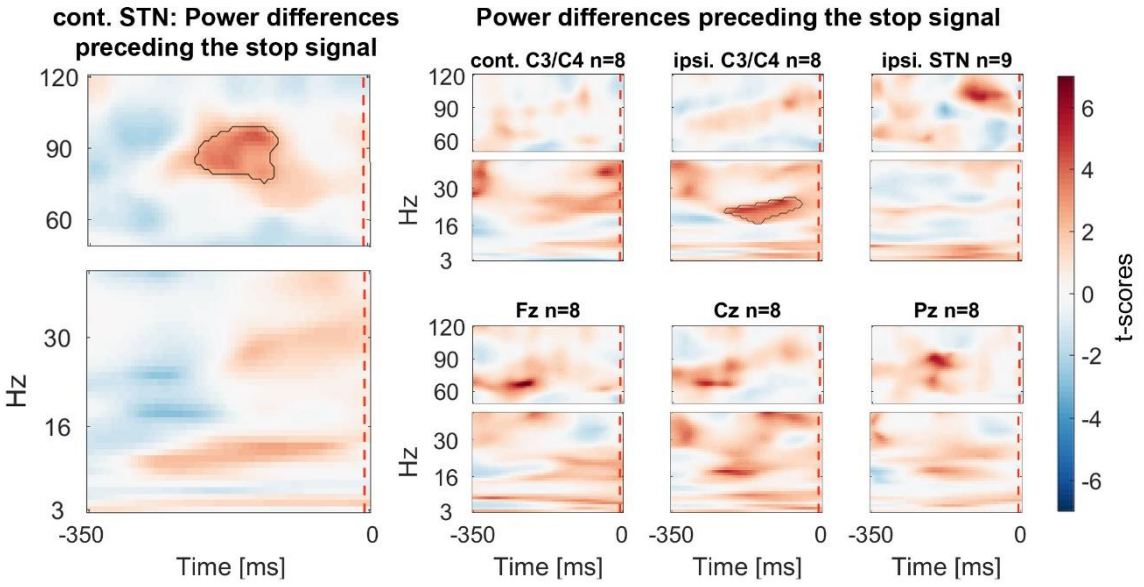

Figure 5.9 Power differences preceding the stop signal averaged across all patients. Around 150ms before the stop signal (at 0 ms) gamma activity was significantly higher in the STN if stopping was successful. Beta power in ipsilateral C3/C4 was also increased prior to successful stops.

5.3.4 Power differences preceding the stop signal

Finally, we assessed if gamma power was already tonically elevated prior to the stop signal, before participants knew they had to stop. We tested for significant differences within a 350 ms window before the stop signal. If the upcoming tap was inhibited more successfully, STN gamma power was already higher prior to the stop signal (

Figure 5.9). 20-30 Hz beta power over C3/C4 ipsilateral to the tapping hand also was significantly higher preceding successful stops. If the data were re-aligned to the last regular tap instead of the stop signal, a second significant cluster at 20-30 Hz over C3/C4 contralateral to the tapping hand was found, in line with previous reports (Fischer et al., 2016) (*Supplementary Figure A.6*).

5.4 Discussion

We found that when finger tapping had to be stopped abruptly, the stop signal elicited a fast increase in 60-90 Hz gamma activity in the contralateral STN and a pronounced theta increase in cortex. However, only the former was significantly higher when stopping was successful. The gamma increase occurred within 156ms, which was the brief time window between the stop signal and the average failed tap. In a control condition, in which participants were presented with the same stop signal while tapping, but stopping was not attempted, only cortical theta but not STN gamma power increased. This shows that STN gamma activity does not only reflect pro-kinetic activity as previously suggested (Litvak et al., 2012) nor does it merely reflect processing of the salient stop signal.

The alternative hypothesis that stopping of the tapping movement itself involved an active movement seems unlikely on two grounds. First, the gamma increase was less if the tap was terminated mid-flight rather than before the downward finger movement was started. Second, gamma connectivity between the STN and C3/C4 also sharply decreased directly after the stop cue, which differs from the movement-related increase usually observed (Litvak et al., 2012) and may indicate disengagement from the obsolete motor plan.

Two previous studies have reported a different relationship between gamma and stopping success to the one that we have found (Alegre et al., 2013; Ray et al., 2012). Ray and colleagues (2012b) reported a gamma increase in response to the stop signal as we do (see Ray, 2012b: Fig. 4b) but did not detect significantly higher gamma during successful stops. This discrepancy may result from extensive temporal smoothing (their sliding window was 333ms long), and from the pre-selection of a window of interest between 200-400ms after the stop signal, which also would have failed to detect the gamma difference in our data occurring right after the cue. If we apply the same temporal smoothing to our data, the power trajectories of successful and failed stops would look very similar (data not shown) as extensive smoothing flattens the brief

gamma increase, such that part of it appears before the stop signal. The late gamma increase during failed stopping, which would be too late to affect the stopping outcome, would remain as a prominent difference about 300ms after the stop signal.. In Alegre et al.'s (2013) study, which differed methodologically in using a visual stop signal, one conclusion was that successful inhibition was associated with a bilateral gamma power decrease. The precise time-frequency decomposition parameters used in that study are unclear and so we have not re-analysed our data in the same way. However, as their window of interest was relatively long (0-0.4 s), they might have predominantly captured the pro-kinetic gamma component that is relatively reduced when a motor response is withheld. Even so, similar as in our study, gamma appeared to increase briefly when aligned to the stop signal in patients on medication during both successful and failed stopping attempts (Alegre, 2013: Fig. 5) and a drop in STN-M1 coherence during successful inhibition also was found (Alegre, 2013: Fig 7).

Periods of high gamma activity in the STN have been reported to coincide with an overall increase in firing rate and phase-locking of spikes to the gamma cycle peak (Pogosyan et al., 2006; Trottenberg et al., 2006). From the LFP we cannot infer changes in firing rate, but it suggests that the number of neurons or inputs to these neurons synchronizing at 60-80Hz was coupled with stopping outcome, and that increased synchronisation occurred early enough to influence such outcome. After observing that the strength of gamma synchronization in the STN or its coherence with C3/C4 did not depend on the exact movement performed, Litvak and colleagues suggested that STN gamma activity modulates rather than explicitly encodes motor commands (Litvak et al., 2012). Our results take this hypothesis further by extending the concept of modulation to include a possible role for movement cancelation. This notion is also compatible with observations that have linked STN gamma activity to effort (Jenkinson et al., 2013; Oswal et al., 2013; Tan et al., 2013) and arousal (Brücke et al., 2013; Jenkinson et al., 2013; Kempf et al., 2009). The fact that stopping was more likely successful after STN gamma was relatively high already 200ms before the

stop cue (i.e. before patients knew they had to stop) may reflect such arousal-related function and the need for proactive inhibition.

The present study is correlative in nature, so we cannot infer that gamma oscillations are causally involved in stopping. However, we would like to speculate that a strong surge in STN gamma activity may shift the excitable period of the otherwise observed pro-kinetic gamma increase such that presynaptic spikes arrive at a period of relative inhibition and motor output thus may be interrupted. Inter-individual variability of the peak frequency and the strength of the STN gamma increase may have been related to differences in disease progression, individual stopping speed or electrode placement and type. We did not find a significant gamma increase in cortical electrodes, which may be due to the reduced signal-to-noise ratio of the EEG. However, a broad gamma increase was observed during stopping in electrocorticography recordings from the pre-supplementary motor area and right inferior frontal gyrus (Swann et al., 2012), raising the possibility of cortical involvement in generating the gamma increase via the hyperdirect pathway.

In comparison to tetrode recordings in rats (Schmidt et al., 2013), our study is limited in that the recording contacts may not have been directly in the STN. The SNr is located in close proximity, ventrally adjacent to the STN, and thus we cannot exclude that we picked up activity from neighbouring structures. However, gamma has been reported to be specifically localized in the dorsal part of the STN (Trottenberg et al., 2006), so that contacts selected according to the strongest gamma modulation are likely located closer to the dorsal border of this nucleus. However, this remains speculative.

It may also be argued that stopping may have involved muscle contractions, which were not picked up by the FDI EMG. But the short latency of the gamma increase and the absence of a similar increase in motor cortex in combination with the decrease in connectivity between STN and C3/C4, which would be expected to increase during movements (Litvak et al., 2012), renders this possibility unlikely. Additionally, we observed that gamma increased most strongly in trials where participants were able to

stop fully instead of interrupting the downward movement halfway, showing that gamma increased not only during braking in the middle of a movement but that it increased even more in the absence of any movement.

As reported in Chapter 5, we confirmed a link between higher post-movement C3/C4 beta activity and subsequently improved stopping performance, which we suggest was related to fluctuations in cognitive load (Fischer et al., 2016). Beta has also been implicated in time estimation (Kononowicz and van Rijn, 2015), thus it may also reflect an intention to delay the next tap's timing, which would allow for more time to stop. Stopping success indeed was correlated with the tap-to-sound offset of the last regular tap in seven patients, such that relatively early taps (early with respect to the sound, which should be compensated for by delaying the next tap) were followed by higher stopping success. Note that this effect was not present in the STN. We also observed significantly higher beta power over contralateral motor and frontal cortex when stopping was successful in comparison to when it failed. As beta oscillations are less likely to occur during movement execution (Feingold et al., 2015; Kilavik et al., 2013), this difference was expected. In the past, a number of studies have suggested that beta plays an active role in motor inhibition (Bastin et al., 2014; Brittain et al., 2012; Wessel et al., 2016a). Importantly, in the present study no beta increase was observed after the stop signal in comparison to the previous regular tap – not even when only successful stop trials were considered. Thus it seems unlikely that bursts of beta oscillations *per se* implemented active braking in our task. Increased beta in other studies may have reinforced the resting position as current motor state to be maintained (Gilbertson et al., 2005). Such resting posture was not present in our task given that the stop signal was delivered during ongoing tapping.

How can we reconcile the above with the results reported by Benis et al. (2014), who observed a weaker STN beta decrease during "proactively inhibited" go-trials ("proactively inhibited" as participants were aware that a stop signal may come after the cue, although it did not appear in these trials) in comparison to go-trials with a cue, which was never followed by a stop signal and thus resulted in faster reaction

times? The stronger beta decrease may have been related to a more vigorous response in fast go-trials (Tan et al., 2015, 2013) or reduced response uncertainty (Tzagarakis et al., 2010) and thus does not necessarily need to reflect an inhibitory process. A stronger difference in beta decrease between the two trial types was also linked to shorter stop signal reaction times across patients. But this correlation may be mediated by symptom severity, as more severe symptoms could result in less beta reactivity (Little et al., 2012), reduced modulation of response vigour and longer stop signal reaction times.

Finally, our results may also be reconciled with those reported by Wessel *et al.* (2016) if elevated beta activity reflects better connectivity across task-relevant areas (Gross et al., 2004) or reduced cognitive load (particularly for <20 Hz beta) (Fischer et al., 2016; Rouhinen et al., 2013), it could support motor suppression without actually implementing movement inhibition.

Recently, an influential hypothesis suggesting that motor suppression is implemented by fronto-central low-frequency activity has received further support (Wessel et al., 2016b). Even though the authors also observed an STN gamma increase concurrent with response slowing, this increase was associated with the cognitive demands of the verbal working memory task rather than motor inhibition. Similar to classical stop signal tasks, our auditory stop cue also elicited a slow-wave power increase. However, this increase occurred also when stopping was not even attempted. If the slow-wave power increase over Cz would have induced slowing or braking, then the intertap interval in the CONTINUE control condition between the tap before and the tap immediately after the stop signal, should have been increased, and this was not the case.

Our data suggest an alternative account, namely that the stop signal-evoked slow-wave response does not directly correspond to movement inhibition but instead registers salient sensory stimuli and alerts stopping-relevant areas, which in turn may trigger the STN gamma increase. The increase in cortico-subthalamic low-frequency connectivity

might underpin this sequence, enabling the STN to trigger the stopping process. The event-related low-frequency response would thus be necessary for, but not equivalent to motor suppression *per se*. In Fz and M1 the average low-frequency response seemed to be diminished in the control condition. We would expect that registration of a salient stop signal and efficiency of the transmission process (in terms of speed or extent of neuronal recruitment) depends on endogenous fluctuations in arousal, attention and cognitive load, which would reconcile the hypothesis of low-frequency power-mediated salient stimuli processing with previous results regarding motor inhibition (Wessel and Aron, 2014).

An fMRI study, which investigated the BOLD response in stop and continue trials in a similar design, found bilateral IFG activation regardless of whether motor inhibition was attempted or not (Sharp et al., 2010). Only pre-SMA activity seemed to be specifically related to response inhibition or slowing. The authors proposed that the IFG is involved in the evaluation and decision-making processes when registering a salient cue, as they are required in both conditions. The fast temporal dynamics of neural firing activity in the IFG, which are not captured by fMRI, should nevertheless differ depending on the decision outcome. Further electrophysiological studies recording simultaneously from cortex and the STN may thus provide a better understanding of the temporal sequence of neuronal events that enable sudden stopping.Taken together, our results showed that gamma oscillations in the contralateral STN were linked to successful stopping. This indicates that gamma oscillations in the STN are not simply pro-kinetic, but that they can also increase during movement termination. Though we can only infer an association and not causation from observational recordings, our data suggest that the observed gamma rhythm may underpin a fast stopping mechanism involving the STN. Gamma oscillations therefore seem to support fast changes in processing demands not only in cortical but also in cortico-basal ganglia networks in line with theories of gamma synchrony establishing effective, precise and selective neuronal communication (Fries, 2015).

5.5 Summarized findings

- 60-90 Hz gamma activity increased in the STN during successful stopping
- Concurrently, phase-based connectivity between the STN and motor cortex decreased
- These effects were specific to the STN contralateral to the tapping hand
- Beta or theta power seemed less directly linked to stopping as the former did not increase relative to the tapping hand and the latter also increased when movement inhibition was not even attempted
- Yet, higher beta power after the last tap before the stop signal was again related to better stopping, confirming the results reported in Chapter 5.

6 Activation of motor networks without moving

So far we have looked at oscillations in the STN during bipedal coordination, sensorimotor synchronization and sudden stopping. In our final experiment, we asked if power changes in the beta and gamma band, which both seem to be relevant for flexible motor control, can be regulated by intention. We were specifically interested to see if the extent of intended muscle contractions would induce changes in the absence of movements, which would suggest that these changes do not only passively mirror motor activity but may have a causal role in regulating motor vigour.

6.1 Introduction

Here we hypothesize that motor imagery involves the basal ganglia in humans in a similar fashion to real movements. We test this by investigating if activity recorded during motor imagery in the basal ganglia is modulated in a task-dependent manner similarly as during real movements. It has already been shown that beta activity decreases in the subthalamic nucleus (STN) local field potential (LFP) during mental imagery of brief wrist extension movements, and that this is not the case during non-motor visual imagery (Kühn et al., 2006). Similar decreases in beta activity have also been reported during passive action observation in the STN (Alegre et al., 2010; Marceglia et al., 2009). But it is still not established whether the extent of such beta changes depends on the intended effort or force of the movement that is imagined. In addition, in motor cortex, mu and beta activity are reduced during motor imagery whereas gamma activity tends to increase, with the latter outperforming changes in mu/beta for decoding of individual imagined finger movements (Liao et al., 2014). Whether gamma activity also increases in the STN during motor imagery is not known. However, there is some reason to suspect that reciprocal changes in beta and gamma activity in the STN might occur during motor imagery and scale with task demands. When patients with Parkinson's disease perform real manual grips at different force levels, beta and gamma activity in the STN are modulated such that the change in the

gamma-band subtracted by the change in the beta-band linearly scales with the amount of force applied (Tan et al., 2013). If imagined gripping involves similar network dynamics as real gripping (Jeannerod, 2001), we would predict not only a beta decrease in the STN but also a gamma increase that is amplified with increasing force. Here we test this prediction by analysing local field potential recordings from the STN in Parkinson's disease patients who have undergone deep brain stimulation surgery.

Answering this question does not only have implications for our understanding of motor control but may even lead to clinical applications. It may help us to understand why mental imagery, in addition to physical practice boosts motor performance in comparison to physical practice alone (Avanzino et al., 2009). Two studies in patients with Parkinson's disease have indicated that physical training combined with mental imagery or autogenic training can improve motor performance more than physical exercises alone (Ajimsha et al., 2014; Tamir et al., 2007). Accordingly, it has been suggested that motor imagery exercises might be useful in improving motor control during physical rehabilitation in Parkinson's disease (Abbruzzese et al., 2015). This might be fruitful, as in Parkinson's disease not only motor execution, but also motor planning seems to be impaired (Avanzino et al., 2013; Conson et al., 2014). The idea is corroborated by imaging and transcranial magnetic stimulation studies that have demonstrated abnormal network activity during motor imagery in this patient group (Cunnington et al., 2001; Helmich et al., 2007; Maillet et al., 2015; Rienzo et al., 2014; Thobois et al., 2000; Tremblay et al., 2008). However, the neural basis of the rehabilitating effect of motor imagery in Parkinson's disease is still not known. Better understanding of the network activity underpinning motor imagery might help inform how to optimally leverage this potential therapeutic adjunct to physical rehabilitation in Parkinsonian patients.

6.2 Materials and methods

6.2.1 Participants

We recorded 11 Parkinson's disease patients who had undergone bilateral implantation of deep brain stimulation (DBS) leads in the STN 2-7 days prior to the recording. In this relatively small cohort the number of post-operative days before recording had no obvious effect on the spectral reactivity patterns. One patient had to be excluded because of excessive movement artefacts during real gripping. This patient had Boston Scientific DB-2201™ leads implanted. Clinical details of all patients included (mean age 61.3±7 years, mean disease duration 9.6±4 years, all right-handed, three female) are listed in *Table 6.1*. Recordings were performed in three surgical centres: King's College hospital and University College hospital in London and the John Radcliffe hospital in Oxford, UK. For each patient one of the following three macroelectrode models was used: Medtronic 3389 (quadripolar, n=6), Boston Scientific DB-2201 Vercise (octopolar, n=2) and Boston Scientific DB-2202 Vercise directional (octopolar, directional, n=3).

Table 6.1 Clinical details. Age and disease duration are given in years. UPDRS-III: Unified Parkinson's disease rating scale part III. Levodopa equivalent dose was calculated according to Tomlinson et al. (2010). JR=John Radcliffe hospital, KC=King's College hospital, UCL=University College London hospital.

ID	Age /Sex	UPDRS-III OFF/ON levodopa	Disease duration	Main symptom	Medication (mg / day)	DBS lead	Surgical Centre
1	71/m	22/8	12	Tremor	923 mg	Medtronic 3389™	KC, London
2	55/m	27/8	6	Rigidity, gait	1009 mg	Medtronic 3389™	JR, Oxford
3	56/m	17/9	3	Tremor	328 mg	Boston Scientific DB-2201™	KC, London
4	75/m	31/10	11	Gait, tremor	565 mg	Medtronic 3389™	KC, London
5	55/f	84/25	7	Gait, dystonia	1618 mg	Boston Scientific DB-2202™	JR, Oxford
6	62/m	27/4	12	Freezing of gait	955 mg	Medtronic 3389™	KC, London
7	60/m	52/30	8	Freezing of gait	1282 mg	Medtronic 3389™	UCL, London
8	59/m	53/18	7	Tremor, bradykinesia, dyskinesia	1195 mg	Boston Scientific DB-2202™	JR, Oxford
9	60/f	56/31	14	Tremor, dyskinesia	1750 mg	Medtronic 3389™	KC, London
10	64/f	66/36	16	Rigidity, tremor	1628 mg	Boston Scientific DB-2202™	JR, Oxford

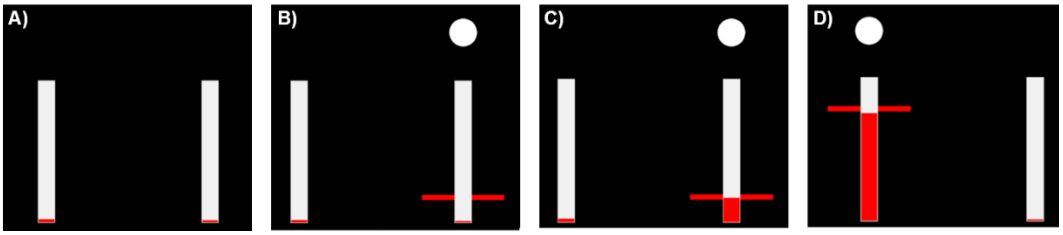

Figure 6.1 Sequence of visual cues. A) In inter-trial intervals the arms were relaxed and the red cursor bars indicating the grip force registered by the dynamometers were down at the bottom of the white vertical bars. B) At the start of each trial, a white dot and a red horizontal bar appeared either behind the left or the right white bar corresponding to the left and right hand respectively. The cue displayed here instructs patients to grip with their right hand at the lightest level (15% of maximum sustainable force). C) Patients adjusted their grip force such that the red vertical column rises to the same level of the red horizontal bar. D) Example of a trial instructing gripping at the strongest level (85% of maximum sustainable force) with the left hand. In the imagined condition, the red horizontal cues indicate the force level and effector side as during real gripping, however the red vertical bar remained down.

6.2.2 Task

Patients were seated in a comfortable chair with their elbows flexed at about 90°. They held a dynamometer (G200; Biometrics Ltd, Cwmfelinfach, Gwent, UK) in each hand and were asked to grip it with maximal effort three times to obtain the maximum sustainable force before starting the main session. They had to hold the grip for as long as a white dot was presented on a computer screen (4.5 seconds), and performed this procedure separately for each hand. The time point of the most stable force production was selected manually in each trial and the maximum sustainable force was then computed as the maximum of the three trials.

In the first part of the main experiment, patients were presented with a red bar on the screen that instructed them to grip at 15, 50 or 85% of the maximum sustainable force (*Figure 6.1*). The white dot and red bar both appeared either on the left or right field of the screen, which instructed them with which hand they should grip (left or right respectively). These were selected in a pseudo-random order. The red horizontal bars were presented at three different heights, corresponding to the different desired forces. The horizontal red bars were presented for 4.5 s in each trial. The exerted grip force was presented in real time as a vertical red column that increased in proportion to the

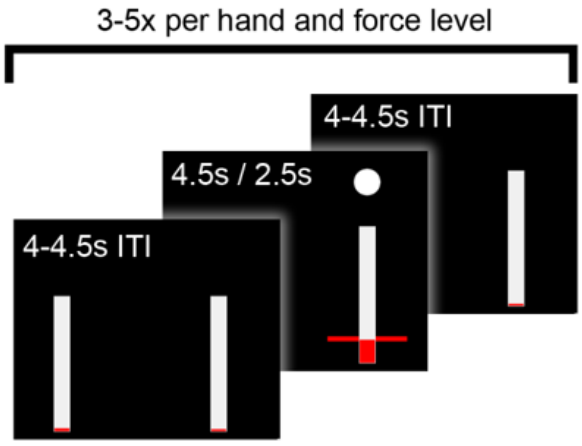

Figure 6.2 Time course of one block. *The inter-trial interval (ITI) was followed by the cue onset (horizontal red bar), which remained present for 4.5s in the executed gripping condition and for 2.5s in the imagined gripping condition. Patients relaxed their arms between each trial in the ITI, which varied randomly between 4-4.5s. Each hand and force level was performed 3-5 times depending on the patient's fatigue.*

force delivered. It replaced a vertical white column that corresponded to maximal sustainable force. The inter-trial interval was chosen randomly between 4 and 4.5 s. The time windows and force levels requested were set such that fatigue was kept to a minimum in the context of a time-limited post-operative study. Prior to the first recorded block, patients performed practice trials until they were comfortable with the task. We recorded three blocks in each condition. Each block contained 3-5 trials for each hand and force level (depending on the patient's fatigue, see *Figure 6.2*). After completion of a block, patients were allowed to rest for as long as they wished. This resulted in an overall average number of 11 ± (SD) 2.8 trials per hand and force level.

In the second part of the main experiment, the dynamometers were put aside and patients were asked to rest their arms still on their lap for imagined gripping. Patients were instructed to imagine the gripping action they had just performed without activating any muscles. They were told to keep their arms fully relaxed, and it was pointed out that this would be assessed via recordings from the electromyographic (EMG) electrodes placed on their forearm (*Figure 6.3*). However, they were not provided with real-time visual feedback of EMG or electrophysiological activity. The duration of the cue presentation was shortened to 2.5 seconds for the imagery condition to make it easier for patients to maintain imagery at the correct level for the whole trial duration and to avoid mind-wandering. Otherwise timings were kept the same as above. The imagery recordings were also split into three blocks allowing for breaks

between blocks. Each block contained three trials per hand and force level resulting in an overall average number of 9 ± 1 trials for each hand and force level.

6.2.3 Recordings

Monopolar LFPs were recorded with a TMSi Porti amplifier simultaneously with the force data from two dynamometers and two EMG electrodes placed on the left and right extensor muscles of the forearm. The data were re-referenced offline to obtain spatially focal bipolar signals by subtracting the data from neighbouring electrode contacts. If single channels were saturated or inactive, the remaining surrounding contacts were used instead.

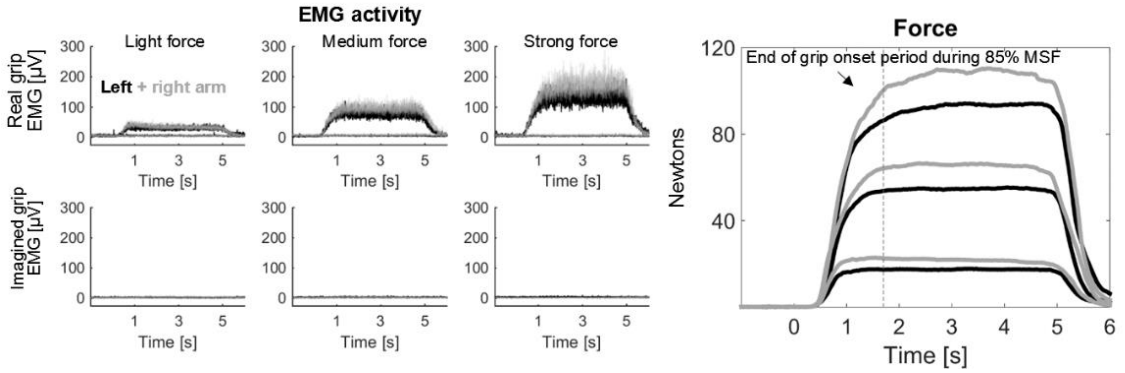

Figure 6.3 EMG and dynamometer data averaged across patients. Left panels show EMG activity during real gripping (upper row) and imagined gripping (lower row). The three columns show the three different force levels requested by the visual cue. EMG activity at y=0 in the upper row shows activity of the arm contralateral to the cued one, which was flat and shows that this arm remained relaxed. During imagined gripping no muscle activation was registered. The rightmost plot shows the average force trajectories. The black traces are slightly below the grey ones showing that the maximum force was weaker for the left arm. MSF=Maximum sustainable force.

Subjective performance ratings after each of the three motor imagery blocks were recorded with a questionnaire that asked "How well were you able to imagine gripping?" Patients indicated their subjective perception on a visual analogue scale ranging from 0 to 10 with 10 corresponding to "Very well" and 0 to "Not at all".

6.2.4 Data pre-processing

Trials containing artefacts in the force signal or movement artefacts in the LFP signal were removed following visual inspection. Data were down-sampled from 2048 to 1000 Hz and high-pass filtered with a 5 Hz cut-off (Butterworth filter with a filter order of 6, passed forwards and backwards). Continuous wavelet transform with Morlet wavelets was then applied using the *fieldtrip*-function *ft_freqanalysis* (Oostenveld et al., 2011). The wavelet width was set to 8 cycles for frequencies below 30 Hz and to 26 cycles for frequencies higher than 50 Hz. For the gamma-band, power was averaged between 55 and 85 Hz. This range was selected to avoid line interference and to capture the reactivity observed particularly in this range (*Figure 6.4*; results were highly similar if statistics were computed with a 55-81 Hz band). 26 cycles thus provided an estimate of power within a window of about 0.37s, which was similar to the 0.40s window including 8 cycles at 20 Hz.

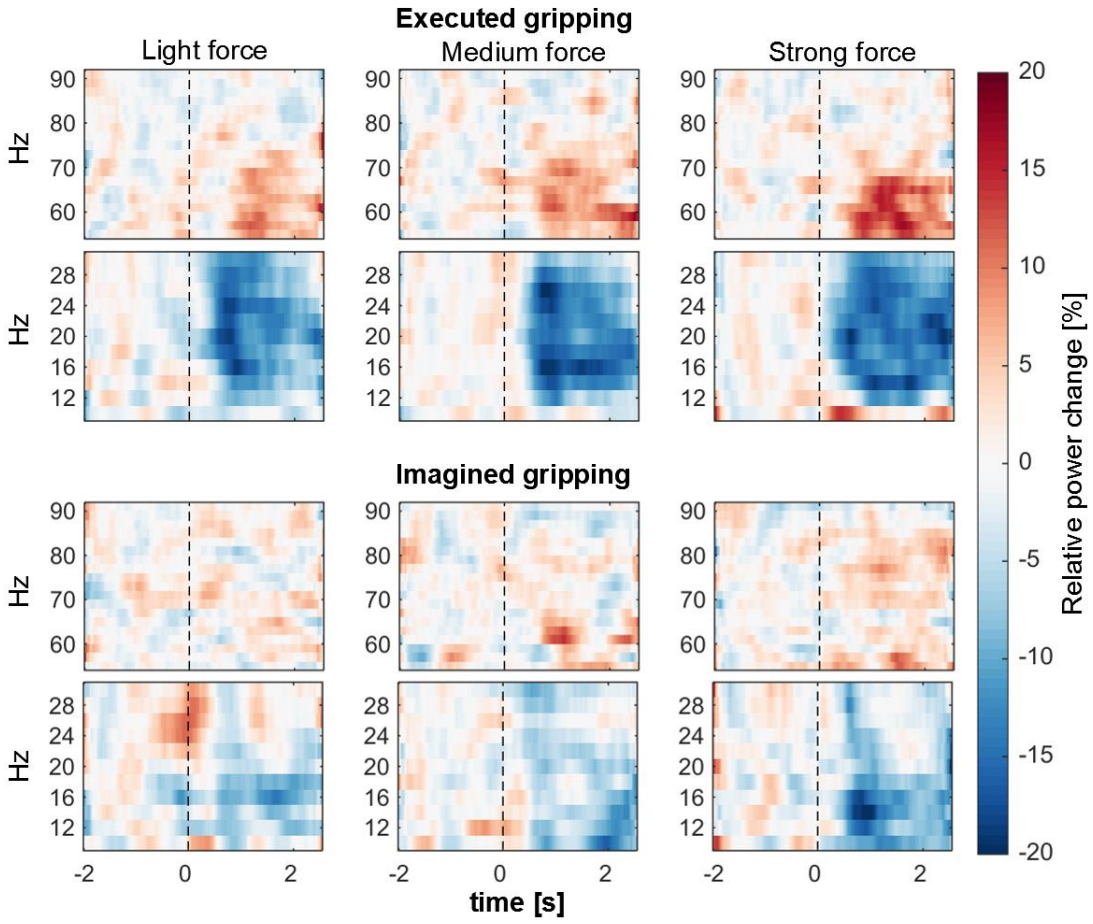

Figure 6.4 Time-frequency spectrograms during contralateral gripping.Red is a % increase and blue a % decrease relative to baseline, which was the average within -2:-0.5s relative to the onset of the visual cue (shown as the vertical dotted line at t = 0). The three columns are light, medium and strong force levels (from left to right). The upper row of three plots shows gamma (55-90 Hz) and the lower row shows beta (10-30 Hz) power changes in each panel during the task. The upper panel (pair of rows of three plots) is for real gripping and the lower panel shows power changes during motor imagery. Data averaged across 18 STN from 10 patients. To reduce noise in these plots, smoothing was applied for each frequency by computing the average within a 0.5 s moving window.

Next, the power of the resulting time-frequency decomposition was down-sampled to 50 Hz and baseline-normalized. After computing the median across trials, a window ranging from -2 to -0.5s prior to cue onset was chosen as baseline (-0.5s to limit inclusion of any preparatory beta decrease that might have occurred close to the cue). We analysed only bipolar contacts that showed a significant movement-related beta decrease upon real gripping across all contralateral grip trials irrespective of force level (assessed by one-sample t-tests against zero) and thus should be located close to the

dorsal, i.e. sensorimotor region, of the STN (Levy et al., 2002; Weinberger et al., 2006; Williams et al., 2005). From these bipolar contacts, the bipolar contact and the frequency (± 2 Hz) with the largest beta decrease was selected. If none of the bipolar contacts of an electrode recorded a significant beta decrease, this electrode was excluded from further analyses. In total, 1 of 20 electrodes was excluded.

To assess the spectral change, we tested the time-averaged normalized power from 0.5 to 2.5s after the cue for frequencies in the beta range (12-30 Hz in 2 Hz steps). The window started at 0.5s to allow for reaction times, which were around 0.5s as displayed in *Figure 6.3*. EMG activity was filtered between 3-400 Hz (Butterworth filter with a filter order of 6, passed forwards and backwards) and rectified. To examine if the velocity of grip onset differed between force levels, the peak rate of force generation was calculated as the maximum of the differentiated force.

6.2.5 Statistical analyses

Gripping consists of an onset phase and a later period during which grip force is more or less sustained. Thus, we separated the data into an early and late time window. *Figure 6.3* shows that movement started only about 0.5s after the cue and that it took up to 1.7s after the cue to reach the desired level across the different cued grip strengths. Thus, the early window was defined to span 0.5-1.7s and the late window 1.7-2.5s. As durations of executed and imagined movements have been reported to be similar (Papaxanthis et al., 2002), we assumed that these windows adjusted to the time course observed during real gripping reflected similar time periods related to the motor process in the imagined condition.

For each subject, the median power change across trials was computed for each force level to obtain a robust estimate of power changes, and then this was averaged within the two time-windows. The data were then subjected to the following repeated-measures ANOVA in SPSS:

A 2 (*task:* real and imagined gripping) * 2 (*effector side:* contra- and ipsilateral grips) * 3 (*force level:* low, medium and high force) ANOVA with the gamma-beta power changes (Tan et al., 2013) as dependent variable to test for significant differences across force levels and to see if the degree of modulation was lateralized. We then examined within-subject contrasts to test if the linear component of the factor *levels* was also significant with beta or gamma modulation alone as dependent variable. To test if the linear component of the factor levels was significant, we computed within-subject contrasts in SPSS.

Correlations of power changes (beta, gamma and gamma-beta power changes) between the real and imagined gripping at the strongest force level were computed as Spearman's rank correlation coefficients with bootstrapped confidence intervals using the *Spearman* function from the Robust correlation toolbox (Pernet et al., 2013). Finally, we also tested if the gamma-beta power change from the lightest to the strongest level during motor imagery was correlated with subjects' self-rating of how well they were able to imagine gripping (again using the *Spearman* function).

6.3 Results

6.3.1 Behavioural data

Force and EMG trajectories show that patients were able to adjust their grip force according to the cues provided during real gripping (*Figure 6.3*). The average maximum sustainable force was 132 ± (SD) 69 Newtons for the right and 121±54 Newtons for the left hand. The force applied in the sustained period (1.7-2.5s) during low, medium and high force trials was on average 17±3%, 49±4% and 81±8% of the maximum sustainable force. A 2x3 ANOVA with peak velocity of the force onset as dependent variable and *side* (left, right) and *force levels* as factor showed that only the factor *force level* was significant ($F_{2,18} = 6.1$, $P = .010$), and not the factor *side* ($P = 0.083$) nor the interaction ($P = 0.780$). Peak rate of force generation during light grips differed significantly from the peak velocity of medium ($P = .002$) and strong (P

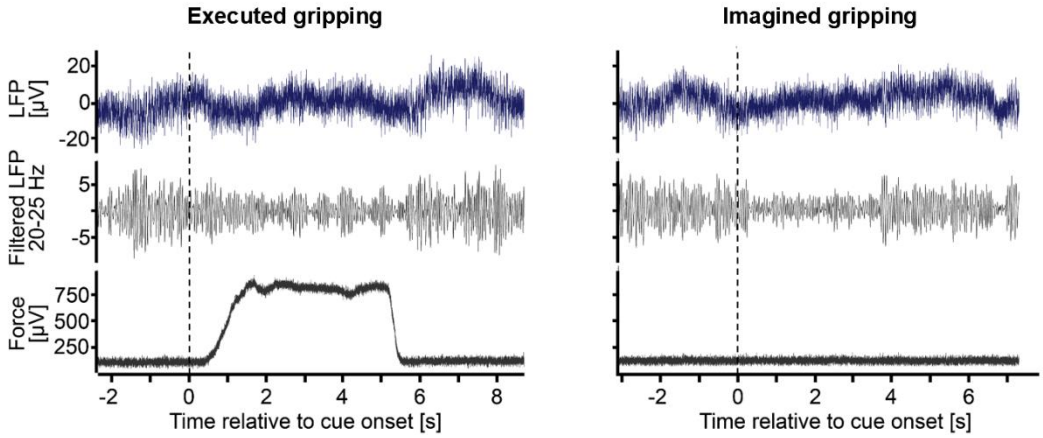

Figure 6.5 LFP recording from one representative patient. The first row shows the raw bipolar local field potential (2s drift correction removal applied), the second row shows the beta oscillations within the same data filtered between 20-25 Hz and the third row shows the force trajectory recorded with the dynamometer. The left panel shows one trial of gripping with the contralateral hand and strongest force (4.5s cue duration, onset at 0s). The right panel shows the same channel in a trial prompting imagination of gripping with the same hand and same force level (2.5s cue duration).

= .002) grips, whereas peak rate of force generation did not differ significantly between medium and strong grips (P = .084). The EMG activity of the arm contralateral to the cued one was flat showing that muscles in this arm were not co-activated (*Figure 6.3*).

In the imagined condition, no EMG activity was visible on either side, confirming that patients kept their arms relaxed as instructed (*Figure 6.3*, bottom row). Patients' subjective rating of how well they were able to imagine gripping was on average 6.6 ± 1.3 on a scale from 0 to 10, with 0 meaning "Not at all" and 10 meaning "Very well".

6.3.2 Contact and frequency band selection

In one patient, beta was significantly modulated only in the right electrode, and in another patient the maximum sustainable force was set too low for one side because of a technical error and thus was discarded. In total, 18 STN from 10 patients were included for analysis of the LFP data. The average beta frequency with the highest movement-related reactivity was 22 ± 6 Hz. *Figure 6.5* shows LFP recordings from one patient performing a representative trial of executed and of imagined gripping at

the strongest force level. The 20-25 Hz filtered beta oscillations decrease clearly with cue onset.

6.3.3 Gamma-beta power changes depend on the force level

To assess if the observed power changes (*Figure 6.4*) were modulated in a force-dependent manner, and if these changes were lateralized, we performed a 2 (*task:* real and imagined gripping) * 2 (*effector side:* contra- and ipsilateral grips) * 3 (*force level:* low, medium and high force) ANOVA with the gamma-beta power changes as the dependent variable (see Tan *et al.*, 2013).

Table 6.2 Linear within-subject contrasts of the factor levels. The F-statistic, which tests if power changes were linearly related to the increasing force levels, was significant and highest for the combined change in gamma - beta.

Power	Early window	Late window
Gamma - Beta	$F_{1,\ 17} = 9.4,\ P = .007$	$F_{1,\ 17} = 9.0,\ P = .008$
Beta only	$F_{1,\ 17} = 6.3,\ P = .023$	$F_{1,\ 17} = 6.2,\ P = .024$
Gamma only	$F_{1,\ 17} = 5.9,\ P = .027$	$F_{1,\ 17} = 5.0,\ P = .040$

All three main effects were significant for both the early (*task*: $F_{1,\ 17} = 13.8,\ \varepsilon = 1.0,\ P = .002$; *effector side:* $F_{1,\ 17} = 28.8,\ \varepsilon = 1.0,\ P < .001$; *force level:* $F_{2,\ 34} = 5.0,\ \varepsilon = .98,\ P = .013$) and the late time window (*task:* $F_{1,\ 17} = 14.1,\ \varepsilon = 1.0,\ P = .002$; *effector side:* $F_{1,\ 17} = 37.9,\ \varepsilon = 1.0,\ P < .001$; *force level:* $F_{2,\ 34} = 4.3,\ \varepsilon = .92,\ P = .026$). Post-hoc pairwise comparisons between force levels are shown in *Figure 6.6*. Within-subject contrasts were also computed to test if the linear component of the factor levels was significant, which was confirmed again for both the early and the late time window (*Table* 6.2).

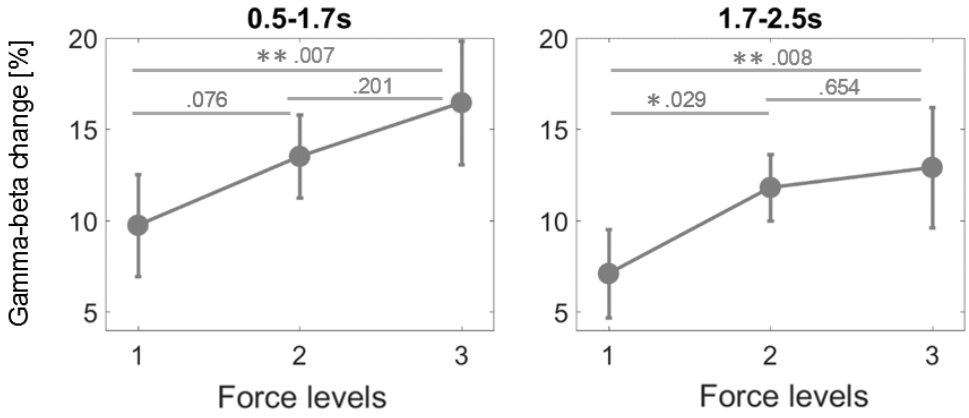

*Figure 6.6 Force-dependent changes of gamma-beta activity averaged across task and effector side.Force-dependent contralateral power changes are separately displayed for each task in Figure 6.6. In both the early and late time window force increases with force level. The difference between power at the highest and lowest force level is significant in both windows. * denotes that power significantly differed between levels after controlling for multiple comparisons with FDR-correction (*<.05, **<.01).*

In addition to the main effect, we found a significant interaction of *effector side*task* in both the early ($F_{1,\,17} = 6.4$, $\varepsilon = 1.0$, $P = .022$) and late window ($F_{1,\,17} = 5.2$, $\varepsilon = 1.0$, $P = .037$). Post-hoc pairwise comparisons for both windows showed that power differed between contra- and ipsilateral grips only significantly in the real gripping condition (*early window:* realContra = 26.0 ± 17.9, realIpsi = 10.9 ± 15.4, $P < .001$; *late window:* realContra = 22.6 ± 14.3, realIpsi = 8.7 ± 15.0, $P < .001$) and not in the imagined condition (*early window:* imaginedContra = 9.9 ± 10.1, imaginedIpsi = 6.2 ± 10.3, $P = .111$; *late window:* imaginedContra = 7.6 ± 9.6, imaginedIpsi = 3.5 ± 10.4, $P = .063$). The beta and gamma power traces in *Figure 6.7* also depict this difference over time. None of the other interactions were significant (*early window:* effector side*force level $P = .503$, task*force level $P = .835$, effector side*task*force level $P = .231$; *late window:* effector side*force level $P = .360$, task*force level $P = .291$, effector side*task*force level $P = .976$).

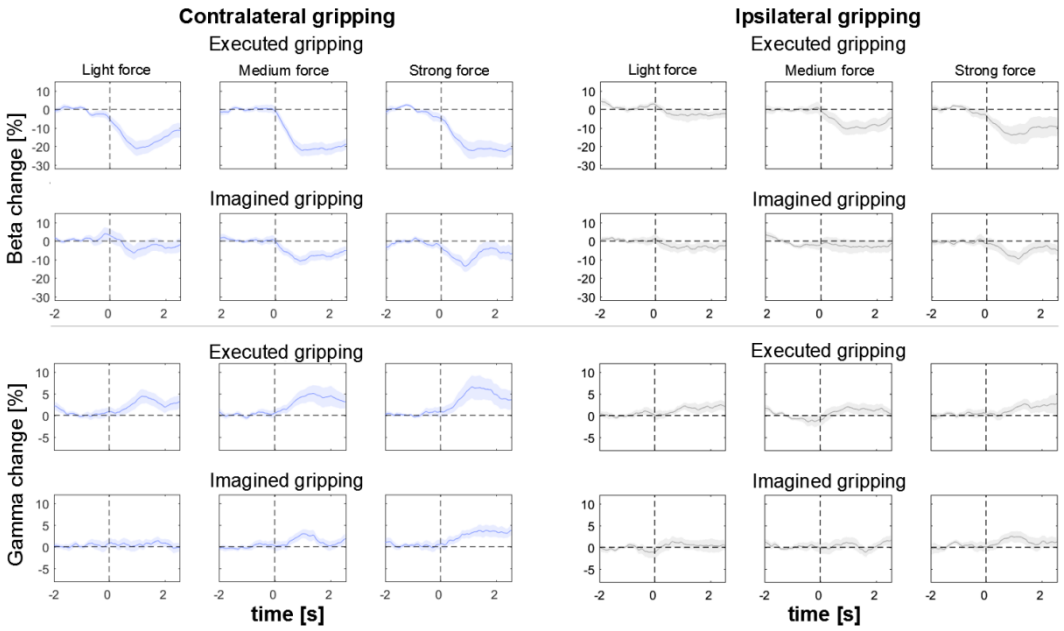

Figure 6.7 Subject-averaged power changes (median across trials). The upper and lower rows show beta and gamma power changes, respectively. The left column shows contralateral grips and the right column ipsilateral grips. Onset of the visual cue is shown as the vertical dotted line at t = 0. To reduce noise, smoothing was applied by computing the average within a 1 s moving window for this visualization. Shaded regions denote standard error of the mean.

Even though the relative power modulation was less in the imagined condition than during real gripping, as confirmed by the main effect of task, the fact that the interaction *task*force level* was not significant indicates that the force-dependent modulation of power observed during real gripping resembled that during imagined gripping.

We also tested if the individual frequency bands, i.e. gamma or beta alone would result in a similar or possibly larger F-statistic for the linear component of the within-subject contrast of levels. The linear component was significant in the late window for both cases, but the F-statistic was reduced indicating that the combination of the two features was superior in detecting a linear relationship (*Table* 6.2).

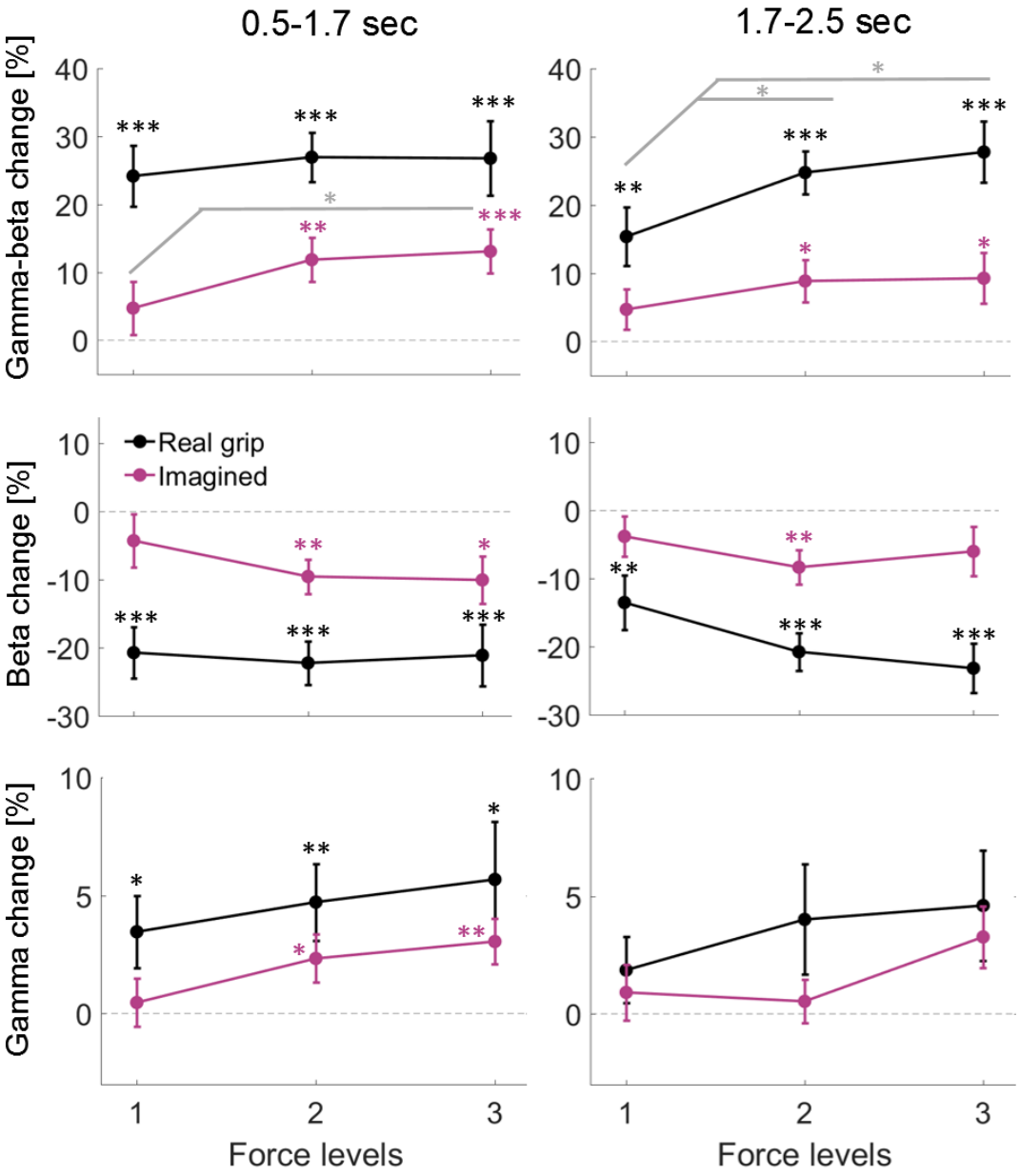

*Figure 6.8 Mean power across patients for the three force levels in the real and imagined gripping condition. * above markers denote that beta ERD was significantly different from zero (*<.05, **<.01, ***<.001, FDR-correction was applied in each plot for the 6 multiple comparisons, grey * did not survive FDR-correction).*

It has not yet been shown whether gamma activity in the STN is modulated during motor imagery. Thus we computed pairwise comparisons between the three combinations of force levels for the gamma and beta-band separately for the two tasks. *Figure 6.8* shows how combined gamma-beta power (top row), and how beta and gamma power separately change across the three different force levels in the two conditions. Beta activity in the sustained period (and in the early window during motor imagery) differed most strongly between the lowest level and the highest two force levels, whereas for gamma activity the increase seemed to be more linear. Such a floor effect of the beta decrease at medium force levels has previously been reported during real gripping (Tan et al., 2013). Gamma activity was significantly increased during imagination of gripping at the highest force level, particularly in the early time window. The average increase in the late time window did not survive FDR-correction.

To examine if reactivity in one task was related to reactivity in the other condition, we also computed correlations between power changes during gripping and imagination at the highest force level. This correlation was significant for gamma-beta and for beta alone in the early time window (*Figure 6.9*).

We also tested if the amount of power reactivity during imagined gripping was correlated with patients' self-ratings of how well they were able to imagine gripping. We correlated the relative power change from the light to the strong force level (averaged across both STN) with the self-rating (averaged across individual ratings following each block). The correlation was positive but it was not significant (Spearman's rho = 0.41, 95% CI = [-0.39, 0.89], $P = .244$).

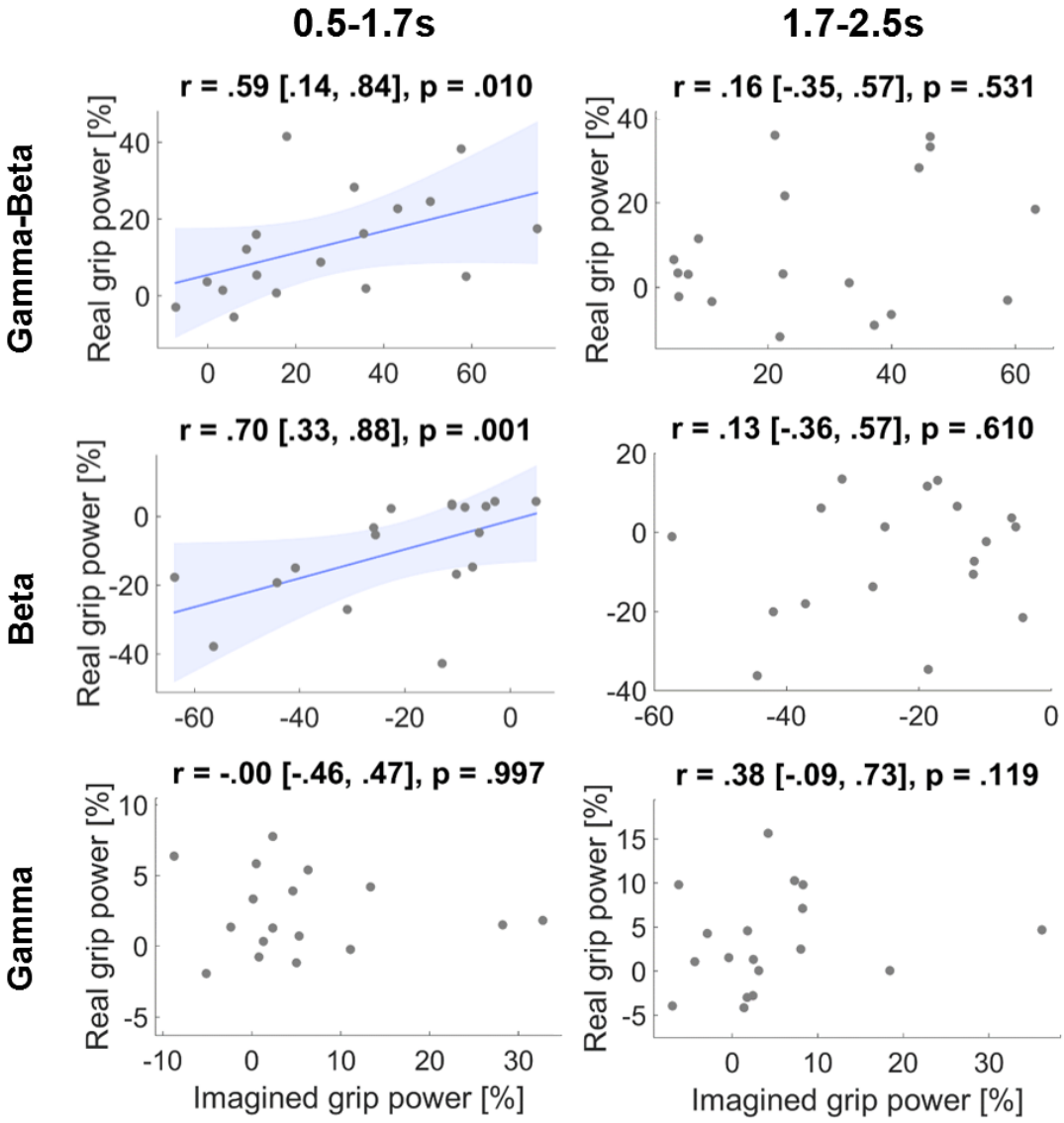

Figure 6.9 Correlations of power changes between the imagined and real grip condition. Each point denotes one recorded STN displaying its power change in the imagined (x-axis) and real grip condition (y-axis). Correlations were significant only for beta power and the combination of gamma-beta power taken from the early window (during grip onset). Plot titles denote Spearman's rho followed by its 95% bootstrapped confidence intervals and p-value. Lines were fitted with a least squares linear regression and shaded areas denote 95% confidence intervals.

6.4 Discussion

We found that STN LFP activity was modulated by the intended force during imagined gripping, suggesting that the STN LFP carries information about force intentions even in the absence of actual muscle activity or movement-related proprioceptive feedback. In addition, to our knowledge, this is the first report of increased STN gamma activity during motor imagery, and shows that the increase of gamma activity in the STN is not only associated with actual movement or muscle activation.

This further strengthens the idea that the observed spectral changes relate to motor effort rather than force coding *per se* (Tan et al, 2015) and that they may actively regulate movement vigour rather than being merely epiphenomenal. The observed modulation of basal ganglia oscillations may then be transcribed into force through the motor cortex and related effectors. The evidence that STN LFP activity is modulated and linearly scaled with force intentions also helps to motivate the exploration of the role of motor imagination in promoting the effects of physical rehabilitation (Abbruzzese et al., 2015). In addition, the results suggest that similar spectral reactivity might be retained within the STN in patients who cannot move and therefore have no movement-related sensory feedback. This is important, as it may mean that the STN LFP could provide an ancillary brain-machine-interface signal for graded response control, such as grasp force control, in paralysed patients.

Although within-subject contrasts confirmed linear scaling of spectral changes during early and later phases of real and imaginary gripping, the average reactivity of beta and gamma oscillations was less in the imagined condition than during real gripping. This may have been due to several reasons. Firstly, patients may have been inattentive or failed to sustain the imagined grip despite the short duration of the imagination blocks. Secondly, although sensory reafference may not be necessary for modulating oscillations it may act to reinforce any modulation. Finally, if changes in beta and gamma activity reflect effort as previously suggested (Tan et al., 2015), then the

reduced modulation might also reflect reduced effort during imagined gripping, assuming that motor imagery might present the motor network with fewer demands than real movement.

We also found that beta-gamma reactivity during imagined gripping at the highest force level significantly correlated with reactivity during real gripping, in the early time window at least. This predominately originated from a relationship within the beta-band. A similar relationship between beta activity modulation during real and imagined movement has also been reported previously in another motor imagery task (Kühn et al., 2006). The correlation provides some evidence that the spectral reactivity during real and imagined tasks comes from a similar generator within the subthalamic area, perhaps the dorsolateral 'motor' STN. Our study thus provides further evidence that imagined and real movements share common pathways (Gerardin et al., 2000).

It should be acknowledged that the observed spectral modulation may not necessarily reflect normal physiological activity, however, vividness of motor imagery seems to be preserved in comparison to age-matched controls even after medication withdrawal (Peterson et al., 2012).

Even though we found that gamma-beta activity during real and imagined gripping at ~15% of the maximum sustainable force differed from gripping at ~50 or ~85%, the latter two levels were not clearly distinguishable in terms of power changes. Moreover, the beta decrease during onset of real gripping seemed to be saturated as it was similar across all three different levels of force. These findings differ from those in our previous report of real gripping (Tan et al., 2013), and may be related to the fact that in the current study the peak rate of force development only differed between the lowest level and the medium or highest force levels but not between the latter two. In addition, Tan et al.'s study had no visual cues and thus task demands may have differed slightly considering that the initial effort of matching grip force to a visual cue may be similarly high for light and strong grips. Also, power changes were aligned to grip onset

in their analysis instead of cue onset as in our study, which was necessary for comparing executed and imagined movements lacking a measurable grip onset.

Although we monitored muscle activity of the arm and closely watched if patients sat still during the task, we cannot entirely rule out subtle contractions of other muscle groups. However, this is a general problem in BCI control and can only ever be tested with certainty in patients who are completely locked-in.

Translational significance of the findings

Beta and gamma activity was not only modulated during imagined gripping of the contralateral, but also of the ipsilateral hand. Significant lateralization only occurred during real gripping. Thus, although the STN LFP signal might provide a potential substrate for force decoding in applications involving brain machine interfaces, selection of an effector would likely require the consideration of additional signals, such as multi-unit or ECoG activity from motor cortex, which also seems to carry, at least to some extent, information about imagined force levels: Cortico-spinal excitability has been found to differ between low and high imagined force levels with higher excitability at higher forces (Helm et al., 2015). In addition, cortical activity during imagery of sustained grasping at different force levels seems to be distinguishable from activity during rest and during imagined alternating movements (Murphy et al., 2016; Yin et al., 2015). Yet it seems difficult to discriminate between different imagined force levels from cortical recordings alone (Murphy et al., 2016; Zaepffel et al., 2013). To our knowledge only one study has successfully extracted features that carry information about imagined force from scalp EEG (Fu et al., 2014). Feature extraction was based only on low-pass filtered data and the contribution of beta or gamma activity was not examined.

Our findings suggest that the combination of gamma-beta is better suited for distinguishing different force intentions than either band in isolation for both real and imagined actions (see also Tan *et al*, 2013). Our results also indicate that force levels

can be differentiated best in the early phase of movement imagination, raising the possibility that STN signals during imagined or fictive gripping of different strengths could potentially provide a relatively fast and dynamic substrate for the control of neuroprostheses, and in particular communication devices, in patients who otherwise cannot move. The only successful approach for communicating with completely locked-in patients to date used functional near infrared spectroscopy to measure hemodynamic changes over sensorimotor and temporal or frontocentral cortex (Chaudhary et al., 2017, 2016; Gallegos-Ayala et al., 2014). However, this communication technique would still benefit from improved decoding accuracy and speed as it depends on relatively slow changes in oxygenation levels.

Another potential application is to combine neuro-feedback and motor imagery to help improve motor symptoms in Parkinson's disease (Subramanian et al., 2011). To this end it would be interesting to explore if gamma and/or beta modulation can be enhanced by repeated practise of mental imagery with concurrent feedback. Importantly, the improvement in motor symptoms in Parkinson's disease after levodopa administration has been linked to a decrease in beta and an increase in gamma activity at the level of the basal ganglia (Brown et al., 2001; Williams et al., 2002). Improved modulation of these oscillations through combined motor imagery and neuro-feedback training might thus facilitate symptom improvement, which was reported after combined motor and mental imagery exercises in patients with Parkinson's disease (Ajimsha et al., 2014; Tamir et al., 2007).

Taken together, beta and gamma modulation in the STN seem to help encode motor effort or vigour rather than actually executed force *per se*. Moreover, this study suggests that spectral changes in STN activity are not dependent on peripheral feedback, opening up the possibility that STN LFP signals might provide a substrate for effort and hence force decoding in the control of neuroprosthetic devices. Finally, the very fact that STN activity is modulated during motor imagery helps motivate further studies of the latter as adjunctive therapy in the physical rehabilitation of

Parkinson's disease (Ajimsha et al., 2014; Tamir et al., 2007; Abbruzzese et al., 2015) and of the use of signals from the STN as a basis for neurofeedback training.

6.5 Summarized findings

- During actual gripping at three force levels, beta and gamma activity is scaled
- Force-dependent modulation of beta and gamma activity also was observed during imagined gripping
- STN neuro-feedback may be useful for improving motor control training or communication via brain-machine interfaces

7 General Discussion

The aim of this thesis was to examine the relationship between neuronal population activity and movement dynamics during flexible motor control. The questions I set out to answer at the beginning of this thesis were:

- How can two or more limbs be flexibly coordinated and this coordination be adjusted to external events in the environment?
- Are beta oscillations indeed related to stopping? How else may fast stopping be mediated?
- What mechanisms could contribute to regulating the extent and speed of transient muscle contractions separately for multiple effectors? Are basal ganglia gamma oscillations only present during movement or can they be generated by the intention to move?

I studied inter-limb coordination in a stepping paradigm, sudden stopping of rhythmic tapping to a metronome, and regulation of movement vigour intentions.

All three experiments indicate an important role of beta and gamma oscillations in flexible motor control. It has long been established that during movement, gamma activity increases while beta decreases in cortex and the STN (Litvak et al., 2012; reviewed in van Wijk et al., 2012). These and other studies (reviewed in Brown, 2003) have formed the basis of theories proposing that beta is an anti-kinetic, or inhibitory, and gamma a pro-kinetic rhythm. I will argue that this view needs to be widened and will propose a new hypothesis of how beta and gamma activity may complement each other to enable flexible interactions with the environment. I will also outline a set of testable predictions, draw links to the symptoms of Parkinson's disease and summarize the clinical significance of the present findings.

7.1 Beta oscillations for segregated sensorimotor integration and timing

In the introduction, we have outlined different components of fluctuations in beta oscillations during motor control: Beta decreases during sensorimotor perturbation, increases during sustained contraction or maintenance of a posture and rebounds after movement completion.

The first experiment of this thesis shows that periods of post-movement beta oscillations alternate between the two STN during gait-like stepping in place. Beta oscillations were elevated when the contralateral foot rested on the floor after each heel strike. This finding is well in line with the previously demonstrated lateralization of movement-related beta modulation (Androulidakis et al., 2007b) and suggests that the 20-30 Hz frequency band could carry segregated information about the left and right leg when they are moved in alternation. The post-movement beta increase was enhanced when auditory cues were provided and step timing accuracy was improved. Events of high beta oscillations thus were more likely to appear when patients performed well. Recently, the idea has been put forward that suppression of the post-movement beta rebound reflects updating of a forward model (Cao and Hu, 2016; Tan et al., 2016b). The present results seem to confirm that beta oscillations are higher when sensorimotor predictions about the timing of a movement are met. If beta oscillations indeed mediate top-down control of behaviour as suggested elsewhere (Bastos et al., 2015; Buschman and Miller, 2007; Siegel et al., 2012), they may even have an active role in adjusting the timing of the next step. A recent study did indicate a role of beta in timing (Kononowicz and van Rijn, 2015), and the present significant second-level within-subjects correlation between beta power and step timing or step interval duration also raises the possibility that elevated beta may contribute to delaying the next step.

In a second experiment, where the rhythmic movement was simplified and reduced to unimanual finger tapping, a similar correlation was found between the timing of a tap

and the subsequent cortical beta rebound. Updating a forward model to achieve desired action outcomes would rely on both bottom-up sensory feedback and top-down information about the goal, such as an instruction to tap with the sound and not between sounds. This ties in again with plenty of evidence for a role of beta in top-down control of sensory processing found within the visual system, where beta oscillations seem to mediate selective routing of visual information (Richter et al., 2017). Similar principles may directly translate to selective re-routing of activity or connectivity within neuronal assemblies to achieve desired action outcomes. Further evidence for a link between beta oscillations and cognitive control stems from prefrontal recordings (Siegel et al., 2009). When the order of two objects had to be held in short-term memory, this information appeared to be maintained in prefrontal cortex by spiking activity that was locked to a 32 Hz oscillation but segregated by appearing at two distinct phases according to object order. This phase-delayed chunking of activity was specific to 32 Hz, which suggests that beta oscillations in PFC present a framework for multiplexed information processing.

Based on my results and the existing literature, I would like to speculate that beta oscillations pose a broad mechanism to integrate sensory information, compare it with goal-dependent predictions and help to feed the result of this comparison selectively back into the motor system. Periods of high beta oscillations, which I will refer to as "beta episodes", may provide an answer to the all-important question "Can I stick with my movement strategy or not?" Only if the answer is yes, when the sampled sensory state is well aligned with the desired state, beta power would be high. Hence, not the status quo (Engel and Fries, 2010) but more generally the current motor strategy would be maintained.

This is not a new idea. Already 20 years ago, William MacKay suggested that "synchronous oscillatory activity may be an integrative sensorimotor mechanism for gathering information that can be used to guide subsequent motor actions." (MacKay, 1997). More recently, Feingold et al (2015) studied post-movement beta episodes in the striatum and cortex and suggested that "a substantial fraction of beta bursts that

follow task completion could be related to modifying or maintaining the strengths of the connections involved in task performance." It has further been argued that beta oscillations play an important role in consolidating and reinforcing muscle synergies (Aumann and Prut, 2015). This seems plausible considering that cortico-spinal beta coherence also was found to correlate with complex motor learning (Houweling et al., 2010).

Alternatively, high post-movement beta oscillations may not have a functional role but may merely appear when less correlated activity is not needed. For motor adjustments or learning that would require connectivity changes, less correlated activity may be necessary considering that highly correlated activity seems to limit information coding capacities (Hanslmayr et al., 2012). The phase of an oscillation has been shown to be critical in providing temporal windows within which information can be relayed (van Elswijk et al., 2010). If beta oscillations indeed mediate selective information routing (Fries, 2015), then one may ask why beta power is reduced during sensorimotor updating (Cao and Hu, 2016), which needs to be selective particularly when complex movements are updated. Subpopulations may still oscillate at beta frequencies, but with a phase shift relative to each other to carry information in a segregated way. If that were the case then the superimposition of fluctuations may result in a reduced rebound in the population average even though individual ensembles may still be entrained to beta rhythms. Phase-locking of STN spikes to cortical beta commonly occurs between two consecutive movements but has also been observed during movements in some cells despite reduced cortical LFP power (Lipski et al., 2017).

Some studies reported reduced sensory detection abilities after periods of high beta power (Jones et al., 2010; Schubert et al., 2008) while others reported an inverse relationship (Donner et al., 2007; Gross et al., 2004; Hanslmayr et al., 2007; Kamiński et al., 2012; Linkenkaer-Hansen et al., 2004; Zhang et al., 2008). Beta episodes may represent a comparison process that occurs not concurrently with but only after the sampling process, i.e. after movement completion (Tan et al., 2014b; Torrecillos et al., 2015). This comparison process may even impair new sensory information from

reaching conscious perception. Motor-evoked potentials were for example found to be reduced during periods of high post-movement beta, which indicates that this particular brain state attenuates information relay (Chen et al., 1998; Schulz et al., 2014).

Anticipation of a tactile stimulus also is preceded by a decrease in pre-stimulus beta power (Bauer et al., 2006), which in turn was associated with faster response times (van Ede et al., 2011) and particularly with better detection probabilities (Jones et al., 2010; Schubert et al., 2008; van Ede et al., 2012). When recorded from the scalp, many cells would need to oscillate synchronously during high-amplitude beta episodes, which presumably implies relatively non-selective processing or low capacity for information encoding (Hanslmayr et al., 2012). If the sensorimotor system already anticipates a sensory change, then pre-emptive suppression of synchronization may allow for more selective and dynamic processing that could mediate enhanced attention.

In the tapping experiment, we also investigated how well an upcoming movement could be adjusted, or more specifically, stopped. Stopping was particularly of interest as beta has been labelled to be inhibitory or anti-kinetic in the past (Ray et al., 2012; Sacchet et al., 2015; Sherman et al., 2016; Wessel et al., 2016a). Thus, if high beta power indeed supports movement inhibition, beta power should increase during stopping. We found that relatively increased cortical post-movement beta was related to successful stopping before participants knew they had to stop in both studies, but not during stopping. This thus does not support the notion that cortical beta mediates actual inhibition of an ongoing movement. Also in the STN – a crucial node in the motor inhibition network (Jahanshahi et al., 2015) – increased beta has been observed in stop tasks in the past (Alegre et al., 2013; Bastin et al., 2014; Benis et al., 2014; Ray et al., 2012). But we found that not even STN beta power increased in our task. Instead, a robust and fast gamma increase became apparent, which will be discussed below. Previously, periods of increased beta were observed when a resting posture was maintained both in Go/NoGo (Kühn et al., 2004) and stop signal tasks (Alegre et al., 2013; Bastin et al., 2014; Benis et al., 2014; Ray et al., 2012). Successful stopping

meant that a brief movement, often a button press, was interrupted before it had been initiated. Instead of having a chance to stop halfway, as in our task, the button press had to be completely cancelled, otherwise stopping would have failed. Beta oscillations thus seemed to appear after the movement initiation process had been stopped and the resting posture was maintained, i.e. no change had to be made. Altogether, this rejects the idea that abrupt stopping of an *already initiated action* is implemented by beta synchrony. Instead, beta oscillations in motor areas seem to appear when a posture is maintained as a consequence of successful stopping rather than as requirement.

Beta oscillations during stopping were previously found to increase in prefrontal cortex and were linked to braking (Aron et al., 2014). Again, if beta oscillations reflect top-down control, this increase could mediate selective instruction- or goal-dependent targeting of only those assemblies corresponding to the effector that needs to be stopped, possibly via fronto-striatal inputs as an fMRI study suggested (Majid et al., 2013).

Yet interestingly, we observed a relationship between beta and stopping success before participants knew they had to stop. Experiment 1 already suggested a possible role of beta in timing. Increased beta may have reflected that the next tap was going to be slightly delayed, which would thus facilitate stopping. If this was the case, then in further experiments, high beta should only correlate with faster stopping of a repetitive movement but not with movement initiation of an effector that is not involved in the ongoing movement itself. Conversely, if elevated beta did not reflect a subsequent movement delay, a relative lack of it may have simply indicated that cognitive resources were occupied. If participants spent more conscious cognitive effort on synchronizing with the sound, which they probably had to when they were late, then reacting to the stop signal likely took longer than when the movement was more automatic. If that was the case, reaction times should not only be slowed down for stopping but also for secondary, newly initiated movements.

Note that when the task was not demanding in the CONTINUE condition, post-movement beta was again relatively high providing more evidence for a relative beta reduction because of high cognitive or attentional load. According to the above outlined hypothesis that high beta may reflect maintenance of a motor strategy, awareness of the fact that the movement strategy may need to be changed at any one point should result in reduced levels of beta activity, similar as in the sensory perception task (Bauer et al., 2006; van Ede et al., 2014) and during sensorimotor adaptation (Tan et al., 2016b). Importantly, this task comparison also suggests that cortical beta oscillations were beyond conscious control. If they had been consciously controlled, they should have been more abundant in the STOP than in the CONTINUE condition as they seemed to be beneficial prior to stopping.

Note also, that in the STN we found no such relationship between post-movement beta and subsequent stopping success despite superior signal-to-noise ratio of LFPs and evidence for a role of STN beta in post-movement evaluation (Tan et al., 2014b).

In the final experiment, the beta decrease during imagined gripping suggests that beta fluctuations in the STN depend on grip force intentions. This indicates that even in the absence of muscle activation and sensory feedback, the level of beta oscillations in the STN reflects the neuronal recruitment during a movement that was only imagined. During prolonged sustained contractions, beta oscillations in the STN reappear (personal communication) similar as in M1 (Baker et al., 1997; Spinks et al., 2008) and seem to aid sustained activation of the current set of motor units. In unstable grip conditions, cortico-muscular beta coherence is relatively reduced (Reyes et al., 2017). As the sensory feedback continuously calls for small motor adjustments under unstable grip conditions, this is also in line with the proposed link between beta and maintenance of the momentary motor strategy

Finally, the high probability of beta oscillations during rest (Engel and Fries, 2010) where motor plans remain the same and about two thirds of sensorimotor cells are entrained to 20-40 Hz oscillations (Murthy et al., 1996) also fits well with this idea.

7.2 Gamma oscillations for fast motor inhibition and movement initiation

Gamma activity in the STN has repeatedly been interpreted as pro-kinetic rhythm (Cassidy et al., 2002; Fogelson et al., 2005; Litvak et al., 2012). But the results of Chapter 5 suggest that gamma oscillations within the basal ganglia have a more flexible role in motor control that is not limited to movement initiation but also extends to motor inhibition. Chapter 6 furthermore suggests that gamma oscillations are also important for regulating movement kinematics.

Why would gamma oscillations be suitable to contribute to these functions?

Gamma oscillations emerge from recurrent inhibitory and often excitatory activity (Gyorgi and Wang, 2012) such that periods of inhibition restrict postsynaptic spiking activity to short temporal windows within each cycle (Fries et al., 2007). In the visual system, gamma oscillations seem to facilitate synchronization between cells that represent coherent objects. This observation has led to theories of gamma oscillations enabling '*binding by synchrony*' (Singer, 1999). Later, gamma oscillations have also been theorised to establish *'communication through coherence'* (Fries, 2005).

During movement initiation, gamma-rhythmic activity seems to propagate from the basal ganglia to motor cortex (Litvak et al., 2012). Movement-related gamma activity in the contralateral thalamus also correlates well with reaction times (Brücke et al., 2013). Gamma-rhythmic activity has been suggested to reflect activation of cortico-subcortical pathways modulating the output of the indirect pathway to facilitate movement execution (Cheyne et al., 2008). In the STN and cortex, neuronal activity was found to be phase-locked to the gamma-cycle (Nir et al., 2007; Trottenberg et al., 2006; Womelsdorf et al., 2007), and thus gamma oscillations indeed come with constrained windows of increased spiking probability. In the STN, this was reported during rest (Trottenberg et al., 2006) and in cortex during auditory and visual processing (Nir et al., 2007; Womelsdorf et al., 2007). The literature also suggests that

gamma oscillations at movement onset reflect an active component of motor control as no similar increase was observed during passive movements, excluding proprioceptive origins (Muthukumaraswamy, 2010). In Chapter 6, we showed that STN gamma oscillations were enhanced during imagined gripping, i.e. already during formation of movement intentions. The power increase with increasing target force suggests recruitment of a larger network of cells oscillating at a gamma rhythm when the motor system prepares for stronger muscle contractions.

It seems that oscillations in the 75-100 Hz gamma range are especially important for dynamic control of muscle activation and less so during static contractions as they soon subside after initial force production onset even when a tonic contraction is maintained (Crone, 1998; Muthukumaraswamy, 2010). The importance of gamma for dynamic motor control has further been corroborated by the observation that corticospinal synchronization increases during force adjustments (Andrykiewicz et al., 2007; Omlor et al., 2007; Schoffelen et al., 2005). Selective motor unit activation thus seems to rely on a gamma-rhythmic mechanism to prevent co-activation of non-selected motor units.

Action stopping as examined in Chapters 4+5, may simply be implemented by overwhelming cortically triggered inhibitory drive from the basal ganglia to the thalamus. But what if stopping should be more selective? It seems that revving up discharge rates of inhibitory cells would not be energy-efficient and may not even successfully silence thalamic firing activity considering that discharge of inhibitory pallidal neurons can cause rebound spikes and thus complex thalamic activity patterns (Goldberg et al., 2013; Person and Perkel, 2005). If the *communication-through-coherence* theory (Fries, 2015) also applies to action selection, then phase-cancellation may be a more elegant mechanism to interrupt actions midway. According to this theory, gamma oscillations, and respective inhibitory neuronal firing activity, allow pre-synaptic spike integration only in very brief temporal windows. If rhythmic STN firing activity is phase-shifted in response to a stop signal, these brief windows, that may allow spike integration across the basal ganglia-motor cortical circuit, would also be shifted. As a result, pre-synaptic spikes may then arrive when the synaptic gain is

strongly reduced. A sudden surge in gamma, as we observed, could easily imply a phase shift and thus might shut the door for descending motor commands, such that any upcoming muscle contractions would be cancelled (*Figure 7.1*).

We did not observe a gamma increase in the stimulus-matched control condition in which patients did not attempt to stop. As the control condition differed only in the instruction, this suggests that the gamma increase is driven by frontal areas exerting executive control (Robbins, 1996; Stuss and Stuss, 1992). Indeed, stop-signal evoked gamma activity was also observed in MEG and ECoG recordings from pre-SMA and right prefrontal cortex (Jha et al., 2015; Swann et al., 2012). Particularly prefrontal cortex seems to provide a flexible selection mechanism for re-routing information flow to allow rapid behavioural changes according to current goals (Stokes et al., 2017). This would need to be implemented via changes in effective connectivity that could be mediated by altered inter-regional coupling and population synchrony or short-term synaptic plasticity (Stokes et al., 2017).

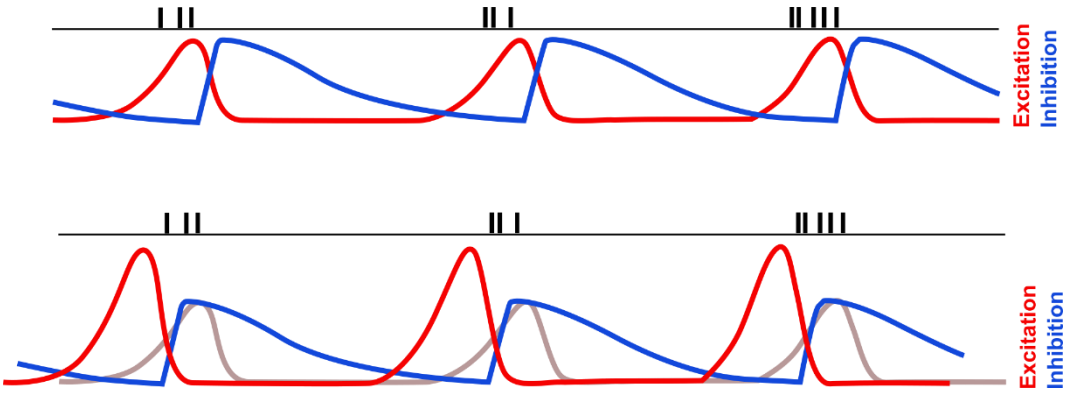

Figure 7.1 Schematic of temporally shifted excitatory and inhibitory post-synaptic potential fluctuations. The upper panel shows how afferent spikes arrive within the brief excitatory window of each gamma cycle (adapted from Fries, 2015). In the lower panel, the windows are shifted by an earlier excitation and spikes would arrive at periods of relative inhibition.

It seems plausible that the stop-related gamma increase originated cortically and was then propagated to the STN via the hyperdirect pathway. In contrast to this, pro-kinetic gamma oscillations may travel through the basal ganglia via the striatum or may even originate within the GPe-STN loop as suggested recently (Blenkinsop et al., 2017). If the pro-kinetic gamma troughs and peaks are superimposed with a temporally shifted stop-related gamma rhythm arriving through the hyperdirect pathway, then this collision may derail cortico-basal ganglia-thalamic coherence such that motor output gets blocked (*Figure 7.1*). Abrupt 180° flips in the phase-offset between two spatially separated ensembles have already been discovered for frequencies in the beta range (Dotson and Gray, 2016; Dotson et al., 2014). These phase-flips occurred between prefrontal and parietal populations at the end of a working memory task and have been termed phase-flip transitions. To date, it has not yet been shown if similar task-dependent phase-flip transitions also occur in the gamma range, probably partly because such transitions would be harder to detect for higher frequencies.

Frequencies in the gamma range seem to be intuitively better suited than lower frequencies to aid interruption of movement-related discharge rates of more than 30 Hz (Baker et al., 2001; Grammont and Riehle, 2003). A recent computational model also proposed that movement-related gamma oscillations are not generated by the neurons encoding an action (Blenkinsop et al., 2017) but by those coding for actions that were not selected. If that were indeed the case, the STN gamma increase in our stop task may also reflect stronger activity of cells that would have not been involved in the tapping movement.

Finally, I would like to discuss how some analyses performed on past data from other motor inhibition tasks may have been biased by the prior belief that gamma is pro-kinetic and that theta and beta oscillations instead are meant to be reliable markers of stopping (Wessel et al., 2016a; Wessel and Aron, 2016, 2014). Theta was shown to correlate with stopping, but this low-frequency phase-reset like response is spatially very broadly distributed and does not seem to be temporally or spatially finely enough resolved to cancel only parts of an action. Much more likely it reflects the brain's

response to an unexpected salient cue that may subsequently lead to stopping but does not implement it. Likewise, the beta increase is also more likely to be epiphenomenal as beta seems to be enhanced when a posture is maintained but not when a movement was interrupted halfway. Further insights about the sequence of cortico-basal ganglia events may be gained from re-analysing past studies that obtained STN LFPs during movement inhibition tasks but used extensive temporal smoothing or did not consider gamma frequencies at all.

7.3 Predictions about beta and gamma oscillations in motor control

Beta and gamma oscillations appear to complement each other during motor control. Beta oscillations seemingly help to integrate and feed sensory feedback into the motor system to strengthen or weaken within-loop connectivity (Aumann and Prut, 2015; Feingold et al., 2015). In turn, gamma oscillations may provide temporal windows to facilitate selection of cell assemblies that are required to execute an action. This temporal framework, mediated by gamma oscillations, may likely be provided by the basal ganglia (Litvak et al., 2012) and rapidly withdrawn with a gamma increase during stopping as discussed above.

Previous work has shown high spatial overlap between concurrently decreasing motor cortical beta power and increasing cortico-spinal gamma coherence during movement anticipation (Schoffelen et al., 2005). This may imply that the very same population oscillating between 15-30 Hz prior to movement switches to a gamma rhythm at movement onset. However, in the STN, the sites of beta and gamma peak activity do not always overlap, with gamma being localized more superior (Trottenberg et al., 2006; van Wijk et al., 2017).

STN gamma and beta oscillations both also seem to reflect the extent of muscle activation. The decrease in STN beta oscillations with increasing vigour (Tan et al.,

2016a, 2013) is probably epiphenomenal and reflects that for stronger contractions more fibres are recruited to fire at increased rates or in a less correlated fashion. If more cells break away from oscillating at beta frequencies by increasing their firing rates, beta power would necessarily drop. Note also, that firing activity during production of low force levels is not necessarily gamma-rhythmic, as a gamma increase was only observed for very high force levels (Tan et al., 2013). Gamma activity thus particularly seems to provide a means to regulate the extent and speed of fast, strong and transient muscle contractions (Brücke et al., 2012; Joundi et al., 2012), and if necessary also to cancel a movement midway.

In the following section, I will outline two predictions following from the discussed observations. My first prediction is that post-movement beta oscillations help to feed sensory consequences back to the motor system selectively to the appropriate assemblies, such that the next movement can be prepared. Experiments in non-human primates may be able to show if post-movement beta episodes indeed play a role in returning modality-specific sensory information to the motor system. The animal would receive feedback about the direction of the next movement upon movement completion either in the visual or auditory domain. I would hope to see that single-cell recordings from direction-selective cells that show preparatory activity already before the next movement (Confais et al., 2012; Grammont and Riehle, 2003; Rao and Donoghue, 2014) are entrained to post-movement beta LFP oscillations obtained from the primary sensory area through which the relevant stimulus arrives (*Figure 7.2*). Additionally, stimuli may also be presented simultaneously in both modalities while the animal is cued to attend only one modality and use its direction information prior to each trial. I would again expect significantly higher beta coherence between motor areas and the primary sensory area (V1 or A1) that processes the attended auditory or visual feedback despite both areas receiving sensory information. If post-movement beta oscillations would result in entrainment only to reinforce a motor strategy, and not only to assist in motor preparation, I would only expect those cells to be entrained that were active in the last movement and will again be active in the next movement.

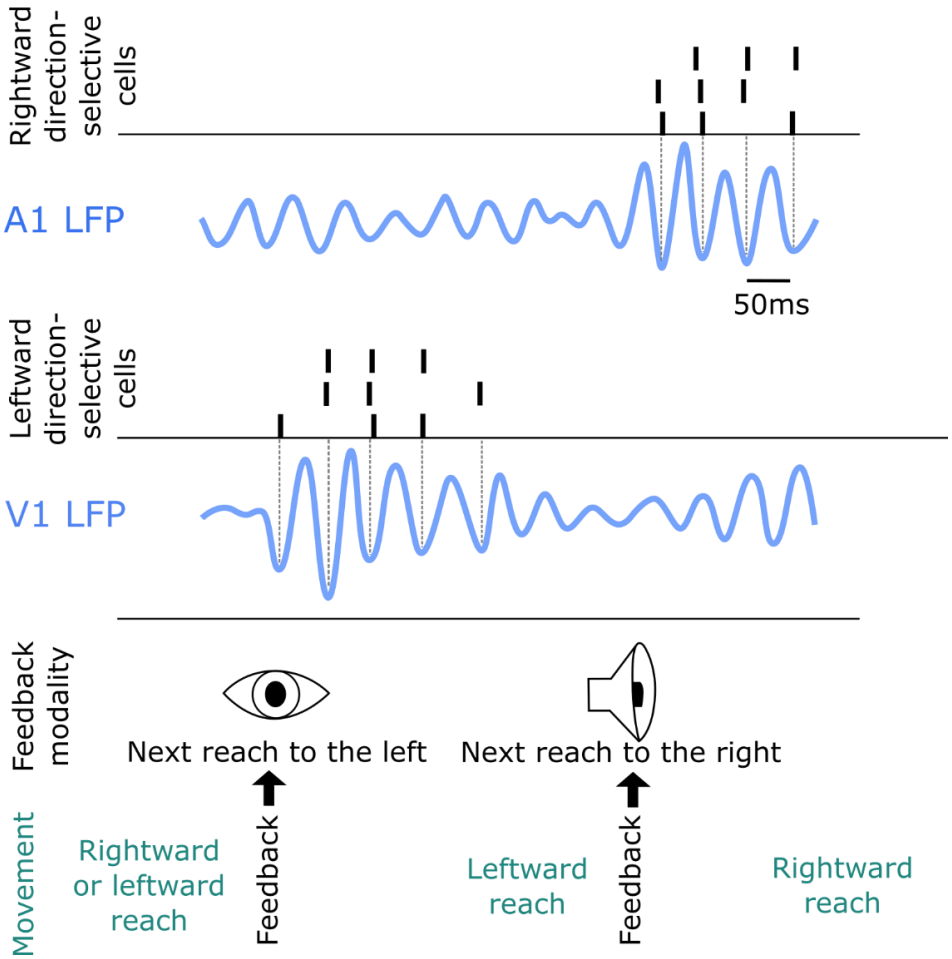

Figure 7.2 Schematic of spike entrainment to post-movement beta oscillations. Feedback is provided after each reaching movement to signal that the next reach should be either a leftward or a rightward reach. The feedback is either a visual or auditory signal. I would expect direction-selective cells that are tuned to the upcoming movement to synchronize with the sensory region that receives the feedback in preparation of the next movement. I would predict that this inter-site locking occurs at beta frequencies.

My second prediction is that the STN gamma increase contributes to action stopping by appearing earlier, with a phase-offset and a higher amplitude than the pro-kinetic gamma rhythm that builds up before action onset. If the movement-related increase in gamma coherence between STN and motor cortex (Litvak et al., 2012) reflects that converging input coincides at a specific phase of the coupled gamma cycle, then a bout of phase-shifted gamma activity in one of the nodes of the network (the STN in this case) may lead to post-synaptic activity cancelation. Laminar LFP recordings from M1,

prefrontal and non-primary motor areas, particularly the pre-SMA, in combination with LFPs from the STN and motor thalamus and M1 layer 5 single cell activity may provide further details of the ongoing dynamic interactions. First, it would be interesting to test if the stop-related gamma-increase in the STN is phase-locked to the one reported in the pre-SMA (Jha et al., 2015; Swann et al., 2012) or if gamma from these two regions is already decoupled, which may be achieved by the recurrent basal ganglia loops. Next, the down-stream effects on the thalamus should be evaluated. If no gamma increase can be observed in the thalamus, as would be expected during movement (Brücke et al., 2013), this would indicate that phase-shift mediated activity cancellation already happens before being propagated to the thalamus. Phase-shift based activity cancellation may happen already within the basal ganglia itself, e.g. in the striatum. Schmidt et al (2013) observed that striatal neurons that would usually fire during action execution remained silent during successful action cancellation, i.e. that they did not even show a stop signal-related increase. They also observed that many STN cells responded to the stop signal only with a single spike. Subsequent STN- or even cortically-driven activation of arkypallidal cells (Mallet et al., 2016), however, may nevertheless result in reverberations that could be reflected in a stop-related gamma power increase.

If action selection indeed involves disinhibition of the thalamus via pro-kinetic basal ganglia gamma oscillations as hypothesized elsewhere (Cheyne, 2013), then two opposing gamma rhythms that would result in fluctuating levels of excitation and inhibition but meet each other within a node of the basal ganglia circuit, as discussed above, may cancel each other out. This may be a very fast and energy-efficient mode of action cancellation. In summary, I would like to propose that the gamma increase reflects a stop-process that can cancel a striatal go-process if it appears early enough.

7.4 Limitations of this thesis

The speculations in the previous section show that, undoubtedly, we are still far from understanding the precise mechanisms behind the functional role of oscillations in motor control. We do not know the origin of the observed oscillatory changes and to which extent spiking activity was entrained. The LFP reflects a superimposition of excitatory and inhibitory synaptic currents, intrinsic membrane oscillations, and fields generated by spikes and afterhyperpolarization (Buzsáki et al., 2012). Hence we would need multi-unit recordings to link our findings to neuronal firing. Unfortunately, we were not able to obtain these in the post-operative recordings.

We designed three different tasks to infer how STN activity is modulated during flexible motor control. One may argue that electrophysiological activity in the basal ganglia from Parkinson's disease patients differs substantially from healthy brain activity, which may mean that the generalizability of our findings is limited. Micro-lesions caused by the electrode insertion procedure may have also affected the spectral dynamics of the LFP recordings. But importantly, patients were able to perform all tasks, which implies that physiological activity must have been present at least to some extent. Basal ganglia and thalamic beta and gamma oscillations have also been shown to be task-modulated in non-Parkinsonian populations, as in dystonia patients (Brücke et al., 2012), essential tremor patients (Brücke et al., 2013), OCD patients (Bastin et al., 2014) and healthy monkeys (Courtemanche et al., 2003). Furthermore, patients were recorded on dopamine replacement therapy, which has been shown to partially normalize pathological activity (Androulidakis et al., 2007b; Doyle et al., 2005; Johnson, 2008). Additionally, some effects, such as increased pre-stop signal cortical beta preceding successful stopping, were not only observed in patients but also in healthy participants.

As we did not have access to post-operative imaging data of sufficient resolution to localize the electrode position, we could not link effect sizes to specific STN subdivisions (Lambert et al., 2012) nor can we exclude contribution of activity from

nearby structures (Buzsáki et al., 2012) such as the thalamus or the SNr given the small size of the STN. However, several studies demonstrated that beta oscillations, and thus presumably also modulation of beta oscillations, which was present in all tasks, are most pronounced in the dorsolateral sensorimotor region of the STN (Accolla et al., 2016; Chen et al., 2006; Horn et al., 2017; Zaidel et al., 2010). Additionally, our analyses were performed not with monopolar recordings but with bipolar recordings of neighbouring contacts, which were shown to be suitable for detecting locally generated neuronal activity (Marmor et al., 2017).

Due to the correlative nature of LFP or EEG recordings, we cannot infer that any of the electrophysiological correlates were causal to the concurrently observed behaviour such as successful stopping. As a next step, one could try to intervene with the system by stimulation with tACS, TMS or even DBS (Herrmann et al., 2016) at critical time-points of a task. However, if one fundamental function of oscillations is to segregate ensembles that may be located nearby but are not meant to be co-activated, such coarse stimulation techniques would fail to mimic how 20 Hz or 60 Hz oscillations would otherwise act in a population- and layer-specific manner. Optogenetic methods would allow for much more fine-tuned targeting of populations, and can even be used to simulate naturally occurring activity (Emiliani et al., 2015). But despite a rapid expansion of stimulation methods, careful manipulations of task conditions while recording unperturbed brain activity (ideally, at multiple sites and scales) are still an important tool to understand the workings of the brain without interference. During rhythmic tapping, post-movement cortical beta seemed to relate at least to some extent to whether the next tap could be successfully stopped. Stopping success crucially depends on the intended time of movement initiation and on whether the stop signal is attended with a certain readiness to stop. As detailed above, this suggests that beta was relatively high either when the next tap was late or when attention was not diverted, which would both imply that post-movement beta oscillations are at least to some extent part of a processing chain for adaptive, flexible behaviour. The amplitude and timing of beta episodes can be highly variable across trials (Feingold et al., 2015;

Williams et al., 2005), which seems to be a major challenge for mapping brain activity to behaviour. This is certainly related to multiple cognitive processes such as cue processing, memory retrieval, movement preparation, time estimation, etc. overlapping at any one time, which cannot be accessed or clearly separated.

7.5 Open questions for future studies

As pointed out in the previous section, it will be important to investigate the link between firing activity and the observed LFP changes in future studies.

Another big open question is, what or where is the origin of the stop-related gamma increase? It may be mediated by synchronous input. But why does it propagate through the STN? Is the STN crucial because of its position within recurrent basal ganglia loops? Or is it its intrinsic organization, with only a small fraction of GABAergic interneurons (Levesque and Parent, 2005) that can achieve the hypothesized shift in excitable periods for movement cancelation? And how does the gamma increase in the STN translate to output onto thalamus and cortex?

Further important considerations are: How do other parts of the brain, such as the cerebellum, contribute to the observed changes? It may well be that the improvement of stepping synchronization with auditory cueing was in part due to stronger involvement of the cerebellum. For example, stronger recruitment of the cerebellum was associated with keeping gait variability relatively low in a similar paradigm when patients were on dopaminergic medication (Gilat et al., 2017). An important role may also fall to the hippocampus for acting according to an instruction, i.e. for remembering whether to stop or to continue, in response to an identical stop signal stimulus. Novelty detection, for example, was proposed to occur within a hippocampus-nucleus accumbens-ventral tegmental dopaminergic loop using gamma activity (Axmacher et al., 2010; Lisman et al., 2005; Marco-Pallarés et al., 2015). If multi-site recordings were

available, dynamic causal modelling or Granger causality (Friston et al., 2013) may be useful tools to investigate functional or effective connectivity between regions.

Another open question is whether the often broadly defined 13-30 Hz beta band should be further divided into sub-bands. Healthy subjects seemed to demonstrate a special role of 12-20 Hz beta in the tapping task whereas STN beta modulation during stepping-in-place was most pronounced between 20-30 Hz. If one takes a closer look at the time-frequency spectrogram of stepping in *Figure 3.3*. 12-20 Hz beta seems to peak twice, i.e. also when the ipsilateral foot was on the ground and the contralateral foot was moved. One may speculate whether 20-30 Hz beta may be more important for limb segregation (i.e. carrying information about the left and right leg in a segregated manner) while 12-20 Hz may be more important for sensorimotor integration and timing irrespective of the effector side. In a delayed movement task in monkeys it has also been shown that peak frequencies of modulated beta activity were lower during temporal expectation than during movement preparation (Kilavik et al., 2012). Shifts in peak frequencies may be critical and thus time-frequency results should always be presented first in two-dimensional frequency-resolved spectrograms that show power changes across a broad frequency spectrum instead of only presenting the average power time course of undifferentiated 12-30 Hz beta.

7.6 Links to the symptoms of Parkinson's disease

The symptoms of Parkinson's disease are characterized by rigidity, i.e. failure to selectively activate or de-activate appropriate motor units, bradykinesia, which resembles failure to invigorate movements, and involuntary stopping as in freezing of gait. As outlined in the introduction, patients also exhibit sensorimotor synchronization and action switching deficits.

Although I would argue that beta oscillations do not implement inhibition of an ongoing movement, pathological beta oscillations may still have a detrimental effect on

motor control in Parkinson's disease. If beta oscillations mediate selection of coherent muscles to perform meaningful actions or to adjust movement strategies, beta hypersynchrony may result in co-activation of ensembles, which would otherwise be segregated if all cells were intact. This non-selectivity would then result in pathological co- and over-activation of muscles as observed in rigidity. In support of this, spiking activity recorded from muscles that exhibited rigidity were locked to thalamic beta oscillations (Narabayashi and Oshima, 2014), and beta was particularly pronounced in patients with rigidity as dominant symptom in comparison to patients with tremor (Beudel et al., 2017; Miyashita et al., 2016; Neumann et al., 2017). Furthermore, reduced STN beta variability was also related to rigidity (Little et al., 2012). DBS at beta frequencies has even been shown to exacerbate motor symptoms (Chen et al., 2007). This does not seem surprising if 20 Hz DBS would force a large set of cells to rigidly follow one and the same rhythm instead of allowing the relevant assemblies to tune in and out of different beta rhythms in a flexible way. If beta indeed plays a role in timing and integrating sensory feedback as our results suggest, then rhythmic interlimb-coordination, and sensorimotor synchronization deficits also likely result from dysfunctional beta that would also restrict a functional increase. For example, the post-movement rebound in patients is reduced (Pfurtscheller, 1998) and only when patients were on medication, beta increased in response to a cue signalling that the current posture should be maintained (Oswal et al., 2012).

Interestingly, beta coherence across cortical regions is elevated in untreated patients whereas beta power within motor cortex seems to be relatively unchanged or even reduced (Heinrichs-Graham et al., 2014; Silberstein et al., 2005). Coherence between the STN and motor regions is increased when patients are off DBS (Oswal et al., 2016) and medication (Hirschmann et al., 2013), and thus increased phase-locking with cortex coincides with local hypersynchrony in the basal ganglia. Yet, the final stage of motor control, i.e. M1 cortico-muscular coherence, was not found to be systematically affected by deep brain stimulation (Airaksinen et al., 2015) or medication when tremor-free data was selected (Hirschmann et al., 2013).

I would like to put forward that episodes of synchronized beta oscillations may not necessarily cause motor inhibition and akinesia per se, but that Parkinsonian symptoms rather originate from a disruption of their original function. It has recently been shown that episodes of STN beta synchronization last particularly long when dopamine levels are low (Tinkhauser et al., 2017), showing that the synchronization dynamics for individual beta episodes are altered. Yet, shorter episodes may still reflect functionally relevant and useful beta in the system.

In patients off dopamine, movement-related contralateral STN gamma synchronization seems absent (Androulidakis et al., 2007b) and STN-M1 gamma coherence is reduced (Litvak et al., 2012). The STN integrates inhibitory pallidal and excitatory cortical input, and thus stark imbalance between these inputs should be detrimental to normal function. It has previously been suggested that gamma oscillations in the basal ganglia contribute to the regulation of movement vigour (Jenkinson et al., 2013), a key function of the basal ganglia (Dudman and Krakauer, 2016). If gamma oscillations indeed provide a framework for initiating or invigorating movements, as supported by Chapter 6, then bradykinesia could result from a failure to establish the right balance or timing of input arriving via the striatum and the hyperdirect pathway such that in M1 not all intended ensembles are activated or that unintended ensembles are wrongly co-activated. A computational model recently suggested that gamma entrains those cells that represent actions that are suppressed instead of activated (Blenkinsop et al., 2017). The proposed mechanism depends on a fine balance of cross-channel-inhibition in the striatum and GPe and cross-channel-excitation from the STN. One can easily imagine that proper segregation fails when reduced dopamine levels result in STN hyperactivity.

Following from Chapter 5, Parkinsonian impairments in switching and inhibiting actions are likely related to dysfunctional gamma activity as well. Other studies have already suggested a role for gamma oscillations in switching in line with this (Anzak et al., 2013, 2011)

Both, the direct and indirect pathway are co-activated during movement (Cui et al., 2013; O'Hare et al., 2016), possibly to suppress competing actions. As suppression needs to happen selectively, both beta and gamma oscillations could play a role in this filtering process considering that oscillations seem to provide a simple mechanism to establish temporal coherence between selected assemblies (Cannon et al., 2014). In Parkinson's disease, movement-related gamma is not only reduced but gamma oscillations seem to be trapped by exaggerated beta-gamma phase-amplitude coupling (de Hemptinne et al., 2015; van Wijk et al., 2016), as if they would lose flexibility that would otherwise be a feature of healthy circuits.

7.7 Implications for using the local field potential as feedback signal

Chapter 6 suggests that beta and gamma activity can be modified by motor imagery without moving and without altered proprioceptive feedback. This may be explored as neuro-feedback signal to enhance beta and gamma changes during physical exercise. Naros et al (2016) have recently demonstrated that motor performance in healthy subjects improved after they received contingent neuro-feedback on the strength of a motor imagery-induced sensorimotor beta decrease. Patients struggle to move fast and are unaware of strategies that may allow them to move faster. If they could practise to either decrease beta or increase gamma activity in sessions in which they receive neuro-feedback, they may improve their mobility by accessing these strategies. Apart from the therapeutic benefit, this research may provide evidence for a causal role of gamma oscillations in motor control if enhancement of movement vigour would exclusively be found after gamma upregulation.

STN LFP activity may also be used as add-on to fNIRS communication in completely locked-in patients to improve decoding accuracy (Chaudhary et al., 2017, 2016; Gallegos-Ayala et al., 2014). Cortical EEG has not been very useful to date, however

activity from the basal ganglia may outperform EEG activity considering that the LFP seems to be a stable signal with a better signal-to-noise ratio (Hanrahan et al., 2016) and that imagined gripping poses an easy mental task.

Finally, I would like to suggest an extension for adaptive deep brain stimulation strategies to improve gait control. If adaptive deep brain stimulation is applied whenever beta oscillations exceed a certain threshold, it would be active exactly in the post-movement period, which I think may be crucial for rhythmic gait. It would not be active during movement, although DBS is provided to facilitate movement (Klostermann et al., 2010; Kumru et al., 2004). An alternative to this would be to stimulate the left and the right STN in an alternating pattern, such that stimulation intensity ramps up before the contralateral foot is lifted to support the naturally occurring beta desynchronization. Stimulation intensity would be high only briefly, such that the post-movement rebound can still occur. Stimulating the two STN at different points may also be helpful to prevent hypersynchrony, which could also arise from inter-hemispheric cross-talk. It remains to be seen if gait needs to be tracked to adjust the stimulation pattern to the gait cycle or if patients automatically adjust to the provided rhythm. Considering that rhythmic cues automatically result in motor entrainment (Thaut et al., 1992; Yoles-Frenkel et al., 2016), alternating DBS at a comfortable pace may even provide benefits without tracking gait.

7.8 Conclusion

I would like to conclude with calling for a more nuanced view of beta and gamma oscillations in motor control. Although with the present experiments I cannot demonstrate a causal role, my work suggests that gamma oscillations are not just pro-kinetic but important for abrupt action stopping as well. Conversely, beta oscillations seem to be more than just anti-kinetic or inhibitory. They seem to aid in sensorimotor integration, in comparing motor outcomes with expectations and in feeding the result back to enable flexible motor control.

8 References

Abbruzzese, G., Avanzino, L., Marchese, R., Pelosin, E., 2015. Action Observation and Motor Imagery : Innovative Cognitive Tools in the Rehabilitation of Parkinson's Disease. Parkinsons. Dis. 2015. doi:10.1155/2015/124214

Abdi, A., Mallet, N., Mohamed, F.Y., Sharott, A., Dodson, P.D., Nakamura, K.C., Suri, S., Avery, S. V, Larvin, J.T., Garas, F.N., Garas, S.N., Vinciati, F., Morin, S., Bezard, E., Baufreton, J., Magill, P.J., 2015. Prototypic and Arkypallidal Neurons in the Dopamine-Intact External Globus Pallidus. J. Neurosci. 35, 6667–6688. doi:10.1523/JNEUROSCI.4662-14.2015

Accolla, E.A., Herrojo Ruiz, M., Horn, A., Schneider, G.-H., Schmitz-Hübsch, T., Draganski, B., Kühn, A.A., 2016. Brain networks modulated by subthalamic nucleus deep brain stimulation. Brain. doi:10.1093/brain/aww182

Airaksinen, K., Mäkelä, J.P., Nurminen, J., Luoma, J., Taulu, S., Ahonen, A., Pekkonen, E., 2015. Cortico-muscular coherence in advanced Parkinson's disease with deep brain stimulation. Clin. Neurophysiol. 126, 748–755. doi:10.1016/j.clinph.2014.07.025

Ajimsha, M.S., Majeed, N.A., Chinnavan, E., Thulasyammal, R.P., 2014. Effectiveness of Autogenic Training in improving motor performances in Parkinson's disease. Complement. Ther. Med. 22, 419–425. doi:10.1016/j.ctim.2014.03.013

Albin, R.L., Young, A.B., Penney, J.B., 1989. The Functional Anatomy of Basal Ganglia Disorders. Trends Neurosci 12, 366–376. doi:10.1146/annurev.ne.06.030183.000445

Alegre, M., Alvarez-Gerriko, I., Valencia, M., Iriarte, J., Artieda, J., 2008. Oscillatory changes related to the forced termination of a movement. Clin. Neurophysiol. 119, 290–300. doi:10.1016/j.clinph.2007.10.017

Alegre, M., De Gurtubay, I.G., Labarga, A., Iriarte, J., Malanda, A., Artieda, J., 2004. Alpha and beta oscillatory activity during a sequence of two movements. Clin. Neurophysiol. 115, 124–130. doi:10.1016/S1388-2457(03)00311-0

Alegre, M., Gurtubay, I.G., Labarga, A., Iriarte, J., Valencia, M., Artieda, J., 2004. Frontal and central oscillatory changes related to different aspects of the motor process: A study in go/no-go paradigms. Exp. Brain Res. 159, 14–22. doi:10.1007/s00221-004-1928-8

Alegre, M., Lopez-Azcarate, J., Obeso, I., Wilkinson, L., Rodriguez-Oroz, M.C., Valencia, M., Garcia-Garcia, D., Guridi, J., Artieda, J., Jahanshahi, M., Obeso, J.A., 2013. The subthalamic nucleus is involved in successful inhibition in the stop-signal task: A local field potential study in Parkinson's disease. Exp. Neurol.

239, 1–12. doi:10.1016/j.expneurol.2012.08.027

Alegre, M., Rodríguez-Oroz, M.C., Valencia, M., Pérez-Alcázar, M., Guridi, J., Iriarte, J., Obeso, J.A., Artieda, J., 2010. Changes in subthalamic activity during movement observation in Parkinson's disease: Is the mirror system mirrored in the basal ganglia? Clin. Neurophysiol. 121, 414–425. doi:10.1016/j.clinph.2009.11.013

Alkemade, A., Schnitzler, A., Forstmann, B.U., 2015. Topographic organization of the human and non-human primate subthalamic nucleus. Brain Struct. Funct. doi:10.1007/s00429-015-1047-2

Allman, M.J., Meck, W.H., 2012. Pathophysiological distortions in time perception and timed performance. Brain 135, 656–677. doi:10.1093/brain/awr210

Almeida, Q.J., Wishart, L.R., Lee, T.D., 2002. Bimanual coordination deficits with Parkinson's disease: the influence of movement speed and external cueing. Mov. Disord. 17, 30–37. doi:10.1002/mds.10030

Androulidakis, A.G., Brücke, C., Kempf, F., Kupsch, A., Aziz, T., Ashkan, K., Kühn, A.A., Brown, P., 2008. Amplitude modulation of oscillatory activity in the subthalamic nucleus during movement. Eur. J. Neurosci. 27, 1277–1284. doi:10.1111/j.1460-9568.2008.06085.x

Androulidakis, A.G., Doyle, L.M.F., Yarrow, K., Litvak, V., Gilbertson, T.P., Brown, P., 2007a. Anticipatory changes in beta synchrony in the human corticospinal system and associated improvements in task performance. Eur. J. Neurosci. 25, 3758–3765. doi:10.1111/j.1460-9568.2007.05620.x

Androulidakis, A.G., Kühn, A.A., Chen, C.C., Blomstedt, P., Kempf, F., Kupsch, A., Schneider, G.-H.H., Doyle, L., Dowsey-Limousin, P., Hariz, M.I., Brown, P., 2007b. Dopaminergic therapy promotes lateralized motor activity in the subthalamic area in Parkinson's disease. Brain 130, 457–468. doi:10.1093/brain/awl358

Andrykiewicz, A., Patino, L., Naranjo, J., Witte, M., Hepp-Reymond, M.-C., Kristeva, R., 2007. Corticomuscular synchronization with small and large dynamic force output. BMC Neurosci. 8, 101. doi:10.1186/1471-2202-8-101

Anzak, A., Gaynor, L., Beigi, M., Foltynie, T., Limousin, P., Zrinzo, L., Brown, P., Jahanshahi, M., 2013. Subthalamic nucleus gamma oscillations mediate a switch from automatic to controlled processing: A study of random number generation in Parkinson's disease. Neuroimage 64, 284–289. doi:10.1016/j.neuroimage.2012.08.068

Anzak, A., Gaynor, L., Beigi, M., Limousin, P., Hariz, M., Zrinzo, L., Foltynie, T., Brown, P., Jahanshahi, M., 2011. A gamma band specific role of the subthalamic nucleus in switching during verbal fluency tasks in Parkinson's disease. Exp.

Neurol. 232, 136–142. doi:10.1016/j.expneurol.2011.07.010

Anzak, A., Tan, H., Pogosyan, A., Foltynie, T., Limousin, P., Zrinzo, L., Hariz, M., Ashkan, K., Bogdanovic, M., Green, A.L., Aziz, T., Brown, P., 2012. Subthalamic nucleus activity optimizes maximal effort motor responses in Parkinson's disease. Brain 135, 2766–2778. doi:10.1093/brain/aws183

Arias, P., Cudeiro, J., 2010. Effect of rhythmic auditory stimulation on gait in parkinsonian patients with and without freezing of Gait. PLoS One 5. doi:10.1371/journal.pone.0009675

Arias, P., Cudeiro, J., 2008. Effects of rhythmic sensory stimulation (auditory, visual) on gait in Parkinson's disease patients. Exp. brain Res. 186, 589–601. doi:10.1007/s00221-007-1263-y

Arlotti, M., Rosa, M., Marceglia, S., Barbieri, S., Priori, A., 2016. The adaptive deep brain stimulation challenge. Park. Relat. Disord. 28, 12–17. doi:10.1016/j.parkreldis.2016.03.020

Aron, A.R., 2011. From reactive to proactive and selective control: developing a richer model for stopping inappropriate responses. Biol. Psychiatry 69, 55–68. doi:10.1016/j.biopsych.2010.07.024.From

Aron, A.R., Behrens, T.E., Smith, S., Frank, M.J., Poldrack, R.A., 2007. Triangulating a Cognitive Control Network Using Diffusion-Weighted Magnetic Resonance Imaging (MRI) and Functional MRI. J. Neurosci. 27, 3743–3752. doi:10.1523/JNEUROSCI.0519-07.2007

Aron, A.R., Cai, W., Badre, D., Robbins, T.W., 2015. Evidence Supports Specific Braking Function for Inferior PFC. Trends Cogn. Sci. 19, 711–712. doi:10.1016/j.tics.2015.09.001

Aron, A.R., Fletcher, P.C., Bullmore, E.T., Sahakian, B.J., Robbins, T.W., 2003. Stop-signal inhibition disrupted by damage to right inferior frontal gyrus in humans. Nat. Neurosci. 6, 115–116. doi:10.1038/nn1003

Aron, A.R., Poldrack, R.A., 2006. Cortical and subcortical contributions to Stop signal response inhibition: role of the subthalamic nucleus. J. Neurosci. 26, 2424–2433. doi:10.1523/JNEUROSCI.4682-05.2006

Aron, A.R., Robbins, T.W., Poldrack, R.A., 2014. Inhibition and the right inferior frontal cortex: one decade on. Trends Cogn. Sci. 18, 177–185. doi:10.1016/j.tics.2013.12.003

Aumann, T.D., Prut, Y., 2015. Do sensorimotor beta-oscillations maintain muscle synergy representations in primary motor cortex? Trends Neurosci. 38, 77–85. doi:10.1016/j.tins.2014.12.002

Avanzino, L., Giannini, A., Tacchino, A., Pelosin, E., Ruggeri, P., Bove, M., 2009. Motor imagery influences the execution of repetitive finger opposition movements. Neurosci. Lett. 466, 11–15. doi:10.1016/j.neulet.2009.09.036

Avanzino, L., Pelosin, E., Martino, D., Abbruzzese, G., 2013. Motor Timing Deficits in Sequential Movements in Parkinson Disease Are Related to Action Planning: A Motor Imagery Study. PLoS One 8, 1–9. doi:10.1371/journal.pone.0075454

Axmacher, N., Cohen, M.X., Fell, J., Haupt, S., Dümpelmann, M., Elger, C.E., Schlaepfer, T.E., Lenartz, D., Sturm, V., Ranganath, C., 2010. Intracranial EEG Correlates of Expectancy and Memory Formation in the Human Hippocampus and Nucleus Accumbens. Neuron 65, 541–549. doi:10.1016/j.neuron.2010.02.006

Baker, S.N., Olivier, E., Lemon, R.N., 1997. Coherent oscillations in monkey motor cortex and hand muscle EMG show task-dependent modulation. J. Physiol. 501, 225–241. doi:10.1111/j.1469-7793.1997.225bo.x

Baker, S.N., Spinks, R., Jackson, A., Lemon, R.N., 2001. Synchronization in monkey motor cortex during a precision grip task. I. Task-dependent modulation in single-unit synchrony. J. Neurophysiol. 85, 869–885. doi:10.1152/jn.00832.2002

Ball, T., Demandt, E., Mutschler, I., Neitzel, E., Mehring, C., Vogt, K., Aertsen, A., Schulze-Bonhage, A., 2008. Movement related activity in the high gamma range of the human EEG. Neuroimage 41, 302–310. doi:10.1016/j.neuroimage.2008.02.032

Bari, A., Robbins, T.W., 2013. Inhibition and impulsivity: Behavioral and neural basis of response control. Prog. Neurobiol. 108, 44–79. doi:10.1016/j.pneurobio.2013.06.005

Bartolo, R., Merchant, H., 2015. Oscillations Are Linked to the Initiation of Sensory-Cued Movement Sequences and the Internal Guidance of Regular Tapping in the Monkey. J. Neurosci. 35, 4635–4640. doi:10.1523/JNEUROSCI.4570-14.2015

Bastin, J., Polosan, M., Benis, D., Goetz, L., Bhattacharjee, M., Piallat, B., Krainik, A., Bougerol, T., Chabardès, S., David, O., 2014. Inhibitory control and error monitoring by human subthalamic neurons. Transl. Psychiatry 2–9. doi:10.1038/tp.2014.73

Bastos, A., M., M., Vezoli, J., Bosman, C.A., Schoffelen, J.M., Oostenveld, R., Dowdall, J.R., DeWeerd, P., Kennedy, H., Fries, P., 2015. Visual areas exert feedforward and feedback influences through distinct frequency channels. Neuron 85, 390–401. doi:10.1016/j.neuron.2014.12.018

Bauer, M., Oostenveld, R., Peeters, M., Fries, P., 2006. Tactile Spatial Attention Enhances Gamma-Band Activity in Somatosensory Cortex and Reduces Low-Frequency Activity in Parieto-Occipital Areas. J. Neurosci. 26, 490–501. doi:10.1523/JNEUROSCI.5228-04.2006

Benis, D., David, O., Lachaux, J.P., Seigneuret, E., Krack, P., Fraix, V., Chabardès, S., Bastin, J., 2014. Subthalamic nucleus activity dissociates proactive and reactive inhibition in patients with Parkinson's disease. Neuroimage 91, 273–281. doi:10.1016/j.neuroimage.2013.10.070

Benis, D., David, O., Piallat, B., Kibleur, A., Goetz, L., Fraix, V., Seigneuret, E., Krack, P., Chabardès, S., 2016. Response inhibition rapidly increases single-neuron responses in the subthalamic nucleus of patients with Parkinson's disease. Cortex. doi:10.1016/j.cortex.2016.09.006

Benjamini, Y., Hochberg, Y., 1995. Benjamini Y, Hochberg Y. Controlling the false discovery rate: a practical and powerful approach to multiple testing. J. R. Stat. Soc. B 57, 289–300. doi:10.2307/2346101

Berchtold, F., Ba, K.T., Pasto, B., Pastötter, B., Berchtold, F., Bäuml, K.H.T., Ba, K.T., Pasto, B., Pastötter, B., Berchtold, F., Bäuml, K.H.T., 2012. Oscillatory correlates of controlled speed-accuracy tradeoff in a response-conflict task. Hum. Brain Mapp. 33, 1834–1849. doi:10.1002/hbm.21322

Beste, C., Saft, C., Andrich, J., M??ller, T., Gold, R., Falkenstein, M., 2007. Time processing in Huntington's disease: A group-control study. PLoS One 2. doi:10.1371/journal.pone.0001263

Beudel, M., Brown, P., 2015. Adaptive deep brain stimulation in Parkinson's disease. Park. &} Relat. Disord. 22, 1–4. doi:10.1016/j.parkreldis.2015.09.028

Beudel, M., Oswal, A., Jha, A., Foltynie, T., Zrinzo, L., Hariz, M., Limousin, P., Litvak, V., 2017. Oscillatory Beta Power Correlates With Akinesia-Rigidity in the Parkinsonian Subthalamic Nucleus. Mov. Disord. 32, 174. doi:10.1002/mds.26860

Bienkiewicz, M.M.N., Craig, C.M., 2015. Parkinson's is time on your side? Evidence for difficulties with sensorimotor synchronization. Front. Neurol. 6, 1–14. doi:10.3389/fneur.2015.00249

Blenkinsop, A., Anderson, S., Gurney, K., 2017. Frequency and function in the basal ganglia: the origins of beta and gamma band activity. J. Physiol. doi:10.1113/JP273760

Bosch-Bouju, C., Hyland, B.I., Parr-Brownlie, L.C., 2013. Motor thalamus integration of cortical, cerebellar and basal ganglia information: implications for normal and parkinsonian conditions. Front. Comput. Neurosci. 7, 1–21. doi:10.3389/fncom.2013.00163

Bosman, C.A., Schoffelen, J., Brunet, N., Oostenveld, R., Bastos, A.M., Womelsdorf, T., Rubehn, B., Stieglitz, T., Weerd, P. De, Fries, P., 2012. Attentional Stimulus Selection through Selective Synchronization between Monkey Visual Areas. Neuron 75, 875–888. doi:10.1016/j.neuron.2012.06.037

Bostan, A.C., Dum, R.P., Strick, P.L., 2010. The basal ganglia communicate with the cerebellum. Proc. Natl. Acad. Sci. 107, 8452–8456. doi:10.1073/pnas.1000496107

Bradford, J.C., Lukos, J.R., Ferris, D.P., 2015. Electrocortical activity distinguishes between uphill and level walking in humans. J. Neurophysiol. jn.00089.2015. doi:10.1152/jn.00089.2015

Brazhnik, E., Novikov, N., McCoy, A.J., Cruz, A. V, Walters, J.R., 2014. Functional correlates of exaggerated oscillatory activity in basal ganglia output in hemiparkinsonian rats. Exp. Neurol. 261, 563–577. doi:10.1016/j.expneurol.2014.07.010

Brittain, J.-S., Watkins, K.E., Joundi, R.A., Ray, N.J., Holland, P., Green, A.L., Aziz, T.Z., Jenkinson, N., 2012. A Role for the Subthalamic Nucleus in Response Inhibition during Conflict. J. Neurosci. 32, 13396–13401. doi:10.1523/JNEUROSCI.2259-12.2012

Brittain, J.S., Brown, P., 2014. Oscillations and the basal ganglia: Motor control and beyond. Neuroimage 85, 637–647. doi:10.1016/j.neuroimage.2013.05.084

Brovelli, A., Ding, M., Ledberg, A., Chen, Y., Nakamura, R., Bressler, S.L., 2004. Beta oscillations in a large-scale sensorimotor cortical network: Directional influences revealed by Granger causality. Proc. Natl. Acad. Sci. 101, 9849–9854. doi:10.1073/pnas.0308538101

Brown, P., 2007. Abnormal oscillatory synchronisation in the motor system leads to impaired movement. Curr. Opin. Neurobiol. 17, 656–664. doi:10.1016/j.conb.2007.12.001

Brown, P., 2003. Oscillatory nature of human basal ganglia activity: relationship to the pathophysiology of Parkinson's disease. Mov. Disord. 18, 357–363.

Brown, P., Oliviero, A., Mazzone, P., Insola, A., Tonali, P., Di Lazzaro, V., 2001. Dopamine dependency of oscillations between subthalamic nucleus and pallidum in Parkinson's disease. J. Neurosci. 21, 1033–1038. doi:21/3/1033 [pii]

Brown, P., Salenius, S., Rothwell, J.C., Hari, R., 1998. Cortical correlate of the piper rhythm in humans. J. Neurophysiol. 80, 2911–2917.

Brücke, C., Bock, A., Huebl, J., Krauss, J.K., Schönecker, T., Schneider, G.H., Brown, P., Kühn, A.A., 2013. Thalamic gamma oscillations correlate with reaction time in a Go/noGo task in patients with essential tremor. Neuroimage 75, 36–45. doi:10.1016/j.neuroimage.2013.02.038

Brücke, C., Huebl, J., Schonecker, T., Neumann, W.-J., Yarrow, K., Kupsch, A., Blahak, C., Lutjens, G., Brown, P., Krauss, J.K., Schneider, G.-H., Kuhn, A.A., 2012. Scaling of Movement Is Related to Pallidal Oscillations in Patients with

Dystonia. J. Neurosci. 32, 1008–1019. doi:10.1523/JNEUROSCI.3860-11.2012

Bruns, A., 2004. Fourier-, Hilbert- and wavelet-based signal analysis: Are they really different approaches? J. Neurosci. Methods 137, 321–332. doi:10.1016/j.jneumeth.2004.03.002

Buschman, T.J., Miller, E.K., 2007. of Attention in the Prefrontal and. Science (80-.). 315, 1860–1862. doi:10.1126/science.1138071

Buzsáki, G., Anastassiou, C.A., Koch, C., 2012. The origin of extracellular fields and currents — EEG, ECoG, LFP and spikes. Nat. Rev. Neurosci. 13, 407–420. doi:10.1038/nrn3241

Byblow, W.D., Summers, J.J., Lewis, G.N., Thomas, J., 2002. Bimanual coordination in Parkinson's disease: Deficits in movement frequency, amplitude, and pattern switching. Mov. Disord. 17, 20–29. doi:10.1002/mds.1281

Cagnan, H., Duff, E.P., Brown, P., 2015. The relative phases of basal ganglia activities dynamically shape effective connectivity in Parkinson's disease. Brain 138, 1667–1678. doi:10.1093/brain/awv093

Calabresi, P., Picconi, B., Tozzi, A., Ghiglieri, V., Di Filippo, M., 2014. Direct and indirect pathways of basal ganglia: a critical reappraisal. Nat. Neurosci. 17, 1022–1030. doi:10.1038/nn.3743

Cannon, J., Mccarthy, M.M., Lee, S., Lee, J., Börgers, C., Whittington, M.A., Kopell, N., 2014. Neurosystems: Brain rhythms and cognitive processing. Eur. J. Neurosci. 39, 705–719. doi:10.1111/ejn.12453

Cao, L., Hu, Y.-M., 2016. Beta Rebound in Visuomotor Adaptation: Still the Status Quo? J. Neurosci. 36, 6365–6367. doi:10.1523/JNEUROSCI.1007-16.2016

Carpenter, M.B., Whittier, J.R., Mettler, F.A., 1950. Analysis of choreoid hyperkinesia in the rhesus monkey. Surgical and pharmacological analysis of hyperkinesia resulting from lesions in the subthalamic nucleus ol luys. J. Comp. Neurol. 92, 293–331. doi:10.1002/cne.900920303

Cassidy, M., Mazzone, P., Oliviero, A., Insola, A., Tonali, P., Di Lazzaro, V., Brown, P., 2002. Movement-related changes in synchronization in the human basal ganglia. Brain 125, 1235–1246. doi:10.1093/brain/awf135

Cassim, F., Monaca, C., Szurhaj, W., Bourriez, J.L., Defebvre, L., Derambure, P., Guieu, J.D., Cassim, F., Monaca, C. a C., Szurhaj, W., Bourriez, J.L., Defebvre, L., Derambure, P., Guieu, J.D., 2001. Does post-movement beta synchronization reflect an idling motor cortex ? Neuroreport 12, 3859–3863. doi:10.1097/00001756-200112040-00051

Chakarov, V., Naranjo, J.R., Schulte-Monting, J., Omlor, W., Huethe, F., Kristeva, R., 2009. Beta-Range EEG-EMG Coherence With Isometric Compensation for Increasing Modulated Low-Level Forces. J. Neurophysiol. 102, 1115–1120. doi:10.1152/jn.91095.2008

Chambers, C.D., Bellgrove, M.A., Stokes, M.G., Henderson, T.R., Garavan, H., Robertson, I.H., Morris, A.P., Mattingley, J.B., 2006. Executive "Brake Failure" following Deactivation of Human Frontal Lobe. J. Cogn. Neurosci. 18, 444–455. doi:10.1162/jocn.2006.18.3.444

Chaudhary, U., Birbaumer, N., Ramos-Murguialday, A., 2016. Brain–computer interfaces for communication and rehabilitation. Nat. Rev. Neurol. 12, 513–525. doi:10.1038/nrneurol.2016.113

Chaudhary, U., Xia, B., Silvoni, S., Cohen, L.G., Birbaumer, N., 2017. Brain Computer Interface Based Communication in the Completely Locked-In State. PLoS Biol. 15, 1–25. doi:10.1371/journal.pbio.1002593

Chen, C.C., Litvak, V., Gilbertson, T., Kühn, A., Lu, C.S., Lee, S.T., Tsai, C.H., Tisch, S., Limousin, P., Hariz, M., Brown, P., 2007. Excessive synchronization of basal ganglia neurons at 20 Hz slows movement in Parkinson's disease. Exp. Neurol. 205, 214–221. doi:10.1016/j.expneurol.2007.01.027

Chen, C.C., Pogosyan, A., Zrinzo, L.U., Tisch, S., Limousin, P., Ashkan, K., Yousry, T., Hariz, M.I., Brown, P., 2006. Intra-operative recordings of local field potentials can help localize the subthalamic nucleus in Parkinson's disease surgery. Exp. Neurol. 198, 214–221. doi:10.1016/j.expneurol.2005.11.019

Chen, R., Yaseen, Z., Cohen, L.G., Hallett, M., 1998. Time course of corticospinal excitability in reaction time and self-paced movements. Ann. Neurol. 44, 317–325. doi:10.1002/ana.410440306

Cheron, G., Duvinage, M., De Saedeleer, C., Castermans, T., Bengoetxea, A., Petieau, M., Seetharaman, K., Hoellinger, T., Dan, B., Dutoit, T., Sylos Labini, F., Lacquaniti, F., Ivanenko, Y., 2012. From spinal central pattern generators to cortical network: Integrated BCI for walking rehabilitation. Neural Plast. 2012. doi:10.1155/2012/375148

Chevalier, G., Vacher, S., Deniau, J.M., 1984. Inhibitory nigral influence on tectospinal neurons, a possible implication of basal ganglia in orienting behavior. Exp. Brain Res. 53, 320–326. doi:10.1007/BF00238161

Cheyne, D., Bells, S., Ferrari, P., Gaetz, W., Bostan, A.C., 2008. Self-paced movements induce high-frequency gamma oscillations in primary motor cortex. Neuroimage 42, 332–342. doi:10.1016/j.neuroimage.2008.04.178

Cheyne, D., Gaetz, W., Garnero, L., Lachaux, J.P., Ducorps, A., Schwartz, D., Varela,

F.J., 2003. Neuromagnetic imaging of cortical oscillations accompanying tactile stimulation. Cogn. Brain Res. 17, 599–611. doi:10.1016/S0926-6410(03)00173-3

Cheyne, D.O., 2013. MEG studies of sensorimotor rhythms: A review. Exp. Neurol. 245, 27–39. doi:10.1016/j.expneurol.2012.08.030

Chikazoe, J., Jimura, K., Asari, T., Yamashita, K.I., Morimoto, H., Hirose, S., Miyashita, Y., Konishi, S., 2009. Functional dissociation in right inferior frontal cortex during performance of go/no-go task. Cereb. Cortex 19, 146–152. doi:10.1093/cercor/bhn065

Chiken, S., Nambu, A., 2016. Mechanism of Deep Brain Stimulation. Neurosci. 22, 313–322. doi:10.1177/1073858415581986

Chu, H.Y., Atherton, J.F., Wokosin, D., Surmeier, D.J., Bevan, M.D., 2015. Heterosynaptic regulation of external globus pallidus inputs to the subthalamic nucleus by the motor cortex. Neuron 85, 364–376. doi:10.1016/j.neuron.2014.12.022

Cohen, M.X., 2017. Where Does EEG Come From and What Does It Mean? Trends Neurosci. 40, 208–218. doi:10.1016/j.tins.2017.02.004

Confais, J., Kilavik, B.E., Ponce-Alvarez, A., Riehle, A., 2012. On the anticipatory precue activity in motor cortex. J. Neurosci. 32, 15359–15368. doi:10.1523/JNEUROSCI.1768-12.2012

Conson, M., Trojano, L., Vitale, C., Mazzarella, E., Allocca, R., Barone, P., Grossi, D., Santangelo, G., 2014. The role of embodied simulation in mental transformation of whole-body images: Evidence from Parkinson's disease. Hum. Mov. Sci. 33, 343–353. doi:10.1016/j.humov.2013.10.006

Corbit, V.L., Whalen, T.C., Zitelli, K.T., Crilly, S.Y., Rubin, J.E., Gittis, A.H., 2016. Pallidostriatal Projections Promote Oscillations in a Dopamine-Depleted Biophysical Network Model. J. Neurosci. 36, 5556–5571. doi:10.1523/JNEUROSCI.0339-16.2016

Courtemanche, R., 2004. Local Field Potential Oscillations in Primate Cerebellar Cortex: Synchronization With Cerebral Cortex During Active and Passive Expectancy. J. Neurophysiol. 93, 2039–2052. doi:10.1152/jn.00080.2004

Courtemanche, R., Fujii, N., Graybiel, A.M., 2003. Synchronous, focally modulated beta-band oscillations characterize local field potential activity in the striatum of awake behaving monkeys. J. Neurosci. 23, 11741–11752. doi:23/37/11741 [pii]

Crone, N., 1998. Functional mapping of human sensorimotor cortex with electrocorticographic spectral analysis. II. Event-related synchronization in the gamma band. Brain 121, 2301–2315. doi:10.1093/brain/121.12.2301

Crone, N.E., Crone, N.E., Miglioretti, D.L., Miglioretti, D.L., Gordon, B., Gordon, B., Sieracki, J.M., Sieracki, J.M., Wilson, M.T., Wilson, M.T., Uematsu, S., Uematsu, S., Lesser, R.P., Lesser, R.P., 1998. Functional mapping of human sensorimotor cortex with electrocorticographic spectral analysis. I. Alpha and beta event-related desynchronization. Brain 121 (Pt 1, 2271–2299. doi:10.1093/brain/121.12.2271

Cui, G., Jun, S.B., Jin, X., Pham, M.D., Vogel, S.S., Lovinger, D.M., Costa, R.M., 2013. Concurrent activation of striatal direct and indirect pathways during action initiation. Nature 494, 238–242. doi:10.1038/nature11846

Cunnington, R., Egan, G.F., O'Sullivan, J.D., Hughes, A.J., Bradshaw, J.L., Colebatch, J.G., 2001. Motor imagery in Parkinson's disease: A PET study. Mov. Disord. 16, 849–857. doi:10.1002/mds.1181

Cyron, D., 2016. Mental Side Effects of Deep Brain Stimulation (DBS) for Movement Disorders: The Futility of Denial. Front. Integr. Neurosci. 10, 1–4. doi:10.3389/fnint.2016.00017

de Hemptinne, C., Ryapolova-Webb, E.S., Air, E.L., Garcia, P.A., Miller, K.J., Ojemann, J.G., Ostrem, J.L., Galifianakis, N.B., Starr, P.A., 2013. Exaggerated phase-amplitude coupling in the primary motor cortex in Parkinson disease. Proc. Natl. Acad. Sci. 110, 4780–4785. doi:10.1073/pnas.1214546110

de Hemptinne, C., Swann, N.C., Ostrem, J.L., Ryapolova-Webb, E.S., San Luciano, M., Galifianakis, N.B., Starr, P. a, 2015. Therapeutic deep brain stimulation reduces cortical phase-amplitude coupling in Parkinson's disease. Nat. Neurosci. 18, 779–786. doi:10.1038/nn.3997

Delaville, C., McCoy, A.J., Gerber, C.M., Cruz, A. V, Walters, J.R., 2015. Subthalamic nucleus activity in the awake hemiparkinsonian rat: relationships with motor and cognitive networks. J. Neurosci. 35, 6918–6930. doi:10.1523/JNEUROSCI.0587-15.2015

Desmurget, M., Turner, R.S., 2010. Motor Sequences and the Basal Ganglia: Kinematics, Not Habits. J. Neurosci. 30, 7685–7690. doi:10.1523/JNEUROSCI.0163-10.2010

Devos, D., Labyt, E., Cassim, F., Bourriez, J.L., Reyns, N., Touzet, G., Blond, S., Guieu, J.D., Derambure, P., Destée, A., Defebvre, L., 2003a. Subthalamic stimulation influences postmovement cortical somatosensory processing in Parkinson's disease. Eur. J. Neurosci. 18, 1884–1888. doi:10.1046/j.1460-9568.2003.02925.x

Devos, D., Labyt, E., Derambure, P., Bourriez, J.L., Cassim, F., Guieu, J.D., Destée, A., Defebvre, L., 2003b. Effect of L-Dopa on the pattern of movement-related (de)synchronisation in advanced Parkinson's disease. Neurophysiol. Clin. 33, 203–

212. doi:10.1016/j.neucli.2003.10.001

Diedrichsen, J., Shadmehr, R., Ivry, R.B., 2010. The coordination of movement: optimal feedback control and beyond. Trends Cogn. Sci. 14, 31–39. doi:10.1016/j.tics.2009.11.004

Donner, T.H., Siegel, M., Oostenveld, R., Fries, P., Bauer, M., Engel, A.K., 2007. Population activity in the human dorsal pathway predicts the accuracy of visual motion detection. J. ...} 345–359. doi:10.1152/jn.01141.2006.

Donoghue, J.P., Leibovic, S., Sanes, J.N., 1992. Organization of the forelimb area in squirrel monkey motor cortex: representation of digit, wrist, and elbow muscles. Exp. Brain Res. 89, 1–19. doi:10.1007/BF00228996

Dotson, N.M., Gray, C.M., 2016. Experimental observation of phase-flip transitions in the brain. Phys. Rev. E 94, 7–11. doi:10.1103/PhysRevE.94.042420

Dotson, X.N.M., Salazar, X.R.F., Gray, C.M., 2014. Frontoparietal Correlation Dynamics Reveal Interplay between Integration and Segregation during Visual Working Memory 34, 1–14. doi:10.1523/JNEUROSCI.1961-14.2014

Doyle, L.M.F., Kühn, A.A., Hariz, M., Kupsch, A., Schneider, G.H., Brown, P., 2005. Levodopa-induced modulation of subthalamic beta oscillations during self-paced movements in patients with Parkinson's disease. Eur. J. Neurosci. 21, 1403–1412. doi:10.1111/j.1460-9568.2005.03969.x

Dudman, J.T., Krakauer, J.W., 2016. The basal ganglia: From motor commands to the control of vigor. Curr. Opin. Neurobiol. 37, 158–166. doi:10.1016/j.conb.2016.02.005

Eagle, D.M., Baunez, C., Hutcheson, D.M., Lehmann, O., Shah, A.P., Robbins, T.W., 2008. Stop-signal reaction-time task performance: Role of prefrontal cortex and subthalamic nucleus. Cereb. Cortex 18, 178–188. doi:10.1093/cercor/bhm044

Ebersbach, G., Moreau, C., Gandor, F., Defebvre, L., Devos, D., 2013. Clinical syndromes: Parkinsonian gait. Mov. Disord. 28, 1552–1559. doi:10.1002/mds.25675

Edagawa, K., Kawasaki, M., 2017. Beta phase synchronization in the frontal-temporal-cerebellar network during auditory-to-motor rhythm learning. Sci. Rep. 7, 42721. doi:10.1038/srep42721

Emiliani, V., Cohen, A.E., Deisseroth, K., Häusser, M., 2015. All-Optical Interrogation of Neural Circuits. J. Neurosci. 35, 13917–26. doi:10.1523/JNEUROSCI.2916-15.2015

Engel, A.K., Fries, P., 2010. Beta-band oscillations-signalling the status quo? Curr. Opin. Neurobiol. 20, 156–165. doi:10.1016/j.conb.2010.02.015

Fasano, A., Aquino, C.C., Krauss, J.K., Honey, C.R., Bloem, B.R., 2015. Axial disability and deep brain stimulation in patients with Parkinson disease. Nat. Rev. Neurol. 11, 98–110. doi:10.1038/nrneurol.2014.252

Feige, B., Aertsen, a, Kristeva-Feige, R., 2000. Dynamic synchronization between multiple cortical motor areas and muscle activity in phasic voluntary movements. J. Neurophysiol. 84, 2622–2629.

Feingold, J., Gibson, D.J., DePasquale, B., Graybiel, A.M., 2015. Bursts of beta oscillation differentiate postperformance activity in the striatum and motor cortex of monkeys performing movement tasks. Proc. Natl. Acad. Sci. 112, 201517629. doi:10.1073/pnas.1517629112

Fischer, P., Tan, H., Pogosyan, A., Brown, P., 2016. High post-movement parietal low-beta power during rhythmic tapping facilitates performance in a stop task. Eur. J. Neurosci. 44, 2202–2213. doi:10.1111/ejn.13328

Fogelson, N., Pogosyan, A., Kühn, A.A., Kupsch, A., Van Bruggen, G., Speelman, H., Tijssen, M., Quartarone, A., Insola, A., Mazzone, P., Di Lazzaro, V., Limousin, P., Brown, P., 2005. Reciprocal interactions between oscillatory activities of different frequencies in the subthalamic region of patients with Parkinson's disease. Eur. J. Neurosci. 22, 257–266. doi:10.1111/j.1460-9568.2005.04179.x

Foltynie, T., Hariz, M.I., 2010. Surgical management of Parkinson's disease. Expert Rev. Neurother. 10, 903–914. doi:10.1586/ERN.10.68

Fonken, Y.M., Rieger, J.W., Tzvi, E., Crone, N.E., Chang, E., Parvizi, J., Knight, R.T., Krämer, U.M., 2016. Frontal and motor cortex contributions to response inhibition: evidence from electrocorticography. J. Neurophysiol. 115, 2224–2236. doi:10.1152/jn.00708.2015

Fries, P., 2015. Rhythms for Cognition: Communication through Coherence. Neuron 88, 220–235. doi:10.1016/j.neuron.2015.09.034

Fries, P., 2005. A mechanism for cognitive dynamics: Neuronal communication through neuronal coherence. Trends Cogn. Sci. 9, 474–480. doi:10.1016/j.tics.2005.08.011

Fries, P., Nikolic, D., Singer, W., 2007. The gamma cycle. Trends Neurosci. 30, 40–45. doi:10.1016/j.tins.2007.05.005

Friston, K., Moran, R., Seth, A.K., 2013. Analysing connectivity with Granger causality and dynamic causal modelling. Curr. Opin. Neurobiol. 23, 172–178. doi:10.1016/j.conb.2012.11.010

Fu, Y., Xu, B., Li, Y., Wang, Y., Yu, Z., Li, H., 2014. Single-trial decoding of imagined grip force parameters involving the right or left hand based on movement-related cortical potentials. Chinese Sci. Bull. 59, 1907–1916. doi:10.1007/s11434-014-0234-

Fujioka, T., Ross, B., Trainor, L.J., 2015. Beta-Band Oscillations Represent Auditory Beat and Its Metrical Hierarchy in Perception and Imagery. J. Neurosci. 35, 15187–15198. doi:10.1523/JNEUROSCI.2397-15.2015

Fujioka, T., Trainor, L.J., Large, E.W., Ross, B., 2012. Internalized Timing of Isochronous Sounds Is Represented in Neuromagnetic Beta Oscillations. J. Neurosci. 32, 1791–1802. doi:10.1523/JNEUROSCI.4107-11.2012

Fujiyama, F., Sohn, J., Nakano, T., Furuta, T., Nakamura, K.C., Matsuda, W., Kaneko, T., 2011. Exclusive and common targets of neostriatofugal projections of rat striosome neurons: A single neuron-tracing study using a viral vector. Eur. J. Neurosci. 33, 668–677. doi:10.1111/j.1460-9568.2010.07564.x

Gaetz, W., Cheyne, D., 2006. Localization of sensorimotor cortical rhythms induced by tactile stimulation using spatially filtered MEG. Neuroimage 30, 899–908. doi:10.1016/j.neuroimage.2005.10.009

Gallegos-Ayala, G., Furdea, A., Takano, K., Ruf, C.A., Flor, H., Birbaumer, N., 2014. Brain communication in a completely locked-in patient using bedside near-infrared spectroscopy. Neurology 82, 1930–1932.

Gauggel, S., Rieger, M., Feghoff, T., 2004. Inhibition of ongoing responses in patients with Parkinson's disease. J. Neurol. Neurosurg. Psychiatry 75, 539–544. doi:10.1177/1073858403009003009

Gerardin, E., Sirigu, A., Lehéricy, S., Poline, J.B., Gaymard, B., Marsault, C., Agid, Y., Le Bihan, D., 2000. Partially overlapping neural networks for real and imagined hand movements. Cereb. Cortex 10, 1093–1104. doi:10.1093/cercor/10.11.1093

Giladi, N., Shabtai, H., Simon, E.S., Biran, S., Tal, J., Korczyn, A.D., 2000. Construction of freezing of gait questionnaire for patients with Parkinsonism. Park. Relat. Disord. 6, 165–170. doi:10.1016/S1353-8020(99)00062-0

Gilat, M., Bell, P.T., Martens, K.A.E., Georgiades, M.J., Hall, J.M., Walton, C.C., Lewis, S.J.G., Shine, J.M., 2017. Dopamine depletion impairs gait automaticity by altering cortico-striatal and cerebellar processing in Parkinson's disease. Neuroimage. doi:10.1016/j.neuroimage.2017.02.073

Gilat, M., Shine, J.M., Bolitho, S.J., Matar, E., Kamsma, Y.P.T., Naismith, S.L., Lewis, S.J.G., 2013. Variability of Stepping during a Virtual Reality Paradigm in Parkinson's Disease Patients with and without Freezing of Gait. PLoS One 8, 1–6. doi:10.1371/journal.pone.0066718

Gilbertson, T., Lalo, E., Doyle, L., Di Lazzaro, V., Cioni, B., Brown, P., 2005. Existing motor state is favored at the expense of new movement during 13-35 Hz oscillatory synchrony in the human corticospinal system. J. Neurosci. 25, 7771–

7779. doi:10.1523/JNEUROSCI.1762-05.2005

Goldberg, J.H., Farries, M.A., Fee, M.S., 2013. Basal ganglia output to the thalamus: Still a paradox. Trends Neurosci. 36, 695–705. doi:10.1016/j.tins.2013.09.001

Gouvêa, T.S., Monteiro, T., Motiwala, A., Soares, S., Machens, C., Paton, J.J., 2015. Striatal dynamics explain duration judgments. Elife 4, 1–14. doi:10.7554/eLife.11386

Grammont, F., Riehle, A., 2003. Spike synchronization and firing rate in a population of motor cortical neurons in relation to movement direction and reaction time. Biol. Cybern. 88, 360–373. doi:10.1007/s00422-002-0385-3

Gross, J., Schmitz, F., Schnitzler, I., Kessler, K., Shapiro, K., Hommel, B., Schnitzler, A., 2004. Modulation of long-range neural synchrony reflects temporal limitations of visual attention in humans. Proc. Natl. Acad. Sci. U. S. A. 101, 13050–13055. doi:10.1073/pnas.0404944101

Gyorgi, B., Wang, X., 2012. Mechanisms of Gamma Oscillations. Annu. Rev. Neurosci. 35, 203–225. doi:10.1146/annurev-neuro-062111-150444

Hagbarth, K. -E, Jessop, J., Eklund, G., Wallin, E.U., 1983. The Piper rhythm-a phenomenon related to muscle resonance characteristics? Acta Physiol. Scand. 117, 263–271. doi:10.1111/j.1748-1716.1983.tb07205.x

Haider, B., Schulz, D.P.P.A., Häusser, M., Carandini, M., 2016. Millisecond Coupling of Local Field Potentials to Synaptic Currents in the Awake Visual Cortex. Neuron 90, 35–42. doi:10.1016/j.neuron.2016.02.034

Hamada, I., DeLong, M.R., 1992. Excitotoxic acid lesions of the primate subthalamic nucleus result in transient dyskinesias of the contralateral limbs. J.Neurophysiol. 68, 1850–1858.

Hanrahan, S.J., Nedrud, J.J., Davidson, B.S., Farris, S., Giroux, M., Haug, A., Mahoor, M.H., Silverman, A.K., Zhang, J.J., Hebb, A.O., 2016. brain sciences Dynamics of Subthalamic Local Field Potentials in Parkinson â€™ s Disease 1–16. doi:10.3390/brainsci6040057

Hanslmayr, S., Aslan, A., Staudigl, T., Klimesch, W., Herrmann, C.S., Bäuml, K.H., 2007. Prestimulus oscillations predict visual perception performance between and within subjects. Neuroimage 37, 1465–1473. doi:10.1016/j.neuroimage.2007.07.011

Hanslmayr, S., Staudigl, T., Fellner, M.-C., 2012. Oscillatory power decreases and long-term memory: the information via desynchronization hypothesis. Front. Hum. Neurosci. 6, 1–12. doi:10.3389/fnhum.2012.00074

Hariz, M., 2017. My 25 Stimulating Years with DBS in Parkinson's Disease. J.

Parkinsons. Dis. 7, S33–S41. doi:10.3233/JPD-179007

Hausdorff, J.M., Lowenthal, J., Herman, T., Gruendlinger, L., Peretz, C., Giladi, N., 2007. Rhythmic auditory stimulation modulates gait variability in Parkinson's disease. Eur. J. Neurosci. 26, 2369–2375. doi:10.1111/j.1460-9568.2007.05810.x

Heideman, S.G., te Woerd, E.S., Praamstra, P., 2015. Rhythmic entrainment of slow brain activity preceding leg movements. Clin. Neurophysiol. 126, 348–355. doi:10.1016/j.clinph.2014.04.020

Heinrichs-Graham, E., Kurz, M.J., Becker, K.M., Santamaria, P.M., Gendelman, H.E., Wilson, T.W., 2014. Hypersynchrony despite pathologically reduced beta oscillations in patients with Parkinson's disease: a pharmaco-magnetoencephalography study. J. Neurophysiol. 112, 1739–1747. doi:10.1152/jn.00383.2014

Helmich, R.C., de Lange, F.P., Bloem, B.R., Toni, I., 2007. Cerebral compensation during motor imagery in Parkinson's disease. Neuropsychologia 45, 2201–2215. doi:10.1016/j.neuropsychologia.2007.02.024

Hentschke, H., Stüttgen, M.C., 2011. Computation of measures of effect size for neuroscience data sets. Eur. J. Neurosci. 34, 1887–1894. doi:10.1111/j.1460-9568.2011.07902.x

Heremans, E., Nieuwboer, A., Vercruysse, S., 2013a. Freezing of gait in Parkinson's disease: where are we now? Curr. Neurol. Neurosci. Rep. 13, 350. doi:10.1007/s11910-013-0350-7

Heremans, E., Nieuwboer, A., Vercruysse, S., 2013b. Freezing of gait in Parkinson's disease: where are we now? Curr. Neurol. Neurosci. Rep. 13, 350. doi:10.1007/s11910-013-0350-7

Herrmann, C.S., Strüber, D., Helfrich, R.F., Engel, A.K., 2016. EEG oscillations: From correlation to causality. Int. J. Psychophysiol. 103, 12–21. doi:10.1016/j.ijpsycho.2015.02.003

Hirschmann, J., Özkurt, T.E., Butz, M., Homburger, M., Elben, S., Hartmann, C.J., Vesper, J., Wojtecki, L., Schnitzler, A., 2013. Differential modulation of STN-cortical and cortico-muscular coherence by movement and levodopa in Parkinson's disease. Neuroimage 68, 203–213. doi:10.1016/j.neuroimage.2012.11.036

Hirschmann, J., Özkurt, T.E., Butz, M., Homburger, M., Elben, S., Hartmann, C.J., Vesper, J., Wojtecki, L., Schnitzler, A., 2011. Distinct oscillatory STN-cortical loops revealed by simultaneous MEG and local field potential recordings in patients with Parkinson's disease. Neuroimage 55, 1159–1168. doi:10.1016/j.neuroimage.2010.11.063

Högl, B., Agostino, P. V, Peralta, M.C., Gershanik, O., Golombek, D.A., 2014. Alterations in time estimation in multiple system atrophy. Basal Ganglia 4, 95–99. doi:10.1016/j.baga.2014.06.004

Hoover, J.E., Strick, P.L., 1993. Multiple output channels in the basal ganglia. Science (80-.). 259, 819–821. doi:10.1126/science.7679223

Horn, A., Neumann, W.-J., Degen, K., Schneider, G.-H., Kühn, A.A., 2017. Toward an electrophysiological "sweet spot" for deep brain stimulation in the subthalamic nucleus. Hum. Brain Mapp. 0. doi:10.1002/hbm.23594

Houweling, S., van Dijk, B.W., Beek, P.J., Daffertshofer, A., 2010. Cortico-spinal synchronization reflects changes in performance when learning a complex bimanual task. Neuroimage 49, 3269–3275. doi:10.1016/j.neuroimage.2009.11.017

Huster, R.J., Enriquez-Geppert, S., Lavallee, C.F., Falkenstein, M., Herrmann, C.S., 2013. Electroencephalography of response inhibition tasks: Functional networks and cognitive contributions. Int. J. Psychophysiol. 87, 217–233. doi:10.1016/j.ijpsycho.2012.08.001

Huster, R.J., Schneider, S., Lavallee, C.F., Enriquez-Geppert, S., Herrmann, C.S., 2017. Filling the void - enriching the feature space of successful stopping. Hum. Brain Mapp. 38, 1333–1346. doi:10.1002/hbm.23457

Hwang, K., Ghuman, A.S., Manoach, D.S., Jones, S.R., Luna, B., 2014. Cortical Neurodynamics of Inhibitory Control. J. Neurosci. 34, 9551–9561. doi:10.1523/JNEUROSCI.4889-13.2014

Inase, M., Tokuno, H., Nambu, A., Akazawa, T., Takada, M., 1999. Corticostriatal and corticosubthalamic input zones from the presupplementary motor area in the macaque monkey: Comparison with the input zones from the supplementary motor area. Brain Res. 833, 191–201. doi:10.1016/S0006-8993(99)01531-0

Iversen, J.R., Repp, B.H., Patel, A.D., 2009. Top-down control of rhythm perception modulates early auditory responses. Ann. N. Y. Acad. Sci. 1169, 58–73. doi:10.1111/j.1749-6632.2009.04579.x

Jackson, A., Gee, V.J., Baker, S.N., Lemon, R.N., 2003. Synchrony between neurons with similar muscle fields in monkey motor cortex. Neuron 38, 115–125. doi:10.1016/S0896-6273(03)00162-4

Jahanshahi, M., Obeso, I., Baunez, C., Alegre, M., Krack, P., 2015. Parkinson's disease, the subthalamic nucleus, inhibition, and impulsivity. Mov. Disord. 30, 128–140. doi:10.1002/mds.26049

Jankovic, J., 2008. Parkinson's disease: clinical features and diagnosis. J. Neurol. Neurosurg. &} Psychiatry 79, 368–376. doi:10.1136/jnnp.2007.131045

Jeannerod, M., 2001. Neural Simulation of Action: A Unifying Mechanism for Motor Cognition. Neuroimage 14, S103—-S109. doi:10.1006/nimg.2001.0832

Jenkinson, N., Kühn, A.A., Brown, P., 2013. Gamma oscillations in the human basal ganglia. Exp. Neurol. 245, 72–76. doi:10.1016/j.expneurol.2012.07.005

Jha, A., Nachev, P., Barnes, G., Husain, M., Brown, P., Litvak, V., 2015. The Frontal Control of Stopping. Cereb. Cortex 25, 4392–4406. doi:10.1093/cercor/bhv027

Johnson, S.W., 2008. Rebound bursts following inhibition: how dopamine modifies firing pattern in subthalamic neurons. J. Physiol. 586, 2033. doi:10.1113/jphysiol.2008.153643

Jones, C.R.G., Jahanshahi, M., 2014. Contributions of the Basal Ganglia to Temporal Processing: Evidence from Parkinson's Disease. Timing Time Percept. 2, 87–127. doi:10.1163/22134468-00002009

Jones, S.R., Kerr, C.E., Wan, Q., Pritchett, D.L., Hamalainen, M., Moore, C.I., 2010. Cued Spatial Attention Drives Functionally Relevant Modulation of the Mu Rhythm in Primary Somatosensory Cortex. J. Neurosci. 30, 13760–13765. doi:10.1523/JNEUROSCI.2969-10.2010

Joundi, R.A., Brittain, J.S., Green, A.L., Aziz, T.Z., Brown, P., Jenkinson, N., 2012. Oscillatory activity in the subthalamic nucleus during arm reaching in Parkinson's disease. Exp. Neurol. 236, 319–326. doi:10.1016/j.expneurol.2012.05.013

Joundi, R. a., Brittain, J.S., Green, A.L., Aziz, T.Z., Brown, P., Jenkinson, N., 2013. Persistent suppression of subthalamic beta-band activity during rhythmic finger tapping in Parkinson's disease. Clin. Neurophysiol. 124, 565–573. doi:10.1016/j.clinph.2012.07.029

Jurkiewicz, M.T., Gaetz, W.C., Bostan, A.C., Cheyne, D., 2006. Post-movement beta rebound is generated in motor cortex: Evidence from neuromagnetic recordings. Neuroimage 32, 1281–1289. doi:10.1016/j.neuroimage.2006.06.005

Kamiński, J., Brzezicka, A., Gola, M., Wróbel, A., Kaminski, J., Brzezicka, A., Gola, M., Wrobel, A., Kamiński, J., Brzezicka, A., Gola, M., Wróbel, A., Kaminski, J., Brzezicka, A., Gola, M., Wrobel, A., 2012. Beta band oscillations engagement in human alertness process. Int. J. Psychophysiol. 85, 125–128. doi:10.1016/j.ijpsycho.2011.11.006

Kato, K., Yokochi, F., Iwamuro, H., Kawasaki, T., Hamada, K., Isoo, A., Kimura, K., Okiyama, R., Taniguchi, M., Ushiba, J., 2016. Frequency-Specific Synchronization in the Bilateral Subthalamic Nuclei Depending on Voluntary Muscle Contraction and Relaxation in Patients with Parkinson's Disease. Front. Hum. Neurosci. 10, 1–13. doi:10.3389/fnhum.2016.00131

Kato, K., Yokochi, F., Taniguchi, M., Okiyama, R., Kawasaki, T., Kimura, K., Ushiba, J., 2014. Bilateral Coherence between Motor Cortices and Subthalamic Nuclei in Patients with Parkinson&#}x02019;s Disease. Clin. Neurophysiol. 126, 1941–1950. doi:10.1016/j.clinph.2014.12.007

Kawaguchi, Y., Wilson, C.J., Emson, P.C., 1990. Projection subtypes of rat neostriatal matrix cells revealed by intracellular injection of biocytin. J. Neurosci. 10, 3421–3438. doi:http://www.jneurosci.org/content/10/10/3421

Kempf, F., Brücke, C., Salih, F., Trottenberg, T., Kupsch, A., Schneider, G.H., Doyle Gaynor, L.M.F., Hoffmann, K.T., Vesper, J., Wöhrle, J., Altenmüller, D.M., Krauss, J.K., Mazzone, P., Di Lazzaro, V., Yelnik, J., Kühn, A.A., Brown, P., 2009. Gamma activity and reactivity in human thalamic local field potentials. Eur. J. Neurosci. 29, 943–953.

Kilavik, B.E., Ponce-Alvarez, A., Trachel, R., Confais, J., Takerkart, S., Riehle, A., 2012. Context-related frequency modulations of macaque motor cortical LFP beta oscillations. Cereb. Cortex 22, 2148–2159. doi:10.1093/cercor/bhr299

Kilavik, B.E., Zaepffel, M., Brovelli, A., MacKay, W.A., Riehle, A., 2013. The ups and downs of beta oscillations in sensorimotor cortex. Exp. Neurol. 245, 15–26. doi:10.1016/j.expneurol.2012.09.014

Klostermann, F., Wahl, M., Marzinzik, F., Vesper, J., Sommer, W., Curio, G., 2010. Speed effects of deep brain stimulation for Parkinson's disease. Mov. Disord. 25, 2762–2768. doi:10.1002/mds.23381

Kondabolu, K., Roberts, E.A., Bucklin, M., McCarthy, M.M., Kopell, N., Han, X., 2016. Striatal cholinergic interneurons generate beta and gamma oscillations in the corticostriatal circuit and produce motor deficits. Proc. Natl. Acad. Sci. 113, E3159—-E3168. doi:10.1073/pnas.1605658113

Kondylis, E.D., Randazzo, M.J., Alhourani, A., Lipski, W.J., Wozny, T.A., Pandya, Y., Ghuman, A.S., Turner, R.S., Crammond, D.J., Richardson, R.M., 2016. Movement-related dynamics of cortical oscillations in Parkinson's disease and essential tremor. Brain 139, 2211–2223. doi:10.1093/brain/aww144

Kononowicz, T.W., van Rijn, H., 2015. Single trial beta oscillations index time estimation. Neuropsychologia 75, 381–389. doi:10.1016/j.neuropsychologia.2015.06.014

Konorski, J., 1967. Integrative Activity of the Brain. An Interdisciplinary Approach. University of Chicago Press, Chicago.

Krause, V., Bashir, S., Pollok, B., Caipa, A., Schnitzler, A., Pascual-Leone, A., 2012. 1 Hz rTMS of the left posterior parietal cortex (PPC) modifies sensorimotor timing. Neuropsychologia 50, 3729–3735. doi:10.1016/j.neuropsychologia.2012.10.020

Krause, V., Pollok, B., Schnitzler, A., 2010. Perception in action: The impact of sensory information on sensorimotor synchronization in musicians and non-musicians. Acta Psychol. (Amst). 133, 28–37. doi:10.1016/j.actpsy.2009.08.003

Krause, V., Weber, J., Pollok, B., 2014. The Posterior Parietal Cortex (PPC) Mediates Anticipatory Motor Control. Brain Stimul. 7, 800–806. doi:10.1016/j.brs.2014.08.003

Kristeva-Feige, R., Fritsch, C., Timmer, J., Lücking, C.H., 2002. Effects of attention and precision of exerted force on beta range EEG-EMG synchronization during a maintained motor contraction task. Clin. Neurophysiol. 113, 124–131. doi:10.1016/S1388-2457(01)00722-2

Kühn, A.A., Brücke, C., Schneider, G.H., Trottenberg, T., Kivi, A., Kupsch, A., Capelle, H.H., Krauss, J.K., Brown, P., 2008. Increased beta activity in dystonia patients after drug-induced dopamine deficiency. Exp. Neurol. 214, 140–143. doi:10.1016/j.expneurol.2008.07.023

Kühn, A.A., Doyle, L., Pogosyan, A., Yarrow, K., Kupsch, A., Schneider, G., Hariz, M.I., Trottenberg, T., Brown, P., 2006. Modulation of beta oscillations in the subthalamic area during motor imagery in Parkinson's disease. Brain 129, 695–706. doi:10.1093/brain/awh715

Kühn, A.A., Williams, D., Kupsch, A., Limousin, P., Hariz, M., Schneider, G.H., Yarrow, K., Brown, P., 2004. Event-related beta desynchronization in human subthalamic nucleus correlates with motor performance. Brain 127, 735–746. doi:10.1093/brain/awh106

Kumru, H., Summerfield, C., Valldeoriola, F., Valls-Solé, J., J, V.-S., Valls-Solé, J., 2004. Effects of subthalamic nucleus stimulations on characteristics of EMG activity underlying reaction time in Parkinson's disease. Mov. Disord. 19, 94–100. doi:10.1002/mds.10638

Lachaux, J.-P., Rodriguez, E., Le van Quyen, M., Lutz, A., Martinerie, J., Varela, F.J., 2000. Studying single-trials of phase synchronous activity in the brain. Int. J. Bifurc. Chaos. doi:10.1142/S0218127400001560

Lalo, E., Thobois, S., Sharott, A., Polo, G., Mertens, P., Pogosyan, A., Brown, P., 2008. Patterns of bidirectional communication between cortex and basal ganglia during movement in patients with Parkinson disease. J. Neurosci. 28, 3008–3016. doi:10.1523/JNEUROSCI.5295-07.2008

Lambert, C., Zrinzo, L., Nagy, Z., Lutti, A., Hariz, M., Foltynie, T., Draganski, B., Ashburner, J., Frackowiak, R., 2012. Confirmation of functional zones within the human subthalamic nucleus: Patterns of connectivity and sub-parcellation using diffusion weighted imaging. Neuroimage 60, 83–94.

doi:10.1016/j.neuroimage.2011.11.082

Lanciego, J.L., Luquin, N., Obeso, J.A., 2012. Functional neuroanatomy of the basal ganglia. Cold Spring Harb. Perspect. Med. 2, 1–20. doi:10.1101/cshperspect.a009621

Lee, D., 2003. Coherent oscillations in neuronal activity of the supplementary motor area during a visuomotor task. J. Neurosci. 23, 6798–6809. doi:23/17/6798 [pii]

Leventhal, D.K., Gage, G.J., Schmidt, R., Pettibone, J.R., Case, A.C., Berke, J.D., 2012. Basal ganglia beta oscillations accompany cue utilization. Neuron 73, 523–536. doi:10.1016/j.neuron.2011.11.032

Levesque, J.-C., Parent, A., 2005. GABAergic Interneurons in Human Subthalamic Nucleus 20, 574–584. doi:10.1002/mds.20374

Levy, B.J., Wagner, A.D., 2011. Cognitive control and right ventrolateral prefrontal cortex: Reflexive reorienting, motor inhibition, and action updating. Ann. N. Y. Acad. Sci. 1224, 40–62. doi:10.1111/j.1749-6632.2011.05958.x

Levy, R., Ashby, P., Hutchison, W.D., Lang, A.E., Lozano, A.M., Dostrovsky, J.O., 2002. Dependence of subthalamic nucleus oscillations on movement and dopamine in Parkinson's disease. Brain 125, 1196–1209. doi:10.1093/brain/awf128

Liao, K., Xiao, R., Gonzalez, J., Ding, L., 2014. Decoding individual finger movements from one hand using human EEG signals. PLoS One 9, 1–12. doi:10.1371/journal.pone.0085192

Lienard, J.F., Cos, I., Girard, B., 2017. Beta-Band Oscillations without Pathways : the opposing Roles of D2 and D5 Receptors. bioRxiv 1–17.

Linkenkaer-Hansen, K., Nikulin, V. V, Palva, S., Ilmoniemi, R., Palva, J.M., 2004. Prestimulus Oscillations Enhance Psychophysical Performance in Humans. J. Neurosci. 24, 10186–10190. doi:10.1523/JNEUROSCI.2584-04.2004

Lipski, W.J., Wozny, T.A., Alhourani, A., Kondylis, E., Turner, R.S., Crammond, D.J., Richardson, R.M., 2017. Dynamics of human subthalamic neuron phase-locking to motor and sensory cortical oscillations during movement. J. Neurophysiol. jn.00964.2016. doi:10.1152/jn.00964.2016

Lisman, J.E., Grace, A.A., Street, S., 2005. The Hippocampal-VTA Loop : Controlling the Entry of Information into Long-Term Memory 46, 703–713. doi:10.1016/j.neuron.2005.05.002

Little, S., Beudel, M., Zrinzo, L., Foltynie, T., Limousin, P., Hariz, M., Neal, S., Cheeran, B., Cagnan, H., Gratwicke, J., Aziz, T.Z., Pogosyan, A., Brown, P., 2016a. Bilateral adaptive deep brain stimulation is effective in Parkinson's disease.

J. Neurol. Neurosurg. Psychiatry 87, 717–721. doi:10.1136/jnnp-2015-310972

Little, S., Brown, P., 2014. The functional role of beta oscillations in Parkinson's disease. Park. Relat. Disord. 20, S44—-S48. doi:10.1016/S1353-8020(13)70013-0

Little, S., Pogosyan, A., Kuhn, A.A., Brown, P., 2012. Beta band stability over time correlates with Parkinsonian rigidity and bradykinesia. Exp. Neurol. 236, 383–388. doi:10.1016/j.expneurol.2012.04.024

Little, S., Pogosyan, A., Neal, S., Zavala, B., Zrinzo, L., Hariz, M., Foltynie, T., Limousin, P., Ashkan, K., Fitzgerald, J., Green, A.L., Aziz, T.Z., Brown, P., 2013. Adaptive deep brain stimulation in advanced Parkinson disease. Ann. Neurol. 449–457. doi:10.1002/ana.23951

Little, S., Tripoliti, E., Beudel, M., Pogosyan, A., Cagnan, H., Herz, D., Bestmann, S., Aziz, T., Cheeran, B., Zrinzo, L., Hariz, M., Hyam, J., Limousin, P., Foltynie, T., Brown, P., 2016b. Adaptive deep brain stimulation for Parkinson's disease demonstrates reduced speech side effects compared to conventional stimulation in the acute setting. J. Neurol. Neurosurg. &} Psychiatry 87, jnnp—-2016—-313518. doi:10.1136/jnnp-2016-313518

Litvak, V., Eusebio, A., Jha, A., Oostenveld, R., Barnes, G., Foltynie, T., Limousin, P., Zrinzo, L., Hariz, M.I., Friston, K., Brown, P., 2012. Movement-Related Changes in Local and Long-Range Synchronization in Parkinson's Disease Revealed by Simultaneous Magnetoencephalography and Intracranial Recordings. J. Neurosci. 32, 10541–10553. doi:10.1523/JNEUROSCI.0767-12.2012

Litvak, V., Jha, A., Eusebio, A., Oostenveld, R., Foltynie, T., Limousin, P., Zrinzo, L., Hariz, M.I., Friston, K., Brown, P., 2011. Resting oscillatory cortico-subthalamic connectivity in patients with Parkinson's disease. Brain 134, 359–374. doi:10.1093/brain/awq332

MacKay, W.A., 1997. Synchronized neuronal oscillations and their role in motor processes. Trends Cogn. Sci. 1, 176–183. doi:10.1016/S1364-6613(97)01059-0

Magill, P.J., Sharott, A., Bevan, M.D., Brown, P., Bolam, J.P., Peter, J., Sharott, A., Bevan, M.D., Brown, P., 2004. Synchronous Unit Activity and Local Field Potentials Evoked in the Subthalamic Nucleus by Cortical Stimulation 700–714.

Magnani, G., Cursi, M., Leocani, L., Volonté, M.A., Comi, G., 2002. Acute effects of L-dopa on event-related desynchronization in Parkinson's disease. Neurol. Sci. 23, 91–97. doi:10.1007/s100720200033

Maillet, A., Thobois, S., Fraix, V., Redouté, J., Le Bars, D., Lavenne, F., Derost, P., Durif, F., Bloem, B.R., Krack, P., Pollak, P., Debû, B., 2015. Neural substrates of levodopa-responsive gait disorders and freezing in advanced Parkinson's disease: A kinesthetic imagery approach. Hum. Brain Mapp. 36, 959–980.

doi:10.1002/hbm.22679

Majid, D.S.A., Cai, W., Corey-Bloom, J., Aron, A.R., 2013. Proactive Selective Response Suppression Is Implemented via the Basal Ganglia. J. Neurosci. 33, 13259–13269. doi:10.1523/JNEUROSCI.5651-12.2013

Mallet, N., Pogosyan, A., Marton, L.F., Bolam, J.P., Brown, P., Magill, P.J., 2008. Parkinsonian Beta Oscillations in the External Globus Pallidus and Their Relationship with Subthalamic Nucleus Activity. J. Neurosci. 28, 14245–14258. doi:10.1523/JNEUROSCI.4199-08.2008

Mallet, N., Schmidt, R., Leventhal, D., Chen, F., Amer, N., Boraud, T., Berke, J.D., 2016. Arkypallidal Cells Send a Stop Signal to Striatum. Neuron 89, 308–316. doi:10.1016/j.neuron.2015.12.017

Marceglia, S., Fiorio, M., Foffani, G., Mrakic-Sposta, S., Tiriticco, M., Locatelli, M., Caputo, E., Tinazzi, M., Priori, A., 2009. Modulation of beta oscillations in the subthalamic area during action observation in Parkinson's disease. Neuroscience 161, 1027–1036. doi:10.1016/j.neuroscience.2009.04.018

Marco-Pallarés, J., Münte, T.F., Rodríguez-Fornells, A., 2015. The role of high-frequency oscillatory activity in reward processing and learning. TL - 49C. Neurosci. Biobehav. Rev. 49C VN-, 1–7. doi:10.1016/j.neubiorev.2014.11.014

Maris, E., Oostenveld, R., 2007. Nonparametric statistical testing of EEG- and MEG-data. J. Neurosci. Methods 164, 177–190. doi:10.1016/j.jneumeth.2007.03.024

Marmor, O., Valsky, D., Joshua, M., Bick, A.S., Arkadir, D., Tamir, I., Bergman, H., Israel, Z., Eitan, R., 2017. Local vs. Volume Conductance Activity of Field Potentials in the Human Subthalamic Nucleus. J. Neurophysiol. C, jn.00756.2016. doi:10.1152/jn.00756.2016

Marsden, J.F., Werhahn, K.J., Ashby, P., Rothwell, J., Noachtar, S., Brown, P., 2000. Organization of cortical activities related to movement in humans. J. Neurosci. 20, 2307–2314.

Martinez-Gonzalez, C., Bolam, J.P., Mena-Segovia, J., 2011. Topographical Organization of the Pedunculopontine Nucleus. Front. Neuroanat. 5, 1–10. doi:10.3389/fnana.2011.00022

Masimore, B., Schmitzer-Torbert, N.C., Kakalios, J., Redish, a D., 2005. Transient striatal gamma local field potentials signal movement initiation in rats. Neuroreport 16, 2021–2024. doi:10.1097/00001756-200512190-00010

Mastro, K.J., Gittis, A.H., 2015. Striking the right balance: Cortical modulation of the subthalamic nucleus-globus pallidus circuit. Neuron 85, 233–235. doi:10.1016/j.neuron.2014.12.062

Mates, J., Radil, T., Pöppel, E., 1992. Cooperative tapping: Time control under different feedback conditions. Attention, Perception, &} Psychophys. 52, 691–704.

Mazilu, S., Blanke, U., Dorfman, M., Gazit, E., Mirelman, A., M. Hausdorff, J., Tröster, G., 2015. A Wearable Assistant for Gait Training for Parkinson&Rsquo;s Disease with Freezing of Gait in Out-of-the-Lab Environments. ACM Trans. Interact. Intell. Syst. 5, 5:1—-5:31. doi:10.1145/2701431

McCarthy, M.M., Moore-Kochlacs, C., Gu, X., Boyden, E.S., Han, X., Kopell, N., 2011. Striatal origin of the pathologic beta oscillations in Parkinson's disease. Proc. Natl. Acad. Sci. 108, 11620–11625. doi:10.1073/pnas.1107748108

Meijer, D., te Woerd, E., Praamstra, P., 2016. Timing of beta oscillatory synchronization and temporal prediction of upcoming stimuli. Neuroimage 138, 233–241. doi:10.1016/j.neuroimage.2016.05.071

Mena-Segovia, J., Bolam, J.P., Magill, P.J., 2004. Pedunculopontine nucleus and basal ganglia: Distant relatives or part of the same family? Trends Neurosci. 27, 585–588. doi:10.1016/j.tins.2004.07.009

Merchant, H., Bartolo, R., 2017. Primate beta oscillations and rhythmic behaviors. J. Neural Transm. 1–10. doi:10.1007/s00702-017-1716-9

Merchant, H., Luciana, M., Hooper, C., Majestic, S., Tuite, P., 2008. Interval timing and Parkinson's disease: Heterogeneity in temporal performance. Exp. Brain Res. 184, 233–248. doi:10.1007/s00221-007-1097-7

Michael Schüpbach, W.M., 2012. Impulsivity, impulse control disorders, and subthalamic stimulation in parkinson's disease. Basal Ganglia 2, 205–209. doi:10.1016/j.baga.2012.09.005

Mima, T., Simpkins, N., Oluwatimilehin, T., Hallett, M., 1999. Force level modulates human cortical oscillatory activities. Neurosci. Lett. 275, 77–80. doi:10.1016/S0304-3940(99)00734-X

Mink, J.W., 1996. The basal ganglia: Focused selection and inhibition of competing motor programs. Prog. Neurobiol. 50, 381–425. doi:10.1016/S0301-0082(96)00042-1

Miyashita, N., Narabayashi, Y., Oshima, T., 2016. Comparative study of non-parkinsonian and parkinsonian motor symptoms in view of brain activities monitored during thalamotomy. Neurol. Clin. Neurosci. 4, 41–51. doi:10.1111/ncn3.12032

Moro, E., Esselink, R.J. a, Xie, J., Hommel, M., Benabid, a L., Pollak, P., 2002. The impact on Parkinson's disease of electrical parameter settings in STN stimulation. Neurology 59, 706–713. doi:10.1212/WNL.59.5.706

Moshel, S., Shamir, R.R., Raz, A., de Noriega, F.R., Eitan, R., Bergman, H., Israel, Z., 2013. Subthalamic nucleus long-range synchronization-an independent hallmark of human Parkinson's disease. Front. Syst. Neurosci. 7, 79. doi:10.3389/fnsys.2013.00079

Murphy, B.A., Miller, J.P., Gunalan, K., Ajiboye, A.B., 2016. Contributions of Subsurface Cortical Modulations to Discrimination of Executed and Imagined Grasp Forces through Stereoelectroencephalography. PLoS One 11, e0150359. doi:10.1371/journal.pone.0150359

Murthy, V.N., Fetz, E.E., 1992. Coherent 25- to 35-Hz oscillations in the sensorimotor cortex of awake behaving monkeys. Proc. Natl. Acad. Sci. U. S. A. 89, 5670–5674. doi:10.1073/pnas.89.12.5670

Murthy, V.N., Fetz, E.E., Murthy, N., Fetz, E.E., 1996. Synchronization of neurons during local field potential oscillations in sensorimotor cortex of awake monkeys. J. Neurophysiol. 76, 3968–3982.

Musall, S., Von Pföstl, V., Rauch, A., Logothetis, N.K., Whittingstall, K., 2014. Effects of neural synchrony on surface EEG. Cereb. Cortex 24, 1045–1053. doi:10.1093/cercor/bhs389

Muthukumaraswamy, S.D., 2011. Temporal dynamics of primary motor cortex gamma oscillation amplitude and piper corticomuscular coherence changes during motor control. Exp. Brain Res. 212, 623–633. doi:10.1007/s00221-011-2775-z

Muthukumaraswamy, S.D., 2010. Functional Properties of Human Primary Motor Cortex Gamma Oscillations. J. Neurophysiol. 104, 2873–2885. doi:10.1152/jn.00607.2010

Nambu, A., Tokuno, H., Takada, M., 2002. Functional significance of the cortico-subthalamo-pallidal "hyperdirect" pathway. Neurosci. Res. 43, 111–117. doi:10.1016/S0168-0102(02)00027-5

Narabayashi, Y., Oshima, T., 2014. Central origin of parkinsonian rigidity examined with thalamic activities on their temporal relationships. Neurol. Clin. Neurosci. 2, 140–148. doi:10.1111/ncn3.112

Naros, G., Naros, I., Grimm, F., Ziemann, U., Gharabaghi, A., 2016. Reinforcement learning of self-regulated sensorimotor beta-oscillations improves motor performance. Neuroimage 134, 142–152. doi:10.1016/j.neuroimage.2016.03.016

Neubert, F.-X., Mars, R.B., Buch, E.R., Olivier, E., Rushworth, M.F.S., 2010. Cortical and subcortical interactions during action reprogramming and their related white matter pathways. Proc. Natl. Acad. Sci. 107, 13240–13245. doi:10.1073/pnas.1000674107/-/DCSupplemental.www.pnas.org/cgi/doi/10.1073/pnas.1000674107

Neumann, W.J., Kühn, A.A., Kuehn, A.A., Kühn, A.A., 2017. Subthalamic beta power - Unified Parkinson's disease rating scale III correlations require akinetic symptoms. Mov. Disord. 32, 175–176. doi:10.1002/mds.26858

Nevado-Holgado, A.J., Mallet, N., Magill, P.J., Bogacz, R., 2014. Effective connectivity of the subthalamic nucleus - globus pallidus network during Parkinsonian oscillations. J. Physiol. 7, 1429–1455. doi:10.1113/jphysiol.2013.259721

Nikolic, D., Fries, P., Singer, W., 2013. Gamma oscillations : precise temporal coordination without a metronome. Trends Cogn. Sci. 17, 54–55. doi:10.1016/j.tics.2012.12.003

Nir, Y., Fisch, L., Mukamel, R., Gelbard-Sagiv, H., Arieli, A., Fried, I., Malach, R., 2007. Coupling between Neuronal Firing Rate, Gamma LFP, and BOLD fMRI Is Related to Interneuronal Correlations. Curr. Biol. 17, 1275–1285. doi:10.1016/j.cub.2007.06.066

O'Hare, J.K., Ade, K.K., Sukharnikova, T., Van Hooser, S.D., Palmeri, M.L., Yin, H.H., Calakos, N., 2016. Pathway-Specific Striatal Substrates for Habitual Behavior. Neuron 89, 472–479. doi:10.1016/j.neuron.2015.12.032

Obeso, I., Wilkinson, L., Jahanshahi, M., 2011. Levodopa medication does not influence motor inhibition or conflict resolution in a conditional stop-signal task in Parkinson's disease. Exp. Brain Res. 213, 435–445. doi:10.1007/s00221-011-2793-x

Ohara, S., Ikeda, A., Kunieda, T., Yazawa, S., Baba, K., Nagamine, T., Taki, W., Hashimoto, N., Mihara, T., Shibasaki, H., 2000. Movement-related change of electrocorticographic activity in human supplementary motor area proper. Brain 123, 1203–1215. doi:10.1093/brain/123.6.1203

Oldenburg, I.A., Sabatini, B.L., 2015. Antagonistic but Not Symmetric Regulation of Primary Motor Cortex by Basal Ganglia Direct and Indirect Pathways. Neuron 86, 1174–1181. doi:10.1016/j.neuron.2015.05.008

Oldfield, R.C., 1971. The assessment and analysis of handedness: the Edinburgh inventory. Neuropsychologia 9, 97–113.

Omlor, W., Patino, L., Hepp-Reymond, M.C., Kristeva, R., 2007. Gamma-range corticomuscular coherence during dynamic force output. Neuroimage 34, 1191–1198. doi:10.1016/j.neuroimage.2006.10.018

Oorschot, D.E., 1996. Total number of neurons in the neostriatal, pallidal, subthalamic, and substantia nigral nuclei of the rat basal ganglia: A stereological study using the cavalieri and optical disector methods. J. Comp. Neurol. 366, 580–599. doi:10.1002/(SICI)1096-9861(19960318)366:4<580::AID-CNE3>3.0.CO;2-0

Oostenveld, R., Fries, P., Maris, E., Schoffelen, J.M., 2011. FieldTrip: Open source

software for advanced analysis of MEG, EEG, and invasive electrophysiological data. Comput. Intell. Neurosci. 2011. doi:10.1155/2011/156869

Oswal, A., Beudel, M., Zrinzo, L., Limousin, P., Hariz, M., Foltynie, T., Litvak, V., Brown, P., 2016. Deep brain stimulation modulates synchrony within spatially and spectrally distinct resting state networks in Parkinson's disease. Brain 139, 1482–1496. doi:10.1093/brain/aww048

Oswal, A., Litvak, V., Brucke, C., Huebl, J., Schneider, G.-H.G.-H., Kuhn, A.A., Brown, P., Brücke, C., Huebl, J., Schneider, G.-H.G.-H., Kühn, A.A., Brown, P., 2013. Cognitive Factors Modulate Activity within the Human Subthalamic Nucleus during Voluntary Movement in Parkinson's Disease. J. Neurosci. 33, 15815–15826. doi:10.1523/JNEUROSCI.1790-13.2013

Oswal, A., Litvak, V., Sauleau, P., Brown, P., 2012. Beta Reactivity, Prospective Facilitation of Executive Processing, and Its Dependence on Dopaminergic Therapy in Parkinson's Disease. J. Neurosci. 32, 9909–9916. doi:10.1523/JNEUROSCI.0275-12.2012

Pan, M.K., Kuo, S.H., Tai, C.H., Liou, J.Y., Pei, J.C., Chang, C.Y., Wang, Y.M., Liu, W.C., Wang, T.R., Lai, W.S., Kuo, C.C., 2016. Neuronal firing patterns outweigh circuitry oscillations in parkinsonian motor control. J. Clin. Invest. 126, 4516–4526. doi:10.1172/JCI88170

Papaxanthis, C., Pozzo, T., Skoura, X., Schieppati, M., 2002. Does order and timing in performance of imagined and actual movements affect the motor imagery process? The duration of walking and writing task. Behav. Brain Res. 134, 209–215. doi:10.1016/S0166-4328(02)00030-X

Paradiso, G., Cunic, D., Saint-Cyr, J.A., Hoque, T., Lozano, A.M., Lang, A.E., Chen, R., 2004. Involvement of human thalamus in the preparation of self-paced movement. Brain 127, 2717–2731. doi:10.1093/brain/awh288

Parkes, L.M., Bastiaansen, M.C.M., Norris, D.G., 2006. Combining EEG and fMRI to investigate the post-movement beta rebound. Neuroimage 29, 685–696. doi:10.1016/j.neuroimage.2005.08.018

Parkis, M.A., Feldman, J.L., Robinson, D.M., Funk, G.D., 2003. Oscillations in endogenous inputs to neurons affect excitability and signal processing. J Neurosci 23, 8152–8158. doi:23/22/8152 [pii]

Pastötter, B., Dreisbach, G., Bäuml, K.-H.T., 2013. Dynamic Adjustments of Cognitive Control: Oscillatory Correlates of the Conflict Adaptation Effect. J. Cogn. Neurosci. 25, 2167–2178.

Patino, L., Omlor, W., Chakarov, V., Hepp-Reymond, M.-C., Kristeva, R., 2008. Absence of Gamma-Range Corticomuscular Coherence During Dynamic Force in a

Deafferented Patient. J. Neurophysiol. 99, 1906–1916. doi:10.1152/jn.00390.2007

Pavlides, A., Hogan, S.J., Bogacz, R., 2015. Computational Models Describing Possible Mechanisms for Generation of Excessive Beta Oscillations in Parkinson's Disease. PLoS Comput. Biol. 11, 1–29. doi:10.1371/journal.pcbi.1004609

Perez, M.A., Lundbye-Jensen, J., Nielsen, J.B., 2006. Changes in corticospinal drive to spinal motoneurones following visuo-motor skill learning in humans. J. Physiol. 573, 843–855. doi:10.1113/jphysiol.2006.105361

Pernet, C.R., Wilcox, R., Rousselet, G.A., 2013. Robust correlation analyses: False positive and power validation using a new open source matlab toolbox. Front. Psychol. 3.

Person, A.L., Perkel, D.J., 2005. Unitary IPSPs Drive Precise Thalamic Spiking in a Circuit Required for Learning 46, 129–140. doi:10.1016/j.neuron.2004.12.057

Petersen, T.H., Willerslev-Olsen, M., Conway, B. a, Nielsen, J.B., 2012. The motor cortex drives the muscles during walking in human subjects. J. Physiol. 590, 2443–2452. doi:10.1113/jphysiol.2012.227397

Peterson, D.S., Pickett, K.A., Earhart, G.M., 2012. Effects of levodopa on vividness of motor imagery in Parkinson disease. J. Parkinsons. Dis. 2, 127–133. doi:10.3233/JPD-2012-12077

Pfurtscheller, G., 1998. Postmovement Beta Synchronization in Patients With Parkinson's Disease. J. Clin. Neurophysiol. 15, 243–250. doi:10.1097/00004691-199805000-00008

Pfurtscheller, G., Graimann, B., Huggins, J.E., Levine, S.P., Schuh, L.A., 2003. Spatiotemporal patterns of beta desynchronization and gamma synchronization in corticographic data during self-paced movement. Clin. Neurophysiol. 114, 1226–1236. doi:10.1016/S1388-2457(03)00067-1

Pfurtscheller, G., Neuper, C., Brunner, C., Lopes Da Silva, F., 2005. Beta rebound after different types of motor imagery in man. Neurosci. Lett. 378, 156–159. doi:10.1016/j.neulet.2004.12.034

Pfurtscheller, G., Zalaudek, K., Neuper, C., 1998. Event-related beta synchronization after wrist, finger and thumb movement. Electroencephalogr. Clin. Neurophysiol. - Electromyogr. Mot. Control 109, 154–160. doi:10.1016/S0924-980X(97)00070-2

Plotnik, M., Hausdorff, J.M., 2008. The role of gait rhythmicity and bilateral coordination of stepping in the pathophysiology of freezing of gait in Parkinson's disease. Mov. Disord. 23 Suppl 2, S444—-50. doi:10.1002/mds.21984

Pogosyan, A., Kühn, A.A., Trottenberg, T., Schneider, G.H., Kupsch, A., Brown, P.,

2006. Elevations in local gamma activity are accompanied by changes in the firing rate and information coding capacity of neurons in the region of the subthalamic nucleus in Parkinson's disease. Exp. Neurol. 202, 271–279. doi:10.1016/j.expneurol.2006.06.014

Pollok, B., Gross, J., Kamp, D., Schnitzler, A., 2008. Evidence for anticipatory motor control within a cerebello-diencephalic-parietal network. J. Cogn. Neurosci. 20, 828–840. doi:10.1162/jocn.2008.20506

Pollok, B., Gross, J., Schnitzler, A., 2006. How the brain controls repetitive finger movements. J. Physiol. Paris 99, 8–13. doi:10.1016/j.jphysparis.2005.06.002

Ponsen, M.M., Daffertshofer, A., van den Heuvel, E., Wolters, E.C., Beek, P.J., Berendse, H.W., 2006. Bimanual coordination dysfunction in early, untreated Parkinson's disease. Park. Relat. Disord. 12, 246–252. doi:10.1016/j.parkreldis.2006.01.006

Rae, C.L., Hughes, L.E., Anderson, M.C., Rowe, X.B., Rowe, J.B., 2015. The Prefrontal Cortex Achieves Inhibitory Control by Facilitating Subcortical Motor Pathway Connectivity. J. Neurosci. 35, 786–794. doi:10.1523/JNEUROSCI.3093-13.2015

Rae, C.L., Nombela, C., Rodriguez, P.V., Ye, Z., Hughes, L.E., Jones, P.S., Ham, T., Rittman, T., Coyle-Gilchrist, I., Regenthal, R., Sahakian, B.J., Barker, R.A., Robbins, T.W., Rowe, J.B., 2016. Atomoxetine restores the response inhibition network in Parkinson's disease. Brain 139, 2235–2248. doi:10.1093/brain/aww138

Rao, N.G., Donoghue, J.P., 2014. Cue to action processing in motor cortex populations. J. Neurophysiol. 111, 441–453. doi:10.1152/jn.00274.2013

Ray, N.J., Brittain, J.S., Holland, P., Joundi, R.A., Stein, J.F., Aziz, T.Z., Jenkinson, N., 2012. The role of the subthalamic nucleus in response inhibition: Evidence from local field potential recordings in the human subthalamic nucleus. Neuroimage 60, 271–278. doi:10.1016/j.neuroimage.2011.12.035

Redgrave, P., Coizet, V., Comoli, E., McHaffie, J.G., Leriche, M., Vautrelle, N., Hayes, L.M., Overton, P., 2010. Interactions between the midbrain superior colliculus and the basal ganglia. Front. Neuroanat. 4, 1–8. doi:10.3389/fnana.2010.00132

Redgrave, P., Prescott, T.J., Gurney, K., 1999. The basal ganglia: A vertebrate solution to the selection problem? Neuroscience 89, 1009–1023.

Remple, M.S., Bradenham, C.H., Kao, C.C., Charles, P.D., Neimat, J.S., Konrad, P.E., 2011. Subthalamic nucleus neuronal firing rate increases with Parkinson's disease progression. Mov. Disord. 26, 1657–1662. doi:10.1002/mds.23708

Repp, B.H., Su, Y.-H., 2013. Sensorimotor synchronization: A review of recent research

(2006–2012). Psychon. Bull. Rev. 20, 403–452. doi:10.3758/s13423-012-0371-2

Reyes, A., Laine, C.M., Kutch, J.J., Valero-Cuevas, F.J., 2017. Beta Band Corticomuscular Drive Reflects Muscle Coordination Strategies. Front. Comput. Neurosci. 11, 1–10. doi:10.3389/fncom.2017.00017

Richter, C.G., Thompson, W.H., Bosman, C.A., Fries, P., 2017. Top-down beta enhances bottom-up gamma. J. Neurosci. 7, 3716–3771. doi:10.1523/JNEUROSCI.3771-16.2017

Riehle, A., Gruen, S., Diesmann, M., Aertsen, A., 1997. Spike Synchronization and Rate Modulation Differentially Involved in Motor Cortical Function. Science (80-.). 278, 1950–1953. doi:10.1126/science.278.5345.1950

Rienzo, F. Di, Collet, C., Hoyek, N., Guillot, A., 2014. Impact of neurologic deficits on motor imagery: A systematic review of clinical evaluations. Neuropsychol. Rev. 24, 116–147. doi:10.1007/s11065-014-9257-6

Rinvik, E., 1975. Demonstration of nigrothalamic connections in the cat by retrograde axonal transport of horseradish peroxidase. Brain Res. 90, 313–318. doi:10.1016/0006-8993(75)90312-1

Ritter, P., Moosmann, M., Villringer, A., 2009. Rolandic alpha and beta EEG rhythms' strengths are inversely related to fMRI-BOLD signal in primary somatosensory and motor cortex. Hum. Brain Mapp. 30, 1168–1187. doi:10.1002/hbm.20585

Robbins, T.W., 1996. Dissociating executive functions of the prefrontal cortex. Phil. Trans. R. Soc. London 351, 1463–1471.

Romanelli, P., Esposito, V., Schaal, D.W., Heit, G., 2005. Somatotopy in the basal ganglia: Experimental and clinical evidence for segregated sensorimotor channels. Brain Res. Rev. 48, 112–128. doi:10.1016/j.brainresrev.2004.09.008

Rosa, M., Arlotti, M., Marceglia, S., Cogiamanian, F., Ardolino, G., Fonzo, A. Di, Lopiano, L., Scelzo, E., Merola, A., Locatelli, M., Rampini, P.M., Priori, A., 2017. Adaptive deep brain stimulation controls levodopa-induced side effects in Parkinsonian patients. Mov. Disord. 32, 2016–2017. doi:10.1002/mds.26953

Roseberry, T.K., Lee, A.M., Lalive, A.L., Wilbrecht, L., Bonci, A., Kreitzer, A.C., 2016. Cell-Type-Specific Control of Brainstem Locomotor Circuits by Basal Ganglia. Cell 164, 526–537. doi:10.1016/j.cell.2015.12.037

Rouhinen, S., Panula, J., Palva, J.M., Palva, S., 2013. Load Dependence of beta and gamma oscillations predicts individual capacity of visual attention. J. Neurosci. 33, 19023–19033. doi:10.1523/JNEUROSCI.1666-13.2013

Rubino, D., Robbins, K.A., Hatsopoulos, N.G., 2006. Propagating waves mediate

information transfer in the motor cortex. Nat. Neurosci. 9, 1549–1557. doi:10.1038/nn1802

Rueda-Orozco, P.E., Robbe, D., 2015. The striatum multiplexes contextual and kinematic information to constrain motor habits execution. Nat. Neurosci. 18, 453–460. doi:10.1038/nn.3924

Sacchet, M.D., LaPlante, R.A., Wan, Q., Pritchett, D.L., Lee, A.K.C., Hamalainen, M., Moore, C.I., Kerr, C.E., Jones, S.R., 2015. Attention Drives Synchronization of Alpha and Beta Rhythms between Right Inferior Frontal and Primary Sensory Neocortex. J. Neurosci. 35, 2074–2082. doi:10.1523/JNEUROSCI.1292-14.2015

Saleh, M., Reimer, J., Penn, R., Ojakangas, C.L., Hatsopoulos, N.G., 2010. Fast and Slow Oscillations in Human Primary Motor Cortex Predict Oncoming Behaviorally Relevant Cues. Neuron 65, 461–471. doi:10.1016/j.neuron.2010.02.001

Salenius, S., Avikainen, S., Kaakkola, S., Hari, R., Brown, P., 2002. Defective cortical drive to muscle in Parkinson's disease and its improvement with levodopa. Brain 125, 491–500. doi:10.1093/brain/awf042

Salmelin, R., Hämäläinen, M., Kajola, M., Hari, R., 1995. Functional segregation of movement-related rhythmic activity in the human brain. Neuroimage. doi:10.1006/nimg.1995.1031

Sanes, J.N., Donoghue, J.P., 1993. Oscillations in local field potentials of the primate motor cortex during voluntary movement. Proc. Natl. Acad. Sci. U. S. A. 90, 4470–4474. doi:10.1073/pnas.90.10.4470

Schmidt, R., Leventhal, D.K., Mallet, N., Chen, F., Berke, J.D., Joshua, B., 2013. Canceling actions involves a race between basal ganglia pathways. Nat. Neurosci. 16, 1118–1124. doi:10.1038/nn.3456

Schnitzler, A., Salenius, S., Salmelin, R., Jousmäki, V., Hari, R., 1997. Involvement of Primary Motor Cortex in Motor Imagery: A Neuromagnetic Study. Neuroimage 6, 201–208. doi:10.1006/nimg.1997.0286

Schoffelen, J.-M., Oostenveld, R., Fries, P., 2005. Neuronal coherence as a mechanism of effective corticospinal interaction. Science 308, 111–113. doi:10.1126/science.1107027

Scholten, M., Govindan, R.B., Braun, C., Bloem, B.R., Plewnia, C., Krüger, R., Gharabaghi, A., Weiss, D., 2016. Cortical correlates of susceptibility to upper limb freezing in Parkinson's disease. Clin. Neurophysiol. 127, 2386–2393. doi:10.1016/j.clinph.2016.01.028

Schubert, R., Haufe, S., Blankenburg, F., Villringer, A., Curio, G., 2008. Now You'll Feel It-Now You Won't: EEG Rhythms Predict the Effectiveness of Perceptual

Masking. J Cogn Neurosci 2407–2419. doi:10.1162/jocn.2008.2117410.1162/jocn.2008.21174 [pii]

Schulz, H., Übelacker, T., Keil, J., Müller, N., Weisz, N., 2014. Now i am ready - Now i am not: The influence of pre-TMS oscillations and corticomuscular coherence on motor-evoked potentials. Cereb. Cortex 24, 1708–1719. doi:10.1093/cercor/bht024

Seeber, M., Scherer, R., Wagner, J., Solis-Escalante, T., Müller-Putz, G.R., 2015. High and low gamma EEG oscillations in central sensorimotor areas are conversely modulated during the human gait cycle. Neuroimage 112, 318–326. doi:10.1016/j.neuroimage.2015.03.045

Sherman, M.A., Lee, S., Law, R., Haegens, S., Thorn, C.A., Hämäläinen, M.S., Moore, C.I., Jones, S.R., 2016. Neural mechanisms of transient neocortical beta rhythms: Converging evidence from humans, computational modeling, monkeys, and mice. Proc. Natl. Acad. Sci. 113, E4885—-E4894. doi:10.1073/pnas.1604135113

Shine, J.M., Handojoseno, A.M.A., Nguyen, T.N., Tran, Y., Naismith, S.L., Nguyen, H., Lewis, S.J.G., 2014. Abnormal patterns of theta frequency oscillations during the temporal evolution of freezing of gait in parkinson's disease. Clin. Neurophysiol. 125, 569–576. doi:10.1016/j.clinph.2013.09.006

Shine, J.M., Matar, E., Ward, P.B., Bolitho, S.J., Gilat, M., Pearson, M., Naismith, S.L., Lewis, S.J.G., 2013a. Exploring the cortical and subcortical functional magnetic resonance imaging changes associated with freezing in Parkinson's disease. Brain 136, 1204–1215. doi:10.1093/brain/awt049

Shine, J.M., Matar, E., Ward, P.B., Frank, M.J., Moustafa, A.A., Pearson, M., Naismith, S.L., Lewis, S.J.G., 2013b. Freezing of gait in Parkinson's disease is associated with functional decoupling between the cognitive control network and the basal ganglia. Brain 136, 3671–3681. doi:10.1093/brain/awt272

Shreve, L.A., Velisar, A., Malekmohammadi, M., Koop, M.M., Trager, M., Quinn, E.J., Hill, B.C., Blumenfeld, Z., Kilbane, C., Mantovani, A., Henderson, J.M., Bront??-Stewart, H., 2017. Subthalamic oscillations and phase amplitude coupling are greater in the more affected hemisphere in Parkinson's disease. Clin. Neurophysiol. 128, 128–137. doi:10.1016/j.clinph.2016.10.095

Siegel, M., Donner, T.H., Engel, A.K., 2012. Spectral fingerprints of large-scale neuronal interactions. Nat. Rev. Neurosci. 13, 20–25. doi:10.1038/nrn3137

Siegel, M., Warden, M.R., Miller, E.K., 2009. Phase-dependent neuronal coding of objects in short-term memory. Proc. Natl. Acad. Sci. U. S. A. 106, 21341–21346. doi:10.1073/pnas.0908193106

Silberstein, P., Pogosyan, A., Kühn, A.A., Hotton, G., Tisch, S., Kupsch, A., Dowsey-Limousin, P., Hariz, M.I., Brown, P., 2005. Cortico-cortical coupling in

Parkinson's disease and its modulation by therapy. Brain 128, 1277–1291. doi:10.1093/brain/awh480

Singer, W., 1999. Neuronal Synchrony: A Versatile Code for the Definition of Relations? Neuron 24, 49–65.

Singh, A., Plate, A., Kammermeier, S., Mehrkens, J.H., Ilmberger, J., Boetzel, K., 2013. Freezing of gait-related oscillatory activity in the human subthalamic nucleus. Basal Ganglia 3, 25–32. doi:10.1016/j.baga.2012.10.002

Sinha, N., Manohar, S., Husain, M., 2013. Impulsivity and apathy in Parkinson's disease. J. Neuropsychol. 7, 255–283. doi:10.1111/jnp.12013

Skaggs, E.B., 1929. The major descriptive categories of inhibition in psychology. J. Abnorm. Soc. Psychol. 311.

Skodda, S., 2012. Effect of deep brain stimulation on speech performance in Parkinson's disease. Parkinsons. Dis. 2012. doi:10.1155/2012/850596

Smith, Y., Bevan, M.D., Shink, E., Bolam, J.P., 1998. Microcircuitry of the direct and indirect pathways of th ebasal ganglia. Neuroscience 86, 353–387. doi:http://dx.doi.org/10.1016/S0306-4522(98)00004-9

Sochůrková, D., Rektor, I., Jurák, P., Stančák, A., 2006. Intracerebral recording of cortical activity related to self-paced voluntary movements: A Bereitschaftspotential and event-related desynchronization/synchronization. SEEG study. Exp. Brain Res. 173, 637–649. doi:10.1007/s00221-006-0407-9

Soteropoulos, D.S., 2005. Cortico-Cerebellar Coherence During a Precision Grip Task in the Monkey. J. Neurophysiol. 95, 1194–1206. doi:10.1152/jn.00935.2005

Spinks, R.L., Kraskov, A., Brochier, T., Umilta, M.A., Lemon, R.N., 2008. Selectivity for Grasp in Local Field Potential and Single Neuron Activity Recorded Simultaneously from M1 and F5 in the Awake Macaque Monkey. J. Neurosci. 28, 10961–10971. doi:10.1523/JNEUROSCI.1956-08.2008

Stokes, M.G., Buschman, T.J., Miller, E.K., 2017. Dynamic Coding for Flexible Cognitive Control. Wiley Handb. Cogn. Control 221–241.

Stuss, D.T., Stuss, T., 1992. Biological and psychological development of executive functions. Brain Cogn. 20, 8–23. doi:10.1016/0278-2626(92)90059-U

Subramanian, L., Hindle, J. V, Johnston, S., Roberts, M. V, Husain, M., Goebel, R., Linden, D., 2011. Real-Time Functional Magnetic Resonance Imaging Neurofeedback for Treatment of Parkinson's Disease. J. Neurosci. 31, 16309–16317. doi:10.1523/JNEUROSCI.3498-11.2011

Surmeier, D.J., Ding, J., Day, M., Wang, Z., Shen, W., 2007. D1 and D2 dopamine-receptor modulation of striatal glutamatergic signaling in striatal medium spiny neurons. Trends Neurosci. 30, 228–235. doi:10.1016/j.tins.2007.03.008

Swann, N., Tandon, N., Canolty, R., Ellmore, T.M., McEvoy, L.K., Dreyer, S., DiSano, M., Aron, A.R., 2009. Intracranial EEG reveals a time- and frequency-specific role for the right inferior frontal gyrus and primary motor cortex in stopping initiated responses. J. Neurosci. 29, 12675–12685.

Swann, N.C., Cai, W., Conner, C.R., Pieters, T.A., Claffey, M.P., George, J.S., Aron, A.R., Tandon, N., 2012. Roles for the pre-supplementary motor area and the right inferior frontal gyrus in stopping action: electrophysiological responses and functional and structural connectivity. Neuroimage 59, 2860–2870. doi:10.1016/j.neuroimage.2011.09.049.

Swick, D., Ashley, V., Turken, U., 2011. Are the neural correlates of stopping and not going identical? Quantitative meta-analysis of two response inhibition tasks. Neuroimage 56, 1655–1665. doi:10.1016/j.neuroimage.2011.02.070

Szurhaj, W., Bourriez, J.L., Kahane, P., Chauvel, P., Mauguière, F., Derambure, P., 2005. Intracerebral study of gamma rhythm reactivity in the sensorimotor cortex. Eur. J. Neurosci. 21, 1223–1235. doi:10.1111/j.1460-9568.2005.03966.x

Szurhaj, W., Derambure, P., Labyt, E., Cassim, F., Bourriez, J.L., Isnard, J., Guieu, J.D., Mauguière, F., 2003. Basic mechanisms of central rhythms reactivity to preparation and execution of a voluntary movement: A stereoelectroencephalographic study. Clin. Neurophysiol. 114, 107–119. doi:10.1016/S1388-2457(02)00333-4

Tachibana, Y., Iwamuro, H., Kita, H., Takada, M., Nambu, A., 2011. Subthalamo-pallidal interactions underlying parkinsonian neuronal oscillations in the primate basal ganglia. Eur. J. Neurosci. 34, 1470–1484. doi:10.1111/j.1460-9568.2011.07865.x

Tamir, R., Dickstein, R., Huberman, M., 2007. Integration of motor imagery and physical practice in group treatment applied to subjects with Parkinson's disease. Neurorehabil. Neural Repair 21, 68–75. doi:10.1177/1545968306292608

Tan, H., Jenkinson, N., Brown, P., 2014a. Dynamic neural correlates of motor error monitoring and adaptation during trial-to-trial learning. J. Neurosci. 34, 5678–5688. doi:10.1523/JNEUROSCI.4739-13.2014

Tan, H., Pogosyan, A., Anzak, A., Ashkan, K., Bogdanovic, M., Green, A.L., Aziz, T., Foltynie, T., Limousin, P., Zrinzo, L., Brown, P., 2013. Complementary roles of different oscillatory activities in the subthalamic nucleus in coding motor effort in Parkinsonism. Exp. Neurol. 248, 187–195. doi:10.1016/j.expneurol.2013.06.010

Tan, H., Pogosyan, A., Ashkan, K., Cheeran, B., Fitzgerald, J.J., Green, A.L., Aziz, T., Foltynie, T., Limousin, P., Zrinzo, L., Brown, P., 2015. Subthalamic Nucleus Local Field Potential Activity Helps Encode Motor Effort Rather Than Force in Parkinsonism. J. Neurosci. 35, 5941–5949. doi:10.1523/JNEUROSCI.4609-14.2015

Tan, H., Pogosyan, A., Ashkan, K., Green, A.L., Aziz, T., Foltynie, T., Limousin, P., Zrinzo, L., Hariz, M., Brown, P., 2016a. Decoding gripping force based on local field potentials recorded from subthalamic nucleus in humans. Elife 5, 1–24. doi:10.7554/eLife.19089

Tan, H., Wade, C., Brown, P., 2016b. Post-Movement Beta Activity in Sensorimotor Cortex Indexes Confidence in the Estimations from Internal Models. J. Neurosci. 36, 1516–1528. doi:10.1523/JNEUROSCI.3204-15.2016

Tan, H., Zavala, B., Pogosyan, A., Ashkan, K., Zrinzo, L., Foltynie, T., Limousin, P., Brown, P., 2014b. Human Subthalamic Nucleus in Movement Error Detection and Its Evaluation during Visuomotor Adaptation. J. Neurosci. 34, 16744–16754. doi:10.1523/JNEUROSCI.3414-14.2014

te Woerd, E.S., Oostenveld, R., De Lange, F.P., Praamstra, P., 2017. Impaired auditory-to-motor entrainment in Parkinson's disease. J. Neurophysiol. jn.00547.2016. doi:10.1152/jn.00547.2016

Tecuapetla, F., Jin, X., Lima, S.Q., Costa, R.M., 2016. Complementary Contributions of Striatal Projection Pathways to Action Initiation and Execution. Cell 166, 703–715. doi:10.1016/j.cell.2016.06.032

Thaut, M.H., Mcintosh, G.C., Prassas, S.G., Rice, R.R., 1992. Effect of Rhythmic Auditory Cuing on Temporal Stride Parameters and EMG Patterns in Normal Gait. J Neuro Rehab 6, 185–190.

Thobois, S., Dominey, P.F., Decety, J., Pollak, P., Gregoire, M.C., Bars, D. Le, 2000. Motor imagery in normal subjects and in asymmetrical Parkinson's disease - A PET study. Neurology 55, 996–1002.

Tinkhauser, G., Pogosyan, A., Tan, H., Herz, D., Kühn, A., Brown, P., 2017. Beta burst dynamics in Parkinson's disease OFF and ON dopaminergic medication. Brain.

Toma, K., Nagamine, T., Yazawa, S., Terada, K., Ikeda, A., Honda, M., Oga, T., Shibasaki, H., 2000. Desynchronization and synchronization of central 20-Hz rhythms associated with voluntary muscle relaxation: A magnetoencephalographic study. Exp. Brain Res. 134, 417–425. doi:10.1007/s002210000483

Tomlinson, C.L., Stowe, R., Patel, S., Rick, C., Gray, R., Clarke, C.E., 2010. Systematic review of levodopa dose equivalency reporting in Parkinson's disease. Mov. Disord. 25, 2649–2653. doi:10.1002/mds.23429

Torrecillos, F., Alayrangues, J., Kilavik, B.E., Malfait, N., 2015. Distinct Modulations in Sensorimotor Postmovement and Foreperiod -Band Activities Related to Error Salience Processing and Sensorimotor Adaptation. J. Neurosci. 35, 12753–12765. doi:10.1523/JNEUROSCI.1090-15.2015

Trager, M.H., Koop, M.M., Velisar, A., Blumenfeld, Z., Nikolau, J.S., Quinn, E.J., Martin, T., Bronte-Stewart, H., 2016. Subthalamic beta oscillations are attenuated after withdrawal of chronic high frequency neurostimulation in Parkinson's disease. Neurobiol. Dis. 96, 22–30. doi:10.1016/j.nbd.2016.08.003

Tremblay, F., Léonard, G., Tremblay, L., 2008. Corticomotor facilitation associated with observation and imagery of hand actions is impaired in Parkinson's disease. Exp. Brain Res. 185, 249–257. doi:10.1007/s00221-007-1150-6

Trottenberg, T., Fogelson, N., Kühn, A.A., Kivi, A., Kupsch, A., Schneider, G.H., Brown, P., 2006. Subthalamic gamma activity in patients with Parkinson's disease. Exp. Neurol. 200, 56–65. doi:10.1016/j.expneurol.2006.01.012

Turner, R.S., Desmurget, M., 2010. Basal ganglia contributions to motor control: A vigorous tutor. Curr. Opin. Neurobiol. 20, 704–716. doi:10.1016/j.conb.2010.08.022

Tzagarakis, C., Ince, N.F., Leuthold, A.C., Pellizzer, G., 2010. Beta-band activity during motor planning reflects response uncertainty. J. Neurosci. 30, 11270–11277.

van Ede, F., de Lange, F., Jensen, O., Maris, E., 2011. Orienting Attention to an Upcoming Tactile Event Involves a Spatially and Temporally Specific Modulation of Sensorimotor Alpha- and Beta-Band Oscillations. J. Neurosci. 31, 2016–2024. doi:10.1523/JNEUROSCI.5630-10.2011

van Ede, F., de Lange, F.P., Maris, E., 2012. Attentional Cues Affect Accuracy and Reaction Time via Different Cognitive and Neural Processes. J. Neurosci. 32, 10408–10412. doi:10.1523/JNEUROSCI.1337-12.2012

van Ede, F., Szebényi, S., Maris, E., 2014. Attentional modulations of somatosensory alpha, beta and gamma oscillations dissociate between anticipation and stimulus processing. Neuroimage 97, 134–141. doi:10.1016/j.neuroimage.2014.04.047

van Elswijk, G., Maij, F., Schoffelen, J., Overeem, S., Stegeman, D.F., Fries, P., 2010. Corticospinal Beta-Band Synchronization Entails Rhythmic Gain Modulation. J. Neurosci. 30, 4481–4488. doi:10.1523/JNEUROSCI.2794-09.2010

van Wijk, B., Pogosyan, A., Hariz, M., Foltynie, T., Limousin, P., Zrinzo, L., Brown, P., Litvak, V., 2017. Localization of beta band and high-frequency oscillations within the subthalamic nucleus. NeuroImage Clin. 16, 4. doi:10.1016/j.nicl.2017.07.018

van Wijk, B.C.M., Beek, P.J., Daffertshofer, A., 2012. Neural synchrony within the

motor system: what have we learned so far? Front. Hum. Neurosci. 6, 1–15. doi:10.3389/fnhum.2012.00252

van Wijk, B.C.M., Beudel, M., Jha, A., Oswal, A., Foltynie, T., Hariz, M.I., Limousin, P., Zrinzo, L., Aziz, T.Z., Green, A.L., Brown, P., Litvak, V., 2016. Subthalamic nucleus phase-amplitude coupling correlates with motor impairment in Parkinson's disease. Clin. Neurophysiol. 127, 2010–2019. doi:10.1016/j.clinph.2016.01.015

van Wijk, B.C.M., Daffertshofer, A., Roach, N., Praamstra, P., 2009. A role of beta oscillatory synchrony in biasing response competition? Cereb. Cortex 19, 1294–1302. doi:10.1093/cercor/bhn174

Verbruggen, F., Aron, A.R., Stevens, M.A., Chambers, C.D., 2010. Theta burst stimulation dissociates attention and action updating in human inferior frontal cortex. Proc. Natl. Acad. Sci. 107, 13966–13971. doi:10.1073/pnas.1001957107

Vercruysse, S., Spildooren, J., Heremans, E., Vandenbossche, J., Levin, O., Wenderoth, N., Swinnen, S.P., Janssens, L., Vandenberghe, W., Nieuwboer, A., 2012. Freezing in Parkinson's disease: a spatiotemporal motor disorder beyond gait. Mov. Disord. 27, 254–263. doi:10.1002/mds.24015

von Nicolai, C., Engler, G., Sharott, A., Engel, A.K., Moll, C.K., Siegel, M., 2014. Corticostriatal Coordination through Coherent Phase-Amplitude Coupling. J. Neurosci. 34, 5938–5948. doi:10.1523/JNEUROSCI.5007-13.2014

Voytek, B., Knight, R.T., 2015. Dynamic network communication as a unifying neural basis for cognition, development, aging, and disease. Biol. Psychiatry 77, 1089–1097. doi:10.1016/j.biopsych.2015.04.016

Wang, D.D., de Hemptinne, C., Miocinovic, S., Qasim, S.E., Miller, A.M., Ostrem, J.L., Galifianakis, N.B., San Luciano, M., Starr, P.A., 2016. Subthalamic local field potentials in Parkinson's disease and isolated dystonia: An evaluation of potential biomarkers. Neurobiol. Dis. 89, 213–222. doi:10.1016/j.nbd.2016.02.015

Wei, W., Wang, X., 2016. Inhibitory Control in the Cortico-Basal Ganglia-Thalamocortical Loop: Complex Regulation and Interplay with Memory and Decision Processes. Neuron 92, 1093–1105. doi:10.1016/j.neuron.2016.10.031

Weinberger, M., Mahant, N., Hutchison, W.D., Lozano, A.M., Moro, E., Hodaie, M., Lang, A.E., Dostrovsky, J.O., 2006. Beta Oscillatory Activity in the Subthalamic Nucleus and Its Relation to Dopaminergic Response in Parkinson's Disease. J. Neurophysiol. 96, 3248–3256. doi:10.1152/jn.00697.2006

Wessel, J.R., Aron, A.R., 2016. HHS Public Access 52, 472–480. doi:10.1111/psyp.12374.It

Wessel, J.R., Aron, A.R., 2014. Inhibitory motor control based on complex stopping

goals relies on the same brain network as simple stopping. Neuroimage 103, 225–234. doi:10.1016/j.neuroimage.2014.09.048

Wessel, J.R., Aron, A.R., 2013. Unexpected events induce motor slowing via a brain mechanism for action-stopping with global suppressive effects. J. Neurosci. Off. J. Soc. Neurosci. 33, 18481–18491. doi:10.1523/JNEUROSCI.3456-13.2013

Wessel, J.R., Ghahremani, A., Udupa, K., Saha, U., Kalia, S.K., Hodaie, M., Lozano, A.M., Aron, A.R., Chen, R., 2016a. Stop-related subthalamic beta activity indexes global motor suppression in Parkinson's disease. Mov. Disord. doi:10.1002/mds.26732

Wessel, J.R., Jenkinson, N., Brittain, J.-S., Voets, S.H.E.M., Aziz, T.Z., Aron, A.R., 2016b. Surprise disrupts cognition via a fronto-basal ganglia suppressive mechanism. Nat. Commun. 7, 11195. doi:10.1038/ncomms11195

Whitmer, D., De Solages, C., Hill, B.C., Yu, H., Bronte-Stewart, H., 2013. Resting beta hypersynchrony in secondary dystonia and its suppression during pallidal deep brain stimulation in DYT3+ lubag dystonia. Neuromodulation 16, 200–205. doi:10.1111/j.1525-1403.2012.00519.x

Williams, D., Kühn, A., Kupsch, A., Tijssen, M., Van Bruggen, G., Speelman, H., Hotton, G., Loukas, C., Brown, P., Bruggen, G. Van, Speelman, H., Williams, D., Ku, A., 2005. The relationship between oscillatory activity and motor reaction time in the parkinsonian subthalamic nucleus. Eur. J. Neurosci. 21, 249–258. doi:10.1111/j.1460-9568.2004.03817.x

Williams, D., Tijssen, M., Van Bruggen, G., Bosch, A., Insola, A., Di Lazzaro, V., Mazzone, P., Oliviero, A., Quartarone, A., Speelman, H., Brown, P., 2002. Dopamine-dependent changes in the functional connectivity between basal ganglia and cerebral cortex in humans. Brain 125, 1558–1569. doi:10.1093/brain/awf156

Williams, D.C., 2011. Finite sample correction factors for several simple robust estimators of normal standard deviation. J. Stat. Comput. Simul. 81, 1697–1702. doi:10.1080/00949655.2010.499516

Witte, M., Patino, L., Andrykiewicz, A., Hepp-Reymond, M.C., Kristeva, R., 2007. Modulation of human corticomuscular beta-range coherence with low-level static forces. Eur. J. Neurosci. 26, 3564–3570. doi:10.1111/j.1460-9568.2007.05942.x

Womelsdorf, T., Schoffelen, J.J.-M., Oostenveld, R., Singer, W., Desimone, R., Engel, A.K., Fries, P., 2007. Modulation of Neuronal Interactions Through Neuronal Synchronization. Science (80-.). 316, 1609–1612. doi:10.1126/science.1139597

Wu, Y., Richard, S., Parent, A., 2000. The organization of the striatal output system: A single-cell juxtacellular labeling study in the rat. Neurosci. Res. 38, 49–62. doi:10.1016/S0168-0102(00)00140-1

Xu, B., Sandrini, M., Wang, W.T., Smith, J.F., Sarlls, J.E., Awosika, O., Butman, J.A., Horwitz, B., Cohen, L.G., 2016. PreSMA stimulation changes task-free functional connectivity in the fronto-basal-ganglia that correlates with response inhibition efficiency. Hum. Brain Mapp. 37, 3236–3249. doi:10.1002/hbm.23236

Yeo, S.-H., Franklin, D.W., Wolpert, D.M., 2016. When Optimal Feedback Control Is Not Enough: Feedforward Strategies Are Required for Optimal Control with Active Sensing. PLoS Comput. Biol. 12, e1005190. doi:10.1371/journal.pcbi.1005190

Yin, X., Xu, B., Jiang, C., Fu, Y., Wang, Z., Li, H., Shi, G., 2015. A hybrid BCI based on EEG and fNIRS signals improves the performance of decoding motor imagery of both force and speed of hand clenching. J. Neural Eng. 12, 36004. doi:10.1088/1741-2560/12/3/036004

Yoles-Frenkel, M., Avron, M., Prut, Y., 2016. Impact of Auditory Context on Executed Motor Actions. Front. Integr. Neurosci. 10, 1–13. doi:10.3389/fnint.2016.00001

Yousif, N., Liu, X., 2008. Modelling the current distribution across the depth electrode-brain interface in deep brain stimulation 4, 623–631. doi:10.1586/17434440.4.5.623.Modelling

Zaepffel, M., Trachel, R., Kilavik, B.E., Brochier, T., 2013. Modulations of EEG Beta Power during Planning and Execution of Grasping Movements. PLoS One 8. doi:10.1371/journal.pone.0060060

Zaidel, A., Spivak, A., Grieb, B., Bergman, H., Israel, Z., 2010. Subthalamic span of β oscillations predicts deep brain stimulation efficacy for patients with Parkinson's disease. Brain 133, 2007–2021. doi:10.1093/brain/awq144

Zavala, B., Damera, S., Dong, J.W., Lungu, C., Brown, P., Zaghloul, K.A., 2015. Human Subthalamic Nucleus Theta and Beta Oscillations Entrain Neuronal Firing During Sensorimotor Conflict. Cereb. Cortex bhv244. doi:10.1093/cercor/bhv244

Zhang, Y., Wang, X., Bressler, S.L., Chen, Y., Ding, M., 2008. Prestimulus cortical activity is correlated with speed of visuomotor processing. J Cogn Neurosci 20, 1915–1925. doi:10.1162/jocn.2008.20132

Zheng, T., Wilson, C.J., 2002. Corticostriatal Combinatorics: The Implications of Corticostriatal Axonal Arborizations. J. Neurophysiol. 87, 1007–1017. doi:10.1016/0006-8993(89)91018-4

Appendix - Supplementary Figures

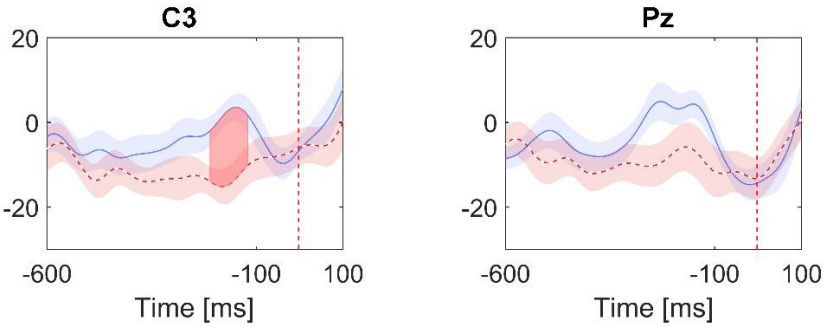

Supplementary Figure A.1 12-20 Hz beta power time course preceding the stop signal (vertical dashed line). Data were split into two clusters by using a k-means clustering algorithm on the movement extent measurement obtained in each trial (initial cluster centres were set to 0% and 100%). The blue line denotes the power average of trials with small movement extents (=successful stopping) and the red dashed line shows the average trials with large movement extents. With this split, the difference in Pz did not survive the cluster-based permutation procedure opposite as in Figure 4.6A.

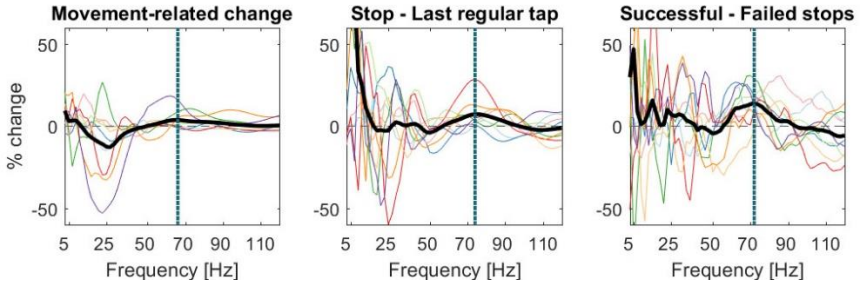

Supplementary Figure A.2 Peak frequencies of movement- and stop-related power changes. Power for individual frequencies between 3-120 Hz was averaged over time between the stop signal and the mean time of failed taps (156ms later) for stop-related changes (right and middle plot). Bold thick lines show the average across subjects and coloured lines show individual subjects. For movement-related power changes (left plot), the window was aligned to the time of each tap onset. The movement-related gamma increase was broader and weaker than the stop-related increase. Dotted lines show the peak frequency in the gamma range (>40Hz). The middle plot shows the difference between power in response to the stop signal irrespective of stopping outcome relative to the last regular tap (corresponding to Figure 5.3A). The right plot shows the difference between successful vs. failed stops (corresponding to Figure 5.3B). Power differences in frequencies lower than 50 Hz were highly variable, whereas power was consistently increased around 70 Hz in response to the stop signal, especially during successful stopping.

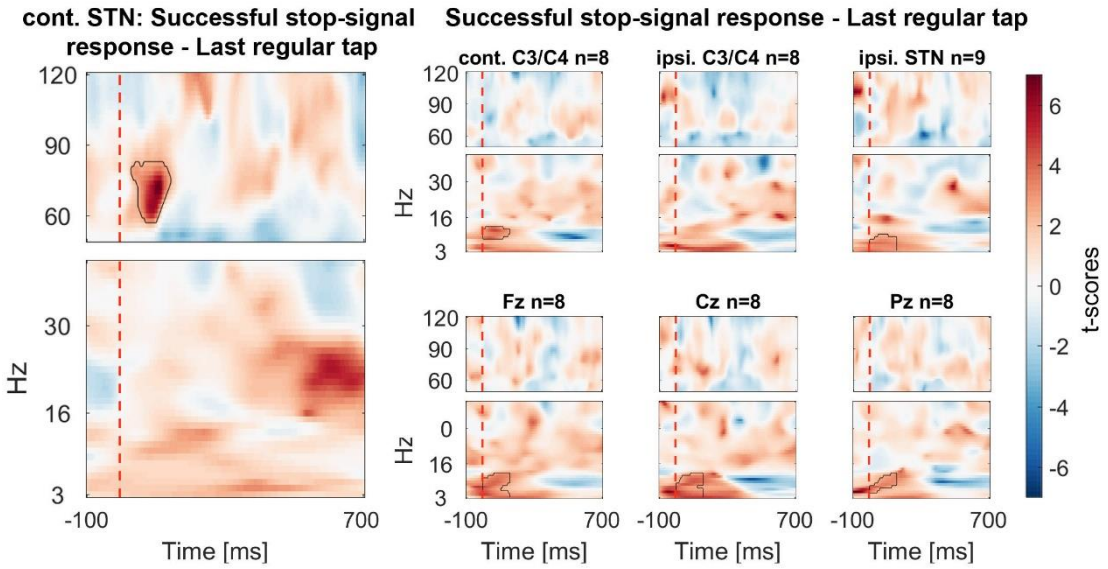

Supplementary Figure A.3 Power changes following the stop signal when only successful stop trials are considered (averaged across all patients). T-scores of the contrast between power of all successful stop trials aligned to the stop signal (vertical dashed line) and the regular tap done before (aligned to where the stop signal would have occurred if it would have been presented one tap earlier). Significant clusters are similar as in the main Figure 5.3A.

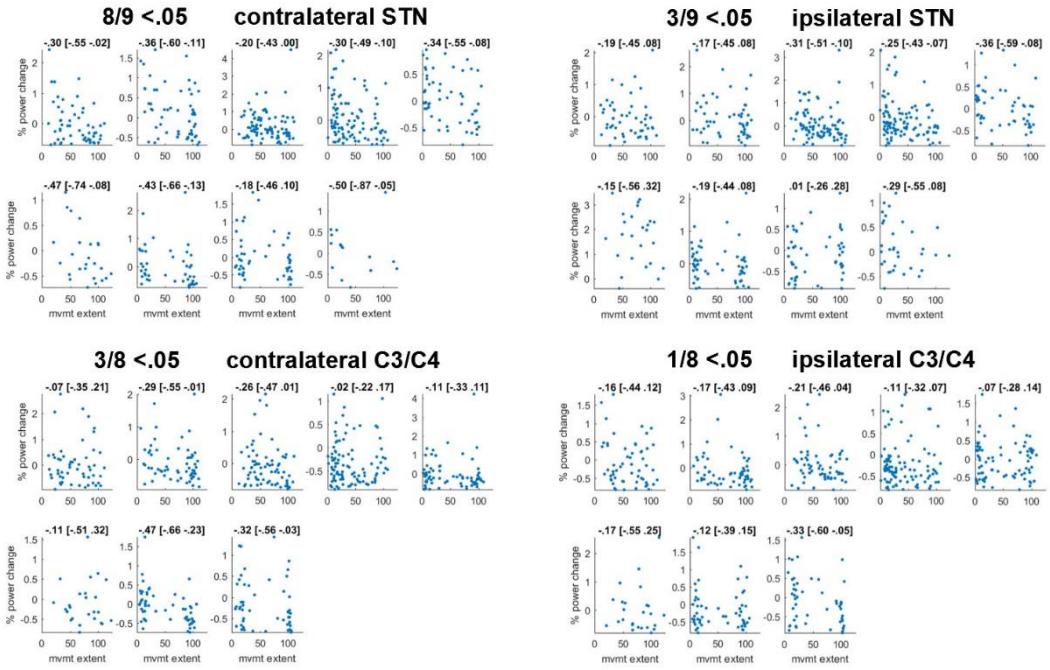

Supplementary Figure A.4 Scatter plot of correlations between movement extent (x-axis) and 60-90 Hz gamma relative to baseline (y-axis).Subplots show individual participants. For each subject, gamma power yielding the maximum correlation (detected anywhere between 60-90 Hz and 0:156ms after the stop signal, considering that optimal frequencies and time points may differ across subjects) is shown. The number of points can differ within each patient if an electrode was more prone to artefacts and thus more trials were excluded. Plot titles denote Spearman's rho followed by its 95% bootstrapped confidence interval. In all but one subject correlations were significant in the contralateral STN.

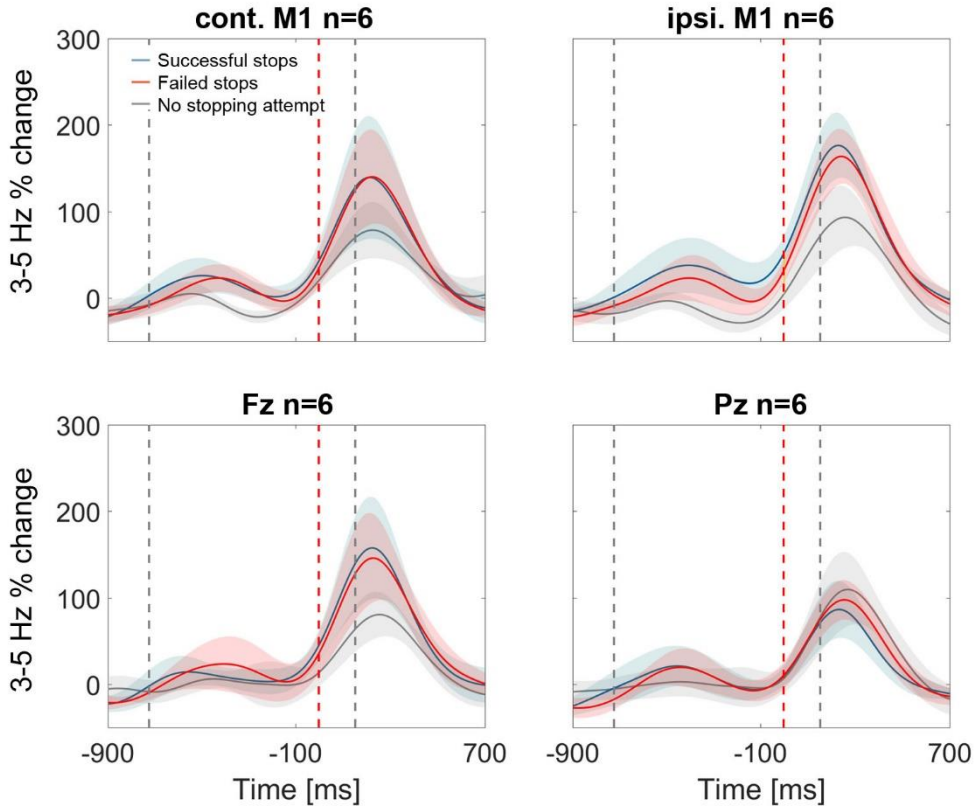

Supplementary Figure A.5 3-5 Hz power increase in contralateral and ipsilateral M1, Fz and Pz. In contralateral and ispilateral M1, as well as Fz, the stop signal-related theta increase seemed to be smaller in the control condition when stopping was not attempted (grey line, n=6) but this difference was not significant. Note also that the blue and red shaded areas (successful and failed stops), denoting standard errors of the mean, were highly overlapping.

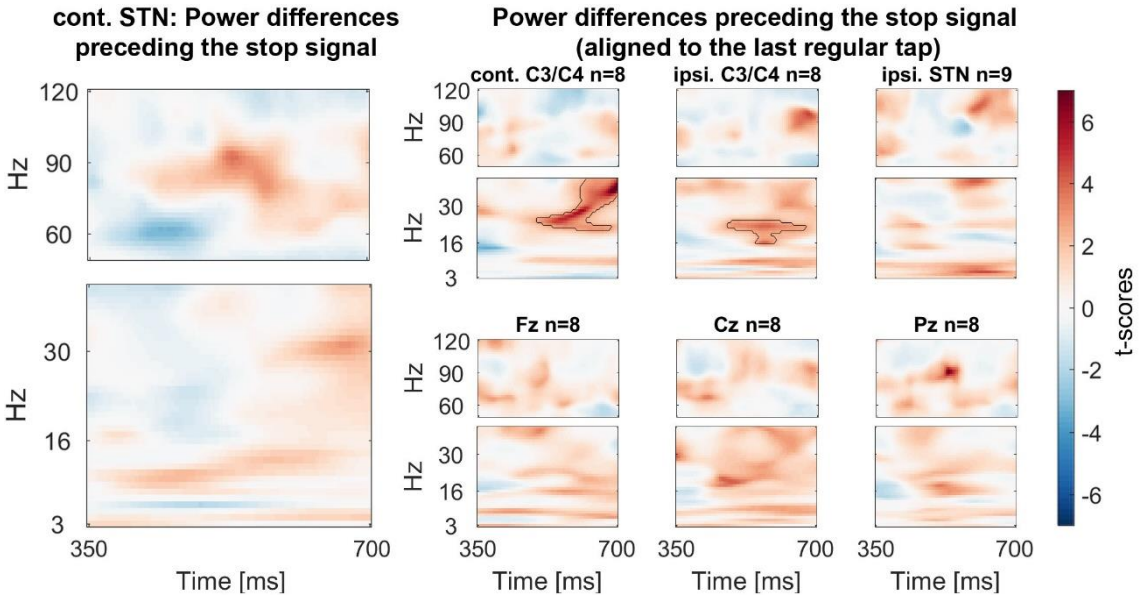

Supplementary Figure A.6 Power differences preceding the stop signal with the data aligned to the last regular tap before stop signal delivery (averaged across all patients). This figure differs slightly from the main Figure 5.8 as the delay between the tap and stop signal differed across patients in spite of being the same across trials in each subject. With the alignment to the last regular tap the beta difference is also significant in contralateral C3/C4. No such difference was present in the STN.